NUREG/CR-4763
SAND86-2280
R3
Printed March 1988

Safety-Related Equipment Survival in Hydrogen Burns in Large Dry PWR Containment Buildings

Donald B. King, Vernon F. Nicolette, Vincent J. Dandini,
Barry L. Spletzer

Prepared by
Sandia National Laboratories
Albuquerque, New Mexico 87185 and Livermore, California 94550
for the United States Department of Energy
under Contract DE-AC04-76DP00789

Prepared for
U. S. NUCLEAR REGULATORY COMMISSION

Available from

Superintendent of Documents
U.S. Government Printing Office
Post Office Box 37082
Washington, D.C. 20013-7082

and

National Technical Information Service
Springfield, VA 22161

NUREG/CR-4763
SAND86-2280
R3

SAFETY-RELATED EQUIPMENT SURVIVAL IN HYDROGEN BURNS IN LARGE DRY PWR CONTAINMENT BUILDINGS

Donald B. King
Vernon F. Nicolette
Vincent J. Dandini
Barry L. Spletzer

March 1988

Sandia National Laboratories
Albuquerque, NM 87185
Operated by
Sandia Corporation
for the
U.S. Department of Energy

Prepared for
Division of Engineering
Office of Nuclear Regulatory Research
U.S. Nuclear Regulatory Commission
Washington DC 20555
Under Memorandum of Understanding DOE 40-550-75
NRC FIN A1270

ABSTRACT

Studies of the threat to safety-related equipment posed by hydrogen burns in both large dry atmospheric and subatmospheric PWR containment buildings have been conducted at Sandia National Laboratories. These studies have taken the form of analyses and experiments.

Analyses for an atmospheric large dry containment used a model of the Three Mile Island containment building. The subatmospheric analyses studied the Surry Nuclear Power Plant. Both analyses used hydrogen source terms as calculated by the MARCH code. The HECTR computer code was used to analyze hydrogen transport and combustion and their effects on heat transfer models of a pressure transmitter.

For hydrogen combustion analyses in which single hydrogen burns were predicted, HECTR calculated that the worst case equipment model temperature would just exceed the qualification temperature (by 6 K) for ten minutes. For multiple hydrogen burns (simulation of ignition by igniters at 7 v/o), HECTR calculated that the safety equipment models could increase in temperature significantly above the qualification temperature for long periods of time. For analyses in which combustion was not allowed, HECTR predicted that potentially detonable hydrogen concentrations could occur in many cases.

A series of experiments was conducted to study the survivability of both aged and unaged nuclear qualified cable and pressure transmitters in a simulated LOCA and hydrogen burn environment. All test specimens survived the single hydrogen burn test environments. However, in the multiple burn tests, the cable specimens and pressure transmitter did not survive the environments.

In conclusion, single hydrogen burns throughout large dry containments do not appear to pose a serious threat to the safety equipment studied in this report. However, a dilemma occurs when considering the effect of igniter-induced multiple burns in large dry containments. Analyses indicate that the absence of igniters (no combustion) can result in potentially detonable mixtures for both the atmospheric and subatmospheric containments. But with igniter use, both analyses and experiments indicate that the multiple burn environment can pose a threat to safety equipment.

CONTENTS

CONTENTS (Continued)

LIST OF FIGURES

LIST OF FIGURES (Continued)

LIST OF TABLES

ACKNOWLEDGMENTS

The tests conducted in the Severe Combined Environment Test Chamber for this report represent a significant step forward in the environmental testing of nuclear-qualified safety-related equipment. The configuration of the chamber in a mode which made the testing possible was the end result of an effort which was, in itself, a significant research and development project.

The authors gratefully acknowledge the contributions of Frank Horine and Mike Ramirez of K-Tech Corporation for their work on the control circuitry and mechanical modifications to the chamber, and to Mike Luker of Sandia Division 6446 for his work on preparation of the test samples.

A special acknowledgment is due to Barry Spletzer of Sandia Division 6447 who designed the chamber and who also developed the scheme for simulating the hydrogen burns and the control circuit for making it work. His tireless enthusiasm and often ingenious solutions to perplexing problems were, in no small measure, responsible for the successful completion of the tests.

The authors also acknowledge Lanny Smith of SAIC for his work in obtaining the Surry and Zion MARCH input decks.

EXECUTIVE SUMMARY

Analytical and experimental investigations of equipment survival in hydrogen burns in large dry PWR containment buildings have been conducted. Both atmospheric and subatmospheric containments were considered. Two sets of analytical studies were carried out for atmospheric large dry containments. One set analyzed the hydrogen burn that occurred as a result of the March 1979, accident at Three Mile Island. The other set considered a hybrid power plant consisting of the Zion reactor housed in the TMI-2 containment building. An analytical study of subatmospheric containments was also carried out using a model of the Surry nuclear power plant. To complement the analyses, a series of experiments simulating hydrogen burns in large dry containments was also conducted using the Sandia severe combined environment test chamber (SCETCh). The experiments investigated the survivability of thermally and radiation aged nuclear qualified Brand Rex power and control cable and a Barton 763 pressure transmitter in a simulated LOCA/hydrogen burn environment.

The analytical studies used the HECTR computer code to calculate the temperature response of equipment models to hydrogen burns in various containment locations. Hydrogen source terms for the analyses were calculated by the MARCH code. Other parameters which were varied in the analyses included LOCA break size, ignition criteria (single burn and multiple burn by igniter simulation) and the operation of engineered safety features. The equipment thermal response models used in the analyses were based on the Barton 763 gauge pressure transmitter.

The results reported below for the atmospheric large dry containment are specific to the TMI-2 containment; however, atmospheric large dry containments have many common structural features. Therefore, the trends of the results reported below and in the main body have significance for all atmospheric large dry containments (applicability of these results to other atmospheric large dry containments is addressed in the main body). The subatmospheric large dry containment results apply to all subatmospheric containments operating in the United States since they are all based on the Surry design.

Equipment model temperature response was a function of the hydrogen burn type to which the equipment was exposed. Single hydrogen burns dispersed their energy throughout containment in relatively short time periods. The atmospheric large dry containment analyses had no cases where single hydrogen burns caused the surface temperature of the three-layer Barton model to exceed 444 K (a typical equipment qualification temperature). In fact, surface temperatures were well below the 444 K temperature limit. The Surry single burn analyses had two cases in which the Barton model surface temperature exceeded 444 K, but the peak temperatures were only slightly above 444 K (447 K and 450 K) for

short time periods (less than ten minutes). It should be noted that the Surry containment represents one of the most severe cases (highest hydrogen mole fractions) for both atmospheric and subatmospheric large dry containments.

Multiple burns simulating ignition by igniters at seven volume-percent hydrogen released most of the hydrogen energy into a relatively small region of containment (the source compartment) over a relatively long period of time. This localized and lengthy release of energy due to multiple burning sometimes forced the Barton model surface temperature to exceed 444 K for long periods of time. Roughly half of the hybrid analyses resulted in equipment model temperatures significantly exceeding the qualification temperature. The worst hybrid case resulted in a peak model surface temperature of 670 K. The surface remained above 444 K for 51 minutes. All the Surry analyses resulted in equipment model temperatures significantly exceeding the qualification temperature. The worst Surry multiple burn case resulted in a peak surface temperature of 670 K which remained above 444 K for 50 minutes.

Analyses were also performed to calculate hydrogen concentrations in large dry containments assuming no hydrogen burning. When no hydrogen burns occur, HECTR predicted potentially detonable gas mixtures would occur briefly (in some cases) in the hybrid analyses. These mixtures occurred only in the source compartments. HECTR predicted potentially detonable gas mixtures would occur for lengthy periods of time in all of the Surry analyses. These mixtures occurred in the source compartments as well as globally throughout the containment and were a direct result of the cold spray water (45°F) stripping out the steam.

The hybrid and subatmospheric analytical results should be viewed in light of HECTR's simple criteria for specifying a detonable concentration. One must also realize that the Barton transmitter served as a surrogate for all safety equipment in these analyses. A more accurate evaluation of the threat to safety equipment posed by hydrogen burns must consider such factors as precise equipment location, function, material properties, susceptibility to thermal stress, and the length of time during the accident for which the equipment is required to function.

The analytical results can also be viewed in light of the results of experiments simulating single and multiple hydrogen burns in large dry containments. Single burn tests of aged and unaged nuclear qualified cable and Barton pressure transmitters indicate that cable and equipment having similar thermal characteristics and sensitivities can withstand a LOCA and single hydrogen burn resulting from a 75 percent core Zircaloy-water reaction in a large dry containment. The observed post-test condition and performance of the test specimens is consistent with the results reported for the EPRI-NTS tests and previous hydrogen burn

simulations at Sandia's Central Receiver Test Facility, as well as observed damage at TMI-2. The results of these tests should not be extrapolated to hydrogen standing flame environments (beyond the scope of this work) where safety equipment may be exposed to plume or flame heat fluxes.

In contrast to the single burn test results, the multiple burn test results indicate that multiple burns can pose a serious threat to safety-related equipment located in small and/or poorly ventilated source compartments. Cable specimens and a Barton pressure transmitter exposed in the multiple burn simulation tests failed to survive.

In conclusion, the results of the single burn tests and HECTR analyses of large dry atmospheric and subatmospheric containments indicate that for a LOCA involving a 75 percent metal-water reaction, a single hydrogen deflagration does not present a serious threat to the survival of nuclear qualified safety-related equipment studied in this report.

However, a conclusion regarding deliberate ignition systems is not as clear. The HECTR results indicate that detonable concentrations of hydrogen may accumulate locally in a source compartment of a large dry atmospheric containment and both locally and globally in a large dry subatmospheric containment unless a deliberate ignition system is employed. A deliberate ignition system would prevent detonations by burning the hydrogen at lower (nondetonable) concentrations. This presents a dilemma since the results of HECTR analyses which model deliberate ignition as well as the results of scoping multiple burn tests indicate that multiple burn (deliberate ignition) environments could pose a serious threat to the survival of safety-related equipment in a source compartment.

1.0 INTRODUCTION

One of the many events that occurred during the Three Mile Island accident was a single hydrogen deflagration which raised the pressure inside the containment building. The integrity of the TMI containment was not compromised, but the event raised concern that a similar event in the future might degrade or incapacitate equipment necessary to monitor the reactor and maintain it in a safe condition. This concern has led to the implementation of hydrogen control schemes at several power plants.

The approach to hydrogen control has largely been dictated by containment type. Because of their small volumes and low design pressures, ice condenser PWR containments and Mark III BWR containments have distributed ignition systems which are intended to burn hydrogen as it is generated. In this way hydrogen is eliminated before it can build up to concentrations which, if ignited, might threaten the ability of the containment to isolate fission products from the environment. The atmospheres in Mark I and II BWR containments are nitrogen inerted, precluding hydrogen combustion completely.

Rulemaking for hydrogen control in large dry and subatmospheric containments has been deferred pending the completion of research into the effects of hydrogen combustion in these structures. This research is based on the premise that hydrogen released as a result of a 75 percent core metal-water reaction is representative of the upper bound of hydrogen release in a hydrogen-producing accident.[1]

This report summarizes the results of recent analytical and experimental research at Sandia National Laboratories dealing with equipment survival in hydrogen burns in large dry and subatmospheric containment buildings. It integrates these new results with the results of earlier work on hydrogen burn equipment survival at Sandia and the Electric Power Research Institute (EPRI).

2.0 DESCRIPTION OF WORK TO DATE

2.1 Recently Reported Work

Recently reported work relevant to hydrogen burn equipment survival in large dry containments has been in the area of experimentation. The Electric Power Research Institute (EPRI) conducted a series of tests at the Nevada Test Site (NTS) which exposed nuclear-qualified safety equipment to hydrogen burns of varying severity in a large, spherical vessel.[2] A series of tests at the Sandia Central Receiver Test Facility (CRTF), which simulated one of the most severe

of the EPRI-NTS tests, augmented equipment performance and thermal response data from the EPRI-NTS series.[3] A second series of CRTF tests investigated the effects of aging on safety equipment exposed to simulations of increasingly severe hydrogen burns.[4]

The EPRI-NTS tests studied the effects of hydrogen burns on several samples of nuclear-qualified safety equipment and cables. The tests were performed in a 74,000 ft^3 dewar at the Nevada Test Site. Deflagrations of hydrogen concentrations up to 13 volume-percent were studied. Instrumentation inside the test vessel provided data on the burn environment. The burns had a deleterious effect on this instrumentation as testing progressed, and, as a result, there is some uncertainty in the environmental descriptions based on data from these instruments.

The safety equipment samples tested in the EPRI-NTS tests were powered and their operation was monitored during and after exposure to the hydrogen burns. The cables were not powered or monitored in any way during the tests. They were, however, evaluated upon removal from the test vessel.

The authors of Reference 2, a summary of the EPRI-NTS results, stated, "The study showed that equipment qualified to operate under LOCA conditions should be able to operate during and after the high-temperature spikes produced by hydrogen burns... Despite substantial external damage to the cables, only those with preexisting defects or cumulative damage from many burns failed."[2]

The CRTF simulation of an EPRI-NTS 13 volume-percent hydrogen burn provided detailed operational and thermal response data on a nuclear-qualified pressure transmitter, solenoid valve, and three brands of nuclear-qualified cable. All samples were unaged.

The transmitter and solenoid valve operated normally during and after exposure to the simulated hydrogen burn. The transmitter displayed a small change in calibration after completion of the tests. Temperature measurements indicated that the transmitter and valve did not reach temperatures which might jeopardize their operation.

Cables were powered during exposure to the simulated hydrogen burn and maintained their electrical integrity throughout exposure. No short circuits were detected. During postexposure insulation testing, none of the conductors failed.

The CRTF sensitivity testing[4] examined the effects of aging on nuclear-qualified cables and pressure transmitters. Artificially aged and unaged cables and transmitters

were exposed to simulations of increasingly severe hydrogen deflagrations. The most severe heat flux pulse had three times the peak flux and total heat content of a deflagration expected to result from the combustion of hydrogen precipitated by an accident involving a 75 percent core metal-water reaction. All samples were electrically powered during exposure to the simulated hydrogen burn fluxes and the transmitters were also pressurized.

All cables maintained their electrical integrity during exposure. During postexposure insulation testing, only one conductor (out of 30) failed. The failed conductor was from the aged cable which had been exposed to the most severe heat flux pulse, and failure occurred at the most severe high-potential withstand voltage. Thermal aging had only a slight effect on the cable insulation properties.

While separate cable samples were used for each pulse, the aged and unaged transmitters were each subjected to the full set of severe pulses. Both transmitters functioned properly throughout the tests. Calibration checks before and after each test demonstrated that exposure to the severe heat flux pulses individually and in toto produced only small changes in calibration.

Overall, aging had little effect on the performance of the cables and transmitters.

2.2 New Work

The new work was initiated to complete issues that had not been addressed by the old work. The EPRI-NTS tests did not address the environmental conditioning of the equipment due to the LOCA which would precede a hydrogen burn and also did not test aged equipment or cable. The Sandia CRTF tests did not address pressure effects on equipment and cables which would occur during a burn as well as pressure and thermal effects due to the LOCA environment.

The new work reported here involved analyses of equipment thermal response to hydrogen deflagrations in large dry and subatmospheric containment buildings and a series of experiments which studied the operational response of safety equipment to a simulated LOCA/hydrogen burn environment in a large dry containment building. Although the TMI Unit 2 containment and Surry containment are both large dry containments, their results will be reported separately because the atmospheric large dry and subatmospheric large dry containments have varying operating conditions. The analyses used the HECTR computer code[5] and the experiments were conducted in Sandia National Laboratories' Severe Combined Environment Test Chamber (SCETCh). The work is discussed briefly here. Details of the work and results are given in the appendices.

Two sets of large dry analyses were conducted. Both used a model of the Three Mile Island Unit 2 containment building. The first set, referred to as the TMI analyses, considered the hydrogen burn which occurred during the TMI accident in March of 1979. The second set, referred to as the TMI-hybrid or hybrid analyses, used a model of the Zion reactor core housed in the TMI-2 containment. The hybrid model was used because of the availability of the Zion reactor model and the TMI Unit 2 containment model.

The TMI analyses considered possible variations in containment surface areas (surface areas in containment are not known exactly), burn time, and combustion completeness. Each of the TMI analyses presumed one of two sets of initial conditions immediately preceding ignition as determined by previous research on the TMI hydrogen burn event.[6,7] The TMI analyses concentrated on containment gas temperature and pressure with some consideration given to equipment thermal response.[8]

The hybrid analyses considered containment conditions and equipment thermal response during LOCAs which had hydrogen burning. The LOCAs were limited to small and intermediate sized coolant system breaks. The parameters of the study included break location, ignition criteria, equipment location, equipment thermal characteristics, and containment compartmentalization.

The subatmospheric analyses studied hydrogen deflagration in the Surry nuclear power plant. The containment building model was similar to that used in the American Nuclear Society Source Term Study.[9] These analyses were concerned primarily with equipment thermal response. The parameters included break size and location, equipment location, equipment thermal characteristics, and ignition criteria.

The experimental tests were performed in Sandia's Severe Combined Environment Test Chamber (SCETCh) and included the simulation of a LOCA/hydrogen burn heat flux, pressure pulse, humidity, and oxygen concentration. Both single burn and multiple burn (deliberate ignition) environments were simulated. Test specimens included aged and unaged samples of nuclear qualified cable and pressure transmitters.

3.0 RESULTS OF NEW WORK

3.1 TMI Analyses Results

3.1.1 Introduction

This section summarizes the analysis of the March 1979 TMI-2 hydrogen burn event. This analysis was requested by DOE and

postulated that hydrogen addition rates calculated by Henrie and Postma be used.[10] Since the Henrie and Postma report was released, a TMI-2 hydrogen burn analysis has also been performed by the Factory Mutual Research Corporation (FMRC).[11] Our report includes and builds upon the analyses of both References 10 and 11. The hydrogen generation in core, release rates, and mixing used in the analysis are based upon the results of References 10 and 11.

The HECTR computer code[5] was used to calculate the containment gas and safety-related equipment thermal response during and after the hydrogen burn. A moderately compartmentalized model of TMI-2 was used. The TMI-2 containment building was divided into eight compartments with 17 intercompartment flow junctions and 46 structural surfaces. The eight compartments selected were: (1) the reactor cavity, (2) the refueling canal, (3) the steam generator compartment with the pressurizer SG1A, (4) the second steam generator compartment without the pressurizer SG1B, (5) the basement level, (6) the second floor, (7) the dome region, and (8) the enclosed stairwell and elevator. The major Engineering Safety Features (ESF) modeled during the burn were the reactor building fan coolers and spray system.

The thermal response models for the safety-related equipment were based on a Barton 763 gauge pressure transmitter. Four models were developed. The model reported in this analysis was a one-dimensional, three-layer representation of the Barton 763. This model accounted for the air gap between the casing and internal electronics. In an analysis, the one-dimensional three-layer model was analytically subjected to an incident heat flux pulse used at the Sandia Central Receiver Test Facility (CRTF) for prior hydrogen burn simulation equipment experiments. The surface temperature response of the model was calculated and compared to the measured surface temperature rise of an actual Barton 763 exposed to the flux pulse at the CRTF. The peak surface temperature of the model was calculated to be approximately 11°K higher (less than 5 percent difference) than the measured Barton 763 surface temperature. The three-layer model and measured Barton 763 thermal time response characteristics were equivalent. This one-dimensional, three-layer model is considered to be the most realistic of the four models and its surface temperature response to hydrogen burning will be reported in this analysis as a basis of evaluating the thermal response of electrical equipment to a hydrogen burn. The surface temperature due to hydrogen burning will be compared to that for which equipment is normally qualified. Environmental qualification test profiles described in IEEE323-74 recommend a maximum pressure of 483 kPa and a maximum temperature of 444°K. The qualification test profiles maintain these maximum values for several hours.

Calculated peak equipment surface temperatures at or below the 444 K qualification temperature were considered not to threaten equipment. Testing of the Barton 763 at the CRTF has shown that the interior equipment temperature substantially lags the surface temperature for large single incident heat flux pulses. However, the interior temperature of the equipment can approach the surface temperature for multiple or repeated incident heat flux pulses such as from multiple hydrogen burns.

The Barton 763 models were placed in five containment locations. The locations were (1) the basement, (2) the second floor, (3) steam generator compartment SG1A, (4) steam generator compartment SG1B, and (5) the dome region.

3.1.2 Containment Conditions Prior to Burn

The initial conditions prior to the burn in containment are dependent upon the hydrogen generated in the primary vessel and released, with steam, through a break in the primary cooling system. This analysis did not attempt to calculate the amount of hydrogen and steam released from the primary but used results from other analyses[10,11] to establish the initial conditions in containment prior to the hydrogen burn.

Approximately 320 to 360 kg of hydrogen were released at TMI into the reactor building over a 7 to 8 hour period before the hydrogen burn.[10-13] Hydrogen and steam were released through the discharge duct from the reactor coolant drain tank (RCDT). The RCDT is located in the basement level with the discharge duct exit near the ceiling of the basement. The hydrogen and steam then entered the second and third floor levels through openings between the floor levels. The hot, buoyant hydrogen and steam mixture might lead to stratification in the compartments into which the mixture would enter, but the stratification would be opposed by phenomena which would promote mixing in containment. These phenomena include (1) circulation of gas by the reactor building fan coolers, (2) circulation of containment gas by hot nuclear steam system surfaces, (3) mixing of containment gas by condensation onto cool surfaces, (4) plume entrainment by released steam and hydrogen, and (5) molecular diffusion. At TMI, the fan coolers circulated containment air roughly once every 12 minutes before the hydrogen burn occurred.

Experiments and analyses[10,11] indicated that average hydrogen concentration differences between containment levels greater than one percent total hydrogen were not likely. A small amount of hydrogen was released approximately 45 seconds before the hydrogen burn occurred, which could have produced a small, enriched hydrogen region in the

basement; however, the bulk of the hydrogen released during the 7 to 8 hours before the burn was well mixed throughout the containment.

The assumed initial conditions at TMI for the hydrogen burn analysis in this report are listed in Table 3.1. Those preignition conditions include an initial hydrogen concentration of 7.3 to 7.9 percent and an initial water vapor concentration of 3.5 to 5.5 percent. The initial gas temperature and pressure were 326.5 K and 110.3 kPa, respectively.

Table 3.1

Initial Conditions Used for the TMI-2 Hydrogen Burn Analysis

Case	XH_2 (%)	XH_2O (%)	P(kPa)	T(°K)
1	7.9	3.5	110.3	326.5
2	7.3	3.6	110.3	326.5
3	7.5	5.5	110.3	326.5

3.1.3 Containment Response to Hydrogen Burn

The containment building pressure is monitored by the Once Through Steam Generator (OTSG) pressure transmitters A and B and by Engineered Safety Features (ESFs) pressure switches. Figure 3.1 shows the pressure data recorded during and after the hydrogen burn. A peak pressure of approximately 302 kPa occurred 10 to 12 seconds after ignition during the accident at TMI. The 12 second pressure rise is a rough indication of the burn time in the containment.

Containment gas temperatures were recorded every 6 minutes. Unfortunately, the hydrogen burn occurred between recording times and no data for gas temperatures during burning is available. However, high-temperature alarm sensors indicated that the hydrogen burn began in the basement and continued upward through the floor levels and steam generator compartments into the dome region.[10]

The completeness of the hydrogen burn at TMI-2 is not precisely known. Henrie and Postma[10] concluded that approximately 86 percent of the hydrogen was consumed during the burn.

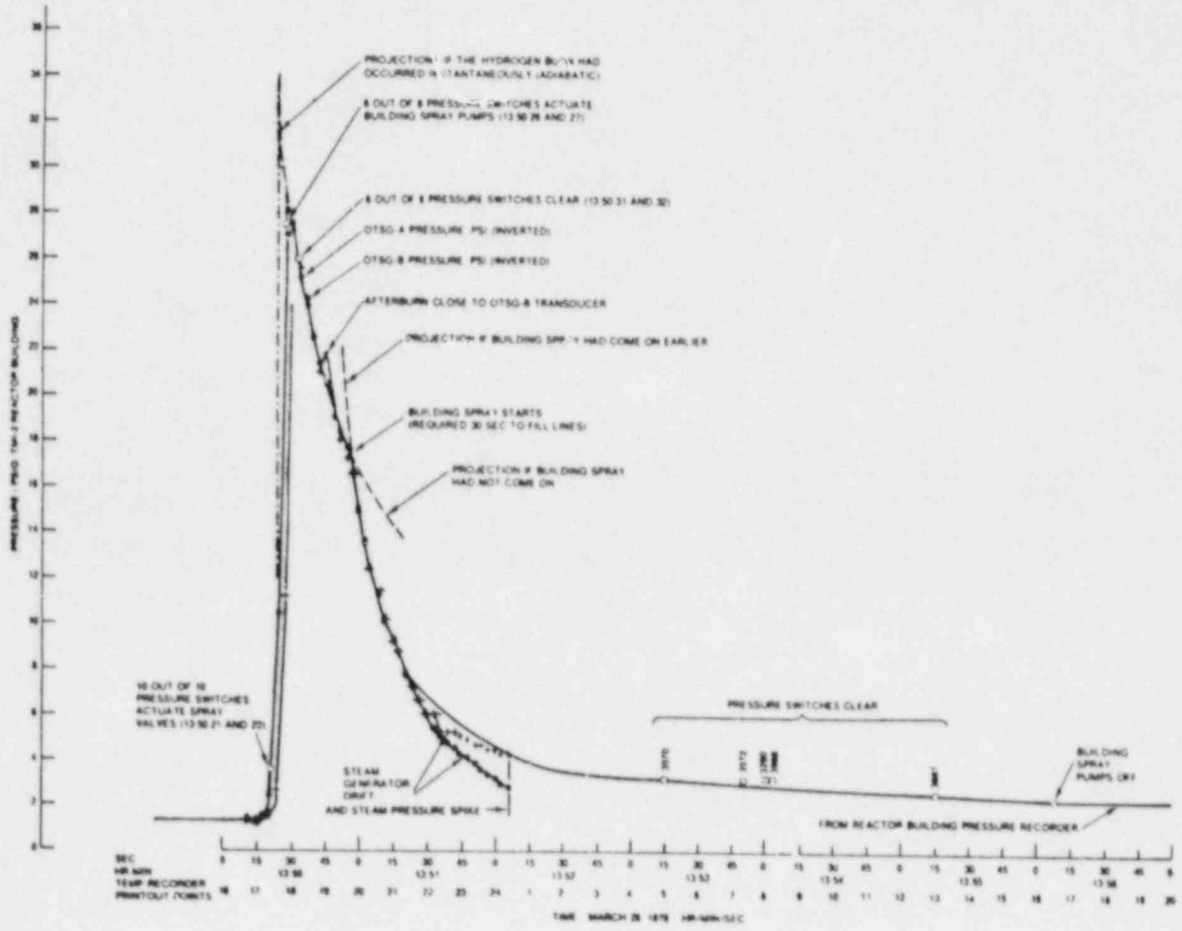

Figure 3.1. TMI-2 Containment Gas Pressure Response to Hydrogen Burning (Reference 6)

3.1.4 Results

Eleven HECTR production runs are reported on in Appendix B for the TMI-2 hydrogen burn analysis. These runs are summarized in Table 3.2. The eleven runs examined the effects of four parameters on the HECTR calculations. Parameters varied included: (1) the initial gas conditions, (2) the burn duration time (burn time mode), (3) the completeness of the hydrogen burn, and (4) the containment surface area. The reader is referred to Appendix B for a detailed description of the production runs.

Table 3.2

HECTR TMI-2 Analyses

Case	Burn Time Mode	Burn Completeness	Surface Area	Initial Gas Conditions
1A	Long BDT	100%	Default	A
1B	Short BDT	100%	Default	A
1C	Short BDT	100%	130%	A
1D	Long BDT	X	Default	A
1E	Long BDT	Y	Default	A
2A	Specified	100%	Default	A
2B	Specified	X	Default	A
2C	Specified	Y	Default	A
2D	Specified	100%	Default	B
2E	Specified	100%	Default	C
2F	Specified	X	Default	A

A Case 1 Initial Gas Conditions, Table 3.1
B Case 2 Initial Gas Conditions, Table 3.1
C Case 3 Initial Gas Conditions, Table 3.1

X 1% H_2 total mole fraction percentage left in dome
2% H_2 total mole fraction percentage left in steam generators
2.2% H_2 total mole fraction percentage left below dome

Y 0% H_2 total mole fraction percentage left in dome
3.5% H_2 total mole fraction percentage left elsewhere in containment

BDT Burn Duration Time

The HECTR code was used to calculate the containment gas temperature and pressure response and the surface temperature response of the one-dimensional, three-layer Barton 763 pressure transmitter model to hydrogen burning. Total incident heat fluxes to the Barton 763 during the hydrogen burning were also calculated.

Peak containment gas pressures for complete hydrogen burning in containment ranged from 300 kPa to 340 kPa. The initial conditions and burn duration times had a significant effect on the peak pressure calculated during the hydrogen burning. Incomplete hydrogen burns as described in Section 3.1.3 had peak gas pressures ranging from 300 kPa to 320 kPa. All peak pressures calculated were significantly below the 483 kPa equipment qualification pressure. A summary of peak gas pressure, gas temperature, Barton model surface temperatures, and incident fluxes to equipment models is presented in Table 3.3. Compartments with no flux listings signify that the Barton was not located in that compartment.

Case 2F results will be presented in this section in detail because it was fairly representative of most of the cases listed in Table 3.3. Figure 3.2 compares a calculated containment gas pressure response for the typical HECTR production run to the actual TMI-2 OTSG A measured containment pressure. Approximately 86 percent of the hydrogen was consumed during the burn. HECTR calculated a quicker pressure increase during hydrogen burning than was measured and a 5 percent higher pressure peak compared to the measured peak. However, the overall agreement is quite good. Sprays were activated at approximately 55 seconds.

The HECTR analyses predicted that peak gas temperatures in containment during hydrogen burning increased with increasing containment elevation. Peak gas temperatures in the dome ranged from 940 K to 1070 K, with the lower peaks occurring for incomplete burning. Second floor peak gas temperatures ranged from 790 K to 1030 K and basement peak gas temperatures ranged from 760 K to 1020 K. Figure 3.3 shows the calculated containment temperature response for the Figure 3.2 pressure response. The burn duration was 12 seconds. The burn was initiated in the basement and propagated almost immediately into SG1A. The burn then propagated into the second floor at approximately 3.5 seconds and into the dome at approximately 6.5 seconds. From 6.5 to 12 seconds, burning was occurring throughout containment. The burn ended at 12 seconds.

Table 3.3

HECTR TMI-2 Deflagration Summaries

Case	Compartment	Gas		Barton	Incident Flux	
		Pm (kPa)	Tm (°K)	Tm (°K)	Tm (kW/m^2)	Rm (kW/m^2)
1A	1	320	870	--	--	--
	2	320	1000	333	52	27
	3	320	1010	333	54	28
	4	320	1020	--	--	--
	5	320	960	334	37	24
	6	320	970	333	50	27
	7	320	1030	338	70	38
1B	1	340	920	--	--	--
	2	340	1020	333	54	29
	3	340	1030	333	55	30
	4	340	1040	--	--	--
	5	340	990	334	44	30
	6	340	1010	335	63	35
	7	340	1060	338	76	42
1C	1	330	920	--	--	--
	2	330	1020	333	54	29
	3	330	1030	333	55	30
	4	330	1040	--	--	--
	5	330	980	333	42	29
	6	330	1000	334	61	34
	7	330	1050	337	74	40
1D	1	310	800	--	--	--
	2	310	900	332	42	19
	3	310	890	332	42	19
	4	310	970	--	--	--
	5	310	850	333	29	18
	6	310	890	333	42	19
	7	310	1000	338	66	36
1E	1	300	710	--	--	--
	2	300	780	333	26	12
	3	300	780	331	26	12
	4	300	780	--	--	--
	5	300	760	331	19	12
	6	300	790	332	26	14
	7	300	1030	339	71	41
1F	1	340	800	--	--	--
	2	340	1010	335	49	35
	3	340	1020	335	50	35
	4	340	1060	--	--	--

Table 3.3

HECTR TMI-2 Deflagration Summaries (Concluded)

Case	Compartment	Gas		Barton	Incident Flux	
		Pm (kPa)	Tm (°K)	Tm (°K)	Tm (kW/m^2)	Rm (kW/m^2)
	5	340	1020	336	56	39
	6	340	1030	337	59	42
	7	340	1070	340	68	48
2B	1	320	720	--	--	--
	2	320	890	332	32	22
	3	320	900	333	33	21
	4	320	1000	--	--	--
	5	320	890	333	35	23
	6	320	900	334	38	25
	7	320	1010	338	57	39
2C	1	310	660	--	--	--
	2	310	790	331	21	12
	3	310	790	331	21	12
	4	310	810	--	--	--
	5	310	800	331	25	14
	6	310	800	332	26	15
	7	310	1060	340	65	46
2D	1	300	730	--	--	--
	2	300	900	332	32	21
	3	300	900	332	32	21
	4	300	930	--	--	--
	5	300	910	333	37	24
	6	300	910	334	39	25
	7	300	940	336	43	28
2E	1	310	750	--	--	--
	2	310	930	333	38	26
	3	310	930	333	39	26
	4	310	970	--	--	--
	5	310	940	334	44	29
	6	310	950	335	46	31
	7	310	980	338	53	35
2F	1	320	750	--	--	--
	2	320	910	333	33	22
	3	320	910	333	34	22
	4	320	1010	--	--	--
	5	320	900	333	37	24
	6	320	900	334	40	25
	7	320	1020	338	64	39

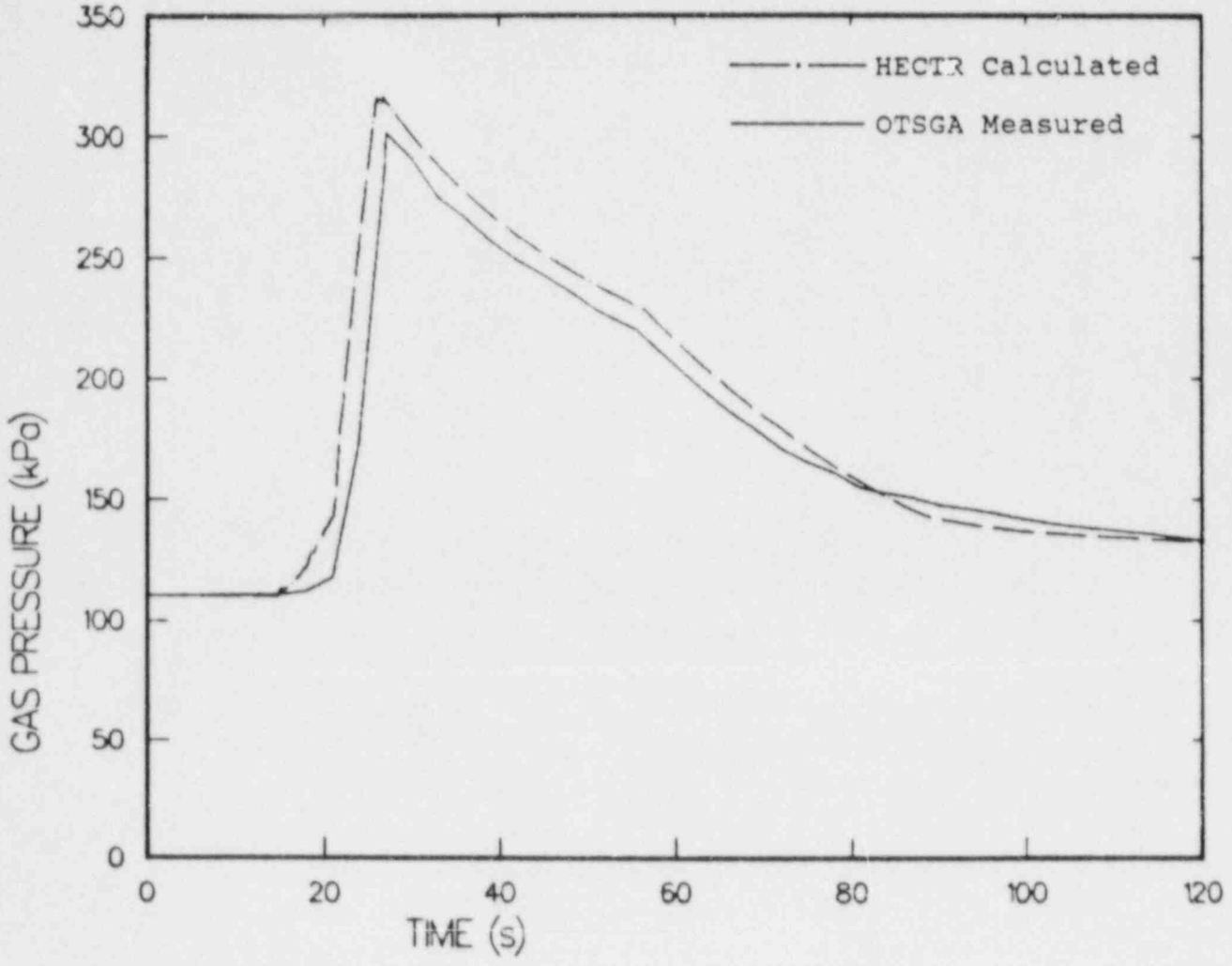

Figure 3.2. HECTR Calculated Pressure Compared to OTSGA Measured Pressure at TMI

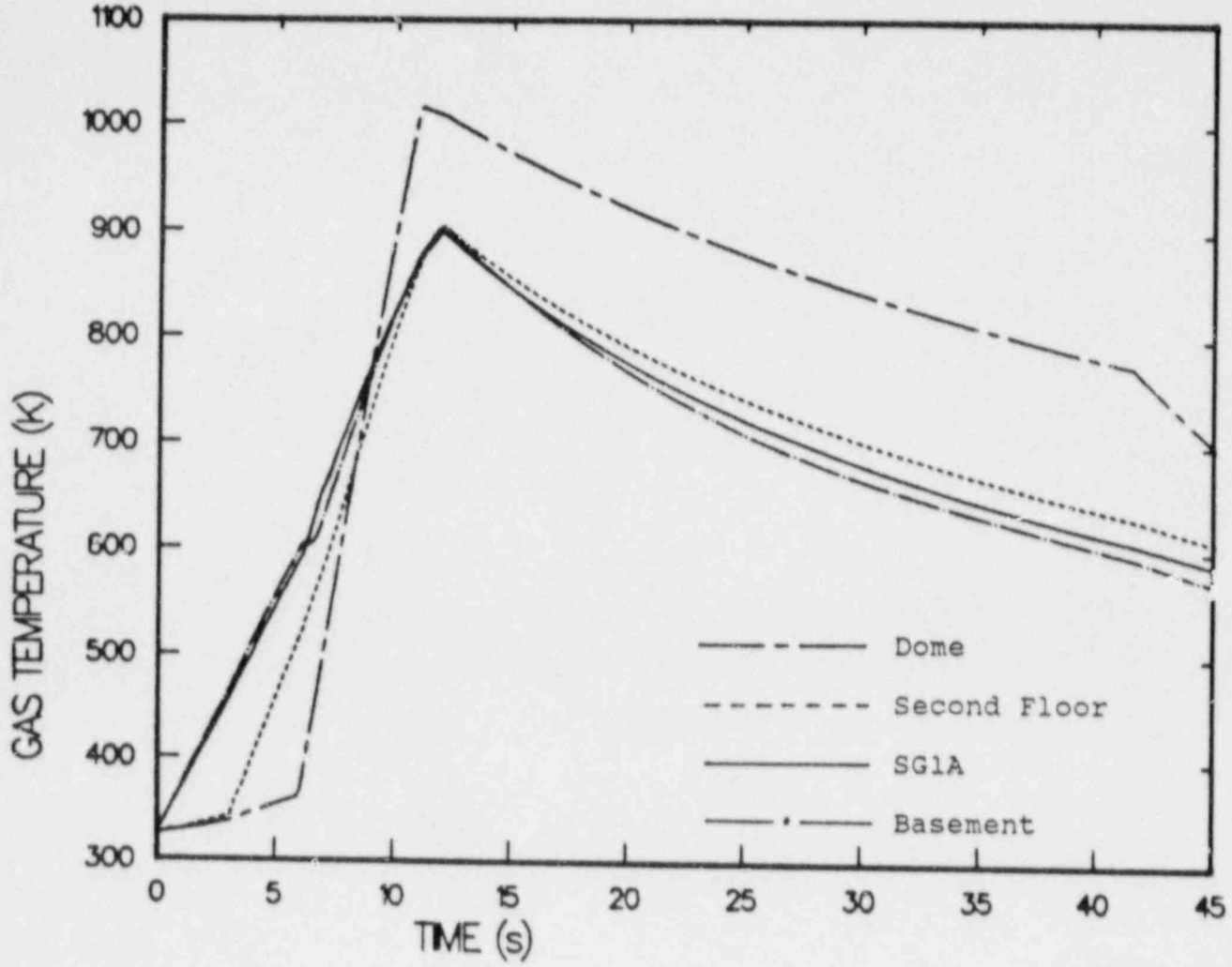

Figure 3.3. HECTR Calculated Containment Gas Temperatures

For the HECTR TMI analysis, the peak surface temperature of the Barton 763 one-dimensional, three-layer model never exceeded the equipment qualification temperature of 444 K. Peak surface temperatures for the models ranged from 333 K to 340 K.

Peak incident total heat fluxes for the Barton 763 model reflected the gas temperatures with respect to containment elevation. Peak total incident fluxes ranged from 43 kW/m^2 to 77 kW/m^2 in the dome region and from 22 kW/m^2 to 64 kW/m^2 in the lower elevations of containment. Figure 3.4 shows the worst-case flux profiles for the dome region and lower containment elevations, respectively. The time-integrated total-incident heat fluxes for Figure 3.4 are shown in Figure 3.5.

Given the containment gas conditions and heat fluxes, these results can be used to estimate the extent of cable damage that might have occurred during the hydrogen burn. Cable flammability studies have been performed at FMRC.[14] The tests conducted at FMRC base cable flammability on two parameters: (1) critical heat flux, and (2) absorbed ignition energy. The critical heat flux is the minimum flux below which ignition of cable cannot occur. The absorbed ignition energy is the minimum time integral of external flux above which a flammable cable vapor/air mixture near the surface of the cable can be maintained as long as the external heat flux is above the critical flux.

Absorbed ignition energy for cable damage (Ed) and cable ignition (Ei) as determined by FMRC range from 900 kJ/m^2 and 1,300 kJ/m^2, respectively, to 1,100 kJ/m^2 and 17,000 kJ/m^2. Typical Ei values for polar crane and power cables are 1,300 to 1,800 kJ/m^2 and 1,300 kJ/m^2, respectively. The absorbed ignition energies are based on an external heat flux of 14 to 27 kW/m^2. The critical heat flux indicates that once Ed or Ei has been obtained, cable damage or ignition will occur as long as the critical heat flux is maintained.

Figures 3.4 and 3.5 indicate that critical heat flux levels of 14 to 27 kW/m^2 do not exist in the basement when integrated flux levels of 900 kJ/m^2 are obtained. Therefore, cable damage or ignition are unlikely below the dome region. Cable damage may occur in the dome region but cable ignition is unlikely. This conclusion is consistent with results reported in Reference 15. An energy damage level of 1,100 kJ/m^2 in the dome region from Figure 3.5 corresponds to a flux level of 24 kW/m^2 in the dome region from Figure 3.4. These observations have been made assuming that incident total heat fluxes to cables would be roughly the same as those to the Barton 763 equipment model.

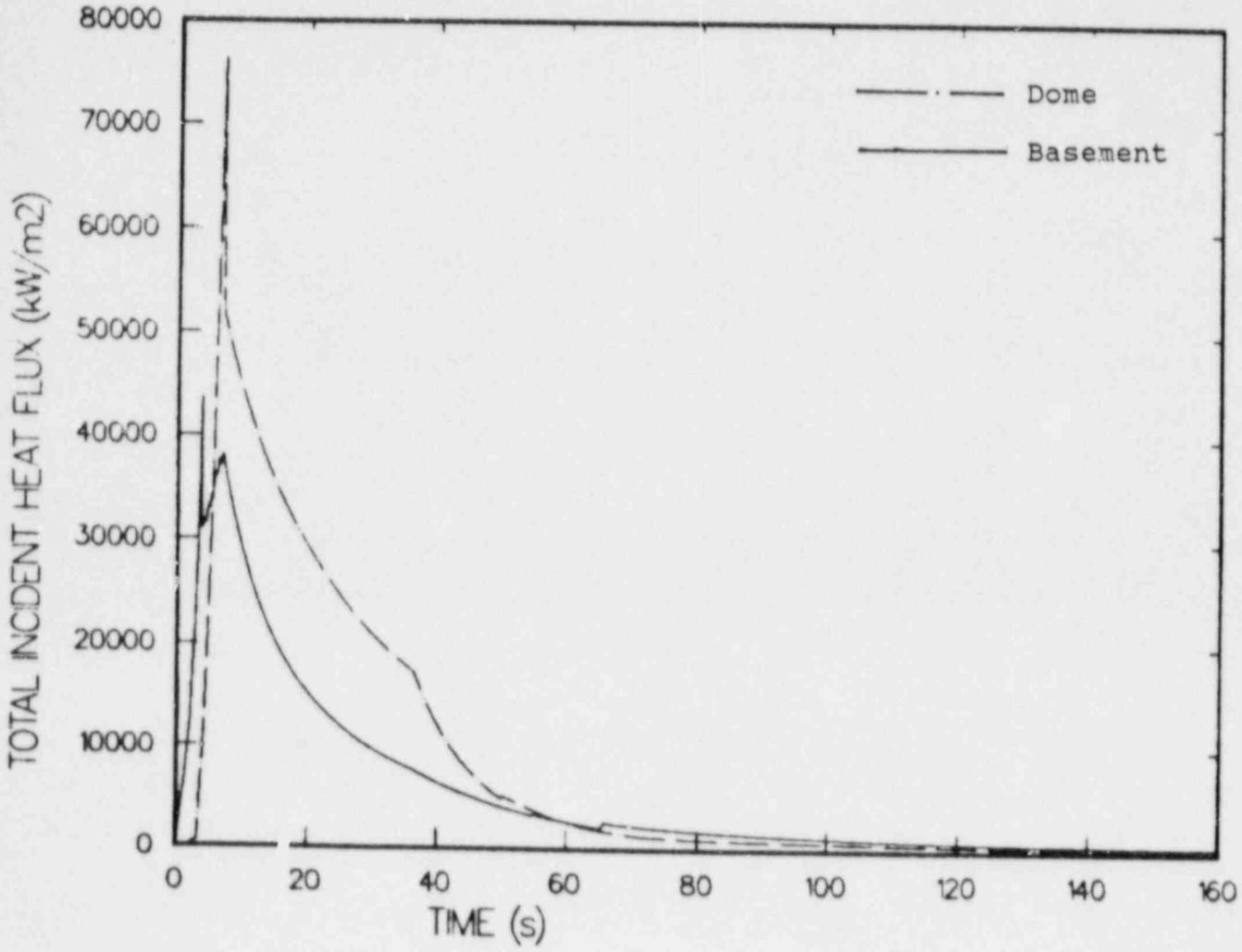

Figure 3.4. Basement-Level and Dome Region Worst-Case Total-Incident Fluxes

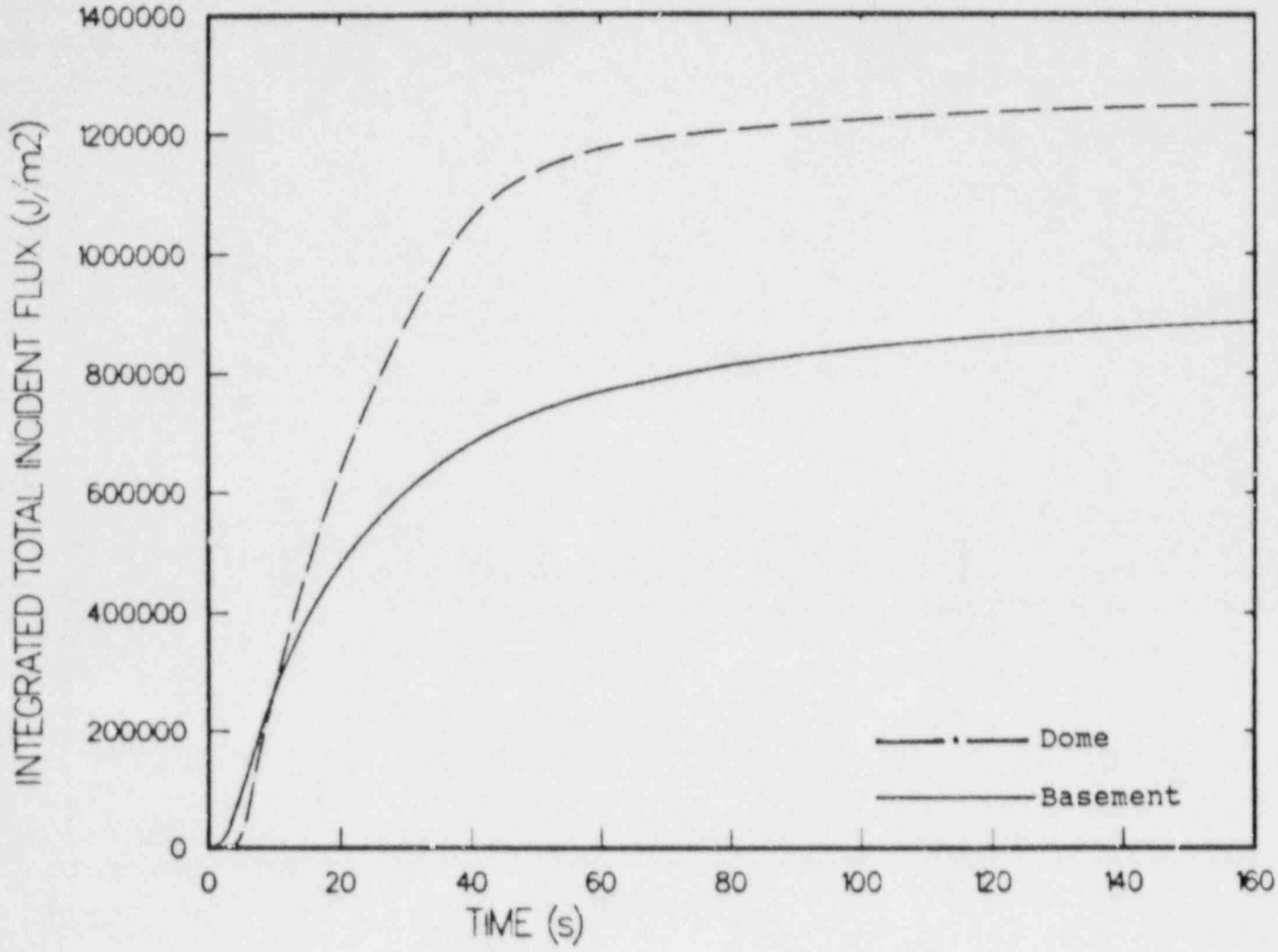

Figure 3.5. Basement-Level and Dome Region Worst-Case Time-Integrated Total-Incident Fluxes

The reader is referred to Appendix B for a more detailed description of containment gas and equipment model responses to the TMI-2 hydrogen burning.

3.1.5 TMI-2 Summary

The HECTR calculated pressures agree well with the measured TMI-2 containment pressures during and after the hydrogen burn. HECTR predicts a quicker pressure rise during hydrogen burning than was measured. HECTR overpredicts pressure by 10 percent or less in all cases during and after the hydrogen burn compared to the measured containment pressure.

HECTR predicts maximum peak gas temperatures during burning to occur in the dome region. Peak temperatures in containment below the dome region are 50 K to 180 K lower than in the dome. The dome peak gas temperatures were higher because the dome region had less heat transfer surface area to volume, allowing less heat transfer to occur out of the dome gas during and after burning.

The one-dimensional, three-layer Barton 763 models never exceeded the equipment qualification temperature of 444 K. The maximum surface temperature calculated was 340 K. The TMI-2 burn appears to pose no threat to equipment with thermal characteristics similar to those of the Barton 763.

Assuming that the Barton model incident total fluxes would be comparable to incident total fluxes to cable in containment, the HECTR analyses indicate that damage to cable in lower containment levels would be unlikely. Damage to cable in the dome region would be possible but burning of cable would be unlikely.

3.2 Hybrid Large Dry Analyses Results

3.2.1 Introduction

Analyses have been performed at Sandia National Laboratories to characterize containment temperature and pressure response and safety-equipment temperature response to hydrogen burning in a large dry containment during degraded core accidents. The hydrogen and steam released from the primary system into containment were calculated by the MARCH code for two small break LOCAs and one intermediate break LOCA. Subsequent hydrogen transport from the break location and hydrogen burning in containment were calculated using the HECTR code.

A "hybrid" large dry nuclear power plant was modeled in this analysis. The containment modeled was that of the Three Mile Island Unit 2 (TMI-2) Nuclear Power Plant. The containment has a net volume of 2,000,000 ft^3. The prima /

system modeled was that of the Zion Nuclear Power Plant. The Zion reactor has a more powerful core than the TMI-2 reactor (3,250 MWt versus 2,772 MWt). Since all large dry PWR nuclear power plants have different containment volumes, zirconium mass, and internal containment structures, the hybrid analyses were intented to be a generic study to identify potential problem zones in containment with respect to hydrogen transport (mixing) and burning.

In Reference 16, prior analyses (for containment loading) had been performed to calculate the final uniform hydrogen concentrations in various PWR containments for LOCAs with 75 percent Zircaloy oxidation. The Zion nuclear power plant was included in this study but the TMI-2 nuclear power plant was not. The final hydrogen mole fraction in the Zion containment was calculated to be .091 (9.1 percent). The 9.1 percent value is based upon dry air calculations without steam present in containment. The Zion containment has a volume of 2,600,000 ft^3, and, by taking the ratio of the Zion to TMI-2 containment volumes (1.3), a possible maximum dry air hydrogen concentration of 12 percent can occur in the TMI-2 containment using the Zion core model.

Table 3.4 lists the containment volume to zirconium mass ratio (Vol/Zr) for the hybrid model as well as fifteen other nuclear power plants. The hybrid volume to mass ratio is within 10 percent of the volume to mass ratio of nine other power plants. Thus the hybrid is representative of a typical large dry nuclear power plant.

Four power plants listed are subatmospheric large drys (North Anna and Surry) and the rest are atmospheric large drys. The ratios were calculated from information reported in Reference 16. Ranges in volume to zirconium mass occur due to differences in fuel designs; newer fuel designs tend to use more zirconium mass. The lower Surry ratio (lower in relation to Reference 16) reflects the larger zirconium mass used in the Surry March calculations (see Table C.4.1). Data for the exact amount of zirconium in a reactor core often does not exist. Therefore, calculations of zirconium mass may vary from one reference to another.

From the ratios of Table 3.4, one might expect the lowest ratio values to produce the highest global concentrations of hydrogen in containment and thus the most severe environments. However, the ratios of containment volume to zirconium mass can be somewhat misleading because the various containments have different operating pressures. Thus containment volume alone is not a true indicator of the moles of air inside containment. Table 3.5 lists the same plants with the ratio of volume of air at one atmosphere inside containment to the mass of zirconium. The corresponding global hydrogen concentration in dry containment air resulting from a 75 percent core metal-water reaction is also

Table 3.4

Containment Volume to Reactor Zirconium Mass Ratio[1] for Various Large Dry Power Plants

	Plant	Vol/Zr (ft^3/lbm)
1.	Ginna	32 - 34
2.	Palisades	35 - 42
3.	Maine Yankee	36 - 37
4.	Ft. Calhoun	37
5.	Arkansas -1, -2	43
6.	Point Beach	45
7.	Millstone-2	46
8.	Trojan	47
9.	Turkey Point	47
10.	Hybrid	50
11.	North Anna -1, -2	52
12.	Surry -1, -2	50 - 55
13.	Robinson	52 - 57
14.	Bellefonte	63
15.	Zion	64

[1]Based on Reference 16

Table 3.5

Containment Air Volume (at 1 atm) to Zirconium Mass Ratio and Resultant Hydrogen Mole Fractions Based Upon 75% Zirconium Oxidation

	Plant	Vol (1 atm)/Zir (ft^3/lbm)	MFH_2[1] x 100
1.	Surry -1, -2[2]	31 - 34	14.7 - 16.5[3]
2.	North Anna[2]	32 - 35	15.4
3.	Ginna	32 - 34	15.5 - 16.6
4.	Palisades	35 - 42	15.2 - 15.6
5.	Maine Yankee	36 - 37	14.8 - 14.9
6.	Ft. Calhoun	37	14.9 - 15.
7.	Arkansas -1, -2	43	13. - 13.1
8.	Point Beach	45	12.5
9.	Millstone-2	46	12.3
10.	Trojan	47	12.1
11.	Turkey Point	47	12.
12.	Hybrid	50	12.
13.	Robinson	52 - 57	10.1 - 11.
14.	Bellefonte	63	9.3
15.	Zion	64	9.1

[1]From Reference 16

[2]Surry and North Anna have operating pressures of 62 - 69 kPa (9 - 10 psi).

[3]The 16.5% hydrogen mole fraction for Surry reflects the zirconium mass and containment volume used in the Surry analyses of this report.

listed in Table 3.5. As can be seen from this table, the ratio of containment air volume at one atmosphere to zirconium mass is a more appropriate indicator of the maximum possible global hydrogen concentration inside containment given a 75 percent zirconium-water reaction.

The values of hydrogen mole fraction (excluding the hybrid and the highest Surry value) shown in Table 3.5 were taken from Reference 16. The 16.5 percent hydrogen mole fraction for the Surry containment reflects the zirconium mass and containment volume used in the Surry analyses of this report. Thus the Surry analyses are representative of the most severe cases (highest global hydrogen concentrations) for atmospheric and subatmospheric large drys.

Based on dry air calculations alone, containment-wide hydrogen deflagrations in atmospheric large drys would be most severe for Ginna and least severe for Zion. Parameters such as containment surface area to volume, initial conditions (caused by a LOCA) prior to burning, and operation of ESFs would also have to be investigated. However, the subatmospheric containment-wide hydrogen deflagration should bound the atmospheric large drys based on Table 3.5.

During a LOCA, large amounts of steam/water can be released into containment. Appreciable amounts of steam in the air will decrease the hydrogen concentration. The amount of steam in the containment will depend upon the heat sinking capability of containment surfaces, operation of ESFs, and the amount of steam released from the primary system.

The Surry subatmospheric spray system is activated when containment pressure exceeds 170 kPa and is maintained at 8°C. In the Surry calculations (see Section 3.3), the spray system was activated during the LOCA and was extremely effective in stripping out steam in containment. Atmospheric large dry spray systems have much higher pressure set points (290 kPa for TMI-Unit 2, for example) and are maintained at temperatures higher than 8°C. For the small break LOCAs analyzed, the hybrid spray system was not activated. Reactor building fan cooler coolant water is also not maintained close to the 8°C level of the Surry spray water and would not be expected to be as effective in stripping steam out of containment. Therefore, including the presence of steam and the effects of ESFs, it is believed that the Surry Plant would still be the most conservative case in terms of containment-wide hydrogen burning.

Two containment models were used for the hybrid analyses. The first model divided the TMI-2 containment into eight compartments: (1) The reactor cavity (RC), (2) the steam generator compartment with the pressurizer (SG1A), (3) the steam generator compartment without the pressurizer (SG1B),

(4) the refueling canal, (5) the basement level (BL), (6) the second floor, (7) the dome region, and (8) the enclosed stairwell and elevator. The compartments were selected based on actual boundaries in containment such as walls and floors. The second model divided the TMI-2 containment into eleven compartments. The basement level was divided into two compartments and SG1A was divided vertically into three equal volume compartments.

The Barton 763 models were placed in four containment locations for this analysis. The locations were (1) the basement level compartment(s), (2) the second floor, (3) the steam generator compartment(s) with the pressurizer (SG1A), and (4) the steam generator compartment without the pressurizer (SG1B). These four locations were considered to be the most likely locations for the safety-related equipment after reviewing the TMI GEND Planning Report (GEND-001). A description of the Barton 763 model is located in Section 3.1.

Two small break LOCAs with 1- and 2-inch diameter breaks (S_2D1 and S_2D2) and one intermediate break LOCA with a 4-inch diameter break (S_1D4) were studied in the hybrid analysis. Core uncovery was allowed until 75 percent of the Zircaloy had oxidized. Emergency cooling was restored to recover the core and stop oxidation at the 75 percent level. The effect of break location in containment on the accident and results was also studied by alternately placing the break in the reactor cavity, the two steam generator compartments, and the lower basement level where the reactor coolant drain tank is located. The compartment in which the break is located will be referred to as the source compartment.

Three hydrogen ignition criteria were used in this analysis. The first study ignited hydrogen at its local maximum concentration in the source compartment during the LOCA. The second study ignited hydrogen at its average (or global) maximum throughout containment at the end of the LOCA. The third study ignited hydrogen at the HECTR default ignition level of 0.07 (7 percent) hydrogen mole fraction level. The HECTR default ignition level is considered to be the most likely minimum hydrogen concentration which can be ignited during a LOCA. This third hydrogen ignition study also represents deliberate hydrogen burning at lower hydrogen levels by some type of ignition system such as glow or spark plugs. The default ignition mode forces hydrogen burning to occur in any compartment that reaches a hydrogen mole fraction of 0.07 during the LOCA; the compartment in which burning first occurred was always the source compartment in these studies.

The effect of ignition location for maximum hydrogen ignition levels at the end of the LOCA was also examined. Ignition locations included the basement, the steam generator compartment, and the dome region.

The effect of spray operation on containment temperature and pressure and the Barton 763 model thermal responses during hydrogen burning was also calculated in this analysis.

3.2.2 Results

The HECTR code was used to calculate: (1) hydrogen transport during the prehydrogen burn LOCA, (2) containment temperature and pressure response to hydrogen burning, and (3) the surface temperature response of the one-dimensional, three-layer pressure transmitter model to hydrogen burning. The hydrogen transport calculations were first performed without hydrogen burning to observe hydrogen transport throughout the containment during the accident.

3.2.2.1 Hydrogen Transport Results

Two types of maximum hydrogen concentrations were calculated in the containment for all of the LOCA studies. The first type occurred in the source compartment at the time of maximum hydrogen release from the break. The release of hydrogen into the source compartment caused the highest local hydrogen concentrations throughout containment to occur in the source compartment during the LOCA. At the same time, hydrogen concentrations in compartments outside of the source compartment were lower because the hydrogen released into the source compartment had insufficient time to be transported to the rest of the compartments in the containment.

Hydrogen concentrations in the source compartment can often result in peak hydrogen mole fractions greater than 0.14. Hydrogen mole fractions above 0.14 are assumed to indicate that hydrogen detonations may be possible. HECTR does not have the capability to analyze detonations. The code only indicates when a potentially detonable concentration of hydrogen is present in a given location. The code uses a simple set of criteria to define a detonable mixture. The HECTR conditions for a detonable mixture are a hydrogen concentration greater than 14 percent, oxygen concentration greater than 9 percent, and a steam concentration less than 30 percent. All three conditions must be satisfied simultaneously. As stated, these are very simple criteria. Whether a detonable concentration actually exists in a given location is very sensitive to compartment geometry, pressure, temperature, and other gases which may be present in the compartment atmosphere. Thus, a HECTR prediction of a detonable mixture indicates the need for detailed analysis

which considers all of these parameters. Should ignition of a detonable concentration occur, HECTR treats the resulting combustion as a deflagration.

The second type of maximum hydrogen concentration calculated occurred at the end of the LOCA hydrogen transport calculations. The hydrogen concentration at the end of the LOCA was relatively uniform throughout the containment (varying by a total mole fraction of approximately 0.01). The hydrogen concentration was relatively uniform because enough time had elapsed for all of the hydrogen to be transported throughout containment. Each compartment (except for the source compartment) also had its maximum hydrogen mole fraction at the end of the LOCA. Therefore the hydrogen concentration at the end of the LOCA will be referred to as the maximum average (or global) hydrogen concentration. However, the local hydrogen peaks in the source compartments during the LOCA were always higher than the global hydrogen concentrations throughout the containment at the end of the LOCA.

Table 3.6 lists the hydrogen transport results for the S_2D2, S_2D1, and S_1D4 scenario calculations. The source compartment, maximum global hydrogen mole fractions, the source compartment peak local hydrogen mole fraction, and the containment model used are presented for each case. The global maximum hydrogen mole fractions are presented as ranges of maxima to demonstrate the range in the final mole fractions of hydrogen for the compartments in the TMI-2 containment models. The source compartments studied in these cases were SG1A, the basement level (BL), and the reactor cavity (RC). Analyses in which the source compartment was SG1B will not be presented because the results were essentially the same as the SG1A source compartment results. The maximum global hydrogen mole fractions which occurred at the end of the LOCA showed no appreciable sensitivity to the break locations. HECTR calculated a hydrogen mole fraction variance throughout containment of approximately 0.01. The almost uniform hydrogen concentrations were caused by turbulence generating mechanisms that occurred during the LOCA such as fan cooler operation, the hydrogen and steam sources from the break, and the hot nuclear steam system surfaces.

The maximum local hydrogen mole fractions for the source compartments were functions of source compartment volume and ventilation to neighboring compartments. In general, smaller source compartments had higher peak hydrogen mole fractions. The reactor cavity was the smallest source compartment and had the highest hydrogen concentrations. Source compartments with large flow path areas and ventilation from the fan coolers had lower peak hydrogen concentrations. SG1A was the best ventilated source compartment resulting in the lowest peak hydrogen mole fractions.

Table 3.6

Hybrid LOCA Hydrogen Transport Results

Case	Scenario	SC	GHM	SCHM	CM
1A	S_2D2	SG1A	0.11 - 0.12	0.12	1
1B		RC	0.11 - 0.12	0.37	1
1C		BL	0.11 - 0.12	0.16	1
2A	S_2D1	SG1A	0.10 - 0.11	0.11	1
2B		RC	0.10 - 0.11	0.27	1
2C		BL	0.10 - 0.11	0.16	1
3A	S_1D4	SG1A	0.11 - 0.12	0.13	1
3B		RC	0.11 - 0.12	0.61	1
3C		BL	0.11 - 0.12	0.16	1
3D		BL	0.10 - 0.12	0.21	2
3E		SG1A	0.11 - 0.12	0.13	2

SC: Source compartment
GHM: Maximum global hydrogen concentration
SCHM: Source compartment peak hydrogen concentration
CM: Containment model: 1 = containment divided into eight compartments, 2 containment divided into 11 compartments

Hydrogen was released at a greater rate in the S_1D4 scenario than in the S_2D2 and S_2D1 scenarios. The S_2D1 had the lowest hydrogen release rate. The high S_1D4 hydrogen release rate resulted in the highest peak hydrogen mole fraction in the small, relatively enclosed reactor cavity.

Detonable messages were received from HECTR during the LOCA for the basement level and reactor cavity source compartments in all of the cases listed. HECTR indicated that detonable mixtures occurred for brief periods of time during maximum hydrogen injection into the source compartments.

3.2.2.2 Hydrogen Deflagration Results

Table 3.7 lists the temperature and pressure calculations performed for the three LOCA scenarios with hydrogen burns. Included in Table 3.7 are the scenario, the source compartment (SC), the ignition criteria (IC), the compartment in which hydrogen burning was initiated (IBC), spray operation, the number of hydrogen burns per compartment (BPC), the peak

Table 3.7

Hybrid Hydrogen Burn Analyses

Case	Scenario	SC	IC	IBC	Spray	BPC	TGM (°K)	PGM (kPa)	TEM (°K)	TDM (°K)
4A	S2D2	SG1A	G	BL	0	1	1210-1290	480	400	1340
4B		SG1A	G	BL	1	1	1210-1290	480	400	1340
4C		SG1A	G	SF	0	1	1330-1340	500	400	1400
4D		SG1A	G	DL	0	1	1300-1350	510	400	1420
4E		SG1A	G	SG1A	0	1	1290-1350	500	400	1390
4F		SG1A	D	SG1A	1	1-2	740- 830	300	420	--
4G		RC	G	BL	1	1	1220-1330	480	400	1370
4H		BL	G	DL	1	1	1250-1350	500	390	1430
4I		BL	D	BL	1	0-11	430- 820	200	440	--
4J		BL	L	BL	1	1	1180-1370	430	380	--
5A	S2D1	SG1A	G	BL	1	1	1100-1160	420	400	1200
5B		SG1A	D	SG1A	1	0-2	450- 840	250	400	--
5C		RC	L	RC	1	0-1	400- 920	210	400	1560
5D		RC	G	DL	1	1	1170-1220	440	400	1300
5E		BL	L	BL	1	0-1	550-1340	230	400	--
5F		BL	G	DL	1	1	1000-1190	410	400	1260
6A	S1D4	SG1A	G	BL	1	1	1210-1310	480	400	1360
6B		BL	D	BL	0	0-12	390- 920	220	540	--
6C		BL	L	BL	1	1	1150-1460	410	420	--
6D		BL	G	DL	0	1	1250-1350	490	420	1430
6E		BL	D	BL	1	0-20	380-1160	220	670	--

SC: source compartment
IC: ignition criteria
IBC: compartment in which hydrogen burn was initiated
BPC: number of hydrogen burns per compartment
TGM: peak gas temperatures
PGM: peak gas pressure
TEM: peak equipment surface temperature
G: global ignition
L: source compartment ignition
D: default ignition

containment gas temperatures and pressures (TGM and PGM, respectively) during the burn, and the peak equipment surface temperature (TEM). The TGM variable is presented as a range of maximum temperatures to demonstrate how the peak gas temperatures in the compartments with the Barton 763 model varied during hydrogen burning in the TMI-2 containment model. The ignition criteria are given as G (global ignition), L (source compartment ignition), and D (default ignition). Spray operation is indicated by 0 for off and 1 for on. The variable TDM is included to show the peak compartment gas temperature calculated for each case when the peak did not occur in a compartment with the Barton 763 equipment model. For global ignition, peak gas temperatures usually were calculated in the dome. Peak gas temperatures were calculated in the source compartments for the local and default ignition cases.

3.2.2.2.1 Global Ignition

Global ignition was initiated at the end of the LOCA with hydrogen mole fractions ranging from 0.10 to 0.12 for the S_2D2, S_2D1, and S_1D4 scenarios. The global ignition burns were characterized by high containment pressures and temperatures throughout the containment building. One hydrogen burn was calculated per compartment as the hydrogen burn propagated throughout the containment. The TGM column from Table 3.7 presents a range of peak gas temperatures which occurred throughout containment during the hydrogen burn. The highest temperatures generally occurred in the dome region during the burn. Higher temperatures were calculated in the dome region because the ratio of heat transfer surface area to volume of burning gas was the smallest in the dome region compared to any other compartment. The smaller heat transfer surface area allowed less energy to be lost by the gas.

For all three scenarios, peak gas temperatures (TGM) ranged from 1000 K to 1350 K and peak gas pressures ranged from 410 kPa to 510 kPa. The peak containment pressures remained above the equipment qualification pressure of 483 kPa for less than 5 seconds.

The spray system was activated during hydrogen burning for all three scenarios, but spray water did not leave the spray headers until after the peak gas temperatures and pressures had been calculated because of the 30-second delay time after pressure activation of the spray system. Therefore, spray operation did not affect the peak gas temperatures and pressures due to hydrogen burning but did cool the containment gas more rapidly than for the cases in which the spray system was shut off. Equipment surface temperatures also decreased at a greater rate during spray operation when compared to no spray operation.

The one-dimensional three-layer model surface temperatures never exceeded the 444 K equipment qualification temperature in any of the cases studied.

3.2.2.2.2 Source Compartment Ignition

Table 3.6 lists the initial hydrogen mole fractions used for the source compartment ignition cases. The source compartment chosen for the S_2D2 scenario was the basement level and had a maximum hydrogen mole fraction of 0.16. The hydrogen mole fractions outside of the source compartment at the time of ignition were lower, ranging from 0.08 to 0.14. The basement level and reactor cavity were selected as source compartments for the S_2D1 scenario and had hydrogen mole fractions of 0.15 and 0.27, respectively, at the time of ignition. Hydrogen mole fractions outside the source compartment ranged from 0.05 to 0.07. The S_1D4 scenario used the basement level as its source compartment and had a peak hydrogen mole fraction of 0.16 at the time of ignition. Although the hydrogen mole fraction was flagged by HECTR to be in the detonable regime, the hydrogen ignition was treated as a deflagration. The hydrogen mole fractions in the rest of the containment compartments at ignition ranged from 0.08 to 0.14.

The S_2D2 and S_1D4 scenarios with source compartment ignition resulted in one burn per compartment with peak gas temperatures occurring in the source compartments (1370 K and 1460 K, respectively). Peak gas temperatures were lower outside the source compartment, ranging from 1180 K to 1270 K for the S_2D2 scenario and 1150 K to 1160 K for the S_1D4 scenario. Gas pressures for the S_2D2 and S_1D4 scenarios ranged from 410 kPa to 430 kPa and did not exceed the equipment qualification pressure of 483 kPa.

The S_2D1 scenario with source compartment ignition resulted in one hydrogen burn occurring in some compartments and none occurring in others. This nonuniform hydrogen burning occurred because of the low hydrogen mole fractions in containment outside of the source compartment at ignition time. These low hydrogen mole fractions were below the HECTR flammability limits in some compartments. Therefore, these burns resulted in high peak gas temperatures in the source compartments (1340 K and 1550 K) and low peak gas temperatures elsewhere in containment (400 K to 920 K). Gas pressures were low (210 kPa and 230 kPa) and did not activate the reactor building spray system.

The peak equipment model surface temperatures did not exceed the 444 K equipment qualification temperature.

3.2.2.2.3 Default Ignition

The default ignition cases calculated multiple hydrogen burning to occur in the source compartments during hydrogen release. The source compartments had from 2 to 20 burns during the LOCA. Multiple burns occurred frequently in the small source compartments since 7 percent hydrogen concentrations were achieved rapidly between burns. Multiple burns in large source compartments occurred less frequently because more time was required for the hydrogen concentration to reach 7 percent after a burn had occurred. The multiple burns caused moderate to high peak gas temperatures to be calculated in the source compartments, ranging from 820 K to 1470 K. The multiple burns consumed large fractions of the hydrogen entering the source compartments allowing less hydrogen to be transported to the rest of the containment. For some cases, multiple burns were also calculated in compartments directly adjacent to the source compartments. For compartments not directly in contact with the source compartment, some had no hydrogen burning or had a single hydrogen burn at low hydrogen concentrations resulting in low peak gas temperatures for those compartments.

The peak gas pressures were calculated to be low because hydrogen burning occurred at low hydrogen mole fractions throughout containment. Peak gas pressures ranged from 200 kPa to 300 kPa. The reactor building spray system was not activated for the default ignition cases.

For the eight compartment containment model, the 444 K equipment qualification temperature was exceeded in one default ignition case (Case 6B). The source compartment was located in the basement and had 12 hydrogen burns. The one-dimensional three-layer model surface temperature was calculated to exceed 444 K for 31 minutes. The peak surface temperature was calculated to be 540 K.

Case 6E used the second containment model with 11 compartments. The multiple burns which were calculated in the source compartment were severe enough to cause the calculated one-dimensional three-layer model surface temperature to exceed 444 K for roughly 51 minutes. The peak surface temperature calculated was 670 K.

3.2.3 Hybrid Large Dry Summary

Containment and safety-related equipment thermal responses were calculated for hydrogen burning in a hybrid large dry containment. Hydrogen was ignited at (1) the average maximum hydrogen concentration throughout containment at the end of the LOCA, (2) at local maximum hydrogen concentrations in the source compartment, and (3) at a hydrogen concentration of 7 percent to simulate igniter burn initiation. The first two ignition cases generally resulted in

one hydrogen burn per compartment, and the third resulted in multiple hydrogen burns in compartments.

The peak qualification pressure of 483 kPa was exceeded in five average maximum burn cases. However, the time above 483 kPa was less than five seconds for the five cases considered.

The one-dimensional, three-layer thermal model of the Barton 763 pressure transmitter was found to be slightly conservative but was determined to be a realistic representation to study equipment surface temperature response to hydrogen burning. The three-layer model exceeded the 444 K qualification temperature in two cases analyzed (6B and 6E). The peak surface temperature calculated was 670 K and remained above the 444 K qualification temperature for 51 minutes. This worst case occurred for an S_1D4 default ignition case with multiple hydrogen burning.

The use of the Zion core in the TMI-2 containment was intended to be a generic study for large dry PWR containments since these PWRs differ with respect to (1) the ratio of containment volume and primary system zirconium mass and (2) the internal structures (rooms or compartments) arrangement inside containment. Table 3.4 illustrated the hybrid model to be within 10 percent of containment volume to zirconium mass ratio for nine of the fourteen power plants listed. Therefore, it is felt that the hybrid analyses can be used to identify potential problems with respect to the release and burning of hydrogen in large dry containments or conclude that no problems exist.

Single hydrogen burns due to global and source compartment ignition and resulting equipment thermal response appear to represent no threat to the hybrid type PWR containment. Peak equipment temperatures were well below the 444 K qualification temperature. From Table 3.5, equipment and containment gas temperatures and pressures could be expected to be lower than the hybrid results for containments 13 to 15 and equivalent to the hybrid results for containments 7 to 12. Containments 3 to 6 should be bounded by the Surry analyses.

The default ignition (multiple burn) analyses resulted in equipment temperatures exceeding 444 K for two cases. The excessive temperatures occurred in small and poorly ventilated source compartments. Large or well ventilated source compartments did not calculate equipment temperatures above 444 K. Since the hybrid studies are generic, these results indicate that further studies might be performed for default ignition cases for large dry PWR containments which could have small and/or poorly vented zones into which hydrogen would be released and ignited at 7 percent.

No assessment was made for equipment damage with respect to detonations. High values of local hydrogen concentration were observed for releases to the reactor cavity and basement level. Again, small source compartments in any large dry PWR could be expected to produce detonable concentrations.

3.3 Surry Subatmospheric Analyses

3.3.1 Summary of Accident Conditions

The Surry analyses used a 15-compartment model of the subatmospheric containment building. The S_2D and S_1D accident sequences were the basis of the studies. These sequences are, respectively, small- and intermediate-size LOCAs with loss of emergency core cooling. The scenarios assumed the reactor core to be uncovered long enough to allow 75 percent of the Zircaloy to react with steam to release hydrogen, at which time core cooling was restored. The break location was varied among all containment compartments which housed portions of the primary coolant system.

Two ignition criteria were studied. The first assumed ignition to occur in the basement at the completion of the 75 percent metal-water reaction. This resulted in a single burn in most containment compartments.

The second ignition criterion simulated deliberate ignition by an ignition system. In these cases ignition occurred at any time the hydrogen concentration reached 7 mole fraction percent in any location. This ignition will be referred to as default ignition.

3.3.2 Results

The HECTR calculations determined the gas temperatures and pressures inside containment and the temperature response, due to hydrogen combustion, of safety equipment modeled in the various containment locations. Because it gave the best fit to experimental data of the four transmitter thermal models, the three-layer model results provide a best estimate of the thermal response of typical safety equipment to hydrogen burns and it is these results which are discussed here. Since the "generic" environmental qualification profile of IEEE323-74[17] has a maximum temperature of 444 K (340 F) which is held for several hours, calculated peak equipment temperatures from these analyses which were at or below this value were considered to be nonthreatening. Peak equipment temperatures above this value were considered potentially threatening to equipment functionality. In these cases the peak temperature and the time the equipment spent above 444 K were noted.

3.3.2.1 Containment Temperature-Pressure Environments

None of the cases studied resulted in a maximum compartment pressure approaching the 483 kPa equipment qualification value. The highest gas temperatures and pressures in any compartment occurred in the single-burn cases. In the S_2D cases the peak gas temperatures were around 1400 K to 1500 K and peak pressures were in the 400 kPa range. For the S_1D events the peak gas temperatures were around 1550 K and peak pressures were around 410 kPa.

3.3.2.2 Detonable Mixtures in Containment

HECTR predicted potentially detonable hydrogen mixtures throughout the containment for S_2D and S_1D cases at the completion of the 75 percent metal-water reaction. These mixtures resulted from the efficient removal of steam from the containment atmosphere by the cold (45°F) sprays. As a result of the steam removal, the hydrogen concentrations rose and HECTR indicated potentially detonable mixtures of hydrogen throughout the containment building. In some cases HECTR indicated detonable concentrations at several different times in the same compartment. These concentrations lasted on the order of minutes before being dispersed.

3.3.2.3 Equipment Model Temperature Response Results

As noted earlier, the three-layer transmitter model is the model which is most representative of an actual piece of safety-related equipment in widespread use in nuclear power plant containments. Thus, the three-layer model of the Barton 763 pressure transmitter served as a surrogate for safety-related equipment in these analyses and results from this model form the basis of the following discussion. Results from the other three models may be useful if their thermal characteristics can be related to those of other known pieces of equipment. For this reason they are included in the results tables of Section C.5.0, Appendix C.

The following discussion of results is divided into sections based on break size and ignition criterion. The S_2D (small break) cases are discussed first, followed by the S_1D (intermediate-size break) cases.

3.3.2.3.1 S_2D Sprays-On Single Burn

These cases had a single burn at the completion of the 75 percent metal-water reaction. There was one case in this scenario for which the three-layer model exceeded 444 K. The equipment model was located in the steam generator A cubicle (which also happened to be the source compartment). The model surface temperature exceeded 444 K for 3 minutes and had a peak temperature of 447 K.

Steam removal by the sprays produced detonable concentrations throughout containment.

3.3.2.3.2 S_2D Sprays-On Default Ignition

One case was run using the largest steam generator cubicle as a source compartment. Thirty-eight multiple burns were calculated to occur in the source compartment which drove the three-layer transmitter model surface temperature above 444 K for 90 minutes. Its peak temperature was 507 K. The three-layer equipment model temperature response is given in Figure 3.6.

A run for a small source compartment was also performed. The source compartment chosen was the pressurizer relief tank cubicle. This case proved to be a demonstration of the strong effect of the combination of the sprays and igniters. All analyses were run on a Cray XMP super computer. For the large source compartment case there were 38 burns in the source compartment and the case required 17.73 minutes of Cray computing time to complete. So many burns occurred in the small source compartment case that the analysis exceeded the allotted 30-minute run time and results could not be obtained. It is therefore expected that the three-layer equipment model in the small pressure relief tank source compartment with the sprays on would reach a higher temperature than it would in the larger source compartment and hence would probably exceed the 507 K calculated for the same model in the largest steam generator cubicle when that cubicle was the source compartment.

3.3.2.3.3 S_1D (Intermediate Break LOCA) Case Selection

Hydrogen transport studies for the S_1D cases were conducted prior to the equipment temperature response analysis. These studies indicated that, regardless of the source compartment, there was an even distribution of hydrogen throughout the containment building at the end of the 75 percent metal-water reaction. Thus, regardless of the source compartment, the results would have been similar for all S_1D single-burn cases with the same spray condition. A review of the S_2D single-burn analyses also indicated that source compartment location was not important at the end of the 75 percent metal-water reaction (in terms of hydrogen concentrations) in those cases. Also, for the igniter cases (which assumed 7 percent hydrogen mole fraction ignition) the combustion and high equipment temperatures are generally confined to the source compartment. The number of burns is determined by the size of that compartment.

Generally, two cases were run: one with a large source compartment, the other with a small one. The large source

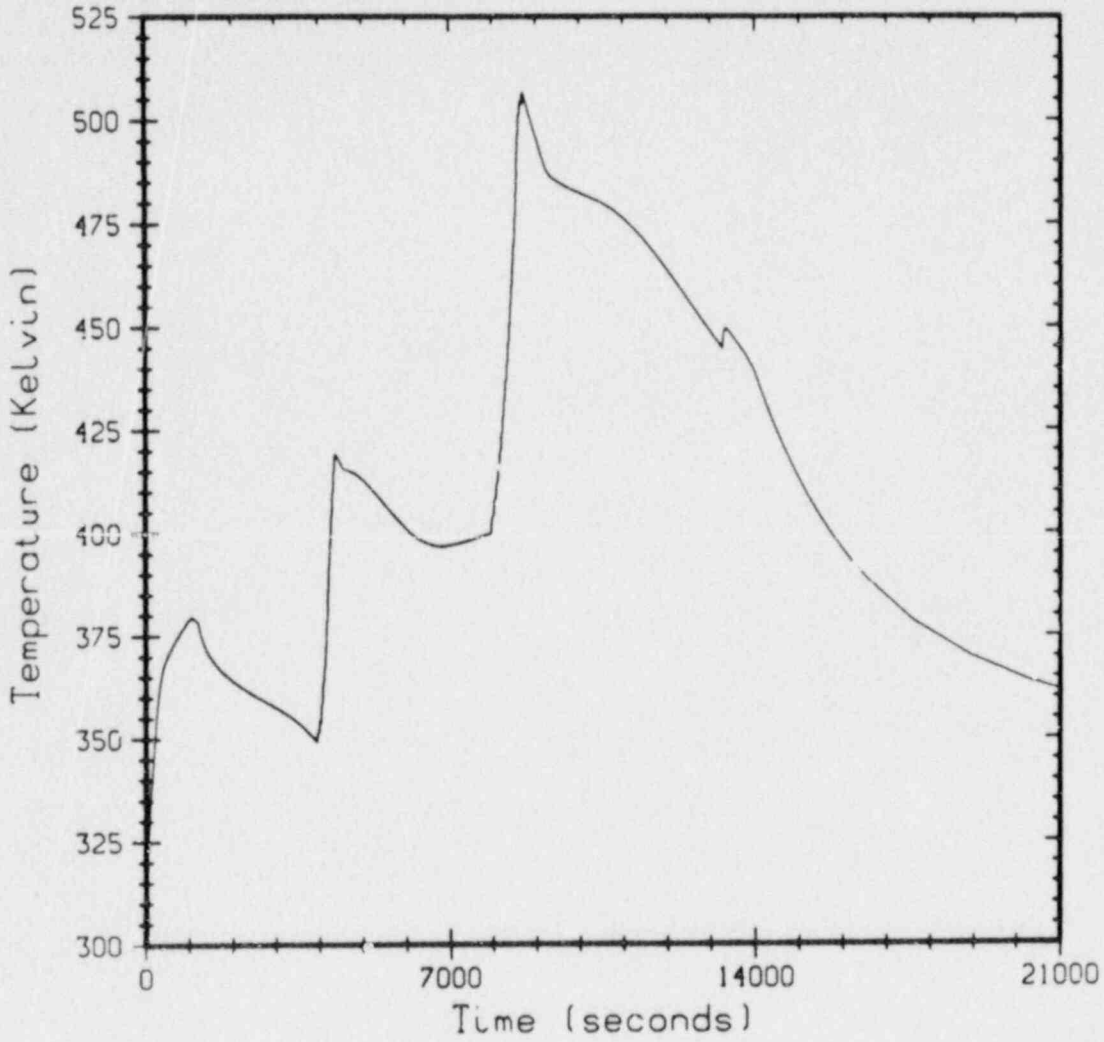

Figure 3.6. Steam Generator Cubicle (Source Compartment) Three-Layer Equipment Model Temperature (S_2D, Spray, w/Igniters)

compartment chosen for these studies was a steam generator cubicle. The small source compartment was the pressurizer cubicle.

3.3.2.3.4 S_1D Sprays-On Single Burn

These cases had a single burn at the completion of the 75 percent metal-water reaction. In addition to the steam generator cubicle and pressurizer cubicle source compartment cases a third case was run using the pressurizer relief tank cubicle as a source compartment. The three-layer equipment model exceeded 444 K for one case in which the model was located in a source compartment. The energy from the hot steam and hydrogen coming out of the break combined with a single hydrogen burn caused the model to exceed 444 K for 10 minutes. The peak temperature calculated was 450 K.

As with the S_2D sprays-on single-burn scenario, HECTR predicted potentially detonable hydrogen mixtures due to steam removal by the sprays. These mixtures occurred more than once in several compartments throughout containment.

3.3.2.3.5 S_1D Sprays-On Default Ignition

One case of this type was run using a steam generator cubicle as a source compartment. There were 59 burns in the source compartment which caused the three-layer equipment model to reach a peak temperature of 670 K. This model remained above 444 K for 50 minutes. The three-layer temperature plot for this case is given in Figure 3.7.

A small source compartment case was not run for this scenario. Given the results of the S_2D sprays-on igniter case which exceeded the allotted computer run time, the large number of burns which occurred in the S_1D no-spray igniter case with the small source compartment, and the inverse relationship between the source compartment volume and the number of burns there for igniter cases, it was determined that nearly 120 burns would occur in a small source compartment for a sprays-on igniter case. Thus the temperature of the three-layer equipment model would probably have exceeded 670 K for this case. This large number of burns would require an inordinate amount of computer time.

3.3.3 Subatmospheric Analyses Summary

By comparison with experimental results, a three-layer model of the Barton 763 pressure transmitter was developed and found to give a mildly conservative yet realistic representation of a device for studying equipment temperature response to hydrogen burns using the HECTR computer code. Equipment temperatures were calculated for S_1D and S_2D scenarios with a 75 percent core metal-water reaction and single and multiple hydrogen burns.

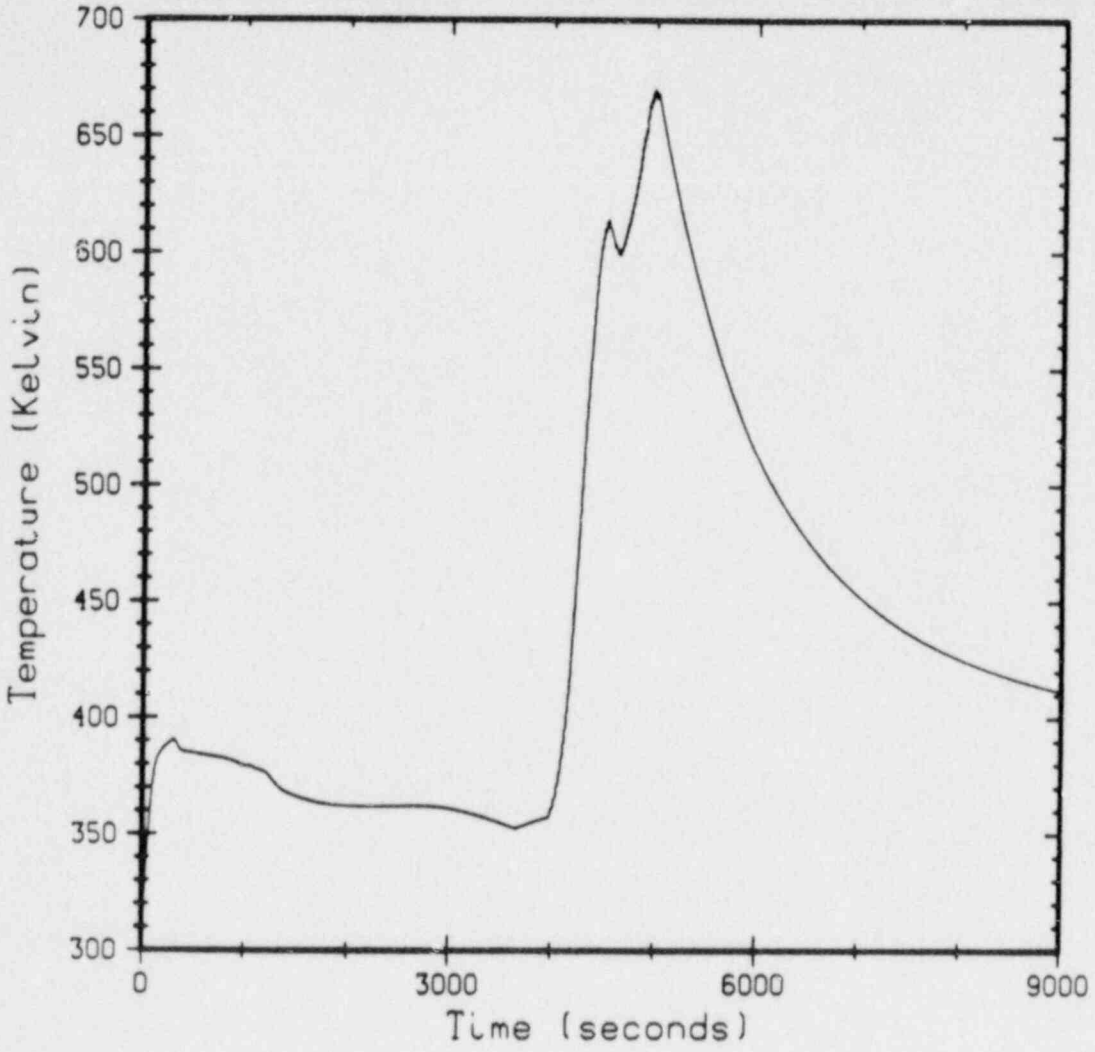

Figure 3.7. Steam Generator Cubicle (Source Compartment) Three-Layer Equipment Model Temperature (S_1D, Sprays-On, w/Igniters)

There were two instances in the S_2D cases in which the three-layer model exceeded the typical equipment qualification temperature of 444 K. One instance occurred for a single burn case. In the single burn case, the three-layer model peak surface temperature (447 K) slightly exceeded the equipment qualification temperature for 3 minutes. The second instance was for a case in which ignition occurred anytime the hydrogen concentration reached 7 mole fraction-percent at any containment location. This ignition criterion corresponds to having igniters in the containment building. The equipment model surface temperature remained above 444 K for 90 minutes and reached a peak temperature of 507 K. The high temperature occurred in a source compartment for both cases.

For the S_1D cases the three-layer equipment model had calculated temperatures which exceeded 444 K twice. One single burn case had a peak model temperature of 450 K and was above 444 K for 10 minutes. The model surface temperature also exceeded 444 K for a seven percent hydrogen ignition case. The peak surface temperature was 670 K and remained above 444 K for 50 minutes. Again, the high temperatures were calculated to occur in source compartments.

In cases which considered deliberate ignition by igniters the majority of the burns and thus high equipment temperatures were generally confined to the source compartments. Smaller source compartments would have resulted in more multiple burns, and therefore even higher equipment temperatures.

The effect of the sprays in these analyses was significant. The spray water is maintained at 45°F prior to spray activation and this low temperature resulted in efficient steam removal from the containment atmosphere. In cases where ignition was delayed until the completion of the 75 percent metal-water reaction, HECTR predicted potentially detonable mixtures throughout containment prior to the completion of the reaction.

The Surry containment is considered to be one of the most conservative plants for both atmospheric and subatmospheric nuclear power plants (see Table 3.5). Because of the effect of spray operation, single deflagrations inside Surry presented a more challenging thermal stress to the Barton than did the TMI hybrid analyses. Multiple burns can be equally severe to equipment for both subatmospheric and atmospheric large drys.

These analyses were carried out for a piece of equipment that is considered to be representative of safety equipment in terms of thermal characteristics. As such these studies considered the three-layer model of the Barton 763

transmitter to be a surrogate for all safety equipment in containment. It is recognized that the sensitivity of different devices to thermal stresses can vary widely depending on the construction and function of the equipment. Therefore, in order to assess the threat to a specific piece of equipment in a containment with a deliberate ignition system (especially in potential hydrogen source compartments) particular attention should be given to the location of the device in containment, its function, thermal characteristics, material properties, and its susceptibility to thermal stress. Based on these considerations, a determination regarding the necessity for the demonstration of equipment survival margins can then be made.

3.4 SCETCh Tests

The SCETCh tests exposed aged and unaged specimens of nuclear qualified cable and pressure transmitters to LOCA and hydrogen burn environments. Single burn and multiple burn simulations were conducted. The tests included simulation of the HECTR predicted heat fluxes, pressures, moisture conditions, and oxygen concentrations during a LOCA and hydrogen burn.

3.4.1 SCETCh Description

The SCETCh facility was designed to simulate severe environments having combined thermal, pressure, and chemical components. The chamber is cylindrical (15.25 inches in diameter by 27 inches long) and is made of Inconel 625.

Heat for the LOCA portion of the tests was provided by 45 quartz lamps (2.5 kW each). The hydrogen deflagration heat fluxes were reproduced using electrically heated stainless steel foils one mil thick. Photographs of the chamber and foils are given in Appendix D.

An external pressure source (air) was used to establish the necessary pre-deflagration oxygen and pressure conditions.

3.4.2 Translation of Environments

Once a representative HECTR generated hydrogen deflagration scenario had been selected, an analysis was performed to determine what would be required to create such an environment in the SCETCh. A computer program (FOILTEMP) was written which combined the appropriate analytical models and was used to predict the required foil temperatures, foil powers, and initial (pre-pulse) conditions necessary to reproduce the HECTR predicted deflagration environment. Details of the analysis can be found in Appendix D. These results were then assimilated into the foil design, control setup, and test plan.

The first point of concern was to match the heat flux absorbed by the equipment during the simulated hydrogen burn. This involved calculation of appropriate thermal radiation viewfactors and consideration of wavelength dependency of the thermal radiation in the HECTR calculations and in the SCETCh. The HECTR predicted radiative plus convective flux was duplicated in the SCETCh using electrically heated foils to provide a mostly radiative flux.

It was also deemed important to match the peak steam and total pressures generated by HECTR, as moisture intrusion through cracks in the cable jacket or through transmitter seals could conceivably lead to electrical failure. This was accomplished by starting the pulse from a LOCA condition of saturated steam at 358°K, and a total pressure (initially) of about 241 kPa (accomplished by injection of an additional 83 to 115 kPa of air immediately before the pulse). This additional air necessitated venting of the SCETCh after the pulse to return to the HECTR LOCA pressure.

Besides matching HECTR predicted peak steam and total pressures inside the SCETCh, this combination of initial SCETCh steam and total pressures results in a SCETCh pre-pulse oxygen concentration of 15 to 16 percent. This is the same initial (pre-deflagration) oxygen concentration predicted in the HECTR results.

The necessary SCETCh foil power versus time profile was calculated using FOILTEMP. The heat flux to equipment produced by this foil power profile in the steam environment could not be directly measured because of erratic behavior of the heat flux gauges due to condensation. Instead the heat flux to equipment versus time curve in the steam environment was inferred from the foil power profile based on calibration of the heat flux gauges versus foil power in dry environments inside and outside the SCETCh. The heat flux versus foil power curve in the steam environment was obtained by modifying the dry environment curves to account for steam absorption. The necessary modification for steam absorption was first estimated analytically and then fine tuned using the experimentally observed pressure response (pressure response is an indirect measurement of gas energy absorption). Using this procedure the heat flux to equipment versus time in the steam environment could be inferred from the measured foil power versus time.

3.4.3 SCETCh Single Burn Tests

Both single and multiple burn tests were conducted in the SCETCh. The following two sections summarize the single burn test results. The multiple burn test results are summarized in Section 3.4.4. Details of the tests can be found in Appendix D. The results indicate that nuclear

qualified class 1E cable can survive a single hydrogen burn resulting from a 75 percent metal-water reaction in a large dry containment.

For the single burn tests, the accident environment simulated was for an S_2D event in the TMI-hybrid power plant which resulted in a 75 percent core metal-water reaction. The particular S_2D event simulated was representative of the most severe environments calculated in the HECTR TMI-hybrid analyses. The hydrogen burn was assumed to occur at the completion of the 75 percent metal-water reaction.

3.4.3.1 Cable Tests

Several specimens of new and artifically aged Brand Rex XLP/CU three-conductor power and control cable were tested in a simulated LOCA/hydrogen burn environment. The cable conductors were connected to a three-phase power supply which established a potential of 480 volts from cable to cable and 277 volts between each cable and the cable mount. This arrangement facilitated the identification, during testing, of specific conductors which might have shorted to each other or to the cable mount.

The LOCA portion of the experiments was conducted after thermal equilibrium had been reached. The SCETCh LOCA environment maintained a temperature of 358 K, a total pressure of 150 kPa, and a steam partial pressure of about 50 kPa (saturation).

Approximately 4.4 hours into the LOCA, the hydrogen burn was assumed to occur (based on the HECTR calculations). At this time, the stainless steel foils were energized to provide the heat flux pulse which would simulate the hydrogen deflagration. Following the hydrogen burn simulation, the LOCA was continued for another 2 hours.

Two tests (one each of an aged and unaged specimen) were conducted at the optimum foil power (i.e., at 100 percent of the foil power necessary to simulate the HECTR-defined hydrogen burn heat flux). These are referred to as the 100 percent tests in Table 3.8. The 110 percent tests used foil powers which resulted in heat fluxes 10 percent higher than the HECTR calculated heat fluxes. These tests were conducted near the limit of foil power.

During two "110 percent" tests conducted with aged cable samples, one or more of the stainless steel foils broke down during the heat flux pulse resulting in test termination prior to the planned end of the test. The foil breakdowns occurred after the peak power had been reached but prior to the completion of the pulse. In both cases the foils were

Table 3.8

Cable SCETCh Test Matrix

Pulse (%)	Number of Samples Aged	Unaged
100	1	1
110	-	3
110+	2	-

replaced and the specimens were subjected to another LOCA simulation and 110 percent pulse; hence, the "110+ percent" test category in Table 3.8.

Results of the 100 percent tests are discussed here. The results of the 110 and 110+ tests were similar and are presented in Appendix D.

A linear ramp up to the peak heat flux was used in all of the cable tests. This was necessary due to the response time of the foil control algorithm. The actual test heat flux profile for the 100 percent unaged cable test is shown in Figure 3.8 along with the HECTR generated profile. The linear ramp up to the peak results in approximately 30 percent more energy incident on the cable specimens (the difference in areas under the curves in Figure 3.8).

Both the aged and unaged 100 percent cables maintained their applied cable-to-cable and cable-to-ground voltages during testing. Conduction voltages for the unaged 100 percent cable are shown in Figure 3.9. (A short to ground which occurred during the aged cable test was traced to the splice connecting the cable to the three-phase power supply. The splice was not a nuclear qualified item and was not a test specimen.)

Physical damage in both the aged and unaged cable tests was primarily confined to the cable jacket. The post-test condition of an unaged and aged cable are shown in Figures 3.10 and 3.11, respectively.

The jacket of the unaged cable showed extensive blistering and charring. There was extensive small surface cracking but no large penetrations to the cable interior.

Damage to the aged cable jacket was different. There was no blistering and the amount of charring was minimal. The most significant damage to the aged cable was the axial cracking of the jacket which penetrated to the interior of the cable. The cracks were wide enough to expose the white

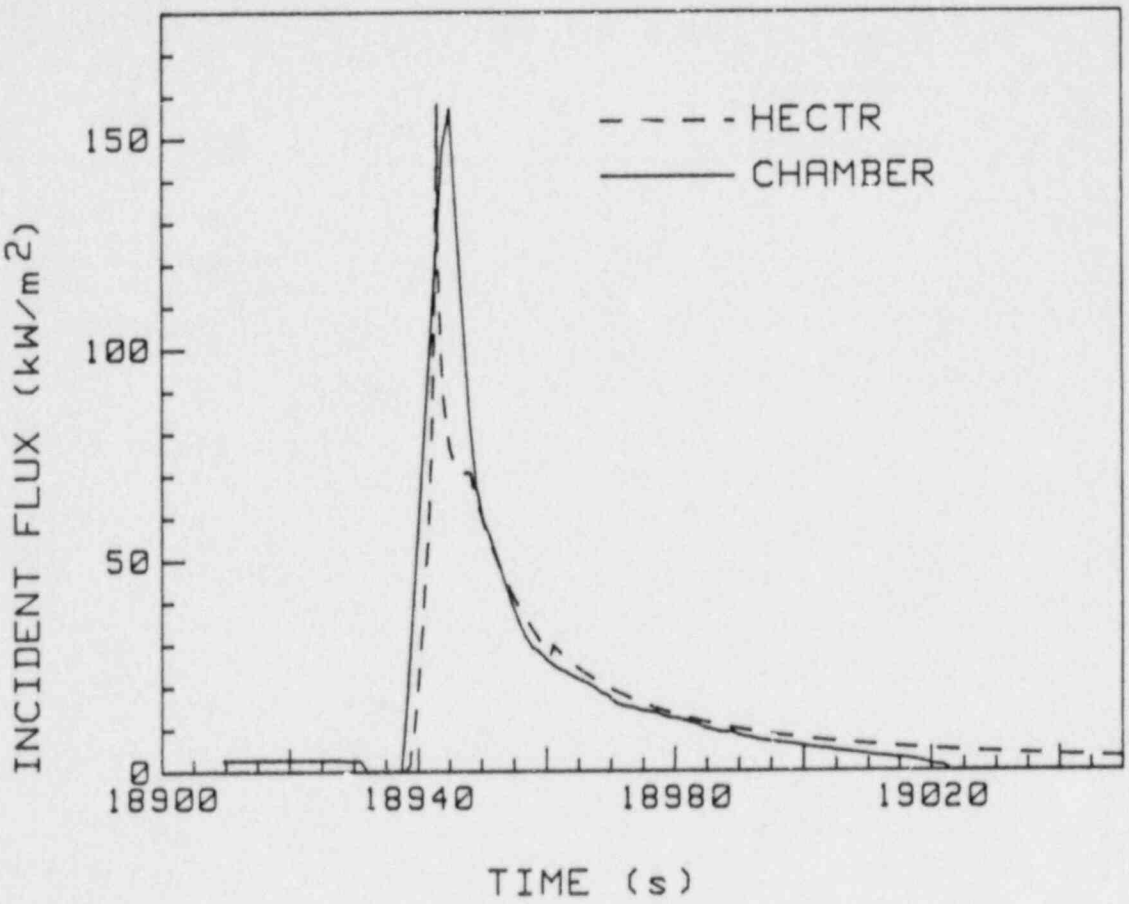

Figure 3.8. Experimental/HECTR 100 Percent Heat Flux Profile Comparison, Unaged Cable

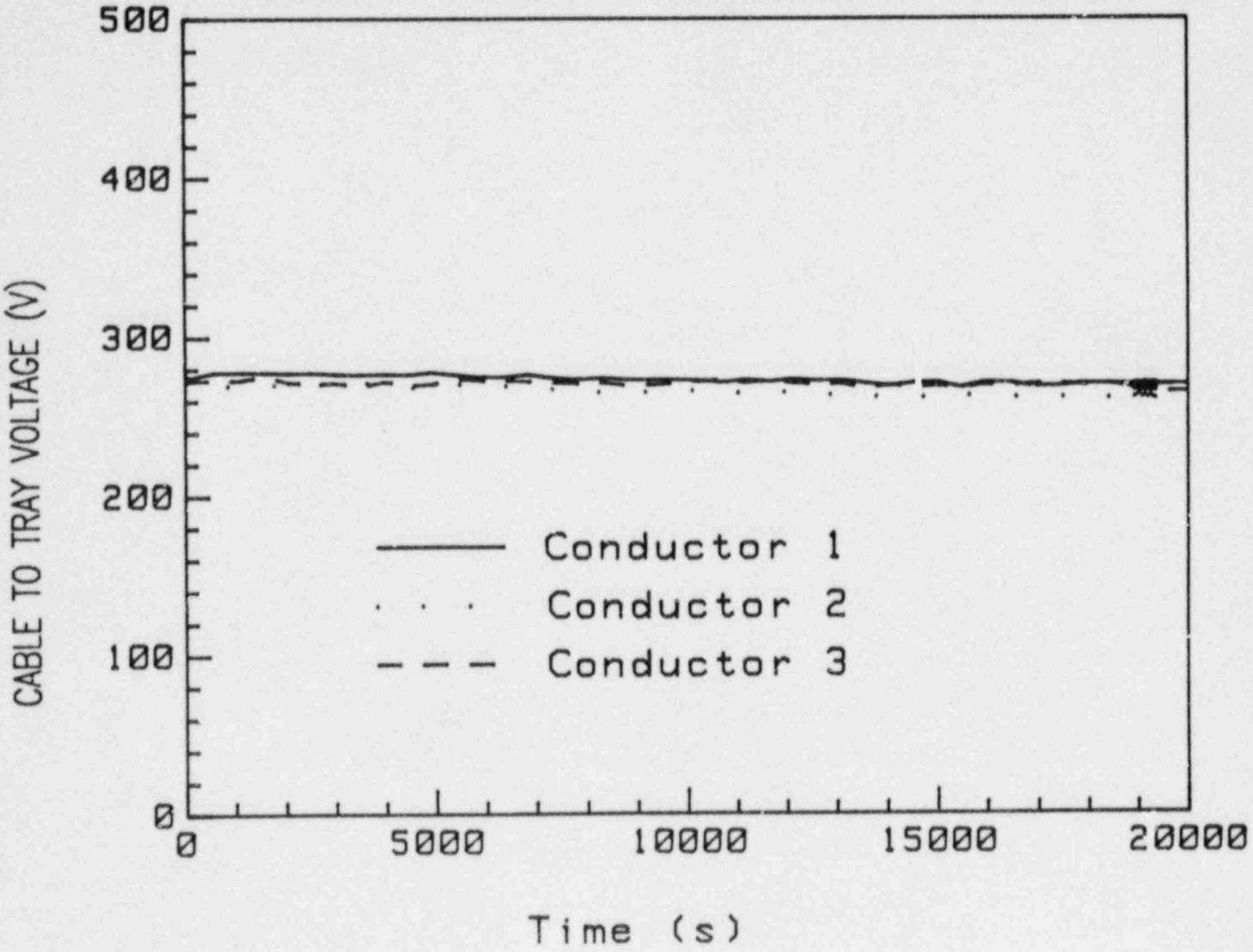

Figure 3.9. Conductor Voltage for an Unaged Cable, 100 Percent Pulse

Figure 3.10. Unaged Cable After 100 Percent Test

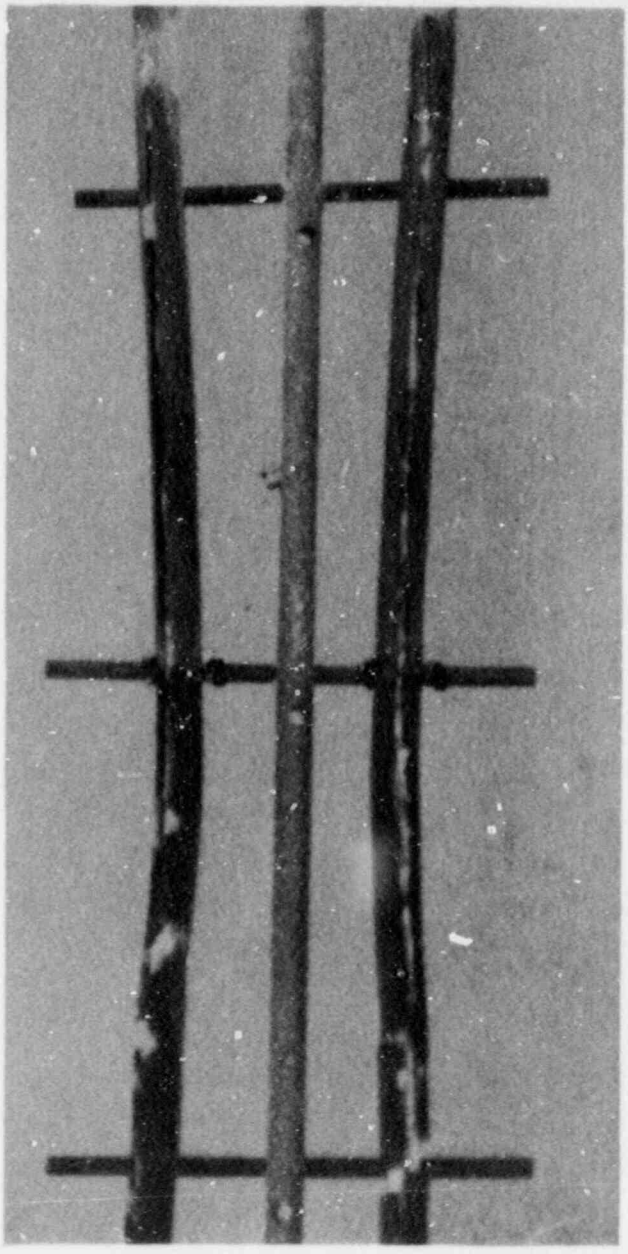

Figure 3.11. Aged Cable After 100 Percent Test

filler material to the heat flux. As a result, this material melted in several places. However, the conductor insulation remained intact.

There was a white crystalline material at the loop in the aged sample. This region of the specimen was outside of the foil assembly. The region inside the foils had no such material. The two 110+ percent aged samples had the same white crystalline material over their entire length after exposure to the partial pulses they experienced. After exposure to the complete pulse the white crystalline material was no longer present on the in-foil portion of those samples.

Also, after exposure to the partial pulses (which reached the peak flux) the 110+ percent aged cables had no cracks in their jackets. Thus, the cracking in the aged 100 percent sample jacket probably occurred during the tail portion of that pulse.

The effects of oxygen availability are significant in this type of testing. The HECTR calculations which defined the test environment indicated that the preburn oxygen concentration was 15 to 16 percent and was approximately 10 percent after the burn. The prepulse oxygen concentration in the SCETCh was 15 percent. In order to assess the effect of increased oxygen, an unaged cable was subjected to a pulse outside the chamber. The cable burned vigorously for 30 to 40 seconds exposing the cable conductors.

As discussed in the previous paragraphs, unaged cable subjected to pulses inside the SCETCh blistered but did not burn. Apparently the 15 to 16 percent oxygen atmosphere in the SCETCh (corresponding to HECTR calculations of containment environments) suppresses cable burning.

As mentioned previously, the linear ramp up to peak heat flux used in the cable tests results in approximately 30 percent more energy incident on the cable specimens compared to the HECTR calculations for the particular S_2D event studied in the TMI-hybrid analysis. Thus all of the single burn cable test environments were more severe than any of the HECTR calculated TMI-hybrid environments.

After completion of these tests, HECTR calculations of the Surry nuclear power plant were completed which indicated more severe environments could exist in Surry than in the TMI-hybrid. This is consistent with Table 3.5 which indicates that Surry is one of the worst (most severe) cases. Although the heat flux profile used in the single burn cable tests was based on one of the worst case TMI-hybrid calculations, the linear ramp up to the peak

heat flux used in the tests results in a 20 percent larger integrated energy deposition in the single burn cable tests than was calculated by HECTR for the worst case Surry environment (see Appendix D). It can therefore be concluded that the cable tests were representative of the most severe environments expected in a LOCA and subsequent single deflagration of the hydrogen resulting from a 75 percent core metal-water reaction in a large dry or subatmospheric power plant.

The single burn cable performance and observed jacket damage from the tests conducted in the SCETCh are consistent with the results of tests at Sandia's Central Receiver Test Facility[3] and the Nevada Test Site.[2] The observed cable damage from these tests is also consistent with cable damage observed inside the TMI-2 containment.[15] The results of the present tests taken in conjunction with the CRTF and EPRI-NTS results indicate that nuclear qualified class 1E cable can survive a single hydrogen deflagration resulting from a LOCA having a 75 percent metal-water reaction in a large dry or subatmospheric power plant.

3.4.3.2 Transmitter Tests

This section summarizes the results of the single burn testing of the Barton 763 pressure transmitter. Detailed results are given in Appendix D.

The transmitter tests were conducted in two phases. The calorimetry phase used a previously tested pressure transmitter[3] equipped with thermocouples to monitor the temperature response of the casing front plate and interior electronics. The performance phase investigated the operational response of the aged Barton 763 transmitter to the LOCA/hydrogen burn environment. The environment used in the transmitter tests was similar to that used in the cable tests with changes in the foil temperatures and geometries to account for differences in the specimen geometry and absorptivity.

By the time the Barton tests were conducted, an improved foil control algorithm had been developed. Thus the linear ramp in heat flux used in the cable tests was not necessary and a more accurate heat flux profile was used for the pressure transmitter tests. This heat flux profile closely follows the HECTR predicted heat flux profile shown in Figure 3.8. Due to the problems encountered in the 110 percent cable tests, only 100 percent transmitter tests were conducted.

The results of the calorimetry tests (Figure 3.12) indicated that the front face temperature reached 133°C (406 K) and the capacitor temperature reached a maximum of 113°C

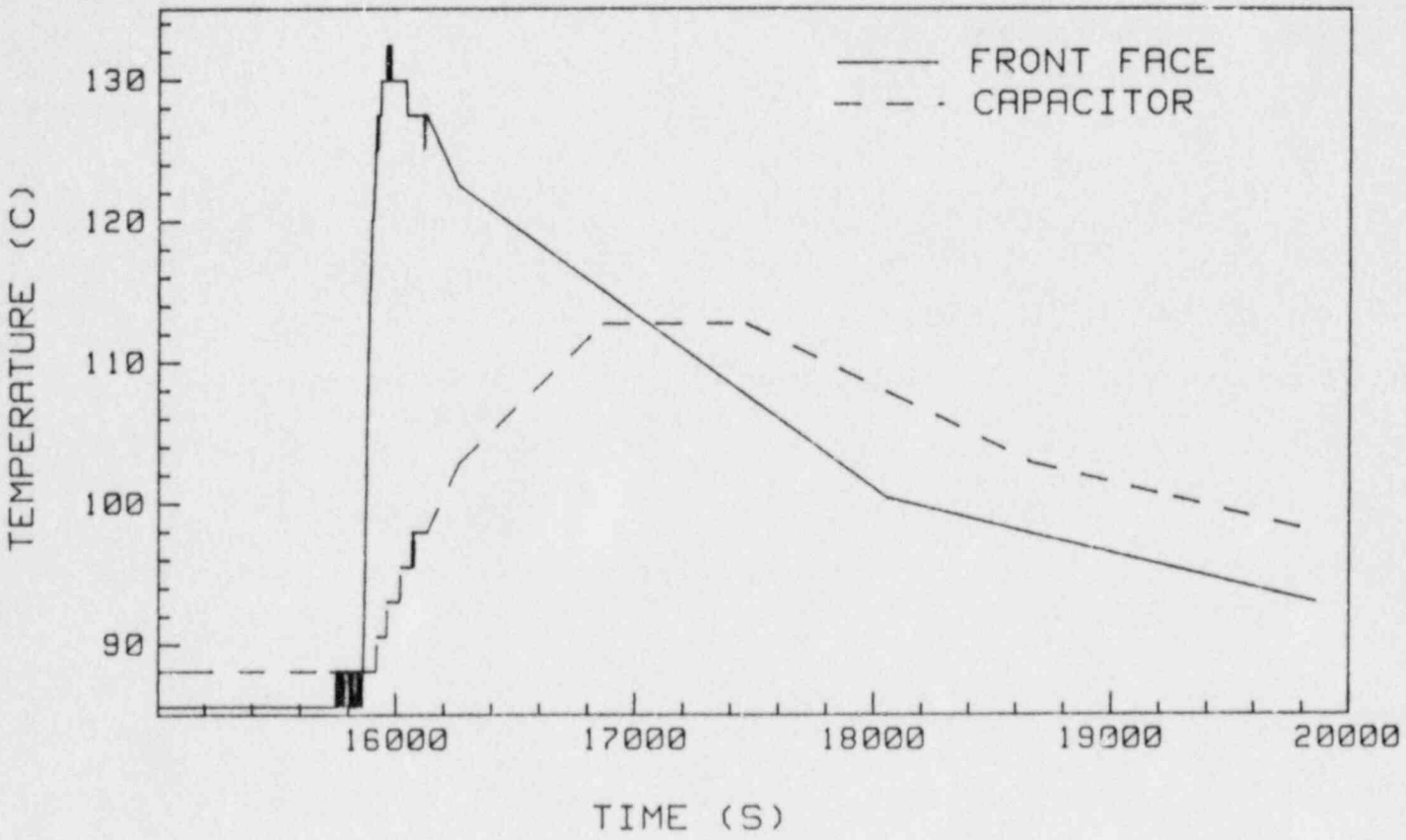

Figure 3.12. Measured Barton Calorimetry Test Temperatures

(386 K). These temperatures are well below the qualification limit of 444 K.[17] It should also be noted that the HECTR three-layer Barton model predictions of the front face temperature were higher by 3°C than the measured temperature, indicating good agreement.

The SCETCh total pressure versus time for the calorimetry test is shown in Figure 3.13 along with the HECTR predicted pressure. The total pressure is an important parameter in the transmitter tests because of the potential to drive moisture through the front face seal.

For all Barton tests, the Barton transmitter was attached to a pressure line which was held continuously at 750 psi. A reference Heise pressure gauge outside of the test chamber was also attached to the pressure line. The output of the Barton and Heise were both monitored.

During both the calorimetry test and the performance test, the Barton transmitters performed well. Slight fluctuations in their readings (<4 percent in the calorimetry test, <2 percent in the performance test) occurred (Figure 3.14), but these were not large enough to be interpreted as indicative of impairment.

Although the transmitter test environments were not as severe as the cable test environments in terms of integrated energy (due to the improved foil control algorithm), the transmitter test environments were still representative of the most severe environments calculated by HECTR for the TMI-hybrid analyses. While the HECTR calculated Surry environments are more severe than the transmitter test environments, the most severe of these HECTR calculated Surry environments resulted in a three-layer model peak front face temperature exceeding the qualification limit of 444 K by about 6 K for less than 10 minutes. In view of the mild conservatism in the HECTR three-layer model and the considerably longer LOCA qualification test which the Barton has been tested to, HECTR predicted front face temperatures exceeding the qualification limit by 6 K for 10 minutes should not be reason for concern. And in light of Table 3.5, this Surry calculation represents the bounding case.

It should be noted that for the single burn scenarios, the most likely threat to the survival of thermally massive equipment such as a Barton pressure transmitter is from moisture penetration through the seals. For the single burn tests, the total pressure and steam concentration used were as severe as any seen in the HECTR single burn calculations.

These results indicate that the Barton 763 pressure transmitter can withstand a large dry containment LOCA and hydrogen burn environment with a single deflagration of hydrogen resulting from a 75 percent core metal-water reaction.

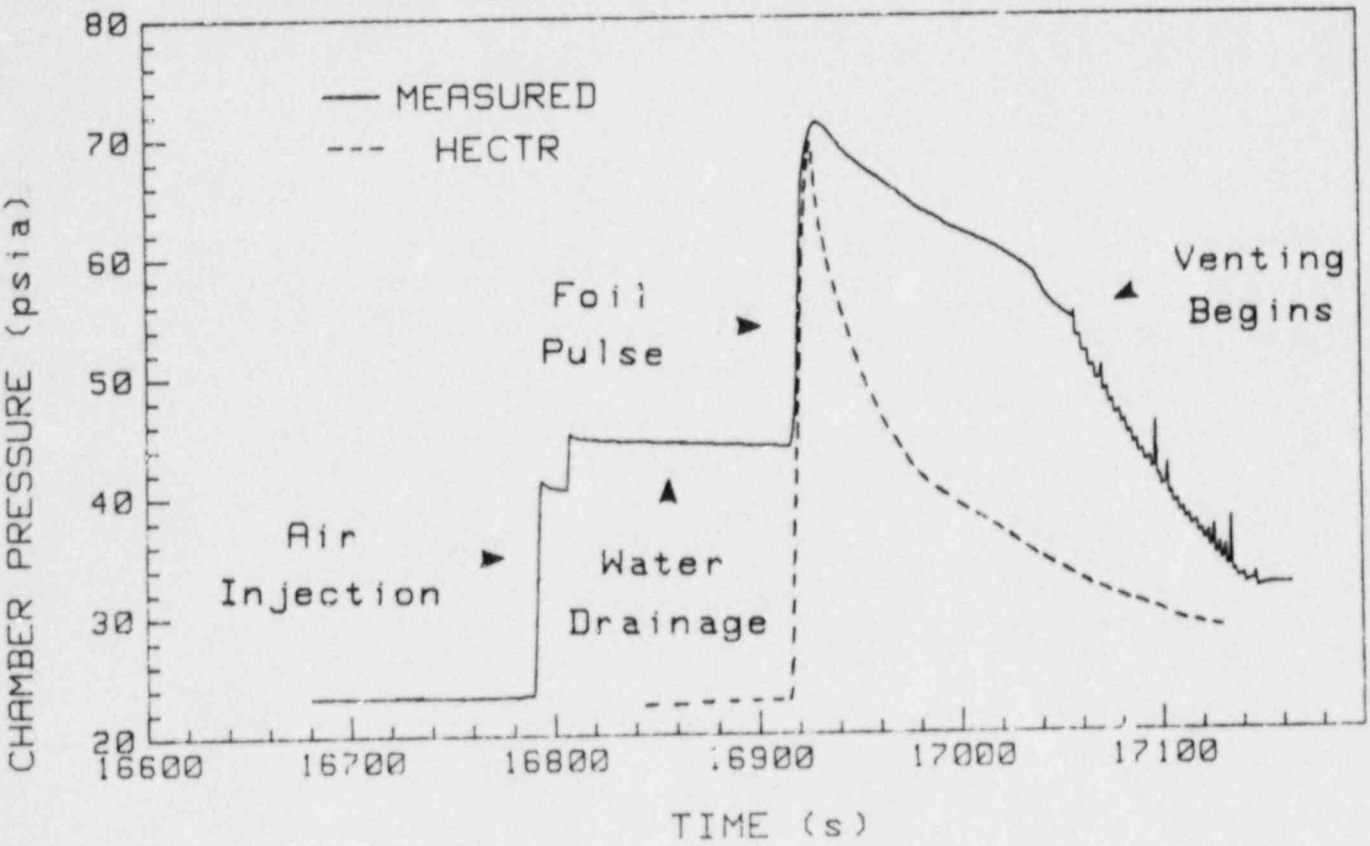

Figure 3.13. HECTR and Measured SCETCh Pressure Versus Time

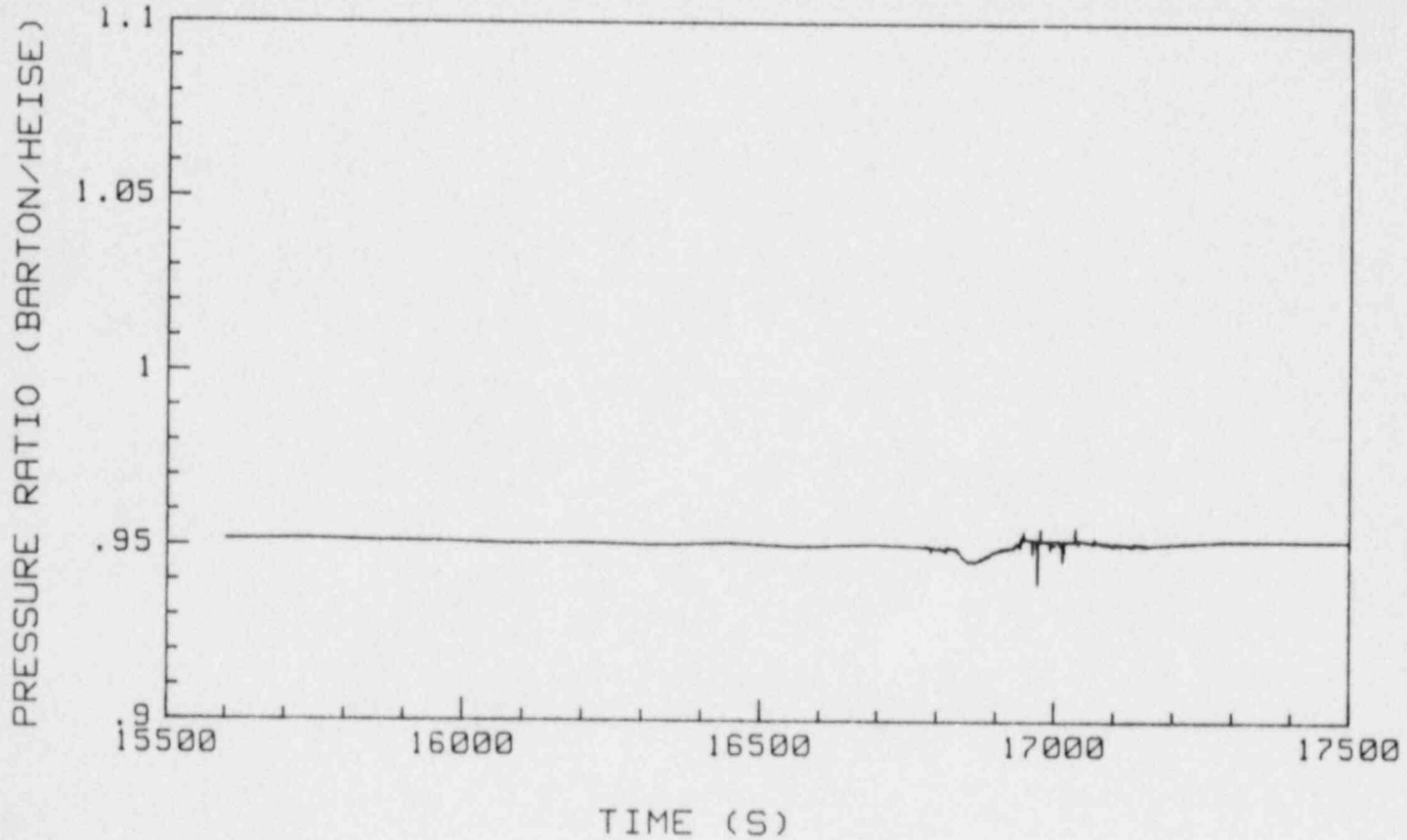

Figure 3.14. Performance Test: Ratio of Measured Barton Pressure to Heise Gauge Pressure

3.4.4 SCETCh Multiple Burn Tests

During the single burn cable tests, most of the visually observed damage occurred after the peak heat flux during the tail portion of the heat flux pulse. The damage to the cable jacket appeared to be a strong function of the energy deposited therein. This raised concern that an environment which results in a considerably larger energy deposition (such as might occur in a multiple burn scenario) may pose a serious threat to the survival of safety-related equipment. Although multiple burn experiments were beyond the program scope, two scoping multiple burn tests were conducted in an attempt to address this concern.

Two cable specimens and one Barton pressure transmitter were exposed in the multiple burn tests. Details of the testing can be found in Appendix D. The results of the tests indicate that multiple burns do pose a serious threat to safety equipment located in a source compartment.

3.4.4.1 Cable Test

Two cable specimens were placed in the SCETCh for the multiple burn test. One specimen was placed in conduit to take advantage of any shielding effects the conduit may provide. The other specimen was fully exposed to the incident foil flux. One half of each specimen had been thermally and radiation aged to the same conditions used for the single burn cable test specimens (the other half had not). The cables were not powered during the test.

The heat flux profile used in the test was calculated using HECTR to model an S_1D event in Surry. The scenario consisted of 59 individual burns as shown in Figure 3.15. This particular profile is believed to be representative of multiple burn scenarios and does not constitute the worst case possible. Calculations have shown that some compartments can see in excess of 100 individual burns.

During the test, the jacket, filler material, and conductor insulation burned off exposing the bare copper wire. The results were similar for the cable specimen in conduit. Thus, both the exposed cable specimen and the cable specimen in conduit did not survive the multiple burn environment simulation. Figure 3.16 shows the cable arrangements after the multiple burn pulses.

These results indicate that multiple burn environments pose a serious threat to cables located in the source compartment.

3.4.4.2 Transmitter Test

The Barton pressure transmitter which had been previously exposed in the single burn calorimetry test was selected for

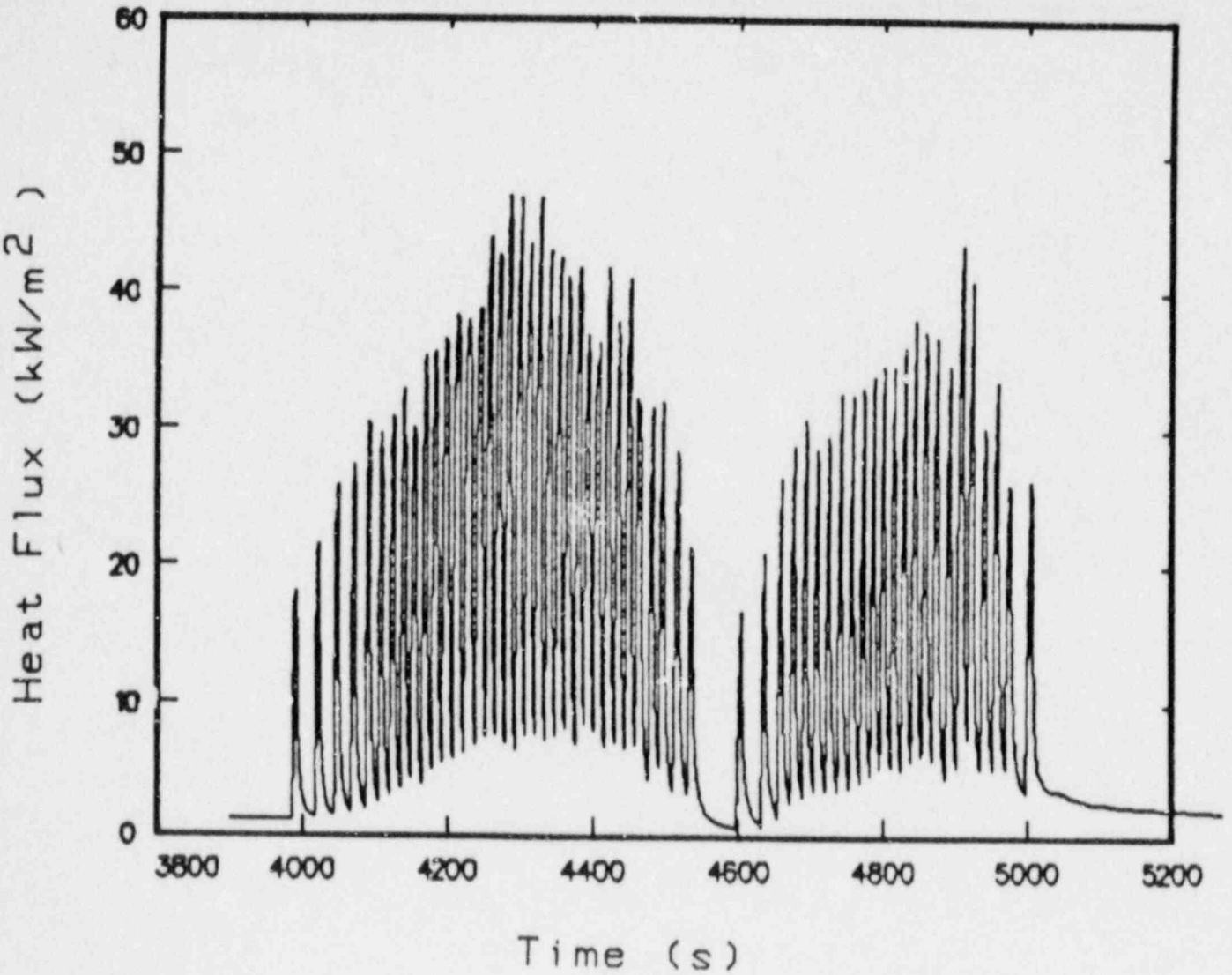

Figure 3.15. S_1D Surry Multiple Hydrogen Burn Heat Flux Profile

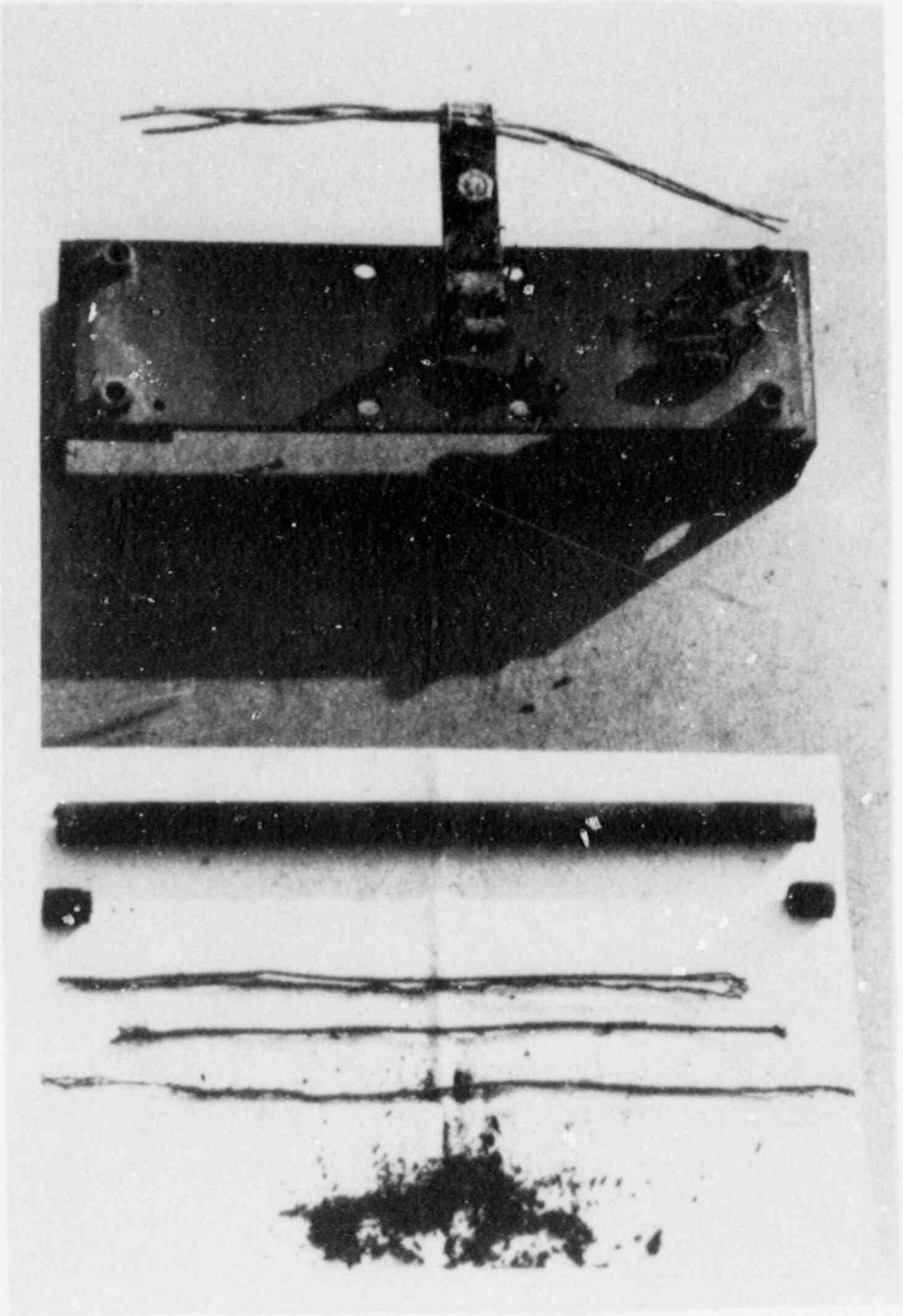

Figure 3.16. Multiple Burn Test Cable Arrangement After Multiple Burn Testing

the multiple burn scenario. The thermocouples and pressure output were monitored during the test. The Barton was maintained at 750 psig during the burn simulations.

There are many combinations of burn frequency, number of burns, incident energy, and peak heat fluxes possible for defining a multiple burn environment. The source compartment volume has a strong influence on which combination of the above occurs in a given scenario. Parametric calculations using HECTR were performed over a range of source compartment volumes to determine possible effects on the multiple burn scenario. The multiple burn scenario selected for the Barton test was a representative scenario and does not constitute the worst case possible. The 39 burn scenario selected produced the heat flux profile shown in Figure 3.17. The source compartment volume used to obtain this heat flux profile is representative of a steam generator cubicle in the TMI containment.

About one third of the way through the multiple burn scenario, the Barton pressure transmitter became erratic and failed. Figure 3.18 presents the ratio of Barton pressure output to that of a Heise gauge. The measured capacitor temperature at the time of failure was approximately 195°C (468 K), while the front face (casing) temperature was in excess of 357°C (630 K). Posttest inspection revealed charring of the electronics and blistering of the painted surface (Figure 3.19).

The results of this test indicate that multiple burns pose a serious threat to pressure transmitters and other similar equipment located in a source compartment.

4.0 SUMMARY AND CONCLUSIONS

Analytical and experimental investigations of equipment survival in hydrogen burns in dry containment buildings have been conducted. Two sets of analytical studies were carried out for large dry containments using a model of the Three Mile Island Unit 2 containment. Another set was carried out for subatmospheric containments using a model of the Surry containment building. The experiments investigated the survivability of thermally and radiation aged nuclear qualified Brand Rex power and control cable and a Barton 763 pressure transmitter in a simulated LOCA/hydrogen burn environment.

The analytical studies used the HECTR code to calculate the temperature response of equipment models to hydrogen burns in various containment locations. Other parameters which were varied in the analyses included LOCA break size, ignition criteria (single burn and ignition simulation) and the operation of engineered safety features.

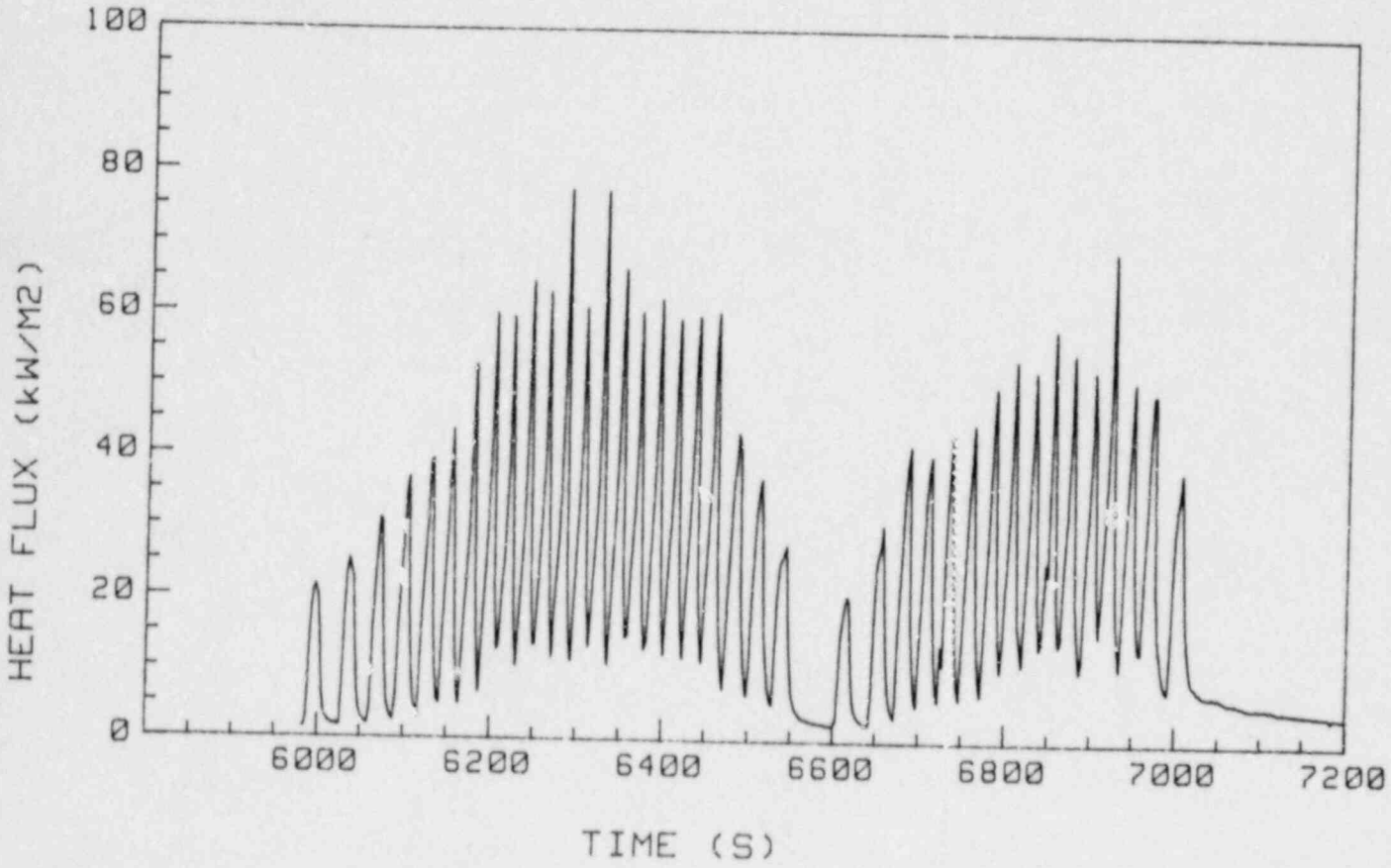

Figure 3.17. Barton Multiple Burn Heat Flux Profile

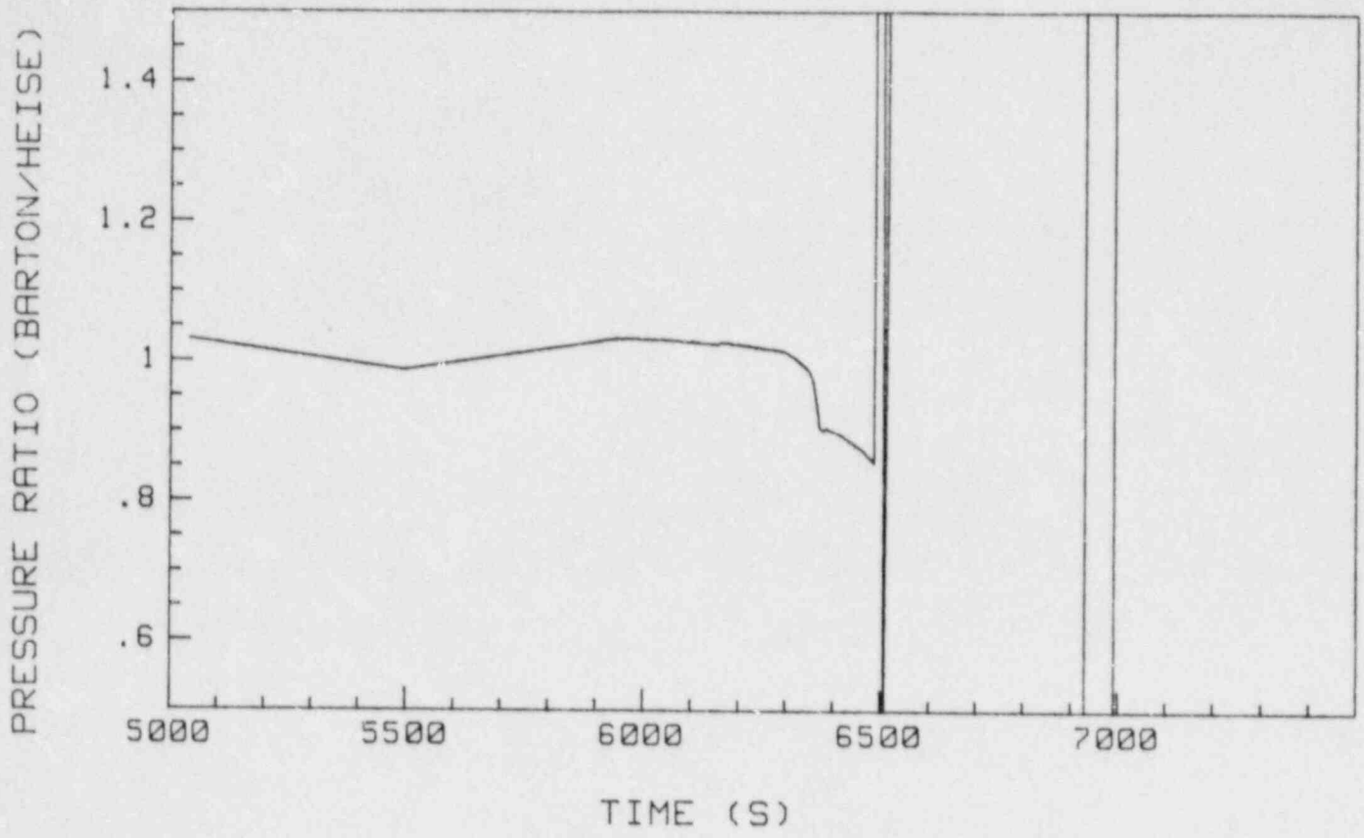

Figure 3.18. Barton Gauge Pressure Output Compared to Heise Gauge Pressure Output

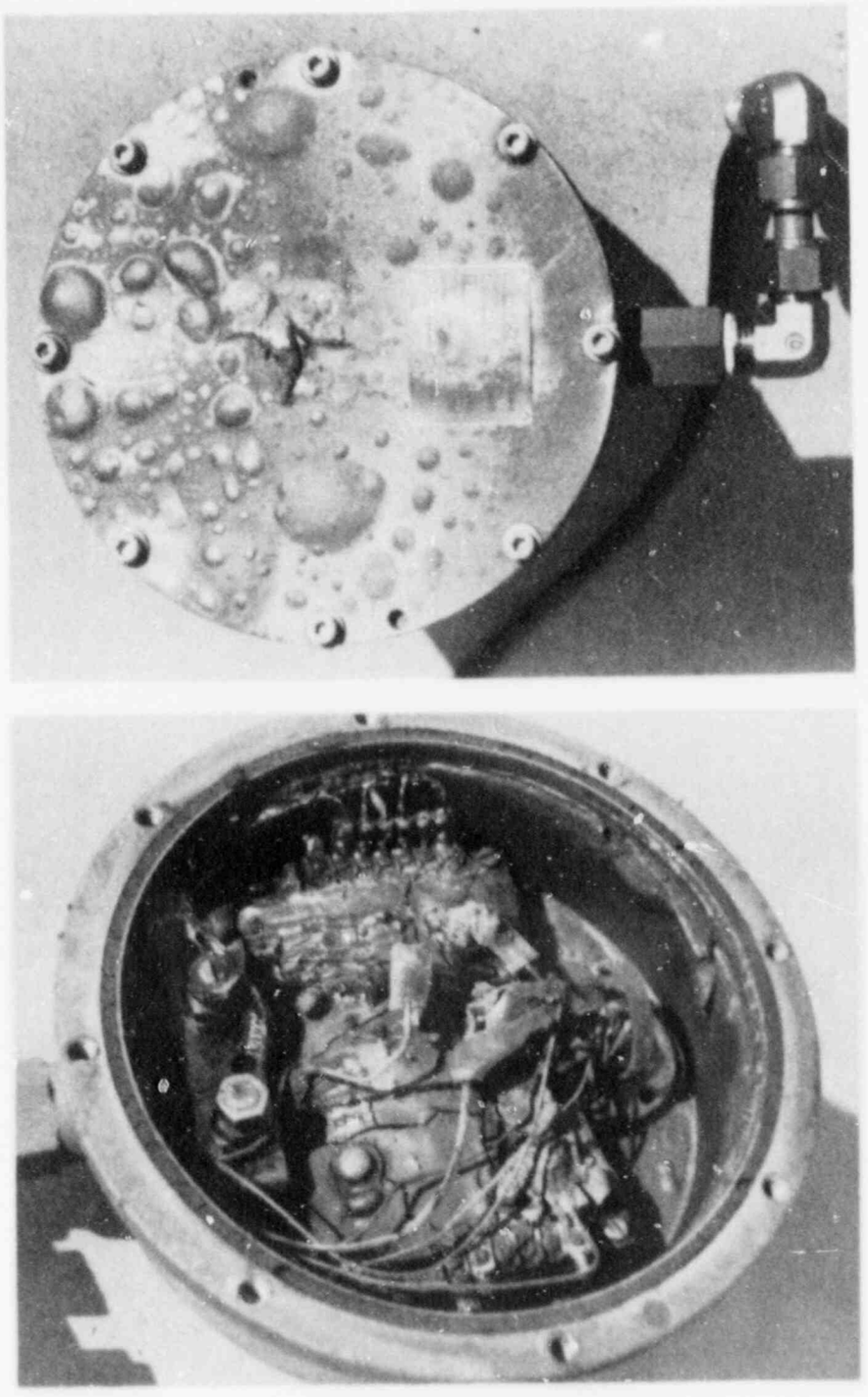

Figure 3.19. Condition of Barton Pressure Transmitter After Multiple Burn Testing

Equipment temperature response was a function of the hydrogen burn type to which the equipment was exposed. Single hydrogen burns dispersed their energy throughout containment in relatively short time periods. The large dry hyb id analyses had no cases where single hydrogen burns caused the surface temperature of the three-layer Barton model to exceed 444 K (a typical equipment qualification temperature). Maximum surface temperatures were well below the 444 K temperature limit. For the Surry analyses it was shown that the Surry containment represents one of the most severe cases (highest hydrogen mole fractions) for both atmospheric and subatmospheric large drys. The Surry single burn analyses had two cases in which the Barton model surface temperature exceeded 444 K, but the peak temperatures were only slightly above 444 K (447 K and 450 K) for short time periods (less than ten minutes).

Multiple burns (simulating ignition by igniters at 7 volume percent hydrogen) released most of the hydrogen's energy into a relatively small region of containment (the source compartment) over a relatively long period of time. This localized and lengthy release of energy due to multiple burning forced the Barton model surface temperature to exceed 444 K for long periods of time. The worst TMI hybrid case resulted in a peak surface temperature of 670 K. The surface remained above 444 K for 51 minutes. Coincidentally, the worst Surry multiple burn case resulted in a peak surface temperature of 670 K which remained above 444 K for 50 minutes.

HECTR calculated potential detonable gas mixtures could occur briefly in the hybrid analyses. These mixtures occurred only in the source compartments. HECTR also calculated potential detonable gas mixtures could occur for lengthy periods of time in the Surry analyses. These mixtures occurred in the source compartments as well as globally throughout the containment and were a direct result of the cold spray water (45°F) stripping out the steam.

Thus, HECTR predicts that the use of igniters presents a dilemma. In the absence of igniters, potentially detonable hydrogen mixtures accumulated in source compartments in the hybrid analysis, and throughout containment in the Surry analysis when sprays were operating. The use of igniters would inhibit the accumulation of detonable hydrogen concentrations because the hydrogen would be burned at lower (nondetonable) concentrations. However, HECTR predicts that a deliberate ignition system could result in excessive equipment temperatures in the source compartment (as high as 670 K for the cases analyzed) for the case of ignition at 7 volume percent hydrogen.

The hybrid and subatmospheric results should be viewed in light of HECTR's simple criteria for specifying a detonable

concentration. One must also realize that the Barton transmitter served as a surrogate for all safety equipment in these analyses. A more accurate evaluation of the threat to safety equipment posed by multiple hydrogen burns in a subatmospheric containment must consider such factors as precise equipment location, function, material properties, susceptibility to thermal stress, and the length of time during the accident for which the equipment is required to function.

Single burn tests of aged and unaged nuclear qualified cable and Barton pressure transmitters indicate that cable and equipment having similar thermal characteristics and sensitivities can withstand a LOCA and single hydrogen burn resulting from a 75 percent core Zircaloy-water reaction in a large dry containment. The observed post-test condition and performance of the test specimens is consistent with the results reported for the EPRI-NTS tests and previous hydrogen burn simulations at Sandia's Central Receiver Test Facility, as well as observed damage at TMI-2. The results of these tests should not be extrapolated to hydrogen standing flame environments where safety equipment may be exposed to plume or flame heat fluxes for a considerably longer period of time. Standing flames were not considered in this work.

In contrast to the single burn test results, the multiple burn test results indicate that multiple burns (at 7 v/o hydrogen ignition) do pose a serious threat to safety-related equipment located in a source compartment. Both cable specimens and a Barton pressure transmitter in the 7 v/o hydrogen ignition multiple burn tests failed to survive. The operability of typical safety-related equipment located in a source compartment in these environments is extremely doubtful.

In conclusion, the results of the single burn SCETCh tests and HECTR analyses of large dry containments and subatmospheric containments indicate that for a LOCA involving a 75 percent metal-water reaction, a single hydrogen deflagration does not present a serious threat to the survival of nuclear qualified safety related equipment.

However, a conclusion regarding deliberate ignition systems is not as clear. The HECTR results indicate that detonable concentrations of hydrogen may accumulate locally in a source compartment of a large dry containment and both locally and globally in a subatmospheric containment unless a deliberate ignition system is employed. A deliberate ignition system would prevent detonations by burning the hydrogen at lower (nondetonable) concentrations. This presents somewhat of a dilemma since the results of HECTR analyses which model deliberate ignition as well as the

results of scoping multiple burn SCETCh simulations indicate that multiple burn (deliberate ignition at 7 v/o hydrogen) environments pose a serious threat to the survival of safety-related equipment in a source compartment.

REFERENCES

1. Hydrogen Control Requirements, Final Rule, 10 CFR Part 50, Federal Register, Vol. 50, No. 17, January 25, 1985.

2. Achenbach, J. A., et al., Westinghouse Electric Corporation, Large Scale Hydrogen Burn Equipment Experiments, (EPRI NP-4354), Electric Power Research Insitute, December 1985.

3. Dandini, V. J. and J. J. Aragon, Simulation of an EPRI-Nevada Test Site (NTS) Hydrogen Burn Test at the Central Receiver Test Facility, NUREG/CR-4146, SAND85-0205, Sandia National Laboratories, June 1985.

4. Dandini, V. J., Testing of Nuclear Qualified Cables and Pressure Transmitters in Simulated Hydrogen Deflagrations to Determine Survival Margins and Sensitivities, NUREG/CR-4324, SAND85-1481, December 1985.

5. Dingman, S. E., et al., HECTR Version 1.5 User's Manual, SAND86-0101, NUREG/CR-4507, Sandia National Laboratories, Albuquerque, NM, April 1986.

6. Henrie, J. O. and A. K. Postma, Analysis of the Three Mile Island Unit 2 Hydrogen Burn, (GEND-INF-0023), Vol. IV, Rockwell International, March 1983.

7. Zalosh, R. G., et al., Analysis of the Hydrogen Burn in the TMI-2 Containment, (NP-3975), Electric Power Research Institute, Palo Alto, CA, April 1985.

8. Letter, W. W. Bixby (U.S. DOE-TMI Site Office) to D. Krenz (U.S. DOE-ALOO), Subject: HECTR Analysis of the TMI-2 Hydrogen Burn--WWB-63-83, May 24, 1983.

9. Report of the Special Committee on Source Terms, American Nuclear Society, September 1984.

10. Henrie, J. O. and A. K. Postma, Analysis of the Three Mile Island (TMI-2) Hydrogen Burn, RHO-RE-SA-8, Vol. 3, July 1982.

11. Analysis of the Hydrogen Burn in the TMI-2 Containment, BPRD NP-3975, Electric Power Research Institute, April 1985.

12. Analysis of the Three Mile Island-Unit 2 Accident, NSAC-1, Electric Power Research Institute, July 1979.

REFERENCES (Concluded)

13. Rogovin, M. and F. J. Frampton, Three Mile Island--A Report to the Commissioners and the Public, Vols. I and II, Part 2, 1980.

14. Lee, J. L., et al., A Study of Damageability of Electrical Cables in Simulated Fire Environments, EPRI NP-1767, Electric Power Research Institute, March 1981.

15. Trujillo, R. E., et al., Analyses of the Polar Crane Pendant Cable From Three Mile Island-Unit 2, GEND-INF-069, General Public Utilities, Electric Power Research Institute, U.S., Nuclear Regulatory Commission, U.S. Department of Energy, January 1986.

16. Wong, C. C., "Hydrogen Production and Combustion-Induced Loadings of the Large-Dry and Subatmospheric PWR Containment," Letter Report to Patricia Worthington, NRC, Sandia National Laboratories, 1986.

17. IEEE Standard for Qualifying Class 1E Equipment for Nuclear Power Generating Stations (IEEE Std 323-1974), Institute for Electrical and Electronics Engineers, 1974.

18. Schutz, H. W., Nagata, P. K., Estimated Temperatures of Organic Materials in the TMI-2 Reactor Building During Hydrogen Burn, GEND-INF-023, Vol. II, EG&G Idaho, December 1982.

APPENDIX A

TMI-HYBRID ANALYSIS

APPENDIX A

TMI-HYBRID ANALYSIS

A.1 Introduction

The hydrogen burn in containment during the accident at Three Mile Island Unit 2 (TMI-2) focused attention on the possible consequences of hydrogen generation during a nuclear core uncovery accident. This accident contributed to the Hydrogen Control Rules for Pressurized Water Reactors (PWR) with ice condenser containments and Boiling Water Reactors (BWR) with Mark III containments. The hydrogen control rule states that containment structural integrity and survivability of needed safety systems during a hydrogen burn must be demonstrated for reactors not relying upon an inerted atmosphere for hydrogen control.[1] The hydrogen control rule for PWRs with large dry containments is presently deferred. To assist in providing a basis for a recommendation on rulemaking for PWRs with large dry containments, the containment environments created by arrested sequences having a 75 percent metal-water reaction were calculated.

The risk significant scenarios selected as sources of water/steam and hydrogen flows into containment were the small break loss-of-coolant accidents (LOCAs) S_1D and S_2D. Three small break LOCAs were analyzed: (1) a 1-inch diameter break, S_2D1; (2) a 2-inch diameter break, S_2D2; and (3) a 4-inch diameter break, S_1D4. The location of the hydrogen and water/steam source terms in containment was varied to observe containment response, and the ignition level of the hydrogen in containment was also varied as a parametric study. The results of this hydrogen burning analysis are presented in terms of temperature response of safety-related equipment during the hydrogen burn.

The HECTR computer code[2] was used to calculate the hydrogen transport and burning and safety-related equipment response to hydrogen burning. HECTR is a lumped parameter containment analysis code developed to analyze nuclear reactor accidents involving the transport and combustion of hydrogen. The gases in each compartment are assumed to be uniformly mixed. Gas flow between compartments can be driven by both pressure and density differences. Included are models for hydrogen burns, radiative and convective heat transfer, condensation, and wall heat conduction. Appropriate engineered safety features (ESFs) such as the reactor building spray system and reactor building fan coolers are also modeled.

The containment input model for HECTR was based on the geometry and operating procedures for the TMI-2 Nuclear Power Plant. Two containment models were used. The first model divided the TMI-2 containment into eight compartments, and the second model divided the TMI-2 containment into 11 compartments.

The steam and hydrogen source terms input into HECTR were calculated with the MARCON 2.0 computer code.[3,4] The nuclear steam system (NSS) modeled was that of the Zion Nuclear Power Plant.

The TMI-2 containment model and the Zion NSS model were used because of the availability of the two models. Placing the Zion NSS into the TMI-2 containment would result in higher hydrogen mole fractions in containment when compared to a TMI NSS in the TMI-2 containment model.

A.2 Models

The MARCON models used to calculate the water and hydrogen source terms and the HECTR containment models are described in this section. The safety-related equipment models used to calculate temperature response are also described in this section.

A.2.1 MARCON 2.0 Model

The MARCON 2.0 computer code was used to generate the steam and hydrogen source terms. The MARCON 2.0 code includes a replacement of the subroutine that calculates the interaction of the molten debris and the concrete floor in the MARCH 2 (Meltdown Accident Response Characteristics) code[3] with the CORCON Mod2 code.[4] MARCON 2.0 also includes an interfacing subroutine to pass key parameters between MARCH and CORCON Mod2 and additional reactor cavity models. Since this analysis addressed arrested sequences, the CORCON and reactor cavity models were not used in the analysis. The water and hydrogen source terms were calculated solely by the models in MARCH 2 version 111. MARCON 2.0 was used because it is being used for other Sandia programs (SASA and Hydrogen Behavior) and the input models were already developed.

The MARCH models in MARCON 2.0 were used to represent the primary and secondary systems. MARCH models the primary system as a single cylindrical volume with liquid at the bottom and gases or vapor at the top when present. Figure A.2.1 shows a representation of the MARCON 2.0 modeling of the primary system. Some characteristics of the Zion primary and secondary systems are listed in Table A.2.1.

The steam source flow rates are primarily dependent on the primary system pressure and the elevation of the flow

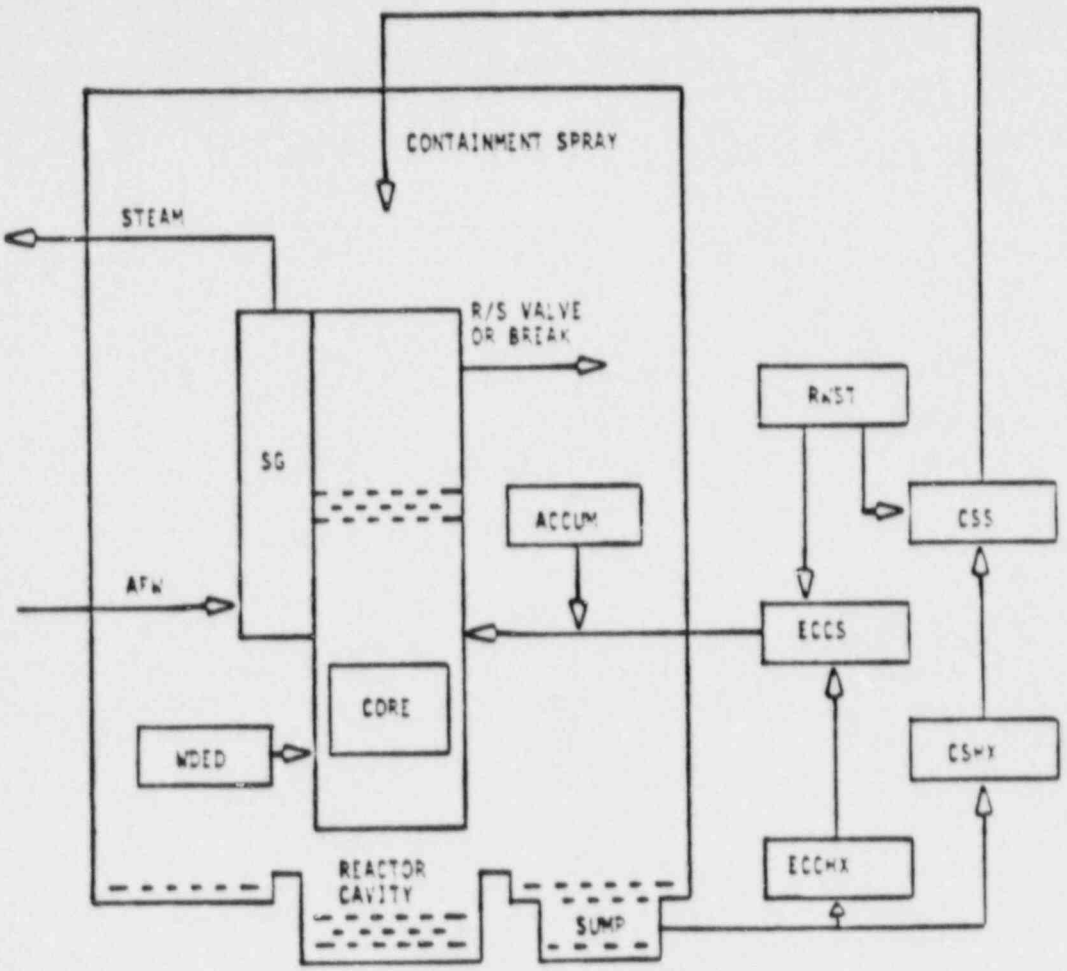

Figure A.2.1. MARCON Model of Primary System

Table A.2.1

Zion Reactor Characteristics for MARCH Analysis

Reactor Power	3238 MWt
Operating Pressure	2265 psia (15.6 MPa)
Operating Temperature	563 F (295 C)
Primary System Volume	12,480 ft^3 (353.4 m^3)
Primary System Water	543,560 lb (246,560 kg)
Steam Generator Water	352,500 lb
Fuel Rods in Core	39,372
Fuel Rod Diameter	0.422 in (0.0107 m)
Clad Thickness	0.023 in (0.0006 m)
Zircaloy in Core	44,550 lb (20,208 kg)
UO_2 in Core	216,600 lb (98,250 kg)

junction break relative to the height of liquid in the primary system. Water flow occurs when the break is below the collapsed liquid level and gas flow occurs when the break is above the water level. Two-phase (liquid-steam) flow is not modeled. The hydrogen source terms are primarily dependent on the hydrogen generation rate from the zirconium-steam reaction and the leak rate from the primary system into containment. The steam and hydrogen leak rates are proportional to their mass fractions in the vessel. For these degraded core scenarios it was assumed that Emergency Core Coolant (ECC) injection was unavailable for a time period long enough for 75 percent of the clad zirconium to oxidize, but was available to arrest the sequence at 75 percent metal-water reaction. Arresting the sequence at 75 percent clad oxidation required performing several computer simulations, varying the time of initiation of high pressure injection (HPI) until 75 percent clad oxidation was calculated. Due to the high head and capacity of the HPI pumps, the oxidation was arrested shortly after the initiation of HPI flow. To obtain the required amount of clad oxidation, very large fractions of the core were melted without core slump.

A.2.2 Containment and Containment Systems

This section describes the Three Mile Island Unit 2 (TMI-2) containment and presents the HECTR models used in the analysis.

A.2.2.1 Large, Dry Containment Description

The TMI-2 general arrangement is shown in Figure A.2.2. The large, dry containment outer structure is a steel-lined concrete cylinder with an elliptic dome roof and is supported

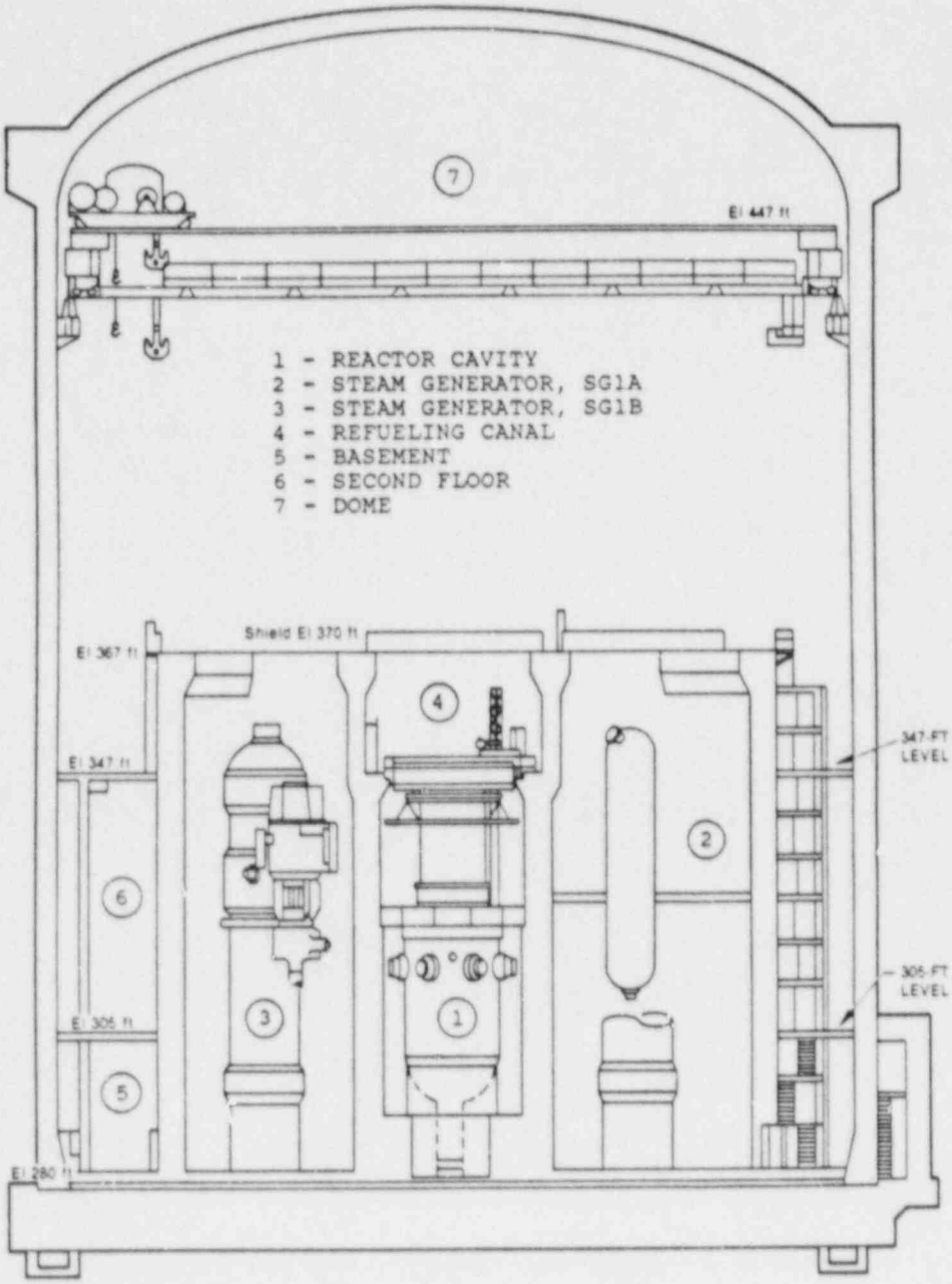

Figure A.2.2. TMI-2 Containment Vertical Cross Section Cut

by a concrete foundation ring. This outer structure encloses the nuclear steam system (NSS) and some of the engineered safety feature (ESF) systems. The net free volume of the containment is 2,100,000 cubic feet. The cylindrical wall has an inside diameter of 130 feet, is 4 feet thick, and is 157 feet in length from the foundation to the spring line. The cylindrical wall is lined with a 3/8-inch steel lining.

The interior structures of the containment consist of a shield wall surrounding the reactor vessel, shield walls surrounding the steam generators, reactor coolant pumps, and pressurizer, and other structures such as walls, floors, and equipment supports. Interior structures are often referred to by the elevation(s) (in feet) at which they occur in containment. The elevation of a structure is measured with respect to sea level. The reactor cavity floor (see Figure A.2.2) is the lowest floor in containment and has an elevation of 280 feet. The internal structures divide the containment building into major zones which affect gas transport and deflagration analyses.

The reactor cavity compartment has cylindrical shield walls which surround the reactor vessel. The reactor cavity is connected to the incore instrumentation chase by a tunnel at the bottom of the cavity. The incore instrumentation chase is sealed at Elevation 305.

The shield walls around the steam generators form the steam generator compartments. The steam generator shield walls are reinforced concrete, "D" shaped structures located on either side of the reactor cavity. The steam generator compartments are illustrated in Figure A.2.3. The D-ring walls are 4.5 feet thick and extend from Elevation 280 to Elevation 367. The two steam generator compartments are connected to each other by two tunnels located on either side of the reactor cavity compartment shield walls.

The refueling canal is a narrow rectangular compartment which sits on top of the reactor cavity compartment and between the D-ring walls of the steam generator compartments. Shield blocks are installed between the refueling canal walls at Elevation 367 during reactor operation to provide biological shielding. The part of the refueling canal not between the steam generator compartments from Elevations 280 to 305 is also called the fuel transfer pit.

The reactor cavity, steam generator compartments, and refueling canal are connected to one another and the rest of the containment building by vent (or flow) paths which allow pressure relief if an accident occurs in one of the NSS compartments. The reactor cavity and steam generator compartments are linked by the reactor vessel hot and cold leg piping penetrations. The reactor cavity and refueling canal

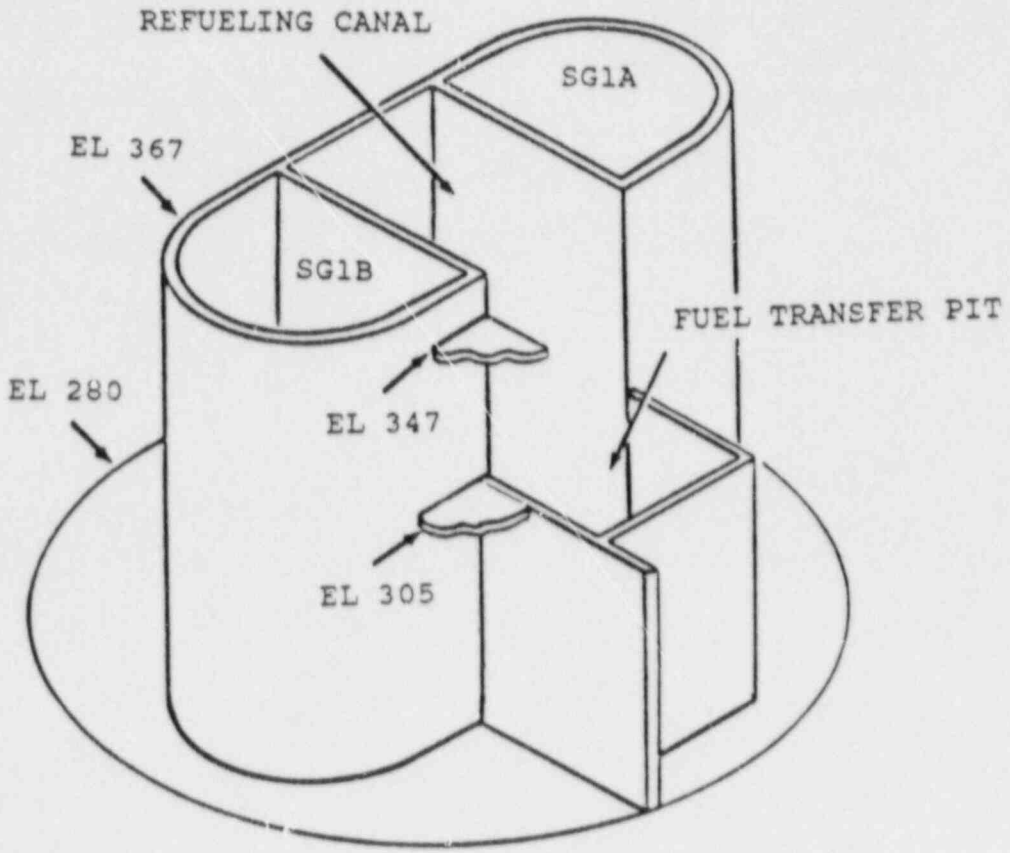

Figure A.2.3. Steam Generator and Refueling Canal Compartments

communicate by a vent path thrcugh shield blocks at the top of the reactor cavity. The refueling canal and steam generator compartments are connected to the rest of containment by openings at the tops of the compartments and by wall penetrations. The remaining internal structures serve chiefly to divide the containment building into three floor levels. The floor levels are located at Elevations 280, 305, and 347. Floor Elevations 305 and 347 are separated from the containment outer wall by a circumferential gap (also known as the seismic gap). The floor levels are located outside of the reactor cavity, refueling canal, and steam generator compartments. The three floor levels are illustrated in Figures A.2.4 to A.2.6.

The first floor level, Elevation 280, has the most internal concrete walls of the three floor levels. However, all of the walls have at least one flow path between neighboring zones of this elevation allowing communication between different regions. The reactor coolant drain tank, leakage coolers, and letdown coolers are located in separate compartments.

The second floor level, 305, is relatively open and has no walls dividing it into smaller compartments. Major equipment structures on this floor include two core flood tanks (CFT) and the reactor building fan coolers. The Elevation 305 floor is penetrated by one stairway, an equipment hatch, and other floor piping penetrations. These penetrations, as well as the seismic gap, allow flow to occur between Elevations 280 and 305.

Elevation 347, the third floor level, is the least obstructed level in containment and has the largest percentage of the containment volume above it. The steam generator and refueling canal compartment walls extend 20 feet above the Elevation 347 floor. Major equipment structures in this level include a machine room and a polar crane. Major penetrations through the Elevation 347 floor include the refueling canal, equipment hatches, a stairwell, and floor penetrations. These penetrations as well as the seismic gap allow flow between Elevations 305 and 347.

A.2.2.2 Containment Heat Removal Systems

Two ESF systems are available to reduce containment pressure and temperature during a LOCA: (1) the Reactor Building Cooler (RBC) system and (2) the Reactcr Building Spray (RBS) system.

The RBC system consists of five air recirculation units. Each air recirculation unit has a fan and a set of coils through which cold water is circulated. The fans blow hot containment air over the cool coils. Three units run during normal reactor operations. All functioning cooler units

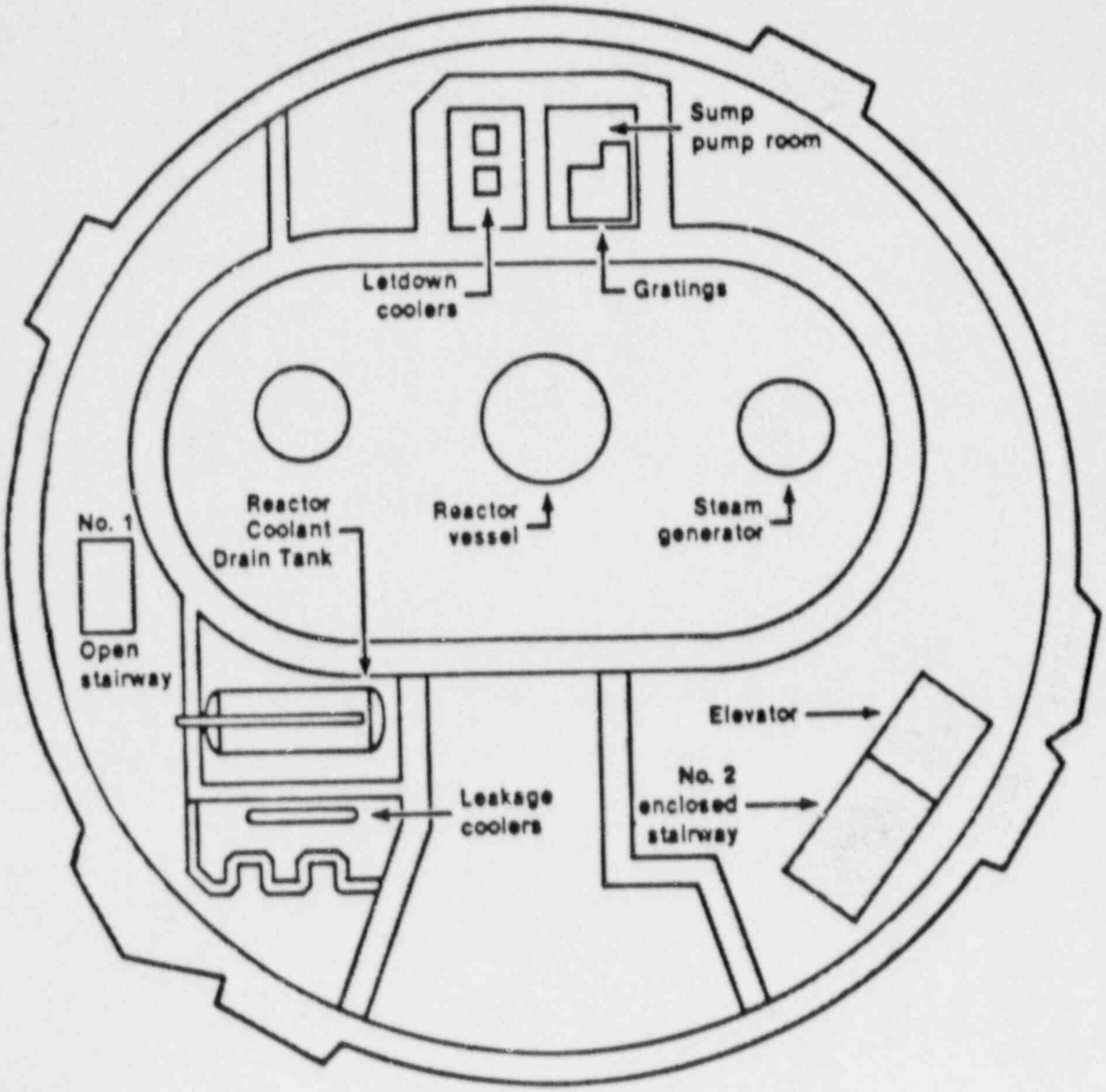

Figure A.2.4. Elevation 280 Containment Floor Plan View

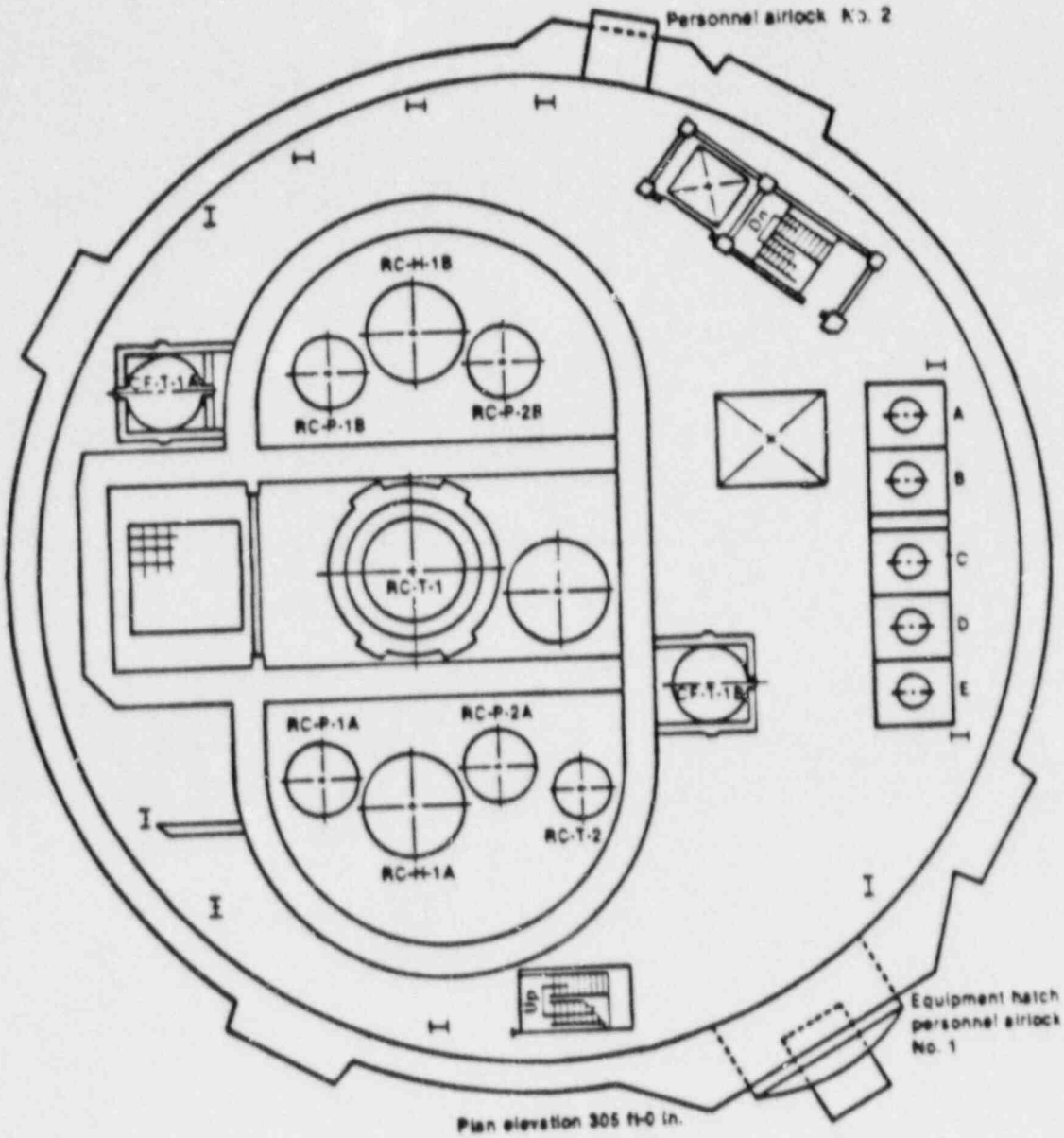

Figure A.2.5. Elevation 305 Containment Floor Plan View

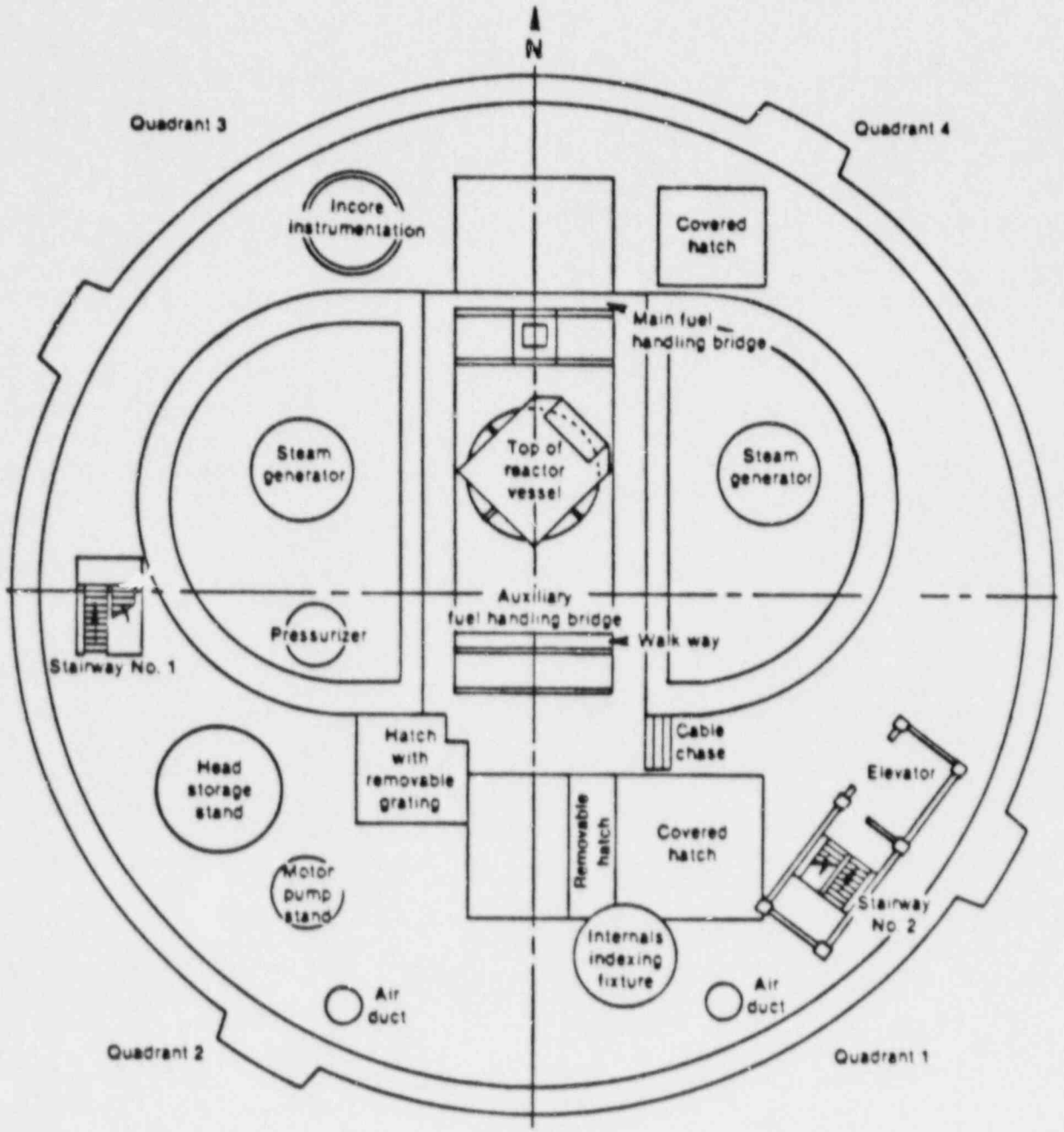

Figure A.2.6. Elevation 347 Containment Floor Plan View

blow cooled containment air into a plenum. Ductwork from the plenum then directs the cooled air to the bottom of each steam generator compartment and the reactor cavity as well as to the basement. All units are located in Elevation 305.

In the event of a LOCA signal (a 4 psig increase in containment pressure), units four and five will be started 30 seconds after the signal. The fans of all five units will be reduced from high speed to low speed operation, and the cooling water rate through the unit coils will be increased. A portion of the LOCA air flow will be diverted into the dome region above Elevation 347. The RBC system will operate in LOCA mode until the reactor building pressure falls below a set value at which time the units are returned to a normal operating mode.

The RBS system consists of two spray systems which operate independently. Emergency operation is initiated by a high containment pressure signal (a 30 psi increase in containment pressure). Water leaves the spray headers 30 seconds after the high pressure signal.

The spray headers are located in the dome region. Water from the headers primarily cools the containment atmosphere above the Elevation 347 floor, but some spray carry-over into the steam generator and refueling canal compartments occurs. Spray water which does not evaporate collects on walls and floors and drains to the building sump at Elevation 280.

A.2.2.3 Containment Model

All of the information needed to construct the TMI-2 containment model was obtained from the TMI-2 Final Safety Analysis Report and communications with TMI-2 personnel.

Compartments are generally chosen to coincide with key internal structures such as walls and floors. Flow junctions or paths occur at compartment boundaries and are based on physical boundaries such as doors, hatches, or penetrations. Most flow junctions are modeled as two-way flow junctions allowing air to flow in either direction through the junction. Five basic heat transfer surfaces were used in the analyses: (1) the liner surface of the outer structure, (2) concrete surfaces of the internal structures, (3) steel structure and equipment surfaces, (4) sump (water) surfaces, and (5) the Barton 763 pressure transducer model surfaces. The Barton models will be discussed in greater detail in Section A.2.3.

Two TMI-2 containment models were developed for the hybrid analysis. These two models were constructed to determine the sensitivity of hydrogen mixing to compartment volume and ventilation.

The first TMI-2 containment model divided the TMI-2 containment building into eight compartments. The eight compartments are connected by 17 flow junctions and contain 45 heat transfer surfaces.

The reactor cavity forms compartment 1. The reactor cavity compartment has three heat transfer surfaces: (1) concrete liner wall, (2) the reactor vessel, and (3) the sump.

Compartments 2 and 3 model the two steam generator compartments, SG1A and SG1B. The steam generator compartment with the pressurizer (SG1A) is compartment 2. Heat transfer surfaces include: (1) equipment, (2) concrete walls, (3) sumps, and (4) pressure transducer models.

The refueling canal and fuel transfer pit make up compartment 4. Its heat transfer surfaces include: (1) a steel liner, (2) equipment surfaces, and (3) a sump surface.

Elevations 280, 305, and 347 form compartments 5, 6, and 7, respectively. Heat transfer surfaces include: (1) the liner wall, (2) concrete walls, (3) steel surfaces, and (4) the pressure transducer model. Compartment 5 also includes a sump (water surface).

Compartment 8 is formed by the enclosed stairwell and elevator. This compartment includes the following heat transfer surfaces: (1) concrete walls and (2) steel surfaces. A summary of the containment model is presented in Table A.2.2.

The second TMI-2 containment model divided the TMI-2 containment building into 11 compartments. The 11 compartments are connected by 21 flow junctions and contain 67 heat transfer surfaces. Compartments 1, 3, 4, 6, 7, and 8 of the first containment model are identical to compartments 1, 3, 4, 6, 7, and 8 of the second containment model.

Compartment 2 (SG1A) of the first containment model was divided vertically into three equal volume compartments (compartments 2, 9, and 10).

Compartment 5 (Elevation 280) of the first containment model was divided into two compartments (compartments 5 and 11).

A summary of the containment model is presented in Table A.2.3.

A.2.3 Equipment Models

The equipment models used in the hybrid analyses were based on the Barton 763 gauge pressure transmitter. This instrument has been tested extensively in the Hydrogen Burn Survival program and its thermal response to simulated hydrogen burn heat flux pulses is well documented.[5]

Table A.2.2

TMI-2 Containment Model 1 Summary

	Compartment	Volume (m^3)	Surface	Description	Area (m^2)
1.	Reactor Cavity	143.	1	C	256.
			2	E	194.
			3	S	29.
2.	SG1A	2885.	4	C	1111.
			5	E	654.
			6	St	389.
			7	S	139.
			5	B	0.0285
			6	B	0.0285
			7	B	0.0285
			8	B	0.0285
3.	SG2A	2885.	9	C	1111.
			10	E	654.
			11	St	389.
			12	S	139.
			13	B	
			14	B	
			15	B	
			16	B	
4.	Refueling Canal	2072.	17	L	886.
			18	E	146.
5.	Elevation 280	6528.	19	L	855.
			20	C	2470.
			21	E	781.
			22	S	985.
			23	B	
			24	B	
			25	B	
			26	B	
6.	Elevation 305	8426.	27	L	1556.
			28	C	2908.
			29	E	1689.
			30	B	
			31	B	
			32	B	
			33	B	
7.	Elevation 347	33140.	34	L	4884.
			35	C	1681.
			36	E	850.
			37	B	
			38	B	
			39	B	
			40	B	

Table A.2.2

TMI-2 Containment Model 1 Summary (Concluded)

Compartment	Volume (m^3)	Surface	Description	Area (m^2)
8. Stairwell	623.	41	C	714.
		42	E	133.

B: Barton 763 equipment model
St: nuclear steam system surface
E: steel structure
C: concrete
S: sump
L: containment liner

Table A.2.3

TMI-2 Containment Model 2 Summary

Compartment	Volume (m^3)	Surface	Description	Area (m^2)
1. Reactor Cavity	143.	1	C	256.
		2	E	194.
		3	S	29.
2. SG1A-1	962.	4	C	370.
		5	E	218.
		6	St	130.
		7	S	139.
		5	B	0.0285
		6	B	0.0285
		7	B	0.0285
		8	B	0.0285
3. SG2A	2885.	9	C	1111.
		10	E	654.
		11	St	389.
		12	S	139.
		13	B	
		14	B	
		15	B	
		16	B	
4. Refueling Canal	2072.	17	L	886.
		18	E	146.
5. Elevation 280-1	2906.	19	L	317.
		20	C	1000.
		21	E	348.
		22	S	404.
		23	B	
		24	B	
		25	B	
		26	B	

Table A.2.3

TMI-2 Containment Model 2 Summary (Concluded)

Compartment	Volume (m^3)	Surface	Description	Area (m^2)
6. Elevation 305	8426.	27	L	1556.
		28	C	2908.
		29	E	1689.
		30	B	
		31	B	
		32	B	
		33	B	
7. Elevation 347	33140.	34	L	4884.
		35	C	1681.
		36	E	850.
		37	B	
		38	B	
		39	B	
		40	B	
8. Stairwell	623.	41	C	714.
		42	E	133.
9. SG1A-2	962.	43	C	370.
		44	E	218.
		45	St	130.
		46	B	
		47	B	
		48	B	
		49	B	
10. SG1A-3	962.	50	C	370.
		51	E	218.
		52	St	130.
		53	B	
		54	B	
		55	B	
		56	B	
11. Elevation 280-2	3621.	57	L	538.
		58	C	1470.
		59	E	433.
		60	S	581.
		61	B	
		62	B	
		63	B	
		64	B	

B: Barton 763 equipment model
St: nuclear steam system surface
E: steel structure
C: concrete
S: sump
L: containment liner

Four models of the Barton were developed. A one-dimensional model of the Barton 763 cover plate alone was the first model. This model was included to provide continuity with a prior analysis of equipment temperature response to hydrogen deflagrations in an ice condenser containment[6]. A second model treated all of the steel in the Barton 763 casing as a one-dimensional steel plate with a frontal area equal to the Barton 763. This model is referred to as the case-as-plate (CAP) model. The third model treated the entire steel casing as a lumped mass with uniform temperature response throughout the mass to incident heat flux. The fourth model was a one-dimensional three-layer representation of the Barton 763. This model accounted for the air gap between the casing and internal electronics.

The fourth model was used in a separate analysis to bound its conservatism. In the analysis, the model was analytically exposed to an incident heat flux pulse used at the Sandia Central Receiver Test Facility (CRTF) for prior hydrogen burn simulation equipment experiments. The surface temperature response of the model was calculated and compared to the measured surface temperature rise of an actual Barton 763 exposed to the flux pulse at the CRTF. The peak surface temperature of the model was calculated to be approximately 11°K (20°F) higher than the actual Barton 763 surface temperature. The model and Barton 763 thermal time response characteristics were equivalent. The comparison of the model and the Barton 763 is shown in Figure A.2.7. The one-dimensional three-layer model is considered to be the most realistic of the four models and its surface temperature response to hydrogen burning will be reported.

The four Barton 763 models were placed into four containment locations for this analysis. The locations were (1) the basement level(s), (2) the second floor, (3) the steam generator compartment(s) with the pressurizer (SG1A), and (4) the steam generator compartment without the pressurizer (SG1B). These four locations were judged to be the most likely locations for the safety related equipment after reviewing the GEND Planning Report (GEND-001).

A.3 MARCON Source Term Calculations

The steam and hydrogen source terms for two small break loss-of-coolant accidents (S_1D and S_2D) were calculated in this analysis. One S_1D scenario was calculated with a 4-inch diameter break (S_1D4), and two S_2D scenarios were calculated with 1-inch diameter (S_2D1) and 2-inch diameter (S_2D2) breaks. Failure of the ECC injection system until 75 percent clad oxidation was also assumed.

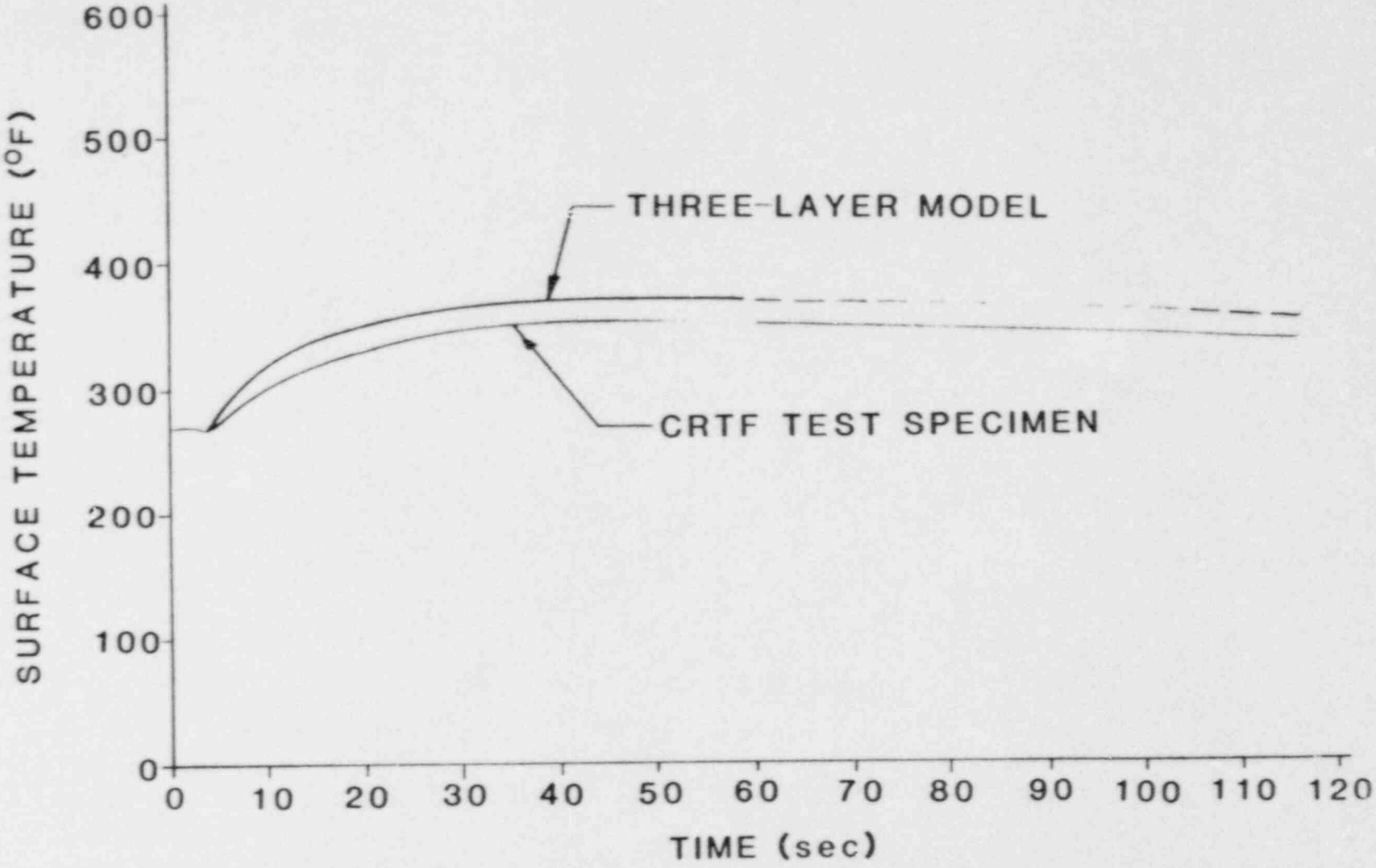

Figure A.2.7. Three-Layer Model/Experiment Barton 763 Temperature Response Comparison

A.3.1 S_2D2 Source Terms

The S_2D2 water mass flow rate into containment is shown in Figure A.3.1. The initial flow rate was approximately 17,500 lb/min and decreased to 14,000 lb/min as the primary system depressurized. The flow remained constant until the break uncovered at 20 minutes allowing the flow to change from liquid to steam. The steam flow continued to decrease as the primary system pressure decreased. At 125 minutes, steam flow stopped when the system pressure decreased below the set pressure of the core flood tanks (CFTs) and their liquid was injected into the primary system. The system pressure increased after CFT injection allowing steam flow to continue out of the break from 130 to 250 minutes. The high pressure injection (HPI) pumps were started at approximately 255 minutes. The break was quickly covered and primary system water flowed out of the break.

The calculated hydrogen mass flow rate into the containment is shown in Figure A.3.2. Hydrogen flow was initiated at 95 minutes. At 125 minutes, CFT injection occurred and covered the core, thereby quenching the core and stopping hydrogen production. The hydrogen mass flow rate decreased to zero by 155 minutes as the amount of hydrogen left in vessel prior to CFT injection was forced out of the break. At 225 minutes, the hydrogen flow began to increase due to the generation of more hydrogen in the primary vessel as the core uncovered a second time. As the flow from the HPI pumps was initiated at 255 minutes, the hydrogen flow out of the break decreased as the core was covered and Zircaloy oxidation was stopped.

A.3.2 S_2D1 Source Terms

Figure A.3.3 shows the calculated water flow rate into the containment for the S_2D1 accident. The initial water flow rate out of the break for the S_2D1 was smaller than that of the S_2D2 (4000 lb/min versus 14,000 lb/min, respectively) and break uncovery occurred later in the S_2D1 than the S_2D2 (80 minutes versus 20 minutes, respectively) due to the smaller break diameter of the S_2D1. Steam was released through the break into containment from 80 minutes to 388 minutes and the primary pressure did not fall below the CFT pressure set point during this period of steam release. HPI flow was initiated at 395 minutes to arrest the clad oxidation. The cycling of water flow after 425 minutes was due to the calculated covering and uncovering of the break. Liquid flowed out of the covered break at high mass flow rates, and gases flowed out of the uncovered break at relatively low mass flow rates.

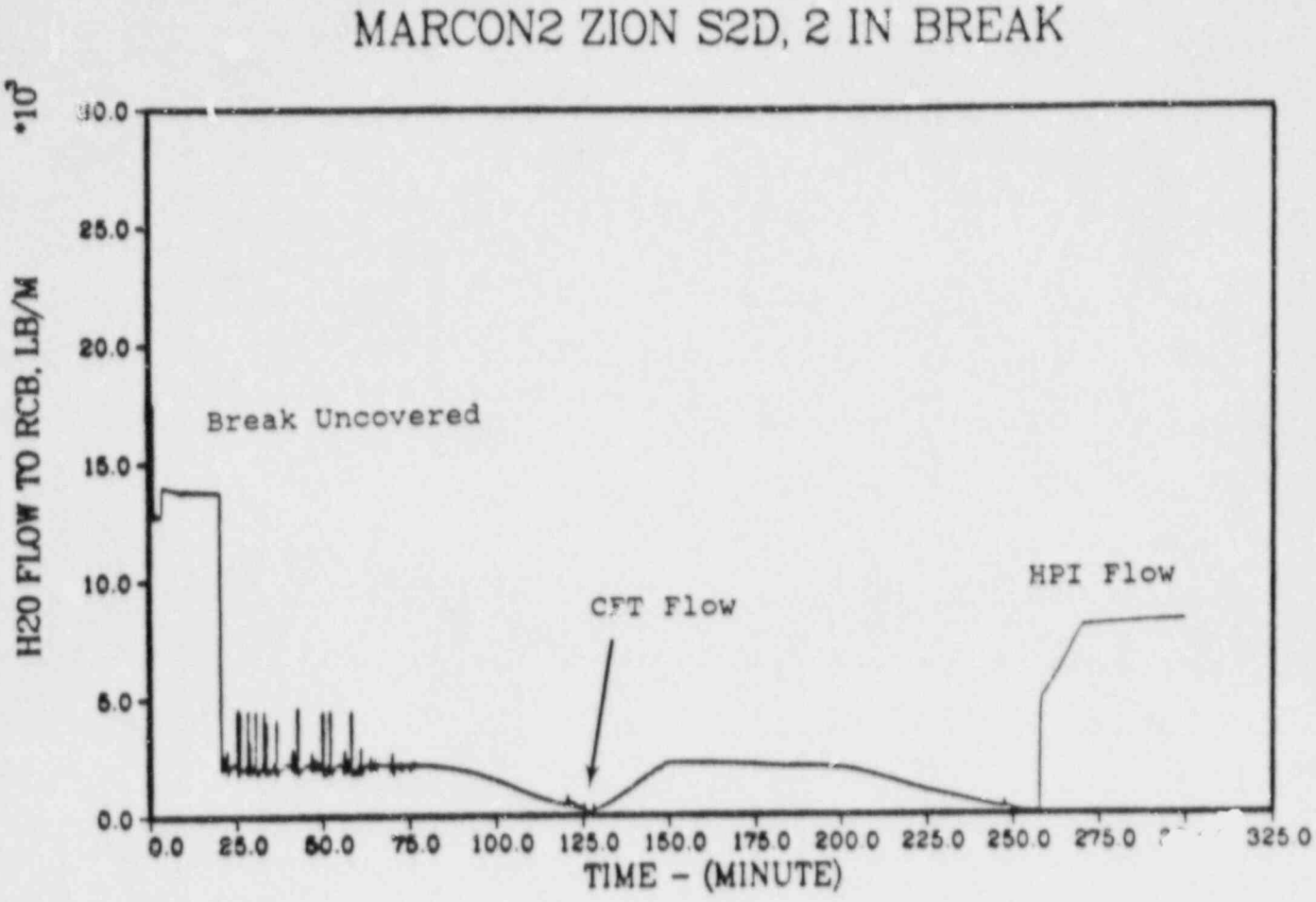

Figure A.3.1. Calculated Water Mass Flow Rate for a Small Break LOCA, S_2D2

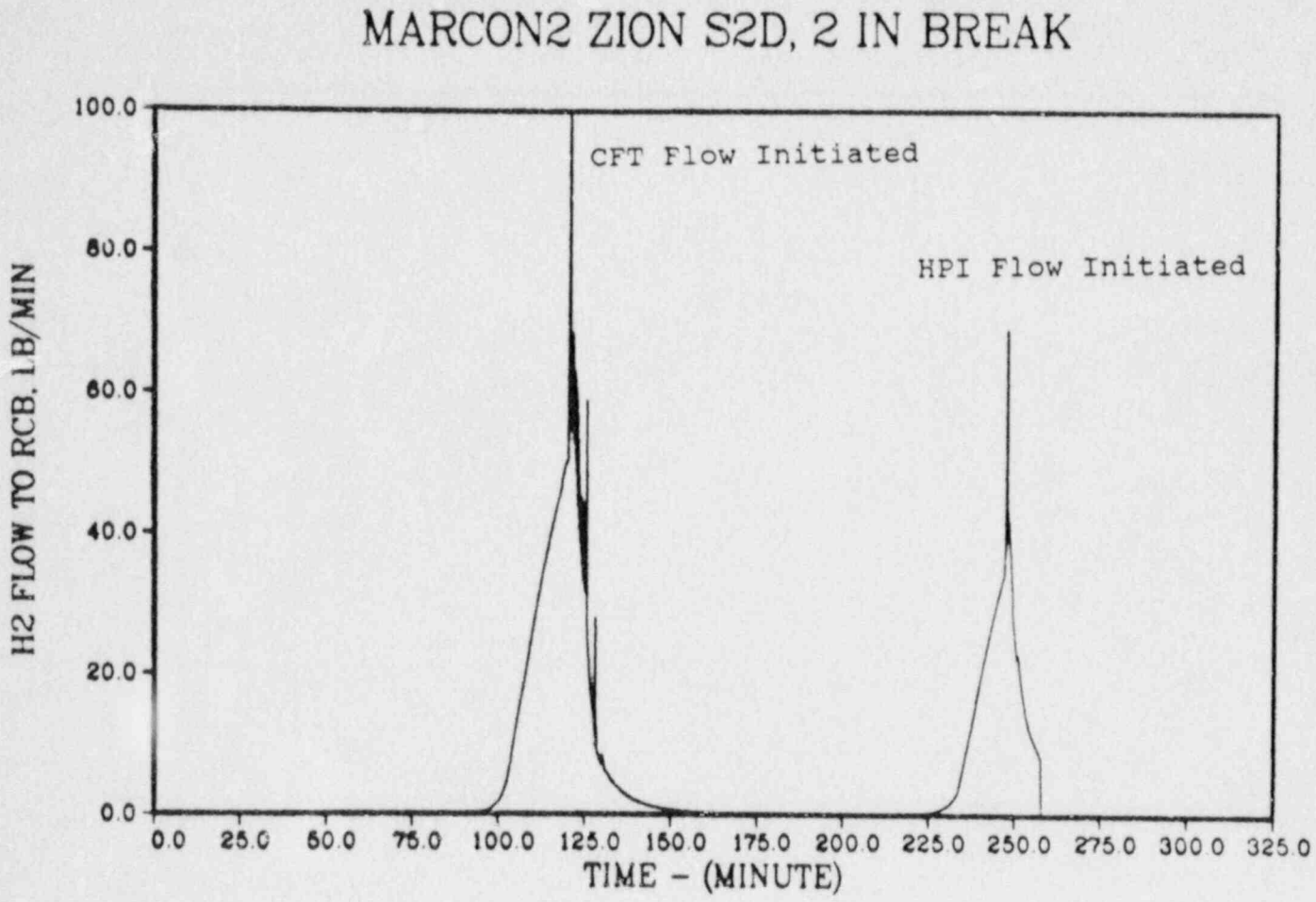

Figure A.3.2. Calculated Hydrogen Mass Flow Rate for a Small Break LOCA, S_2D2

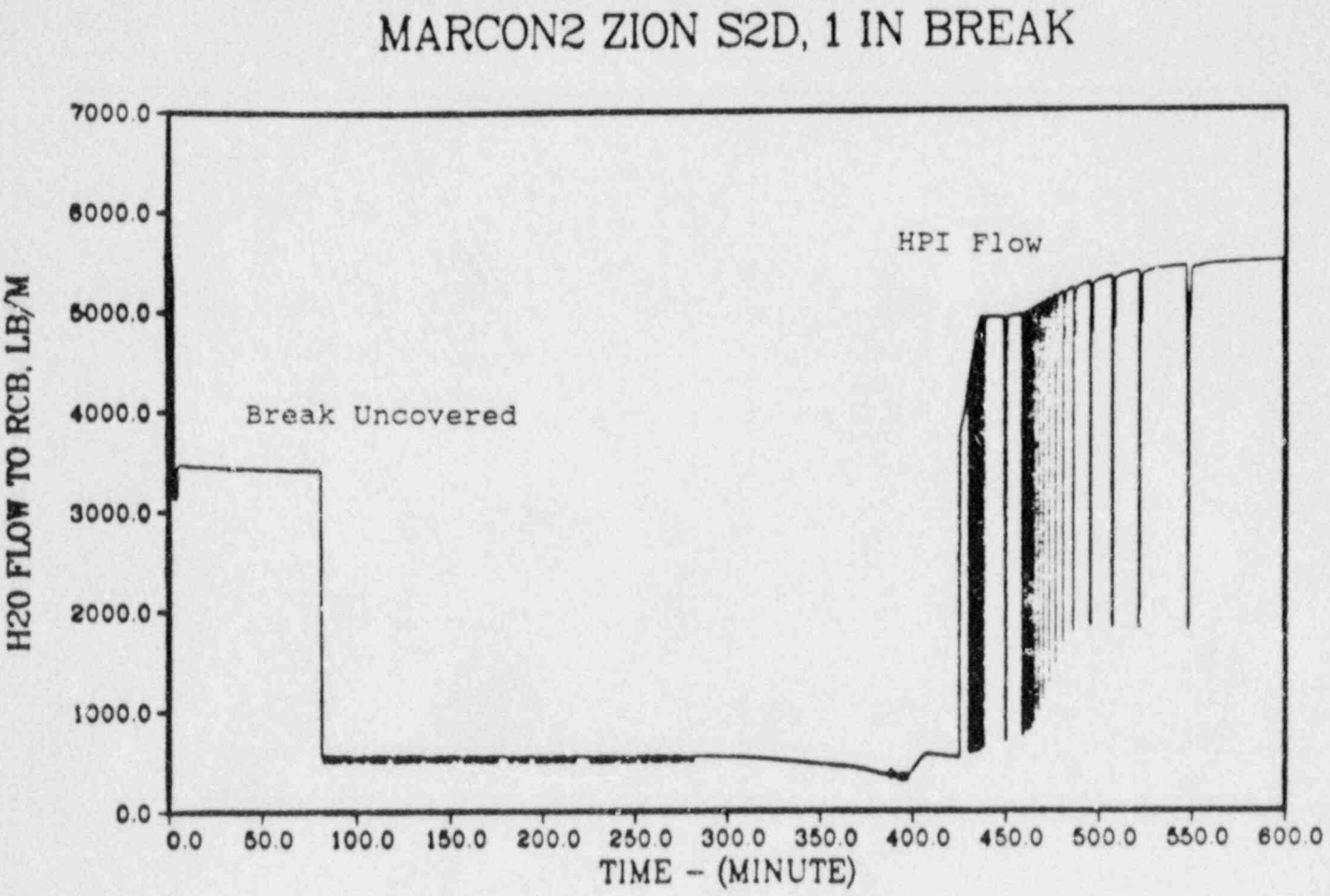

Figure A.3.3. Calculated Water Mass Flow Rate for a Small Break LOCA, S_2D1

The S_2D1 hydrogen mass flow rate into containment is shown in Figure A.3.4. Hydrogen flow began at 345 minutes and was at a peak flow of 41 lb/min when the clad oxidation was stopped due to quenching of the core from HPI initiation. The hydrogen remaining in the primary vessel after core quench at 395 minutes was continuously forced out of the break until the break was covered at 425 minutes. After 425 minutes, hydrogen was released sporadically as the break was uncovered and covered by the HPI flow.

A.3.3 S_1D4 Source Terms

The S_1D4 water mass flow rate into containment is shown in Figure A.3.5. The larger 4-inch diameter break allowed the core break to uncover at 5 minutes due to an initial 50,000 lb/min water flow rate. The system depressurized rapidly resulting in CFT injection at 30 minutes. The break remained uncovered and steam flowed into containment from 30 to 110 minutes. The steam flow stopped as the in-core water/steam inventory was depleted. HPI flow was initiated at 129 minutes. No additional water or steam was added into containment after the break was covered due to an error found in the MARCH input data deck. Steam/water release after HPI injection similar to that of Figure A.3.3 should have been calculated. The MARCH analysis was still used because this error occurred after hydrogen generation and release to containment was stopped.

The hydrogen flow rate into containment (shown in Figure A.3.6) began at 100 minutes and reached a maximum flow rate of 110 lb/min at 115 minutes. The hydrogen flow rate decreased as the incore steam inventory decreased (between 115 minutes and 129 minutes) allowing less clad oxidation to occur. Clad oxidation stopped at 129 minutes when HPI flow covered and quenched the core.

A.4 Transport Results

The HECTR calculated containment pressure response and gas transport results for the small-break-initiated transients are discussed in this section. The accident scenarios analyzed in this report are listed in Table A.4.1. Three small-break loss-of-coolant scenarios were considered. The effects of different break locations were examined for these small-break scenarios. The break locations were placed in: (1) the steam generator compartments SG1A and SG1B, (2) the reactor cavity, and (3) the basement. All of the sequences listed in Table A.4.1 began at the initial conditions given at the bottom of the table.

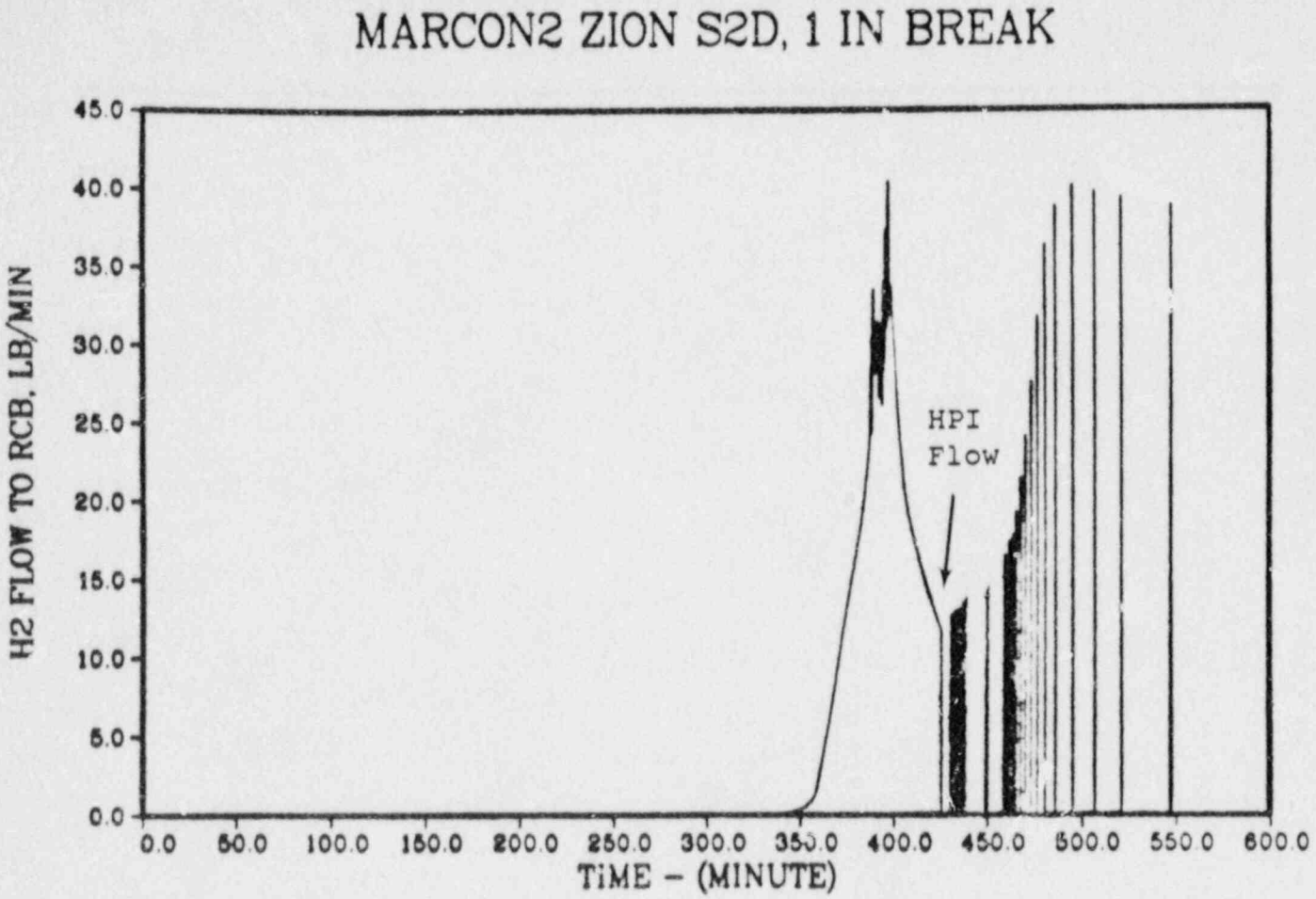

Figure A.3.4. Calculated Hydrogen Mass Flow Rate for a Small Break LOCA, S_2D1

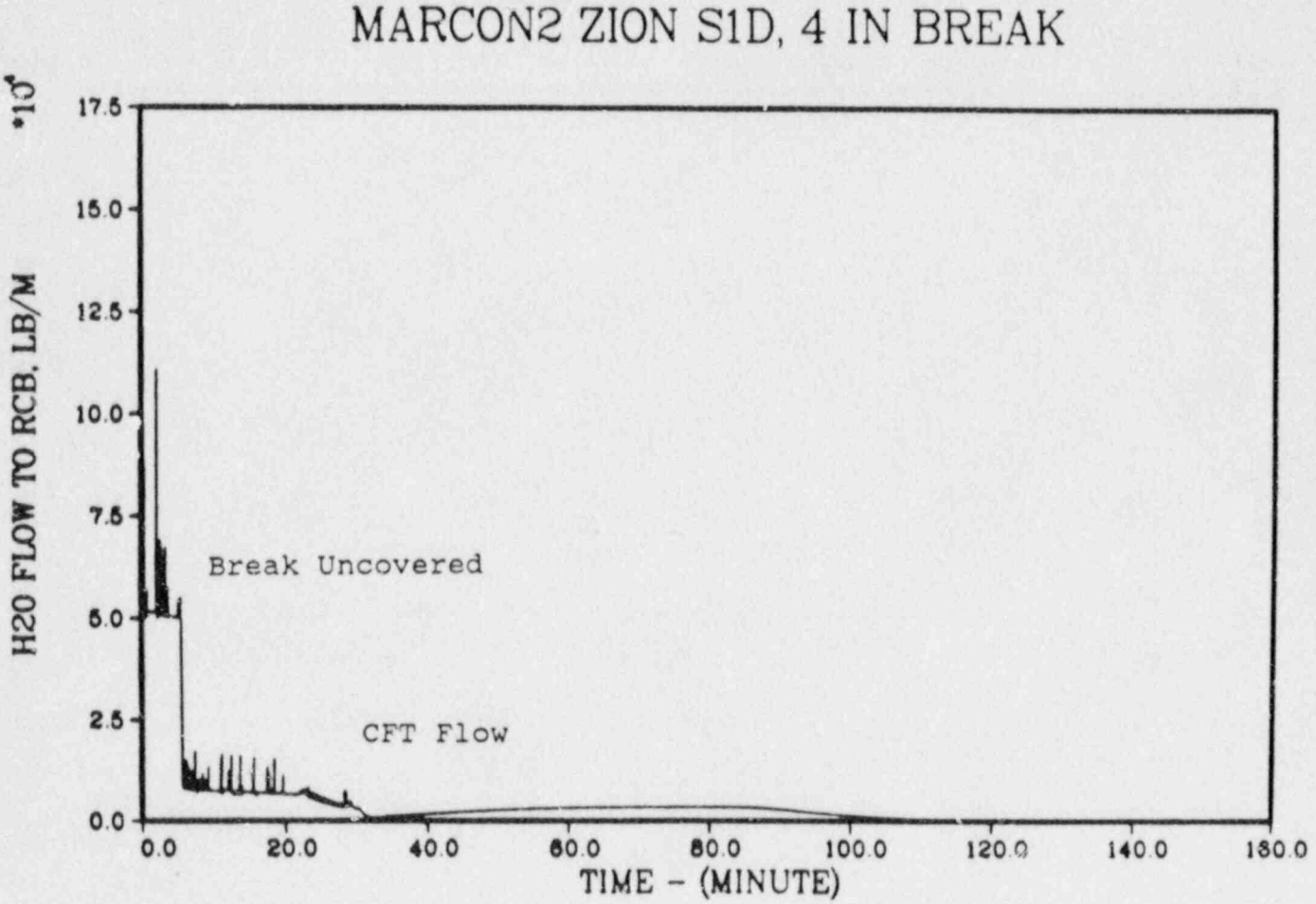

Figure A.3.5. Calculated Water Mass Flow Rate for a Small Break LOCA, S_1D4

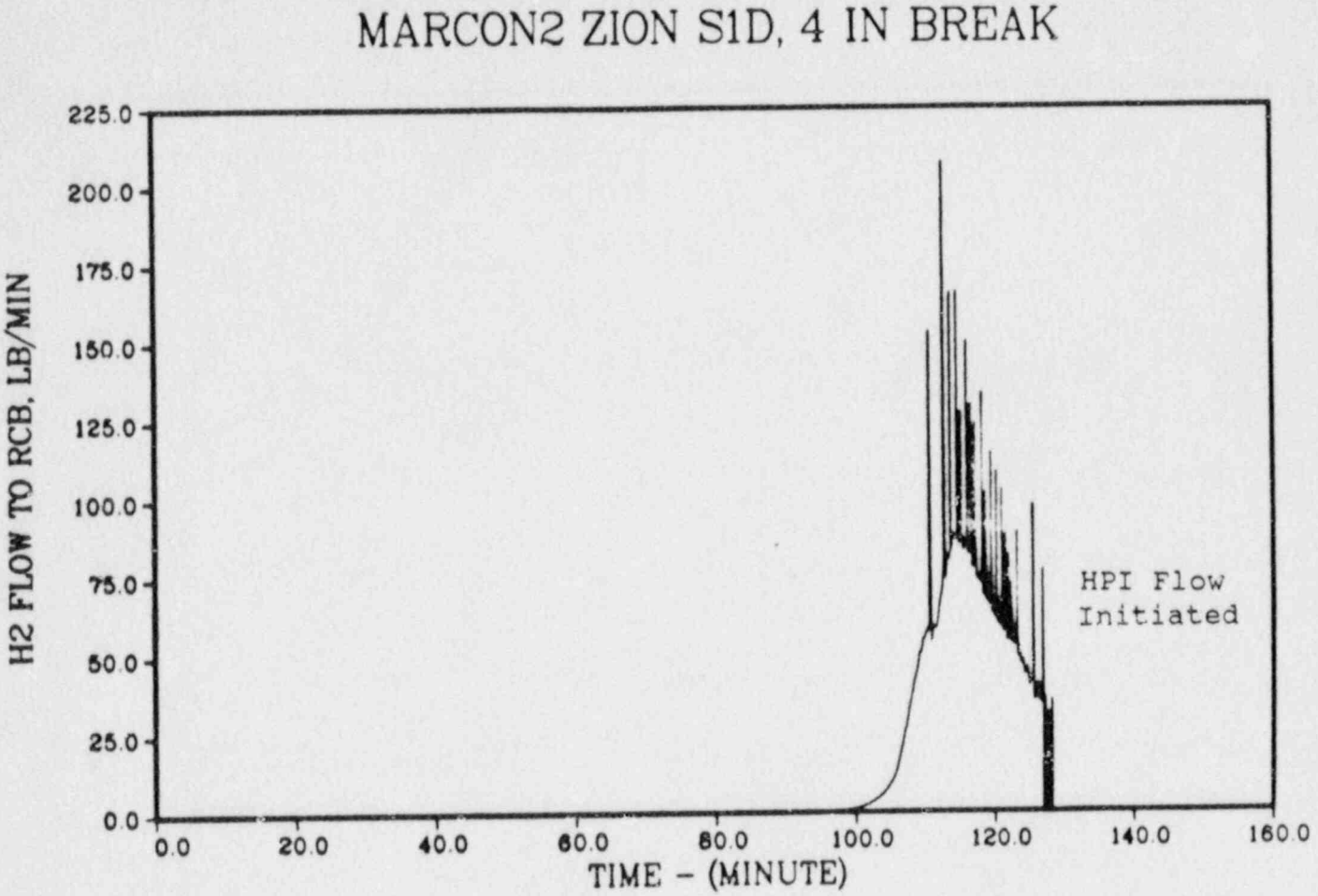

Figure A.3.6. Calculated Hydrogen Mass Flow Rate for a Small Break LOCA, S_1D4

Table A.4.1

Description of Hydrogen Transport Cases Analyzed

Case	Accident Sequence	Source Compartment	ESF System On	Containment Model
1A	S_2D2	2	RBC, RBS*	1
1B	S_2L2	1	RBC, RBS*	1
1C	S_2D2	5	RBC, RBS*	1
1D	S_2D2	3	RBC, RBS*	1
2A	S_2D1	2	RBC, RBS*	1
2B	S_2D1	1	RBC, RBS*	1
2C	S_2D1	5	RBC, RBS*	1
3A	S_1D4	2	RBC, RBS*	1
3B	S_1D4	1	RBC, RBS*	1
3C	S_1D4	5	RBC, RBS*	1
3D	S_1D4	5	RBC, RBS*	2
3E	S_1D4	2	RBC, RBS*	2

Containment Initial Conditions

Temperature	311.°K
Pressure	101. kPa
Mole Fractions	
Steam	6.5%
Nitrogen	73.9%
Oxygen	19.6%

RBS* - Reactor Building Spray System did not activate during LOCA
RBC - Reactor Building Fan Cooler System
Containment Model 1 divided containment into eight compartments
Containment Model 2 divided containment into 11 compartments

Prior analyses for containment loading have been performed to calculate the final uniform hydrogen concentrations in containments for LOCAs with 75 percent Zircaloy oxidation. The Zion nuclear power plant was included in this study but the TMI-2 nuclear power plant was not. The final hydrogen mole fraction in the Zion containment was calculated to be 0.10 (10 percent). The 10 percent value is based upon dry air calculations without steam present in containment. The Zion containment has a volume of 2,600,000 ft^3, and by taking the ratio of the Zion to TMI-2 containment volumes

(1.3), a possible maximum dry air hydrogen concentration of 13 percent can occur in the TMI-2 containment using the Zion core model. The presence of steam in appreciable amounts during the LOCA (10 percent to 20 percent) would reduce the final hydrogen concentrations by 1 percent to 2 percent total mole fraction.

Based on prior experience, hydrogen concentrations in the source compartment can often result in peak hydrogen mole fractions greater than 0.14. Hydrogen mole fractions above 0.14 indicate that hydrogen detonations may be possible. HECTR cannot analyze detonations but does indicate when a detonable mixture of hydrogen, steam, and oxygen may be present in a compartment. HECTR gives detonable mixture messages when the hydrogen mole fraction is greater than 0.14, the oxygen mole fraction is greater than 0.09, and the steam mole fraction is less than 0.30. However, detonations are also geometry, pressure, and temperature dependent and studies are currently in progress to further characterize detonable gas mixtures.

A.4.1 S_2D2 Small Break

Four S_2D2 hydrogen transport cases were analyzed. The four cases examined the effect of break locations on hydrogen concentrations. The four break locations were: (1) SG1A (Case 1A), (2) the reactor cavity (Case 1B), (3) the basement (Case 1C), and (4) SG1B (Case 1D). All S_2D2 cases used containment model 1.

A typical pressure response of the containment building gas for the S_2D2 scenarios for all break locations is shown in Figure A.4.1. The calculated pressure response was dominated by the water/steam mass flow rates calculated by MARCON 2.0. The containment pressure increased continuously until the break elevation was uncovered at 1500s and flow into containment from the primary changed from liquid to steam. After 1500s, the containment pressure response resembles the MARCON 2.0 steam release rate in Figure A.3.1.

Typical calculated water, steam, and oxygen mole fractions in the containment dome are shown in Figure A.4.2 and are almost identical for all four break location calculations. The steam mole fraction indicates a strong dependence on the steam/water flow rate from the primary break. Hydrogen released from the primary from 5700 to 9000 seconds was uniformly mixed in the dome by 9000 seconds. At 13,500 seconds, the hydrogen mole fraction increased due to hydrogen being generated when the core uncovered a second time. The hydrogen mole fraction trend in the dome was representative of most compartments in containment except for the source compartment. The difference in the hydrogen mole fractions

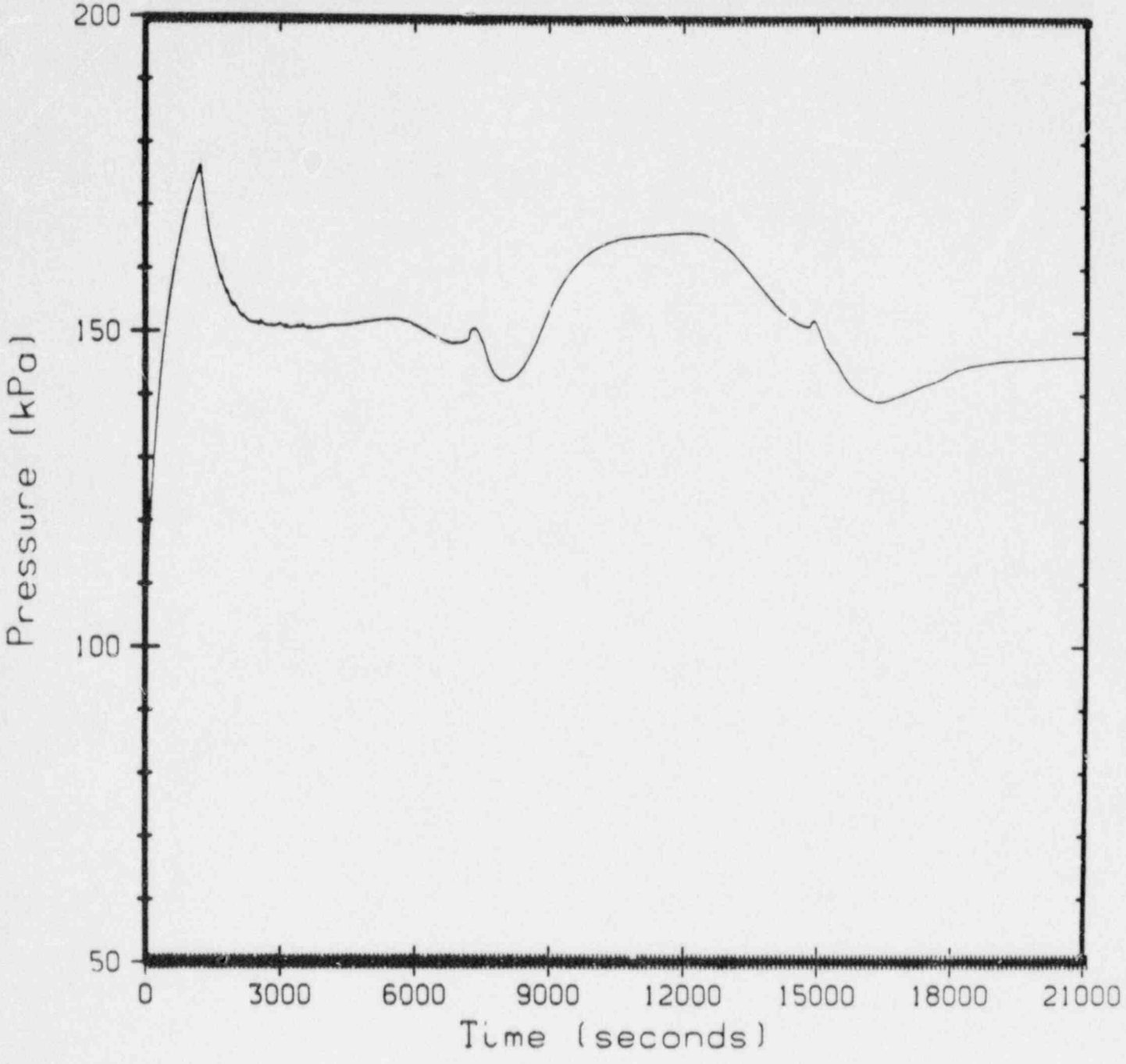

Figure A.4.1. Typical Containment Gas Pressure Response to S_2D2 Source Terms

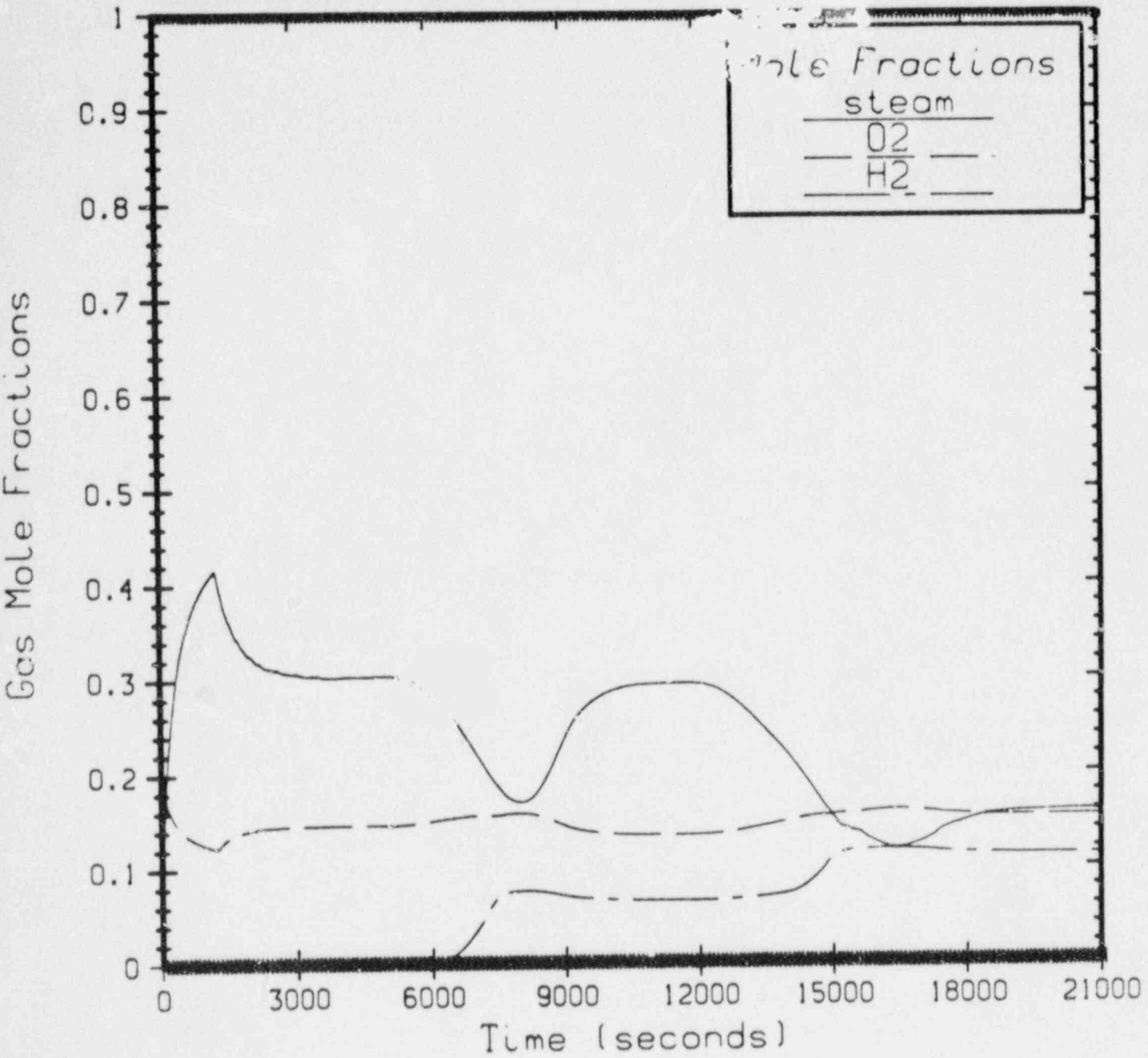

Figure A.4.2. Typical S_2D2 Dome Compartment Gas Mole Fractions

was less than approximately 0.01 total mole fraction throughout the containment by the end of the calculation. The highest average hydrogen mole fractions occurred at the end of the calculation and were approximately 11 percent.

During the early stages of the hydrogen transport calculations, steam mole fractions decreased in magnitude from higher to lower containment elevations by approximately 0.1 total mole fraction except for Case 1C (in which the source compartment was located in the basement). The lower elevations of containment were less influenced thermally by the source terms and remained cooler, which enhanced steam condensation from the containment gas. Steam mole fractions were calculated to be more uniform throughout the containment toward the end of the transport studies but did not achieve the uniformity observed for hydrogen. The lack of steam uniformity was due to: (1) steam source terms being present until the end of the transport calculations which created a steam gradient from the source compartment to the rest of containment, and (2) different condensation rates in each compartment. This trend for steam was also calculated for the S_2D1 and S_1D4 scenarios.

Typical calculated gas mole fractions in a source compartment are shown in Figure A.4.3. Both the hydrogen and steam mole fractions reflected the relative magnitudes of the leak flow rates of steam and hydrogen from the primary system. The maximum hydrogen mole fractions and minimum steam mole fractions at 7000 and 15,000 seconds are dependent on source compartment size and ventilation. Small or poorly ventilated source compartments will have larger hydrogen and steam concentrations. The reactor cavity was the smallest and worst vented source compartment which resulted in the highest peak hydrogen mole fraction of 0.37 at approximately 15,000 seconds. The basement was the largest source compartment but had less venting compared to the SG1A source compartment. The peak hydrogen mole fraction for the basement was 0.16. The SG1A source compartment had a peak hydrogen mole fraction of 0.12.

A summary of peak source compartment hydrogen mole fractions is listed in Table A.4.2. Steam mole fractions for the peak hydrogen mole fractions in Table A.4.2 were below 0.3.

The dominant flow directions in containment during the release of water and hydrogen for the break location in SG1A (Case 1A) are shown in Figure A.4.4. The flow directions are affected by three factors: (1) the hot steam generator surfaces, (2) the reactor building cooler flows, and (3) the leak rates. The D-ring wall of SG1A contained the flow and forced the hot gases up through SG1A into the dome region.

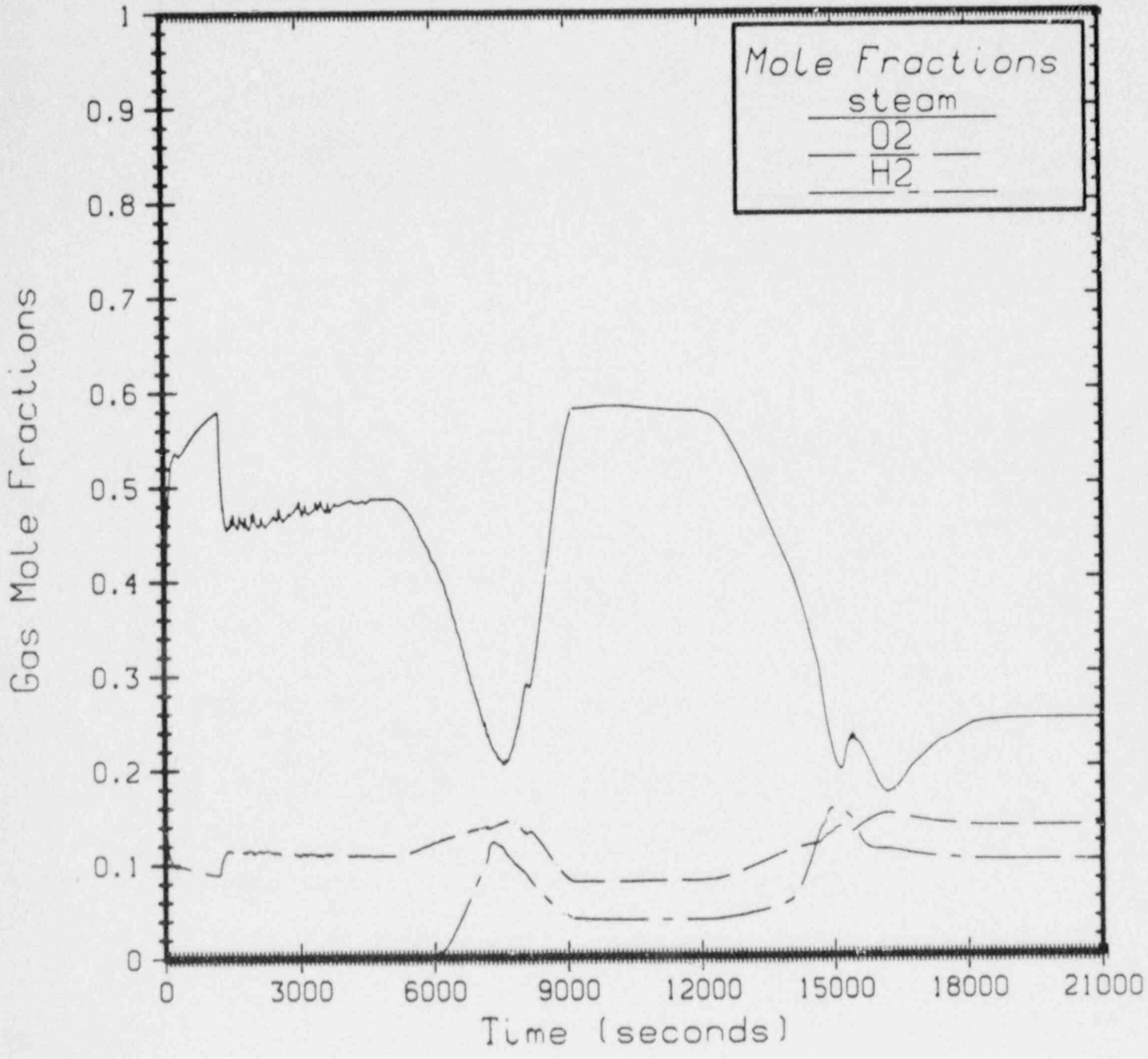

Figure A.4.3. Representative S_2D2 Source Compartment Gas Mole Fractions

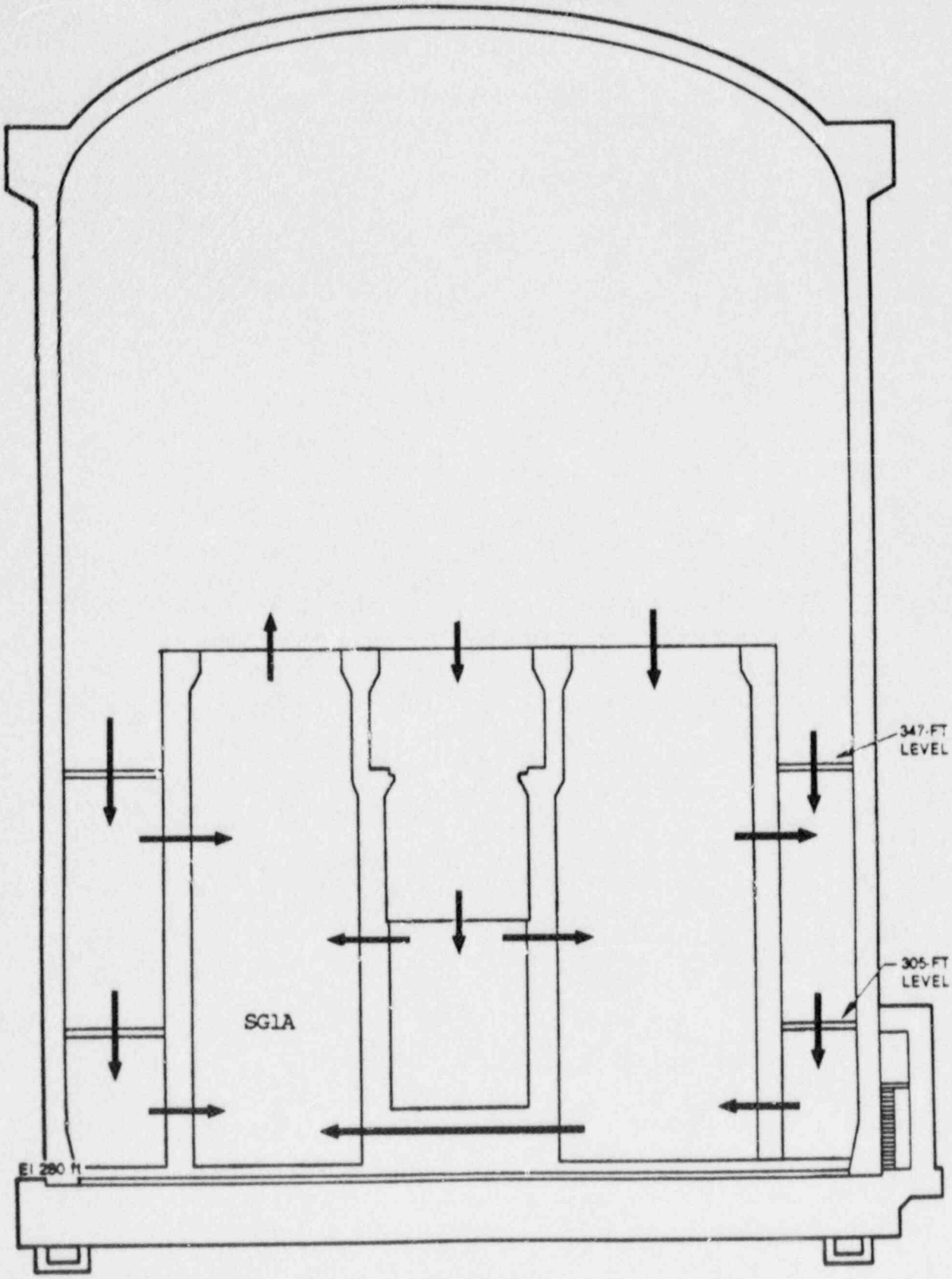

Figure A.4.4. S_2D2 Case 1A Containment Circulation Flow

Table A.4.2

Transport Peak Hydrogen Mole Factions
in Various Source Compartments

Case	Source Compartment	Hydrogen Mole Fraction	Containment Model
1A	Basement	0.12	1
1B	Reactor Cavity	0.37	1
1C	SG1A	0.16	1
2A	Basement	0.11	1
2B	Reactor Cavity	0.27	1
2C	SG1A	0.16	1
3A	Basement	0.13	1
3B	Reactor Cavity	0.61	1
3C	SG1A	0.16	1
3D	Basement	0.21	2
3E	SG1A	0.13	2

Containment Model 1 divided containment into eight compartments
Containment Model 2 divided containment into 11 compartments

The gases in the dome then were forced to the bottom of containment through the Elevation 347 and 305 floors and SG1B. Flow arriving back to the basement was then directed into the bottom of SG1A.

The dominant flow directions in containment for the break location in the reactor cavity (Case 1B) are similar to those described above for the break in SG1A. In Case 1B, the hot gases were directed up through SG1B into the dome region. Gases from the dome then returned to the basement through SG1A and the Elevation 347 and 305 floors

The dominant flow directions in containment for the break location in the basement (Case 1C) were different than those of Case 1A and Case 1B and are illustrated in Figure A.4.5. The primary gases from the break entered the basement and were directed into the second floor compartment (compartment 6). Note that compartment 6 contains the Reactor Building Fan Coolers (RBFC). The RBFCs direct containment gases into SG1A, SG1B, the dome region, the reactor cavity, and the basement. In Case 1C, gases from SG1A, SG1B, and the reactor cavity were directed into the dome region, and gases from the dome region then flowed into compartment 6. This floor pattern is similar to flow patterns during normal reactor operation.

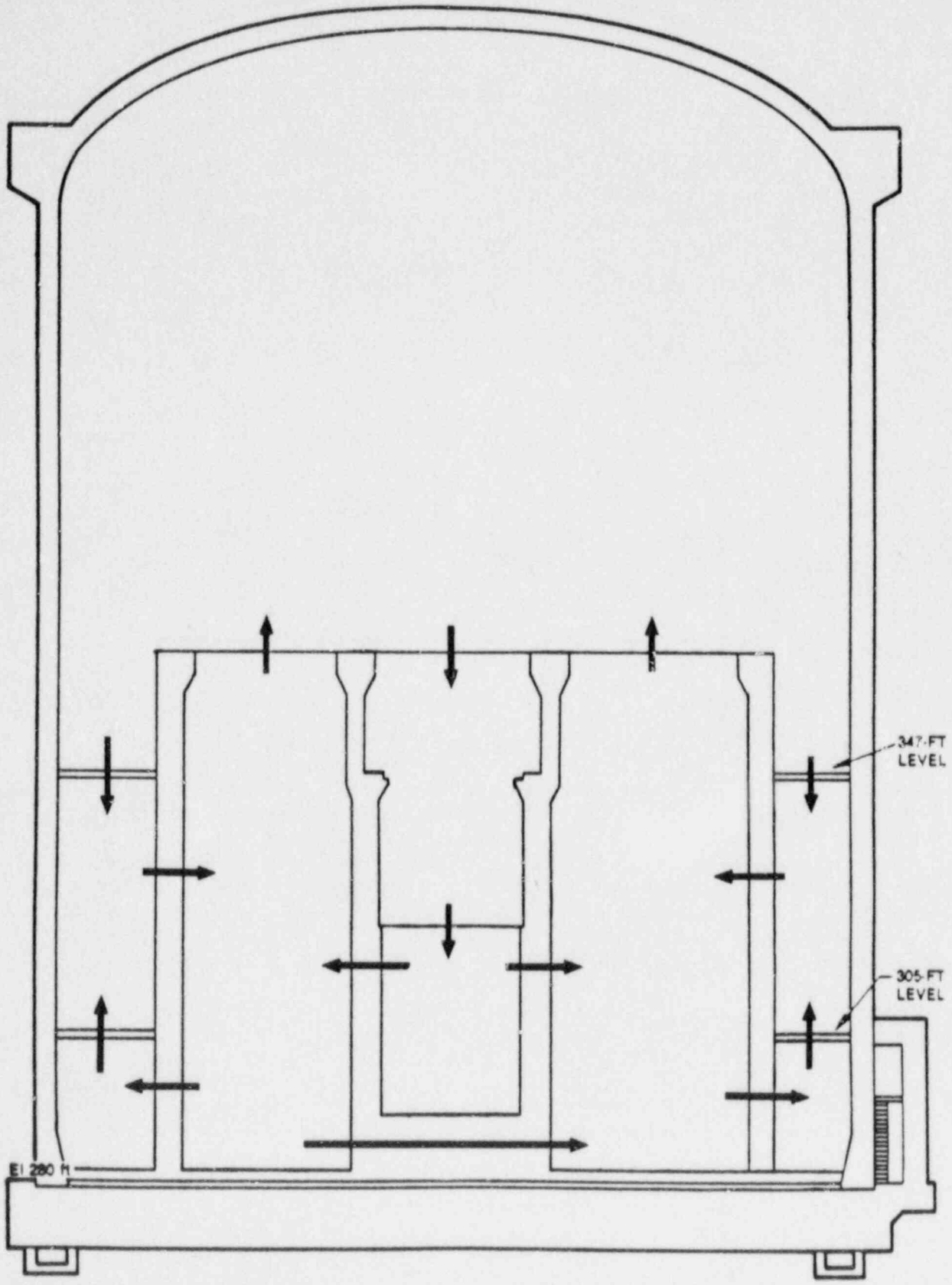

Figure A.4.5. S_2D2 Case 1C Containment Circulation Flow

A.4.2 S_2D1 Small Break

A typical S_2D1 containment building pressure response for all break locations is shown in Figure A.4.6. The water/steam mass flow rates dominated the calculated pressure response. The pressure continuously increased until the break elevation was uncovered at 4800 seconds at which time the flow into containment from the primary system changed from liquid to steam. The reduction in mass flow combined with condensation due to the RBC system and relatively cool containment walls resulted in a decrease in the containment pressure. Containment pressure increased again at 23,000 seconds when hydrogen was released into containment and at 26,000 seconds when the HPI pumps were started.

Typical calculated gas mole fractions in the containment dome for the SG1A break location are shown in Figure A.4.7. The dome gas mole fractions are almost identical for the other break location transport runs. As expected, both the hydrogen and steam mole fractions reflected the relative magnitudes of the leak flow rates of steam and hydrogen. The steam mole fraction reached its peak after 25,000 seconds when the HPI pumps were initiated. The hydrogen concentration reached a local maxima at 25,000 seconds when HPI was initiated and reached a final average (or global) peak at 36,000 seconds as the remaining hydrogen gas in vessel (after core quench) was released into containment.

The dome hydrogen mole fraction profile for the S_2D1 is also typical of hydrogen mole fraction profiles throughout containment except in the source compartment. Hydrogen mole fraction magnitudes varied by roughly 0.01 total mole fraction throughout the containment by the end of the S_2D1 calculation. For roughly the first half of the transport calculations, steam mole fractions decreased in mole fraction magnitude from higher to lower containment elevations by approximately 0.03 to 0.05 except when the source term was located in the basement.

Typical calculated gas mole fractions in a source compartment are shown in Figure A.4.8. Again, the hydrogen and steam mole fractions are dependent on source compartment size and ventilation, but the mole fraction trends would be similar for each source compartment. The small poorly vented reactor cavity compartment reached a peak mole fraction of 0.27. The large poorly ventilated basement compartment reached a peak hydrogen mole fraction of 0.16. The well ventilated SG1A source compartment reached a peak hydrogen mole fraction of 0.11. Peak hydrogen and steam mole fractions occurred at the maximum flow rates of hydrogen and steam from the primary system. The source compartment peak hydrogen mole fractions are shown in Table A.4.2. Corresponding steam mole fractions at the time of peak hydrogen mole fractions were less than 0.30.

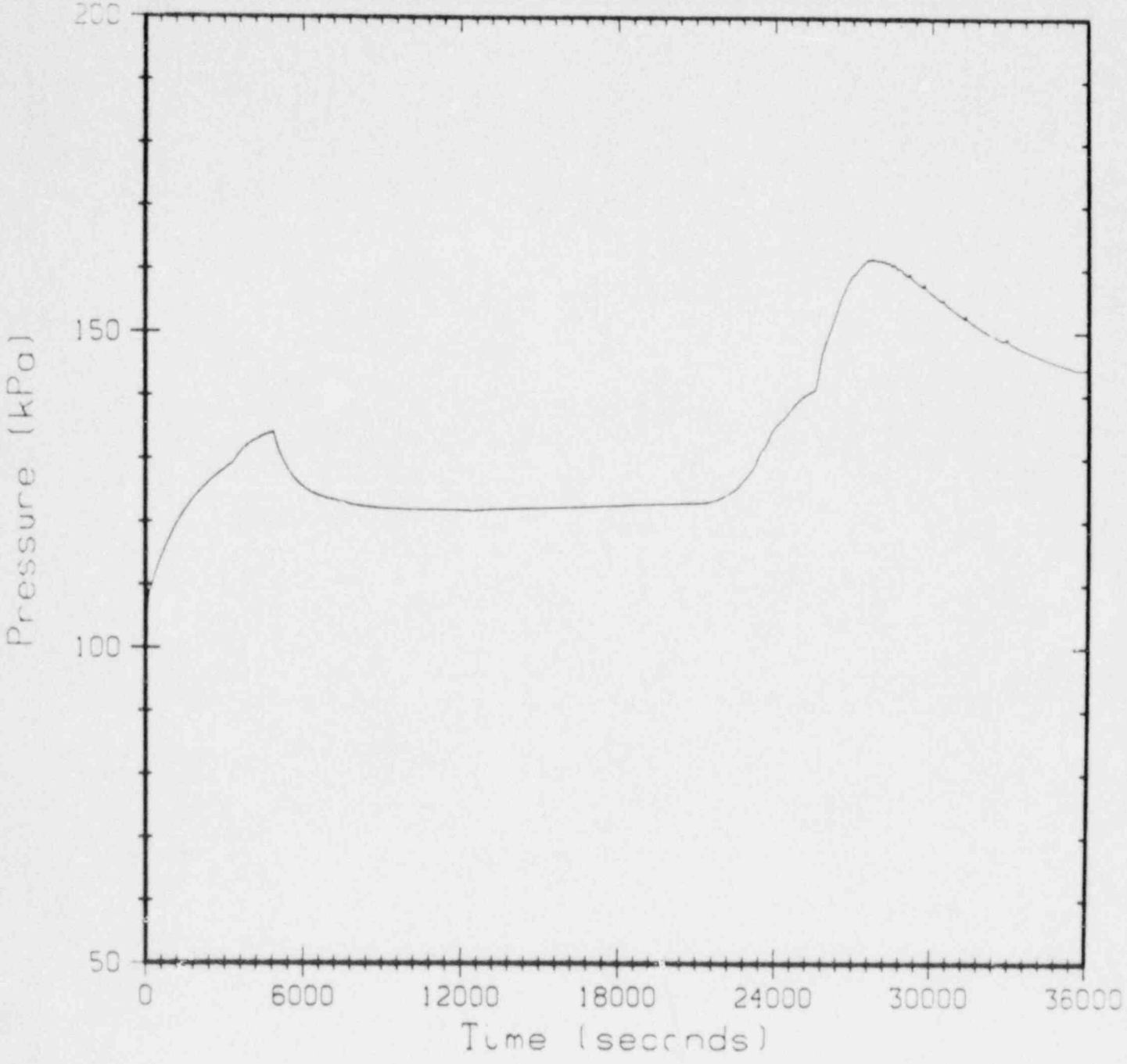

Figure A.4.6. Typical S_2D1 Containment Gas Pressure Response

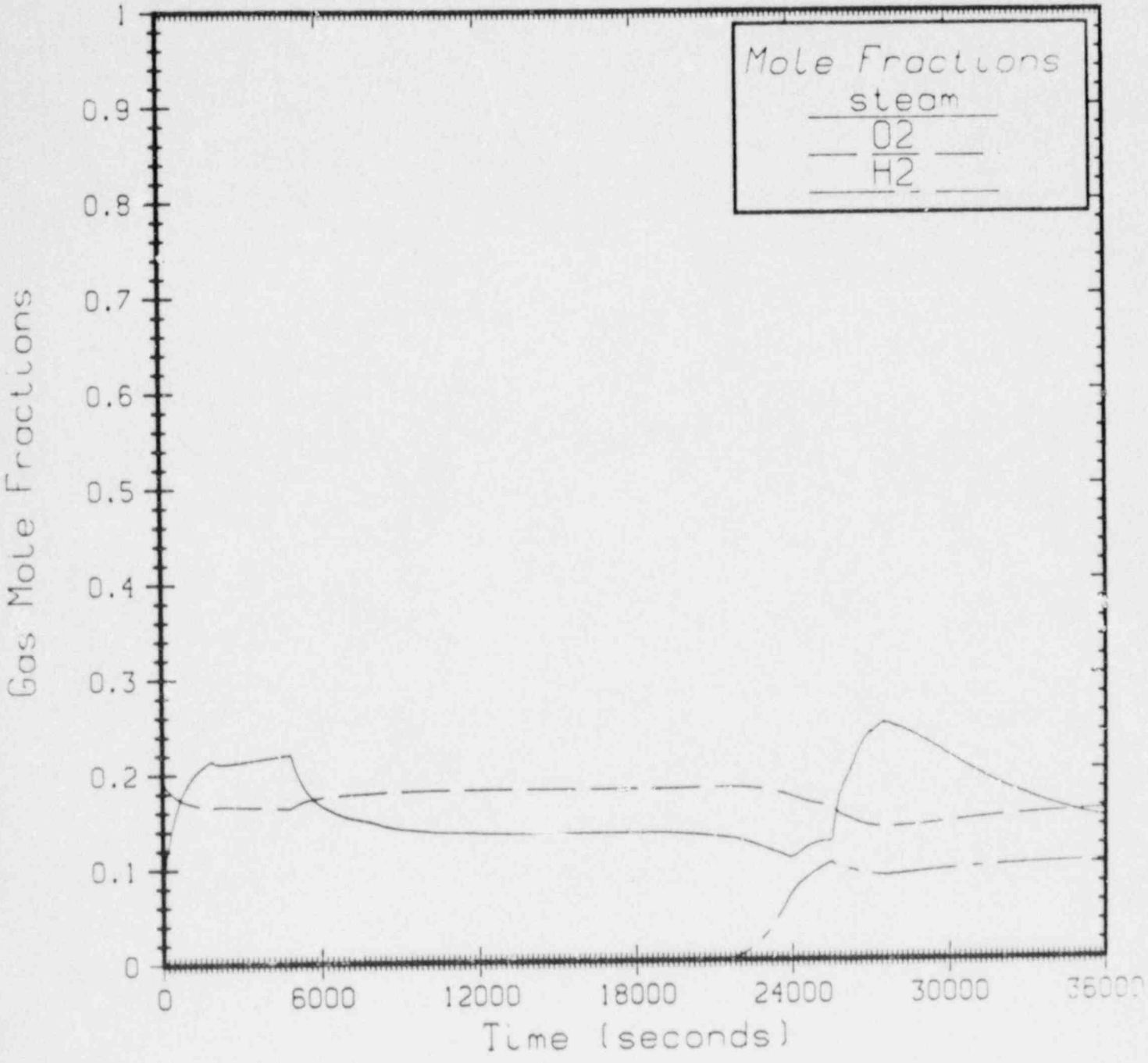

Figure A.4.7. Representative S_2D1 Containment Dome Gas Mole Fractions

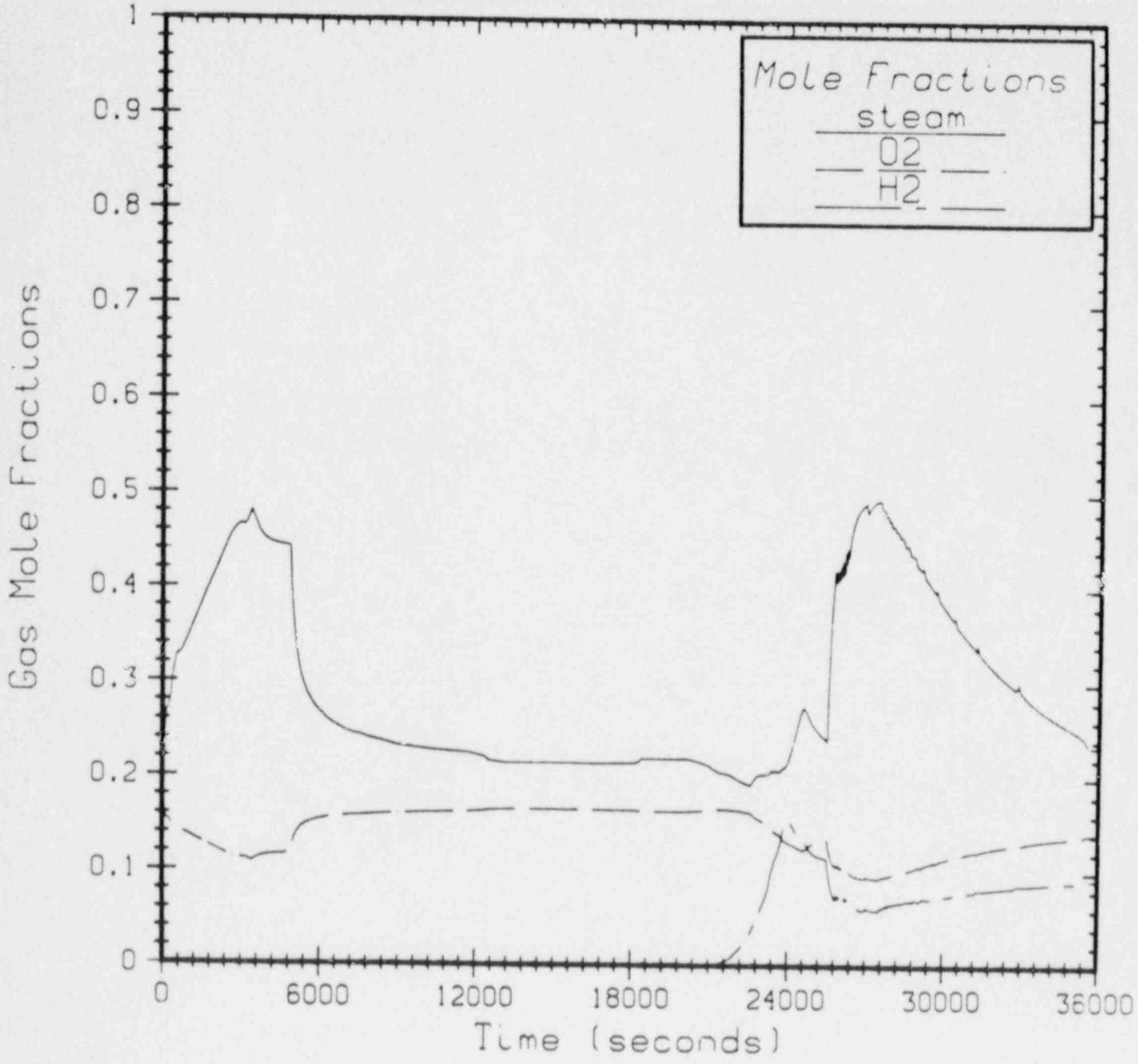

Figure A.4.8. Typical Source Compartment Gas Mole Fractions

The dominant flow directions in containment for Cases 2A, 2B, and 2C were similar to those for the S_2D2 calculation. Flow magnitudes were smaller due to lower primary leak rates.

A.4.3 S_1D4 Small Break

The S_1D4 containment pressure response for all break location cases is shown in Figure A.4.9. The S_1D4 calculations showed much higher initial containment pressures before break uncovery at 400 seconds because of the increased water/steam flow rate from the larger 4-inch-diameter break. Pressure rapidly decreased due to: (1) the relatively low steam flow rate from the primary system after the break was uncovered and (2) condensation of steam out of the containment gas.

Typical containment gas mole fractions in the dome region for each S_1D4 transport are illustrated in Figure A.4.10 and their trends are representative of most compartments in containment except the source compartment. A large flow of water from the primary system was calculated during the first 400 seconds which is reflected in the high initial steam mole fraction. Early into the transport calculations, the decrease in steam mole fraction magnitude in lower elevations ranged from 0.05 to 0.20. The calculated hydrogen concentrations in containment began increasing at 6500 seconds and were typical of a single, relatively large release of hydrogen. The hydrogen concentrations leveled out at 7600 seconds indicating uniform hydrogen mixing throughout containment and varied in magnitude by roughly 0.01 for compartments outside the source compartment.

Representative calculated gas mole fractions in a source compartment are shown in Figure A.4.11. For containment model 1, the reactor cavity source compartment, basement source compartment, and SG1A source compartment peak mole fractions were 0.60, 0.16, and 0.13, respectively and occurred at approximately 7500 seconds.

For containment model 2, the basement source compartment and SG1A source compartment peak hydrogen mole fractions were 0.20 and 0.13, respectively. Source compartment peak hydrogen mole fractions are listed in Table A.4.2.

The dominant flow directions in containment for Cases 3A to 3E were similar to those for the S_2D2 calculation. Flow magnitudes were initially larger due to higher primary leak rates.

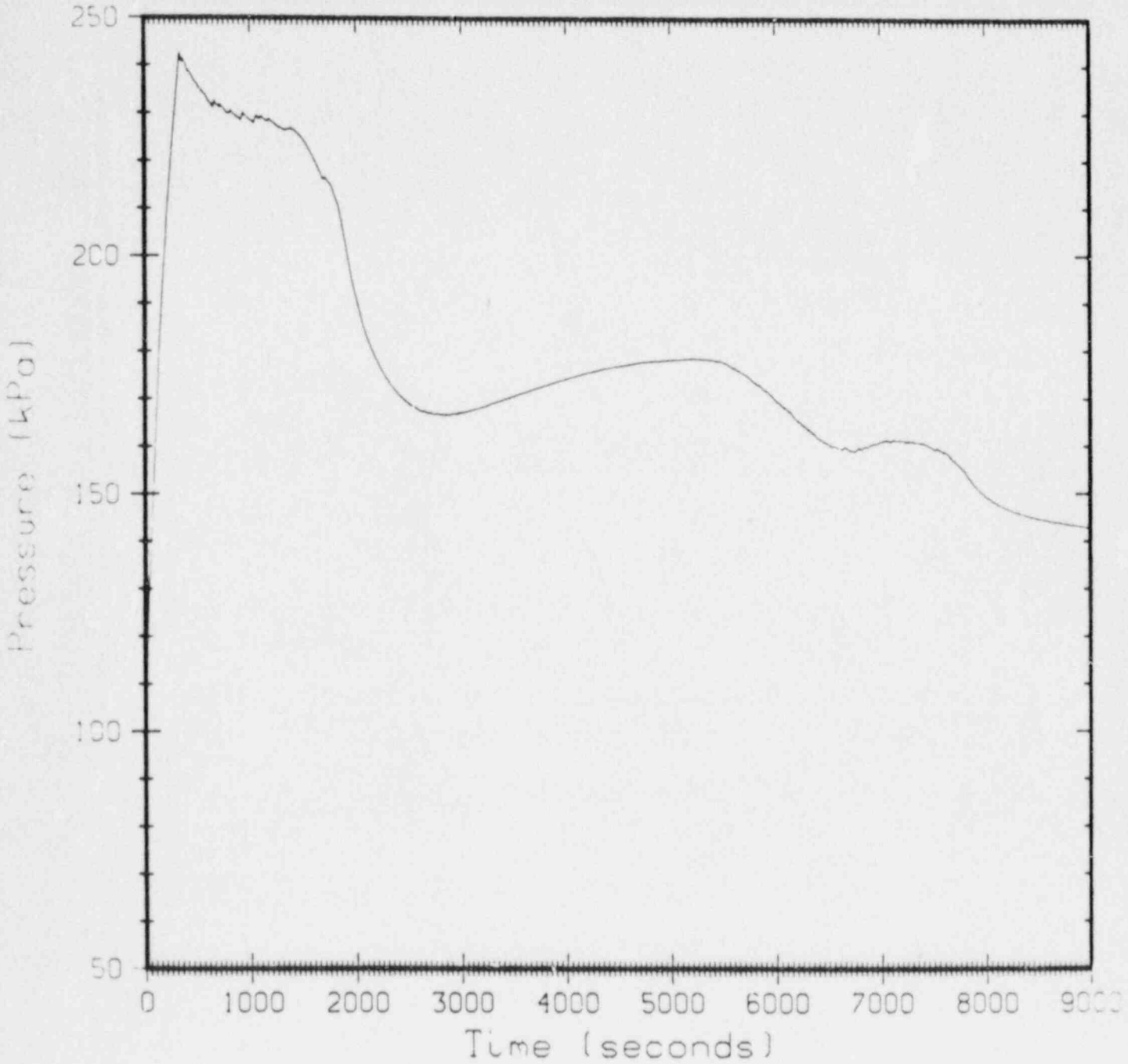

Figure A.4.9. S_1D4 Containment Gas Pressure Response

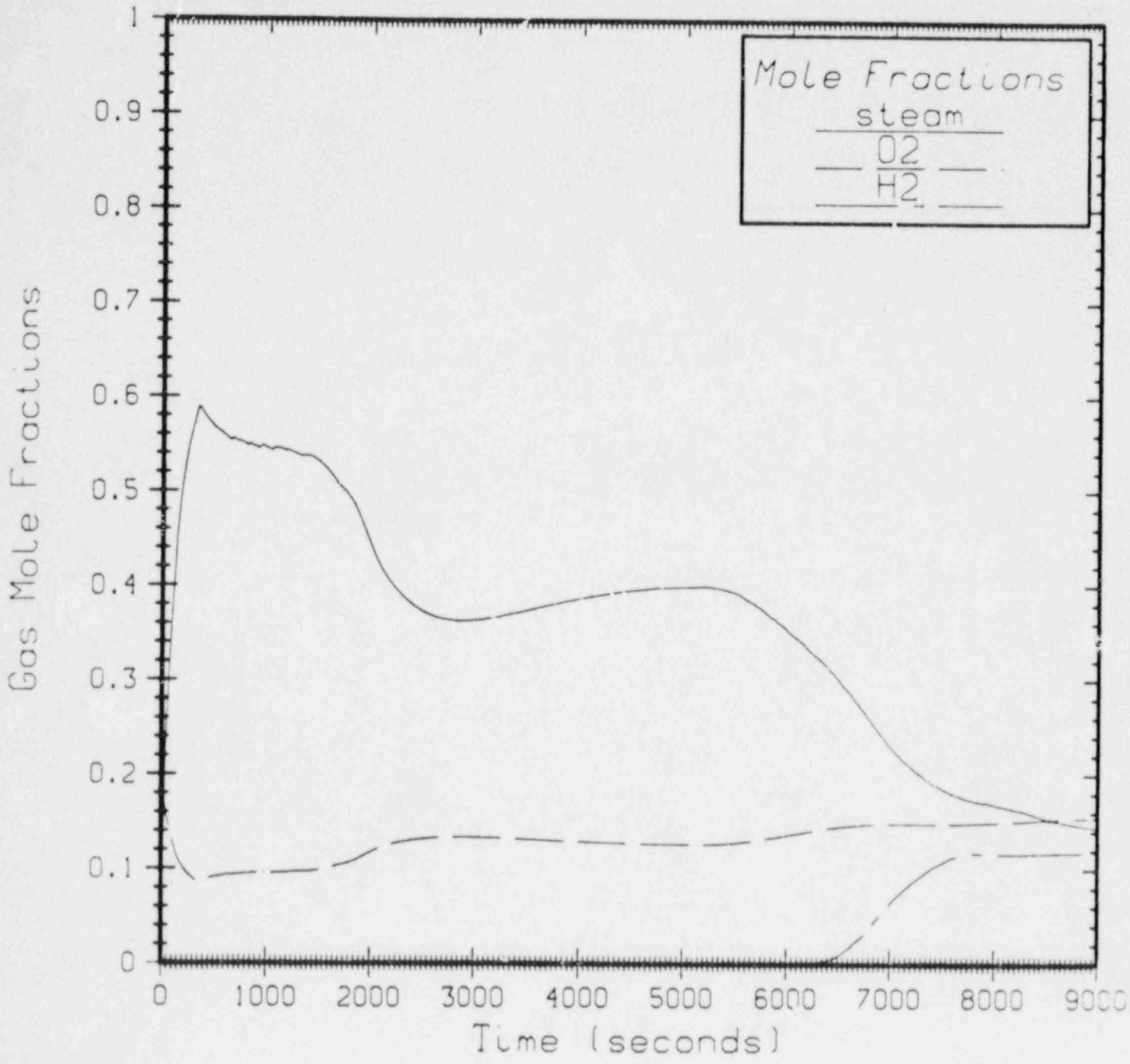

Figure A.4.10. Containment Dome Gas Mole Fractions

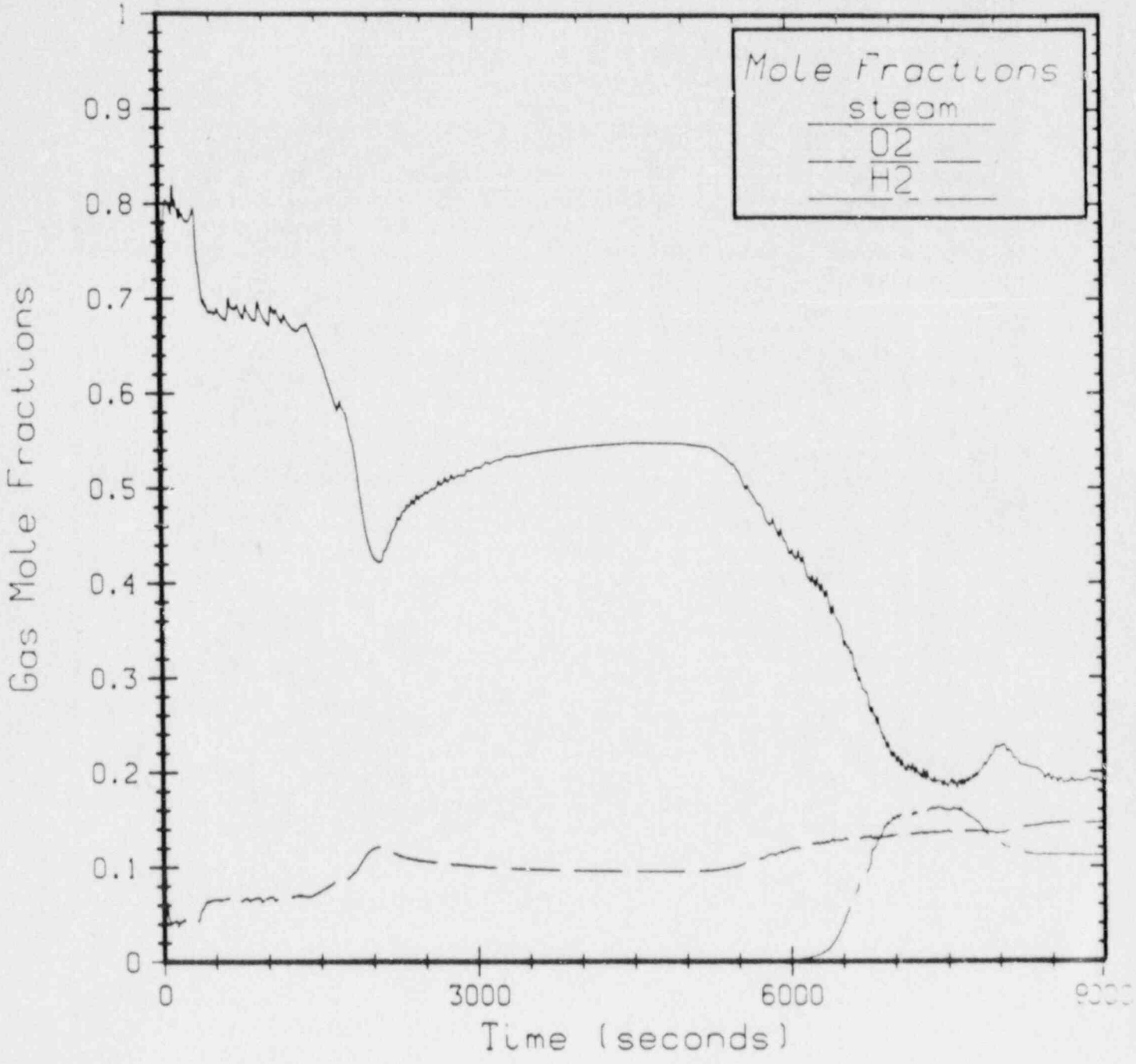

Figure A.4.11. Typical Source Compartment Gas Mole Fraction

A.4.4 Transport Summary

Hydrogen generation and release from the primary occurred once in the S_2D1 and S_1D4 transport calculations. Hydrogen was released late in the scenario transport calculations. Hydrogen generation and release into containment stopped when HPI flow was initiated. Hydrogen was twice generated and released at two intervals during the S_2D2 transport calculation. Hydrogen generation was initially stopped when the CFTs covered the core. Subsequent steam release from the break allowed the core to uncover a second time and regenerate hydrogen. HPI flow initiation re-covered the core and stopped hydrogen generation the second time.

The results from the HECTR calculations showed that the primary leak flow rates and RBC system were influential in establishing the circulation flow in containment. The calculated circulation flows caused relatively uniform mixing of hydrogen after hydrogen injection into containment. Hydrogen mole fractions were slightly lower in the source compartment for some cases at the end of the scenario because steam was still being injected into the source compartment from the primary, which decreased the hydrogen mole fraction in that compartment. Overall containment-wide average hydrogen concentrations were the highest at the end of the transport calculations.

The highest local concentrations of hydrogen were always calculated in the compartment that the steam and hydrogen source flows were injected into. These local peak hydrogen mole fractions occurred at the time of maximum hydrogen injection into the source compartment from the primary. Hydrogen mole fractions in other compartments were lower than the peak mole fractions in the source compartment at the time of maximum hydrogen injection. Cases 1B, 1C, 2B, 2C, 3B, 3C, and 3D had detonable concentration messages printed by HECTR. These messages indicate that further analysis with respect to detonability should be performed.

The volume of the source compartment, the magnitude of flow paths connecting the source compartment, and the amount of RBC flow into the source compartment affected the calculated peak hydrogen concentration. For containment model 1, compartment 1 (the reactor cavity) was the smallest compartment and had the smallest flow path areas; therefore, it showed the highest hydrogen peaks. While compartment 5 (the basement) was the largest, its flow path areas were four times less than those of compartment 2 (SG1A). Compartment 5 showed the second highest peak concentrations. Compartment 2 was half the size of compartment 5 but was

extremely well ventilated during transport scenarios. The high ventilation rates caused the peak hydrogen concentrations to be the smallest in this scenario.

For containment model 2, SG1A was divided into three compartments (2, 9, and 10) with compartment 2 as the source compartment. Although compartment 2 of containment model 2 was one-third the volume of compartment 2 of containment model 1, peak hydrogen mole fractions of both containment models were roughly equal because both compartments were well ventilated by RBC flow.

A.5 Deflagration Results

The hybrid large dry deflagration results are summarized in Section 3.2.2. This section of Appendix A will present in detail a representative single hydrogen burn analysis and a representative multiple burn analysis. The following paragraphs also summarize how single and multiple burns were initiated and trends observed for single and multiple burns.

Table A.5.1 lists the hydrogen burn cases analyzed for the S_2D2, S_2D1, and S_1D4 scenarios. Ten S_2D2 cases were calculated. Seven cases (4A, 4B, 4C, 4D, 4E, 4G, 4H) analyzed average maximum hydrogen ignition. These cases observed effects due to changing source compartment locations, ignition compartment locations, and operation of the spray system. One case (4J) analyzed the local maximum hydrogen ignition. Two cases (4F, 4I) analyzed the default 7 percent hydrogen ignition mode. Six S_2D1 cases were performed. Three cases (5A, 5D, 5F) analyzed average maximum hydrogen ignition, two cases (5C, 5E) analyzed local maximum hydrogen ignition, and one case (5B) analyzed the default hydrogen ignition. Five S_1D4 cases were calculated. Two S_1D4 cases (6A, 6D) were average maximum hydrogen ignition, two cases (6B, 6E) were default ignition cases, and one local maximum hydrogen ignition case (6C) was analyzed.

The mole fraction magnitude at which hydrogen was ignited was based on three criteria: (1) average maximum ignition, (2) local maximum ignition, and (3) default ignition. Average maximum ignition involved igniting hydrogen at the average maximum containment wide hydrogen mole fractions. This ignition occurred at the end of the hydrogen transport calculations. Local maximum ignition was initiated in the source compartment when the peak hydrogen mole fraction was calculated to occur during maximum hydrogen injection into the source compartment. Default ignition ignites the hydrogen in the first compartment in which the hydrogen mole fraction reaches 0.07 (7 percent). The HECTR default ignition level is considered to be the minimum level at which

Table A.5.1

Hydrogen Burn Analyses Performed

Case	Accident Sequence	Source Compartment	Ignition Mode	Initial Burn Compartment	ESFs on	CM
4A	S_2D2	2	AM	5	RBC	1
4B	S_2D2	2	AM	5	RBC, RBS	1
4C	S_2D2	2	AM	6	RBC	1
4D	S_2D2	2	AM	7	RBC	1
4E	S_2D2	2	AM	2	RBC	1
4F	S_2D2	2	D	2	RBC, RBS	1
4G	S_2D2	1	AM	5	RBC, RBS	1
4H	S_2D2	5	AM	7	RBC, RBS	1
4I	S_2D2	5	D	5	RBC, RBS	1
4J	S_2D2	5	LM	5	RBC, RBS	1
5A	S_2D1	2	AM	5	RBC, RBS	1
5B	S_2D1	2	D	2	RBC, RBS	1
5C	S_2D1	1	LM	1	RBC, RBS	1
5D	S_2D1	1	AM	7	RBC, RBS	1
5E	S_2D1	5	LM	5	RBC, RBS	1
5F	S_2D1	5	AM	7	RBC, RBS	1
6A	S_1D4	2	AM	5	RBC, RBS	1
6B	S_1D4	5	D	5	RBC	1
6C	S_1D4	5	LM	5	RBC, RBS	1
6D	S_1D4	5	AM	7	RBC	1
6E	S_1D4	5	D	5	RBC	2

AM: average maximum hydrogen ignition
LM: local maximum hydrogen ignition
D: default hydrogen ignition
CM: containment model
RBC: fan coolers
RBS: spray system

hydrogen burning can occur and was determined by hydrogen burn behavior tests. Source compartments would be the first compartments to have hydrogen burning under the default ignition case. Default ignition could represent deliberate hydrogen burning at lower levels by some type of ignition system such as glow or spark plugs.

Average maximum hydrogen ignition cases for each scenario always resulted in a single hydrogen burn in each compartment. These burns occurred at the end of the scenario when the hydrogen concentrations were uniform throughout containment. Therefore, these burns resulted in elevated temperatures and pressures throughout the containment during hydrogen burning.

Local maximum hydrogen ignition cases usually resulted in a single hydrogen burn in each compartment (S_2D2 and S_1D4 scenarios). The S_2D1 scenario with local maximum hydrogen ignition resulted in one hydrogen burn occurring in some compartments and no hydrogen burns occurring in other compartments. This nonuniform hydrogen burning occurred because of the low hydrogen mole fractions outside of the source compartment at ignition time. These low hydrogen mole fractions were below the HECTR hydrogen flammability limits. When burns occurred in each compartment, high containment gas temperatures and pressures were calculated. The highest gas temperature was calculated in the source compartment. When burns did not occur in every compartment, low containment gas pressures were calculated. Gas temperatures were low in compartments without burning and high in compartments with burning.

Default (7 percent) hydrogen ignition analyses always resulted in multiple burns in the source compartment. These burns occurred shortly after hydrogen began to enter the source compartment. Small and poorly ventilated source compartments had tens of multiple burns while larger, well ventilated source compartments had only several multiple burns. Multiple burns also occurred in compartments adjacent to the source compartment while some compartments removed from the source compartment had no burns in some cases. Generally, the smaller, poorly ventilated source compartments (with their tens of multiple burns occurring) allowed smaller amounts of hydrogen to be transported to the rest of containment when compared to the large, well ventilated source compartments. Therefore, hydrogen burning in small source compartments resulted in hydrogen burning in fewer regions of containment. Low compartment pressures were always calculated in default hydrogen ignition cases. Many multiple burns resulted in high peak gas temperatures while few multiple burns resulted in lower peak gas temperatures.

A.5.1 S_2D2 Single Hydrogen Burn

The hybrid single hydrogen burn analysis presented in this section is listed as Case 4A in Table 3.6. Compartment gas conditions and safety equipment peak surface temperatures caused by the hydrogen burning are listed in Table A.5.2. Compartment gas conditions include the compartment in which burning was initiated, the number of burns which occurred in the compartment, the peak gas pressure, and the peak gas temperature. The equipment temperatures are given in the following order: (1) the transmitter cover plate model, (2) the case-as-plate model, (3) the lumped case model, and (4) the one-dimensional three-layer model.

Table A.5.2

S_2D2 Deflagration Results

Compartment	Number of Burns	Gas P_{max} (kPa)	Gas T_{max} (°K)	Barton 763 Tm_1 (°K)	Barton 763 Tm_2 (°K)	Barton 763 Tm_3 (°K)	Barton 763 Tm_4 (°K)
2	1	480	1320	400	370	370	400
3	1	480	1330	390	360	360	380
5*	1	480	1220	380	360	360	380
6	1	480	1320	390	370	370	390
7	1	480	1370	-	-	-	-

The source compartment was located in the steam generator compartment with the pressurizer (SG1A). Hydrogen ignition was initiated in the basement. At the time of ignition, the hydrogen mole fraction was approximately 0.12 throughout the containment. The hydrogen burning propagated from the basement into the dome region through the second floor and steam generator compartments. Peak gas temperatures for each compartment increased with increasing containment elevation; therefore, the dome region had the highest peak gas temperature. The peak occurred in the dome because the volume to surface area ratio for this compartment was the largest for all the compartments in containment. Large volume to surface area ratios allow less gas energy to escape to surfaces during burning, resulting in higher peak gas temperatures.

Figures A.5.1 and A.5.2 show typical containment gas pressure and temperature responses to a LOCA scenario with a single hydrogen burn at the end of the LOCA. The gas responses are shown for the second floor compartment but their trends are similar for all compartments in the containment. The first 16000 seconds represent the second floor gas response to the steam and hydrogen release from the primary system. In comparison, the burn is a relatively rapid transient.

Figures A.5.3 and A.5.4 show the second floor steam and hydrogen mole fractions, respectively. The steam mole fraction trends are driven by the steam releases as calculated by MARCON 2.0 (see Figure A.2.2). The hydrogen mole fraction trends represent the two releases of hydrogen which occurred during the LOCA (see Figure A.2.3). The steam mole fraction rapidly increased during hydrogen burning due to steam being produced during the combustion process. The hydrogen mole fraction rapidly decreased during the single hydrogen burn.

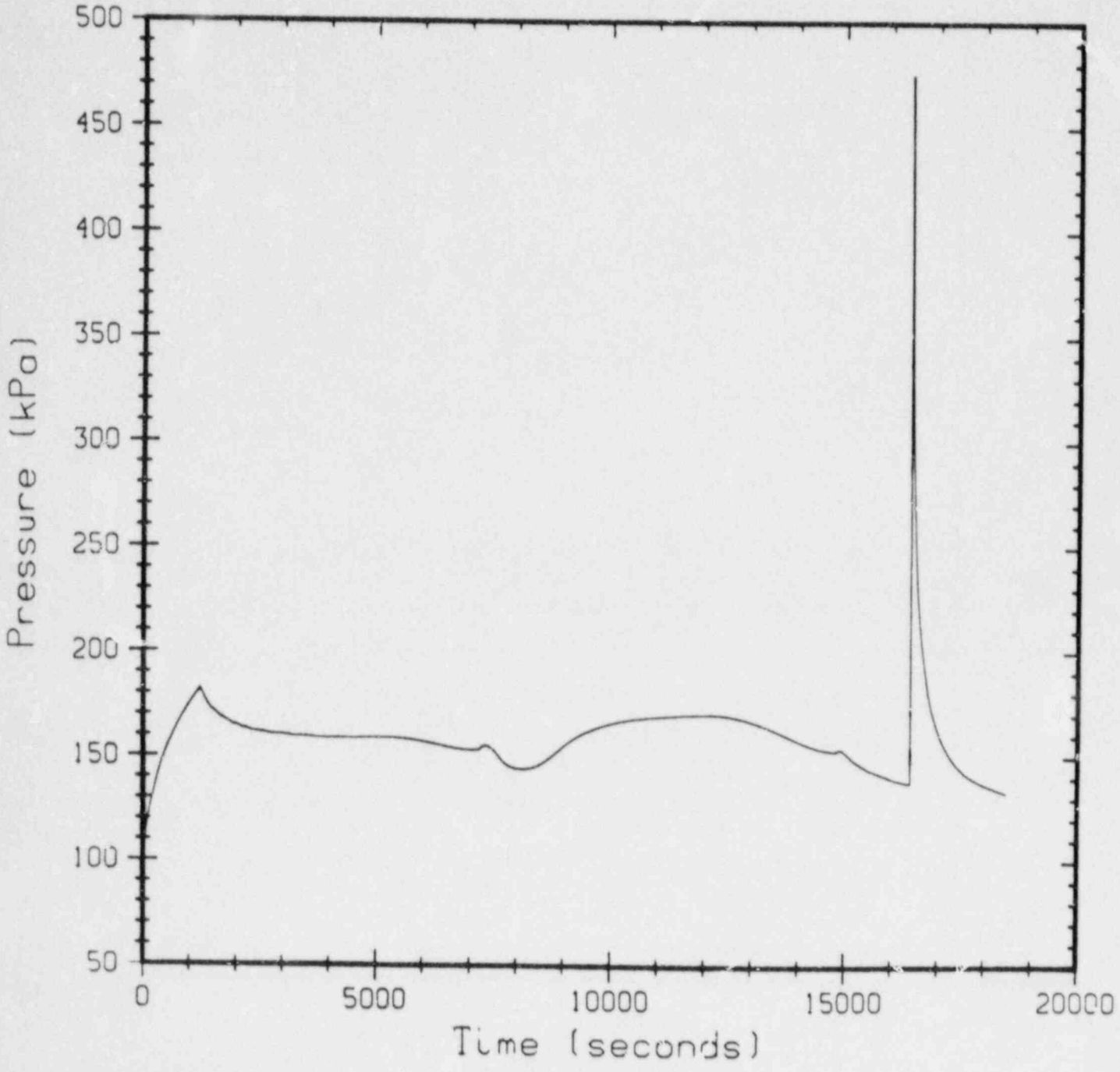

Figure A.5.1. Typical Containment Gas Pressure Response to S_2D2 LOCA and Single Hydrogen Burn

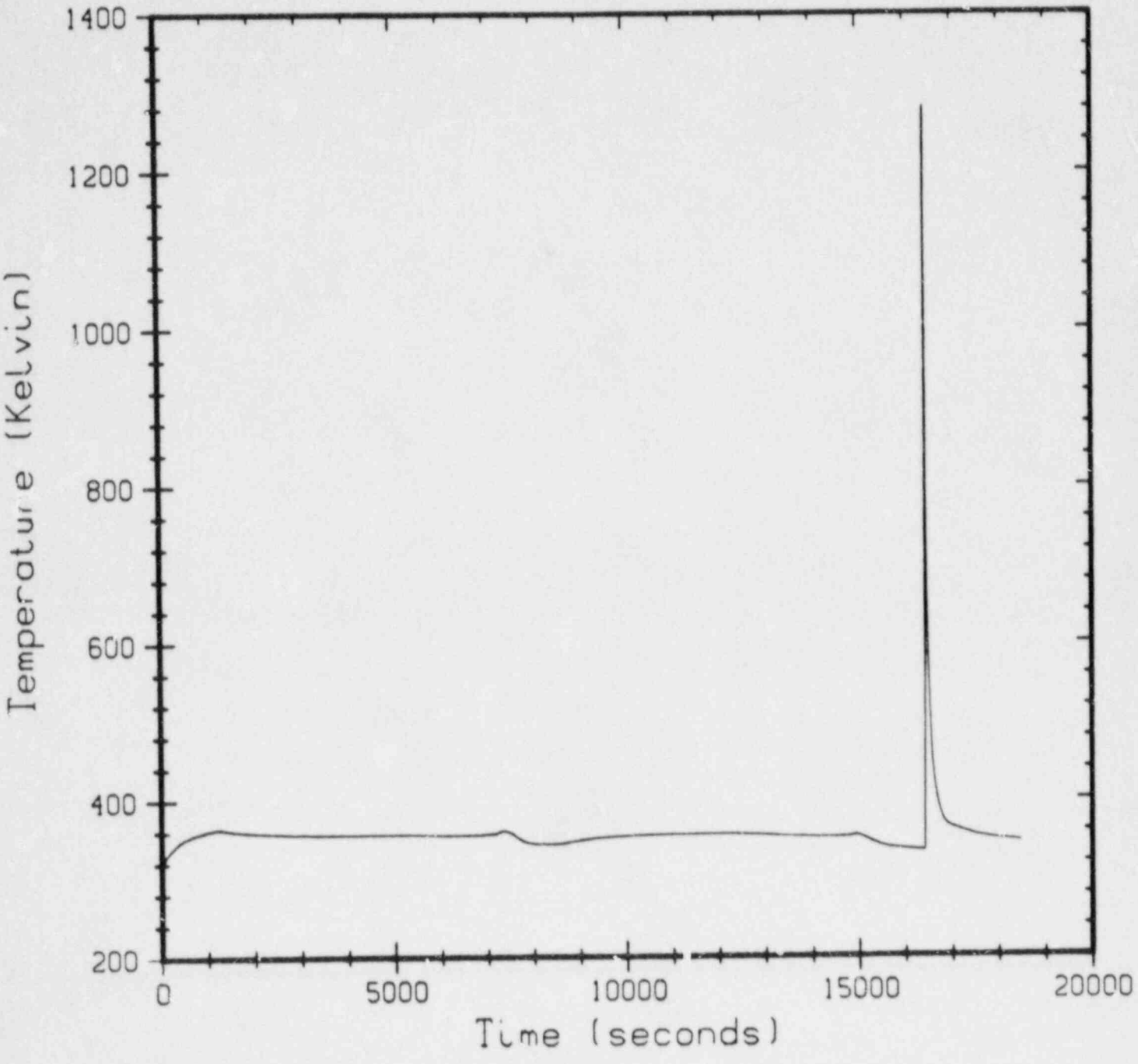

Figure A.5.2. Typical Containment Gas Temperature Response to S_2D2 LOCA and Single Hydrogen Burn

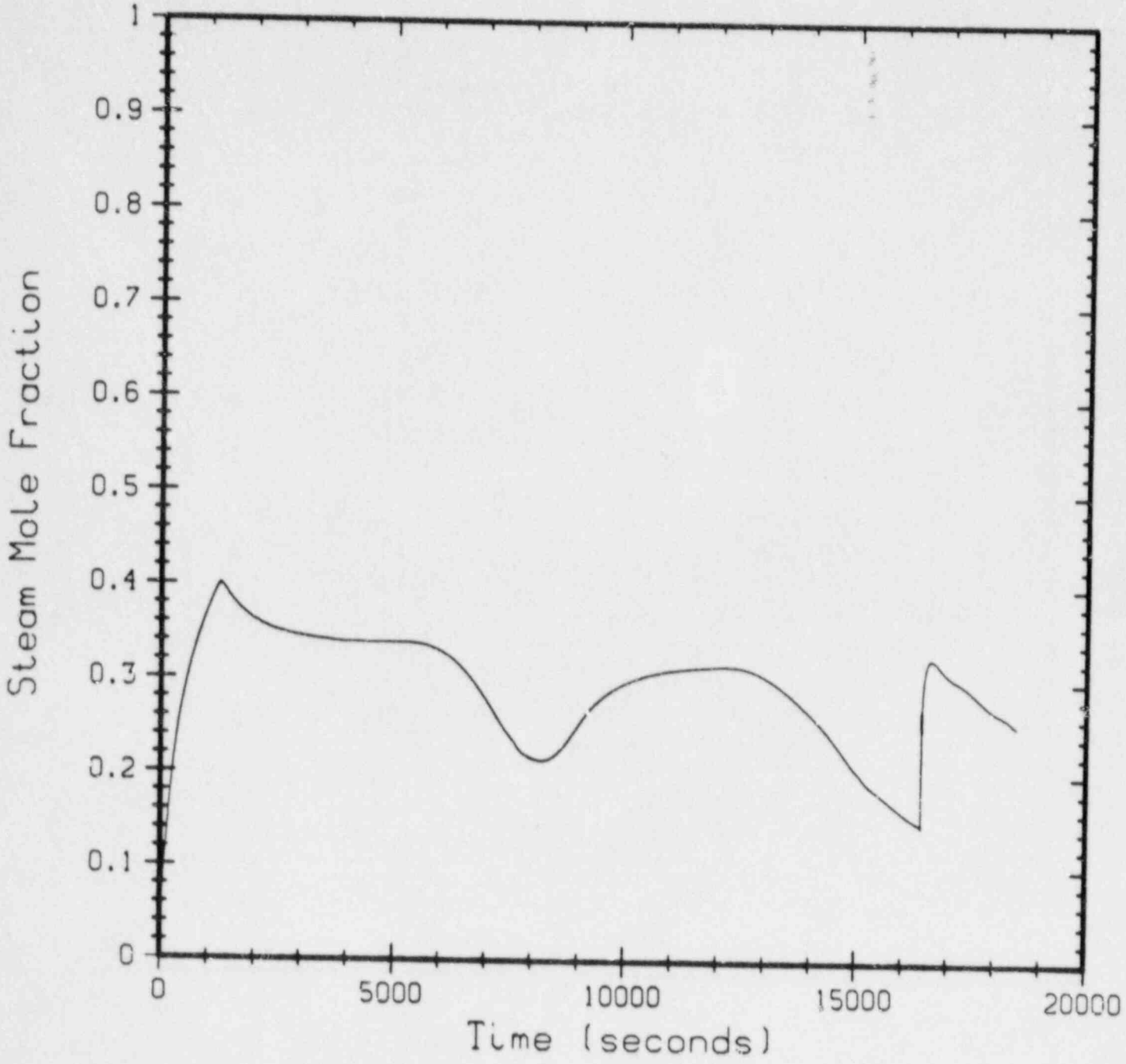

Figure A.5.3. S_2D2 Scenario Second Floor Steam Mole Fraction

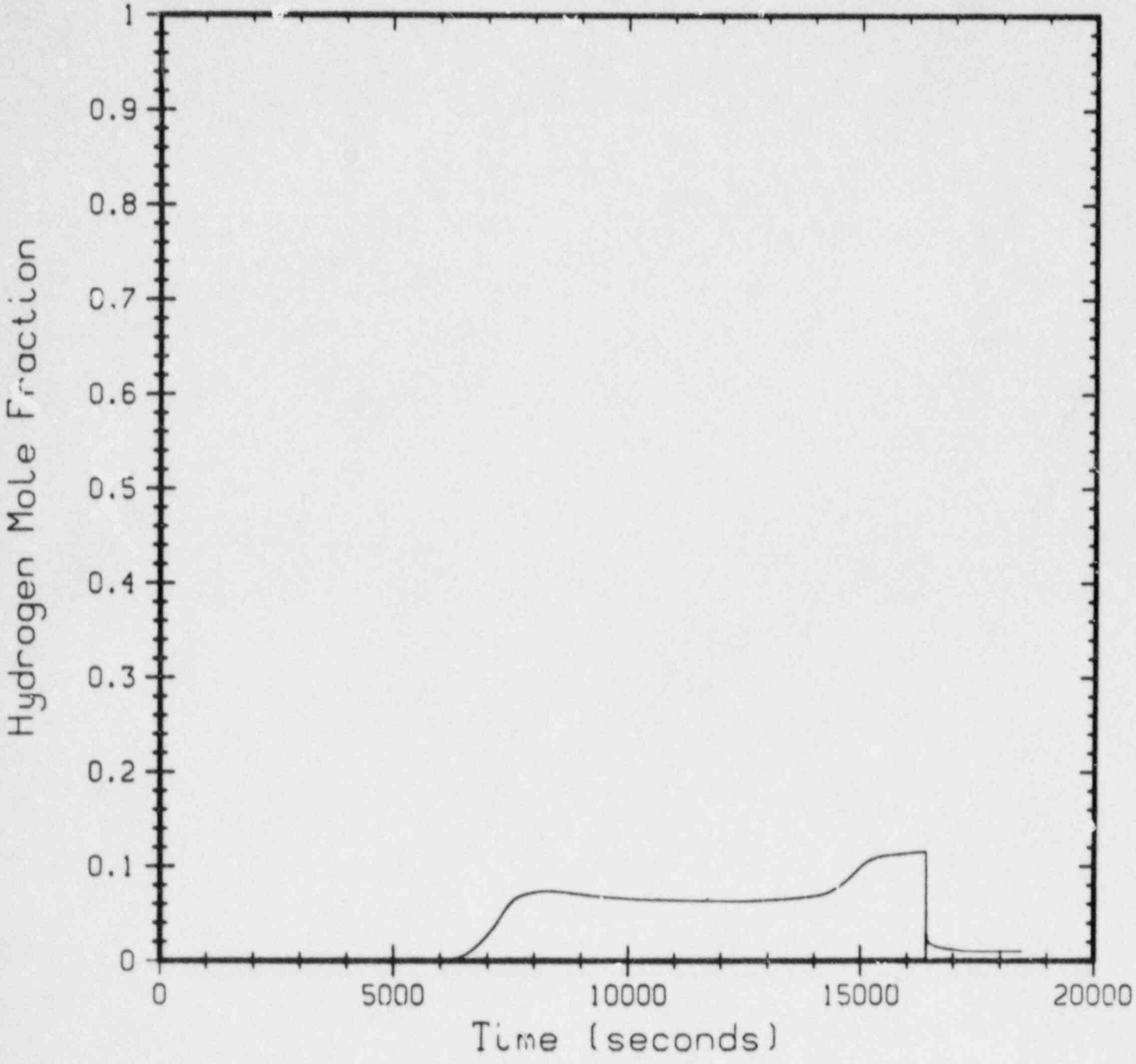

Figure A.5.4. S_2D2 Scenario Second Floor Hydrogen Mole Fraction

Figure A.5.5 shows the one-dimensional three-layer equipment model surface temperature response to the LOCA scenario. The peak temperature occurred during burning with a 50°K increase over the initial temperature of 334°K.

A.5.2 S_1D4 Multiple Hydrogen Burn

The hybrid multiple burn analysis presented in this section is listed as Case 6E in Table 3.6. Compartment gas conditions and safety equipment peak surface temperatures due to the multiple burns are listed in Table A.5.3.

The source compartment was located in the basement and hydrogen was ignited each time that it reached 7 mole fraction percent. This ignition criteria resulted in 18 burns being calculated in the source compartment. Enough hydrogen was transported to the second floor (between multiple burns in the source compartment) to allow five burns to occur in the second floor compartment.

Figure A.5.6 illustrates the source compartment gas temperature during the LOCA. Multiple burning was started at approximately 6500 seconds. Eighteen burns were calculated with peaks briefly reaching 1160°K. The baseline gas temperature was elevated from roughly 400°K to 720°K and remained elevated for approximately 1500 seconds.

Figure A.5.7 shows the second floor gas temperature. Five burns were calculated to occur in this compartment during the LOCA. The individual burns are not readily observed due to thermal influence from the source compartment. The gas temperatures are less than those in the source compartment and are over 440°K for approximately 1000 seconds.

Table A.5.3

S_2D4 Deflagration Results

Compartment	Number of Burns	Gas		Barton 763			
		P_{max} (kPa)	T_{max} (°K)	Tm_1 (°K)	Tm_2 (°K)	Tm_3 (°K)	Tm_4 (°K)
2	0	220	370	370	370	370	370
3	0	220	370	370	370	370	370
5*	18	220	1160	790	630	630	670
6	5	220	540	410	390	390	400
7	0	220	380	-	-	-	-
11	0	220	380	370	370	370	390

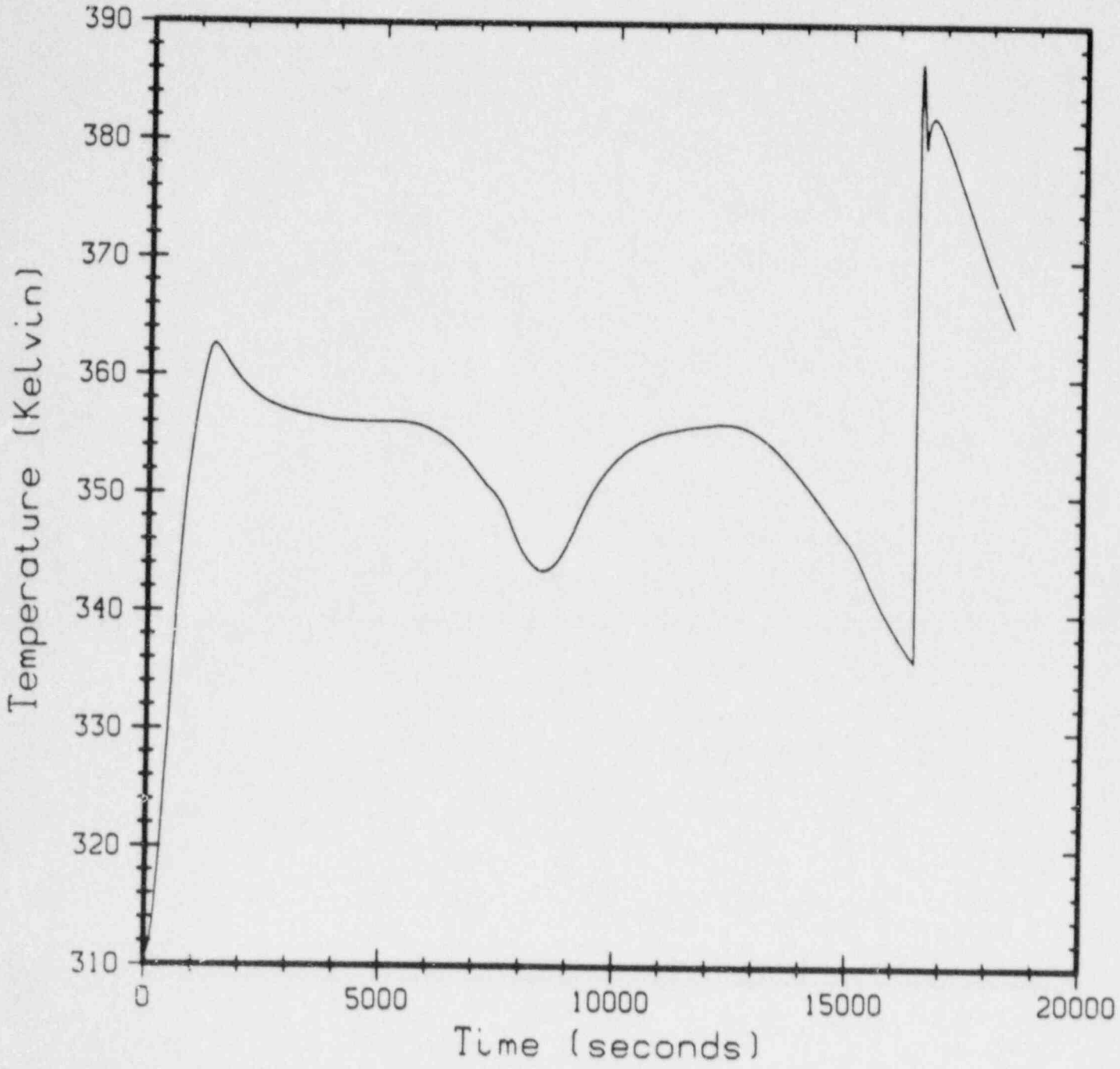

Figure A.5.5. Three-Layer Model Temperature Response to S_2D2 LOCA and Single Hydrogen Burn

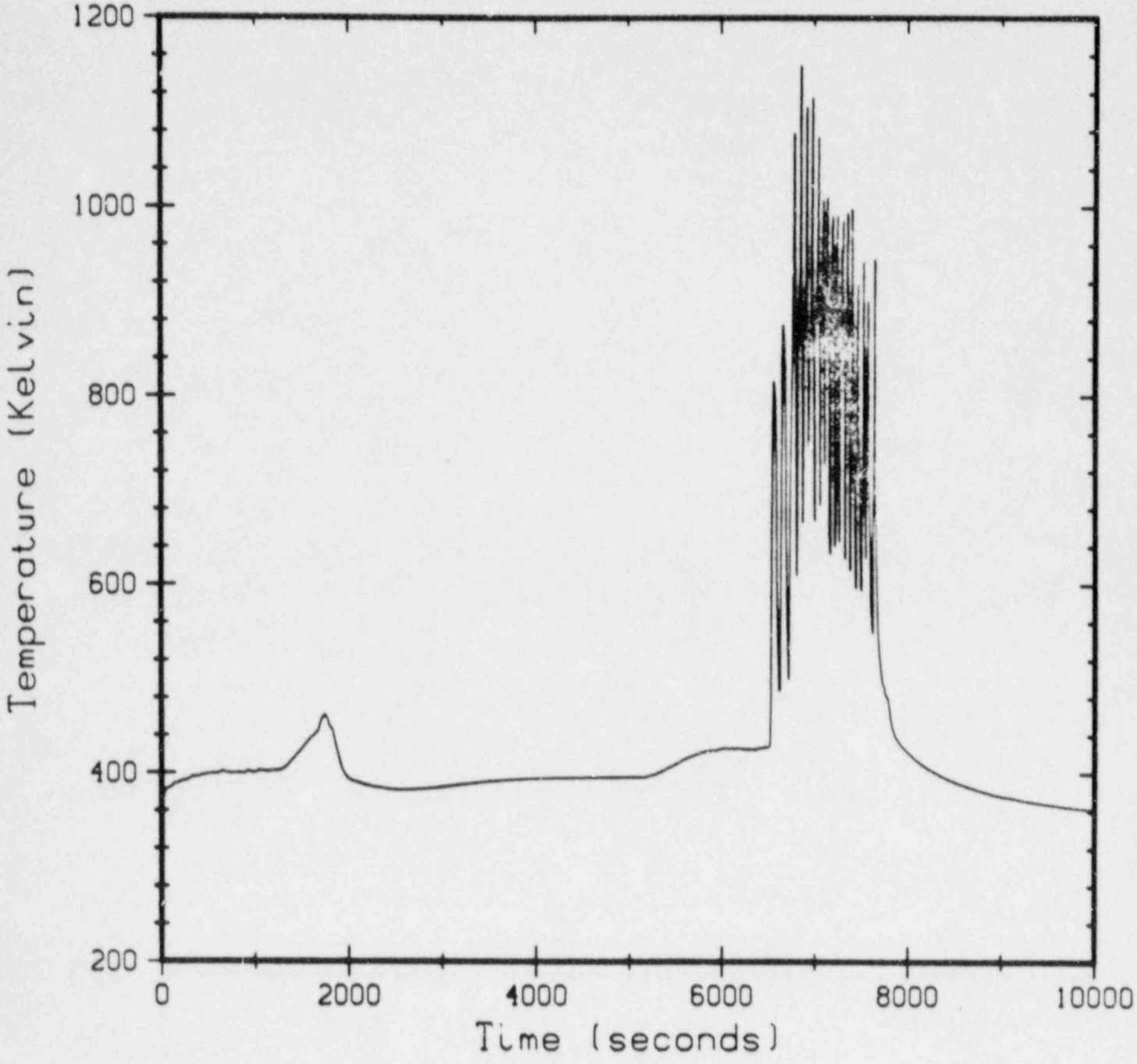

Figure A.5.6. Source Compartment Gas Temperature Response to S_1D4 LOCA and Multiple Hydrogen Burning

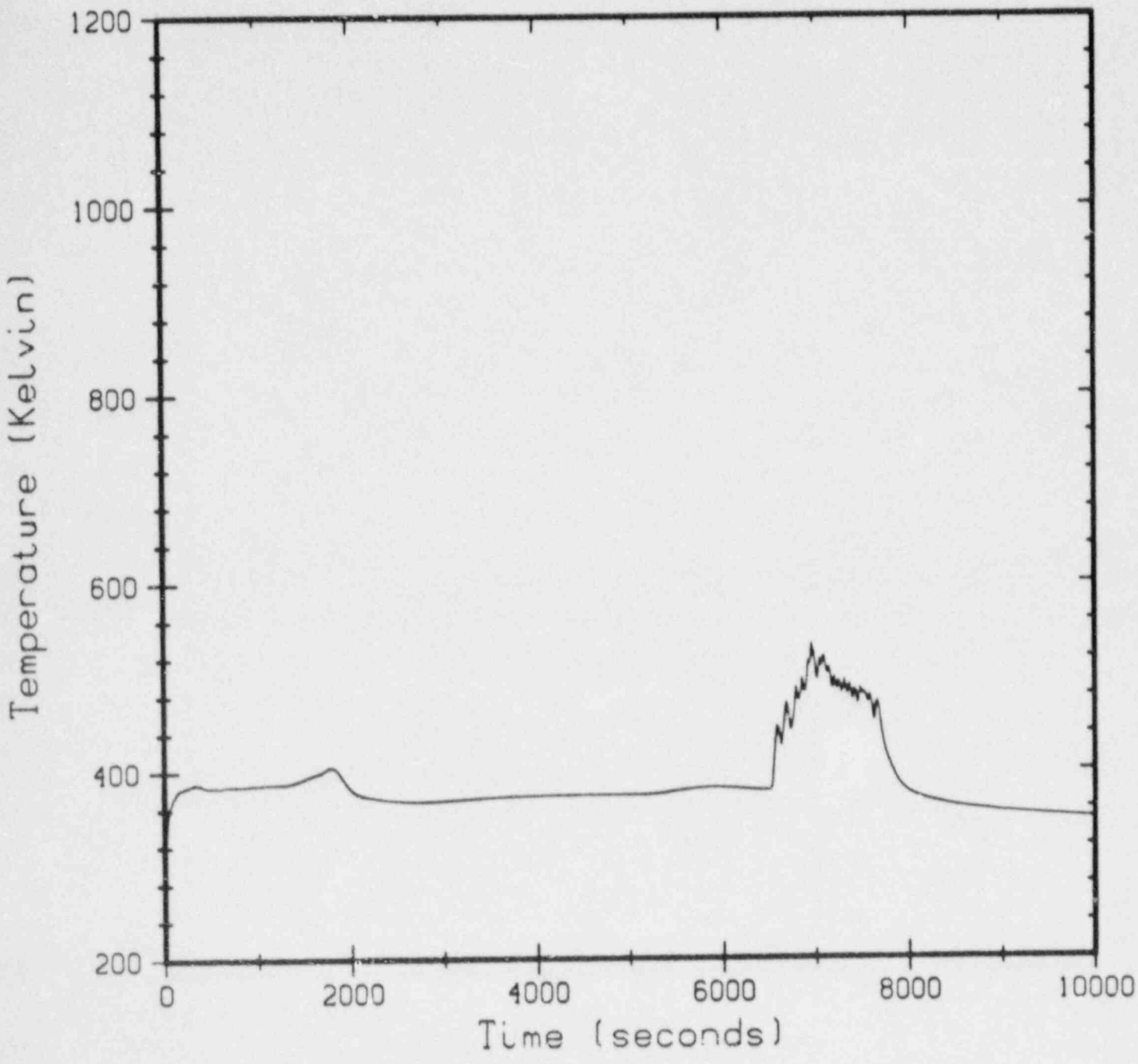

Figure A.5.7. Second Floor Gas Temperature Response to S_1D4 LOCA and Multiple Hydrogen Burning

The dome compartment gas temperature is shown in Figure A.5.8. Its gas trend is typical for other compartments removed from the source compartment. The multiple burn's thermal effect on this compartment compared to the rest of the LOCA is mild.

Figure A.5.9 shows the containment gas pressure response to the LOCA scenario. Note that the initial water blowdown from the primary system (0 to 2000 seconds) has more effect on containment pressure than the multiple burning.

Figure A.5.10 demonstrates the effect of the source compartment multiple hydrogen burn on the one-dimensional three-layer model surface temperature. The equipment surface is unable to cool significantly between burns; therefore, the surface temperature increases almost continuously during the multiple burns. The surface temperature reached a peak of 670°K and remained above 444°K for over 3000 seconds. Recall that experiments have demonstrated that internal equipment temperatures will approach surface temperatures when the equipment is held at elevated temperatures for prolonged periods.

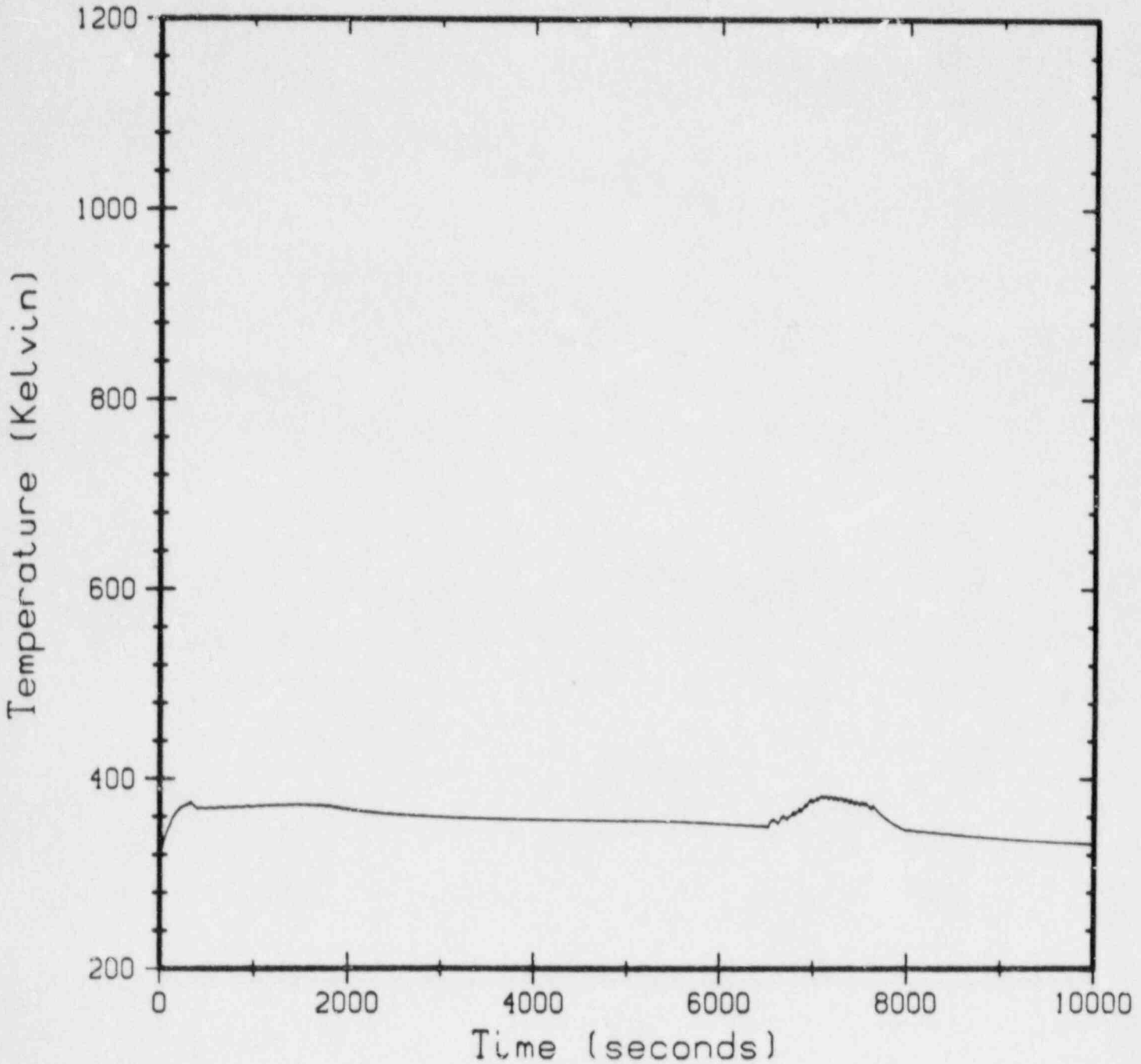

Figure A.5.8. Dome Compartment Gas Temperature Response to S_1D4 LOCA and Multiple Hydrogen Burning

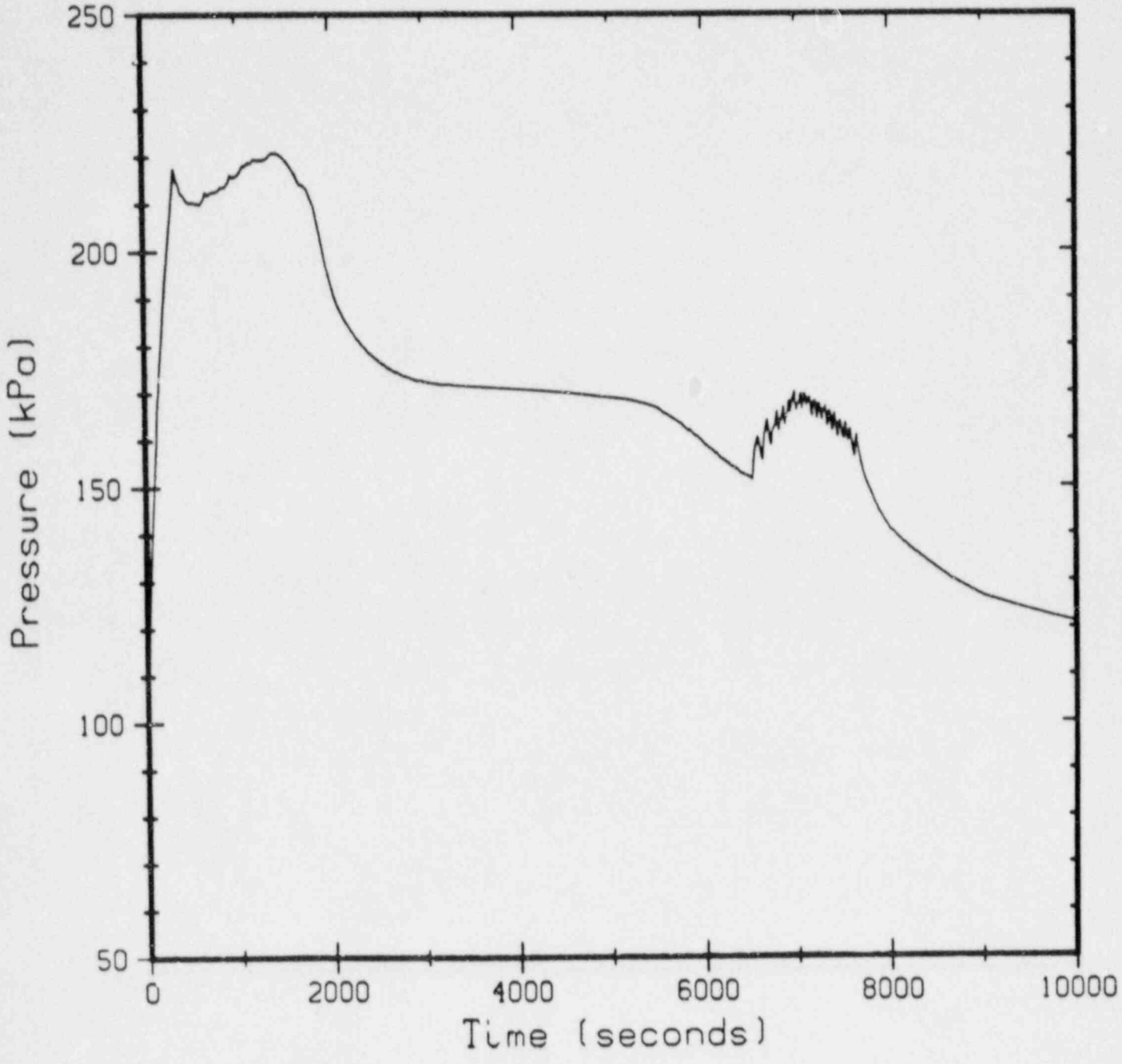

Figure A.5.9. Containment Gas Pressure Response to S_1D4 LOCA and Multiple Hydrogen Burning

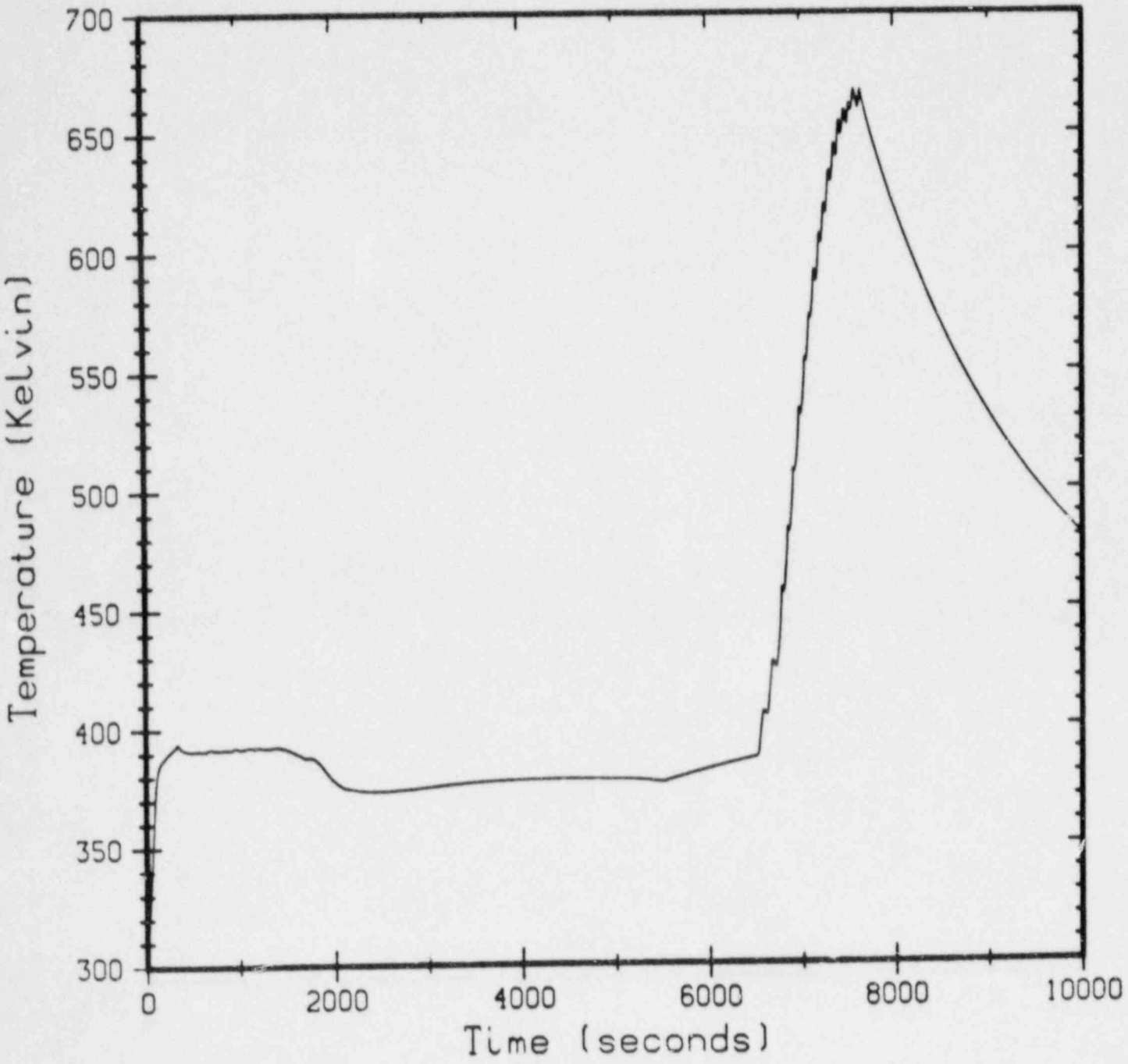

Figure A.5.10. Three-Layer Model Response to S_1D4 LOCA and Multiple Hydrogen Burning, Located in Source Compartment

REFERENCES

1. 10 CFR Part 50, Federal Register, Vol. 50, No. 17, January 25, 1985.

2. Dingman, S. E., et al., HECTR Version 1.5 User's Manual, NUREG/CR-4507, SAND86-0101, Sandia National Laboratories, April 1986.

3. Wooten, R. O., et al., MARCH 2 (Meltdown Accident Response Characteristics) Code Description and User's Manual, NUREG/CR-3988, BMI-2115, August 1984.

4. Cole, R. K., et al., CORCON MOD2 A Computer Program for Analysis of Molten-Core Concrete Interactions, SAND 84-1246, Sandia National Laboratories, August 1984.

5. Dandini, V. J., Testing of Nuclear Qualified Cables and Pressure Transmitters in Simulated Hydrogen Deflagrations to Determine Survival Margins and Sensitivities, NUREG/CR-4324, SAND 85-1481, Sandia National Laboratories, December 1985.

6. Dandini, V. J. and W. H. McCulloch, HECTR Analysis of Equipment Temperature Responses to Selected Hydrogen Burns in an Ice Condenser Containment, NUREG/CR-3954, SAND 84-1704, Sandia National Laboratories, February 1985.

7. IEEE Standard for Qualifying Class 1E Equipment for Nuclear Power Generating Stations, IEEE Std 323-1974, Institute of Electrical and Electronics Engineers, 1974.

APPENDIX B

TMI HYDROGEN BURN ANALYSIS

APPENDIX B

TMI HYDROGEN BURN ANALYSIS

B.1 Introduction

On March 28, 1979, a hydrogen burn occurred in containment during a nuclear core uncovery accident at Three Mile Island Unit 2 (TMI-2). This accident contributed to the Hydrogen Control Rule for Pressurized Water Reactors (PWR), which states that containment structural integrity and survivability of needed safety systems during a hydrogen burn must be demonstrated. The TMI-2 accident data will provide a benchmark of hydrogen burn computer codes which can then be used in analyses of other degraded core accidents.

This report describes the Sandia National Laboratories (SNL) analysis of the TMI-2 hydrogen burn, using the HECTR code to predict the TMI-2 containment pressure and temperature response. This analysis was requested by DOE with the request that postulated hydrogen addition rates calculated by Henrie and Postma be used.[1] Since the Henrie and Postma analysis was released, a TMI-2 hydrogen burn analysis has also been performed by the Factory Mutual Research Corporation (FMRC).[2] This report includes and builds upon the analyses of both Henrie and Postma and FMRC. The hydrogen generation, release rates, and mixing used in this analysis are based upon the results of References 1 and 2.

The HECTR computer code[3] was used to calculate the containment and safety-related equipment response during and after the hydrogen burn. HECTR is a lumped-parameter, multi-compartment containment analysis code developed to analyze nuclear reactor accidents involving the transport and combustion of hydrogen. The gases in each compartment are assumed to be uniformly mixed, and gas flow between compartments can be driven by both pressure and density differences. Included are models for hydrogen burns, radiative and convective heat transfer, and wall heat conduction. Some engineered safety features (ESFs), such as the reactor building spray system and reactor building fan coolers, are also modeled by HECTR. A moderately compartmentalized model of TMI-2 was used: 8 compartments, 17 intercompartment flow junctions, and 46 structural surfaces. More detailed descriptions of the containment model and ESFs systems are presented in Section A.2.2 of this report.

B.2 Containment Conditions Prior to Burn

The initial conditions prior to the burn in containment are dependent upon the hydrogen generated in the primary vessel and released, along with steam, through a break in the

primary cooling system. The analysis in this report did not attempt to calculate the amount of hydrogen and steam released from the primary, but used results from other analyses[1,2] to establish initial conditions in containment prior to the burn.

B.2.1 Hydrogen Generation and Release

The reader is referred to References 1, 2, 4, and 5 for analyses and descriptions of the events leading to hydrogen generation, transport, and release from the primary cooling system. Figure B.2.1 presents several estimates of hydrogen release and accumulation in containment prior to the hydrogen burn. The four curves demonstrate similar trends in hydrogen release; however, the Battelle calculations were performed with an early version of MARCH which calculated hydrogen release rates which were unrealistically low.[2] The important feature of Figure B.2.1 is that the hydrogen release into containment occurred over a 7-hour period. The long release time prior to burn would have enhanced hydrogen transport and mixing processes in the containment building.

B.2.2 Hydrogen Transport in Containment

Hydrogen and steam entered containment through the discharge duct from the reactor coolant drain tank (RCDT). The RCDT is located in the basement level with the discharge duct exit near the ceiling of the basement as shown in Figure B.2.2. The hydrogen and steam would then enter the second- and third-floor levels through floor gratings, hatches, and penetrations, the open stairwell number 1, and an annular 4-inch seismic gap between the containment liner and the second and third floors.

The hot, buoyant hydrogen and steam mixture could lead to stratification in the compartments into which the mixture would enter. However, the stratification or buoyant forces would be opposed by many phenomena in containment which would promote mixing: (1) circulation of containment gas by the reactor building fan coolers, (2) circulation of containment of gas by the hot steam generator surfaces, (3) mixing of containment gas by condensation onto cool surfaces, (4) plume entrainment by released steam and hydrogen, and (5) molecular diffusion. The fan coolers alone circulated containment air once every twelve minutes. The fan cooler inlet drew air from the second floor and exhausted cooled air to multiple locations in the basement, reactor cavity, steam generator compartments, and dome region.

Experiments and analyses described in References 1 and 2 indicated that average hydrogen concentration differences between the dome lower containment regions greater than

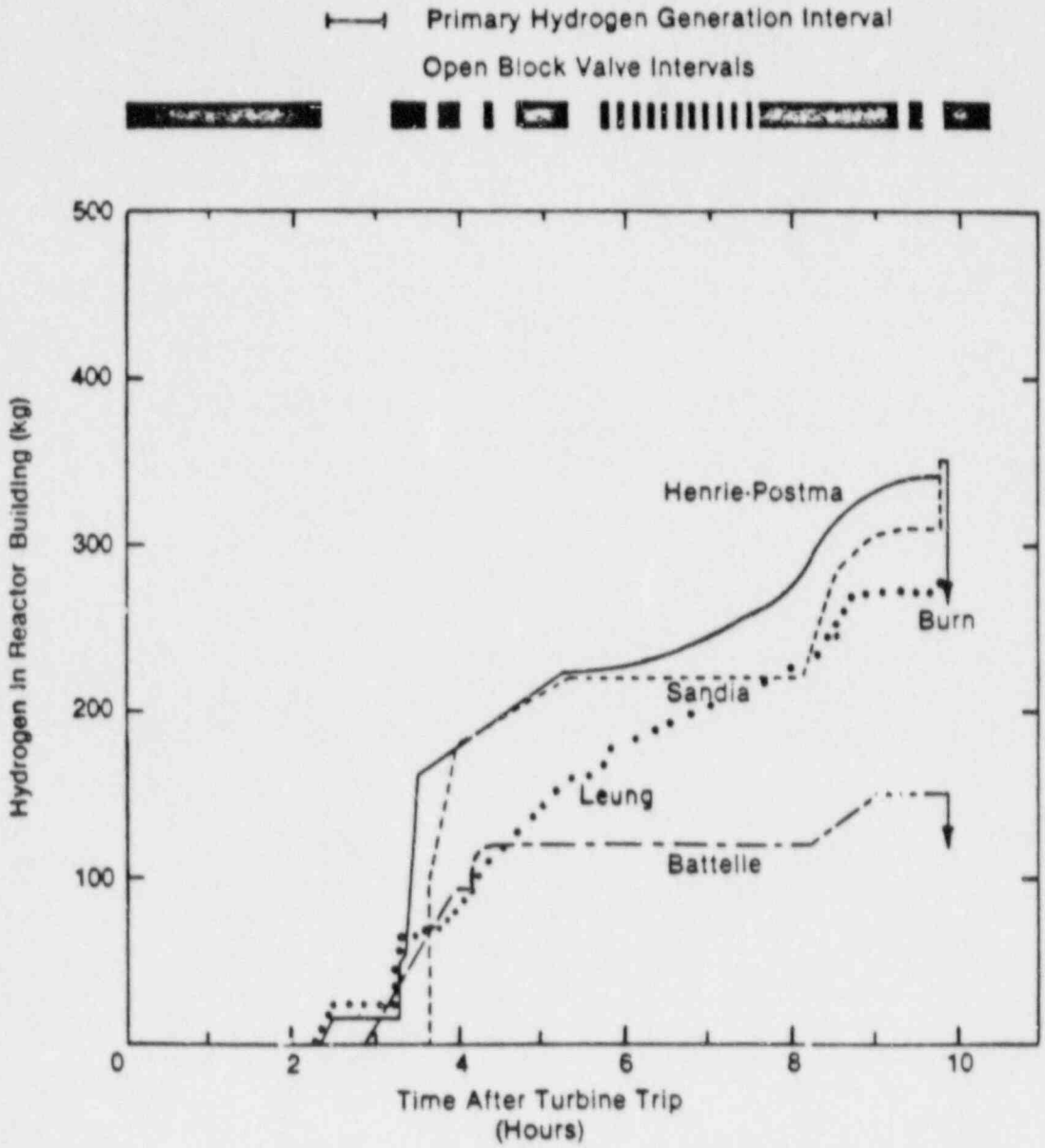

Figure B.2.1. Reactor Building Hydrogen Accumulation Estimates (From Reference 2)

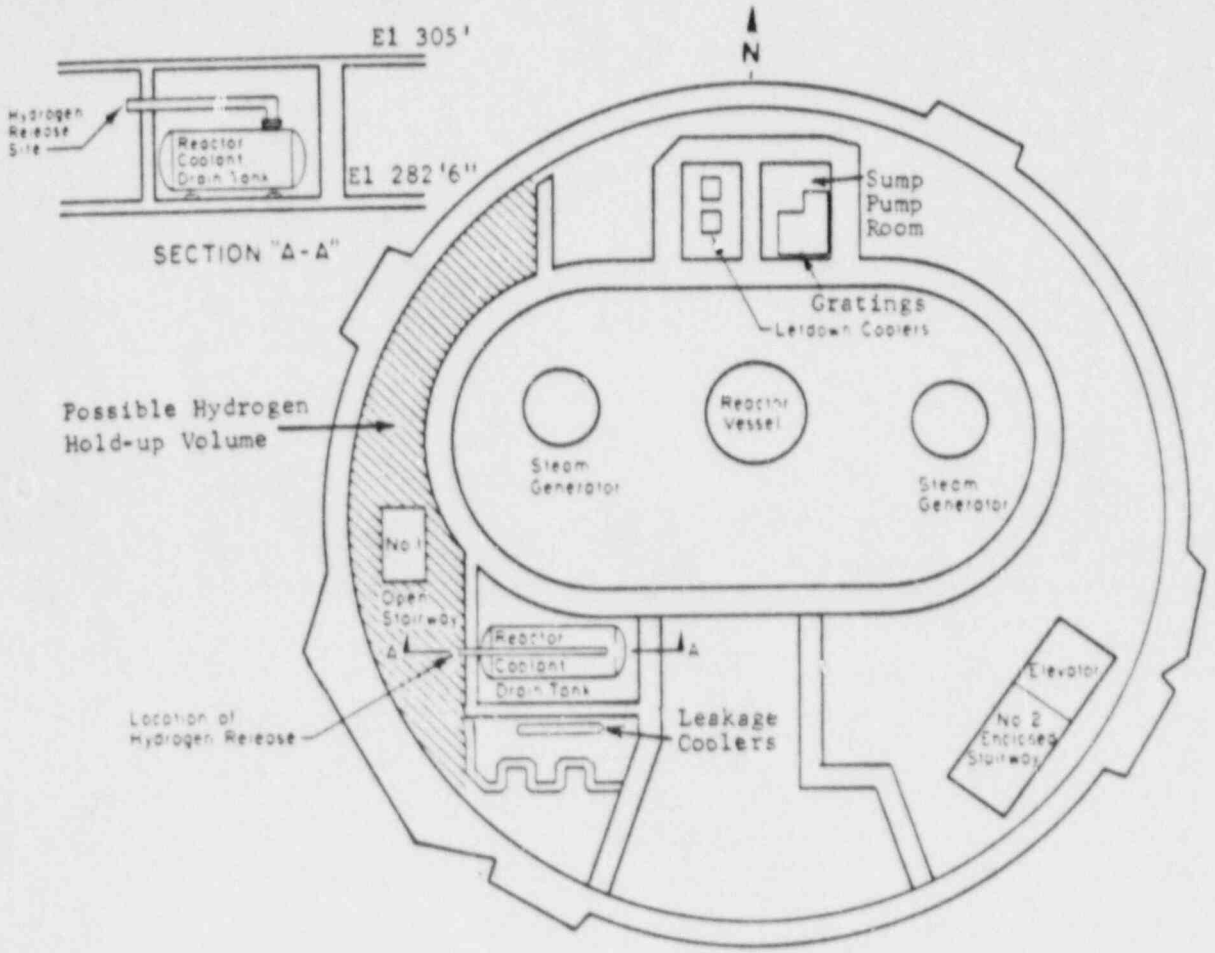

Figure B.2.2. RCDT Location in Containment

1 percent total hydrogen were unlikely. Hydrogen was released approximately 45 seconds prior to the burn which could have produced a small, enriched hydrogen zone in the basement; however, the bulk of the hydrogen released in the sever hours prior to the burn was well mixed throughout the containment.

B.2.3 Hydrogen Burn Initial Conditions

Henrie and Postma and FMRC[1,2] have estimated preignition gas conditions to consist of a hydrogen concentration of 7.3 to 7.9 volume percent and a water vapor concentration of 3.5 to 5.5 volume percent. Containment gas temperature was vertically stratified from 316°K in the basement to 327°K at higher elevations. The containment gas pressure was 110 kPa. Three sets of initial conditions were used in this analysis and are presented in Table B.2.1.

Table B.2.1

Initial Conditions Used for Hydrogen Burn Analysis

Case	XH_2(%)	XH_2O(%)	P(kPa)	T(°K)
1	7.9	3.5	110	327
2	7.3	3.6	110	327
3	7.5	5.5	110	327

B.3 Hydrogen Burn

B.3.1 Containment Response

The containment pressure due to the hydrogen burn was recorded by the Once Through Steam Generators (OTSG), A and B, pressure transmitters as well as by Engineered Safety Features (ESFs) pressure switches. This data is shown in Figure B.3.1. The OTSG A and B data were recorded every 3 seconds while ten ESF pressure switches were calibrated to actuate at 24.7 kPa (3.58 psig) and to reset at 20.7 kPa (3 psig). Six pressure switches were calibrated to actuate at 184 kPa (26.75 psig) and reset at 180 kPa (26 psig). The proximity of the 26.75 psig actuation and 26 psig reset (about a 4-second delay) may indicate that the peak pressure may not have greatly exceeded 193 kPa (28 psig). Henrie shows a peak pressure of 203 kPa (29.5 psig) in Figure 3-1 of Reference 1. The peak pressure occurred 10 to 12 seconds after ignition, which is also a rough indication of the burn time in containment.

Containment gas temperatures were recorded by resistance temperature detectors (RTDs) from twelve locations every 6

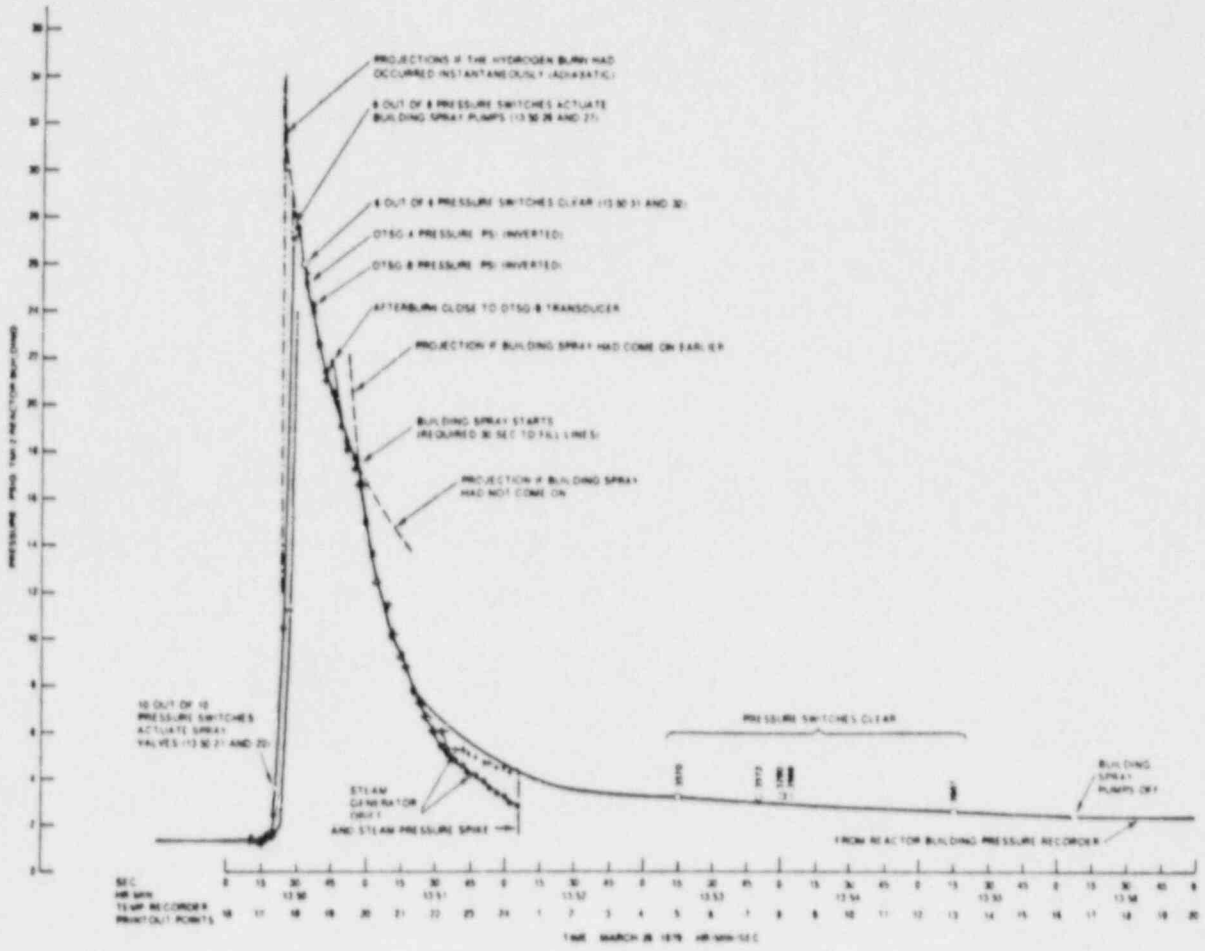

Figure B.3.1. TMI-2 Containment Gas Pressure Response to Hydrogen Burning (From Reference 1)

minutes. The hydrogen burn occurred between recording times and temperatures were logged well into cooldown after combustion. Therefore, the RTDs provided no useful temperature data during the hydrogen burn and gas cooldown period. High temperature alarm sensors monitored by the TMI-2 computer indicate that the burn started in the basement and continued upward through the floor levels and steam generator compartments into the dome region.[1] Therefore, the temperature sensors indicate the origin and direction of burn but do not give any gas temperature data during the burn.

The completeness of the burn at TMI-2 is not precisely known. Oxygen samples taken in containment were not consistent due to changes in sampling procedures to reduce exposure to personnel taking the samples. Henrie and Postma[1] used five different methods to calculate the amount of hydrogen burned in containment and concluded that approximately 86 percent of the initial hydrogen was consumed during the burn. After the burn, 1.1 percent hydrogen (compared to the initial 7.9 percent) would have been in containment.

B.3.2 HECTR Analysis of TMI-2 Hydrogen Burn

B.3.2.1 Containment Model

The TMI-2 containment was divided into eight compartments. These compartments are: (1) the reactor cavity; (2) the steam generator compartment with the pressurizer, SG1A; (3) the steam generator compartment without the pressurizer, SG1B; (4) the refueling canal; (5) the basement, Elevation 280; (6) the second floor, Elevation 305; (7) the third floor or dome region, Elevation 347; and (8) the enclosed stairwell and elevator. The model is shown in Figure B.3.2. The compartments are well connected to one another by equipment hatches, wall and floor penetrations, doorways, open stairwells, and the seismic gap.

The major Engineering Safety Features (ESFs) systems modeled during the burn were the reactor building fan coolers and spray system. The fan coolers operate in normal and LOCA modes. Five fan cooler units are located at Elevation 305 and draw containment air at this location into the cooling coils. During normal operations, three units circulate air from the second floor through the cooling coils to multiple release points in the basement, steam generator compartments, and reactor cavity. Upon a 4 psig increase in pressure signal, the fan coolers switch to LOCA mode operation. Five units circulate air at reduced air flow conditions from the second floor to the dome region as well as the regions mentioned for normal operation. The spray system is activated by a 28 psig increase in containment pressure, and water leaves the spray headers 30 seconds

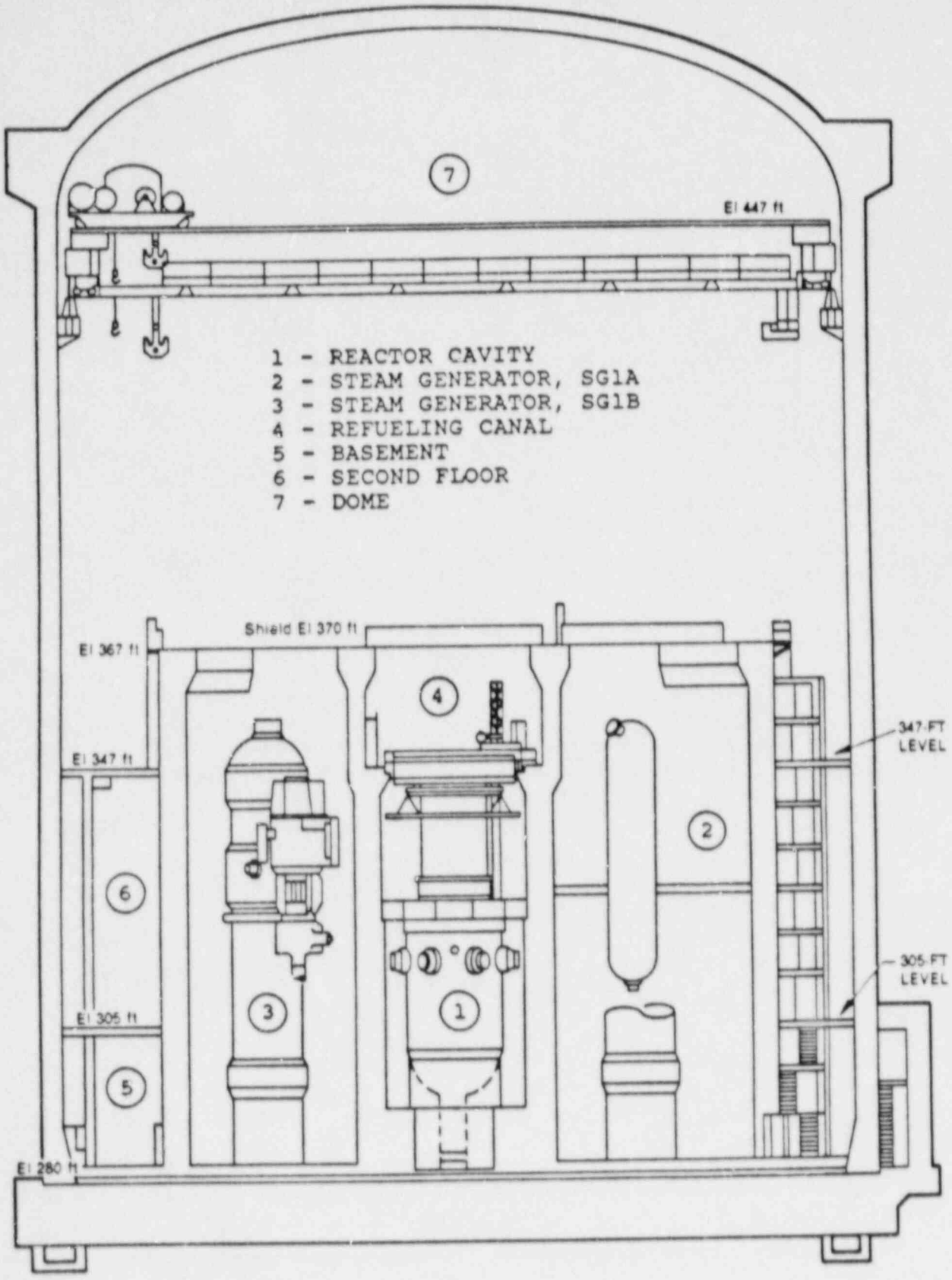

Figure B.3.2. TMI-2 Containment Vertical Section

after the high pressure signal. The effect of spray operation in reducing containment temperature is limited primarily to the dome region. Unevaporated spray reaching the dome region floor above the steam generator compartments and fuel transfer pit is allowed to continue falling through and evaporating in those compartments.

B.3.2.2 Safety-Equipment Model

The thermal response models of the safety-related equipment were based on a Barton 763 gauge pressure transmitter. Four models were developed, each reflecting various degrees of conservatism. Model conservatism indicates that the model surface temperature will respond at a higher temperature to a given incident heat flux when compared to the response of an actual Barton 763 to an identical flux. A one-dimensional model of the cover plate alone from the Barton 763 was the most conservative model. This model was included to provide a comparison with a prior analysis of equipment temperature response to pressure deflagrations in an ice condenser containment.[6] A second model treated all of the steel in the casing of the Barton 763 as a one-dimensional steel plate with a frontal area equal to the Barton 763. This model is referred to as the case-as-plate (CAP) model. The third model treated the entire steel casing as a lumped mass with uniform temperature response throughout the mass-to-incident heat flux. These two models were less conservative than the first model. The fourth model was a one-dimensional three-layer representation of the Barton 763. This model accounted for the air gap between the casing and internal electronics. This model was the least conservative of the four models described.

The fourth model was used in a separate analysis to bound the conservatism of the four models. In the analysis, the model was analytically exposed to an incident heat flux pulse used at the Sandia Central Receiver Test Facility (CRTF) for prior hydrogen burn simulation equipment experiments. The surface temperature response of the model was calculated and compared to the measured surface temperature rise of an actual Barton 763 exposed to the flux pulse at the CRTF. The peak surface temperature of the model was calculated to be approximately 11°K (20°F) higher than the measured Barton 763 surface temperature. The fourth model and measured Barton 763 thermal time response characteristics were equivalent. This fourth model or one-dimensional three-layer model is considered to be the most realistic of the four models and its surface temperature response to pressure burning will be reported in this analysis as a basis of evaluating the thermal response of electrical equipment to a pressure burn.

The Barton 763 model was placed in five containment locations: (1) steam generator compartment SG1A, (2) steam

generator compartment SG1B, (3) the basement, (4) the second floor, and (5) the dome region.

B.3.2.3 Calculations Performed

Eleven HECTR production runs are reported for this analysis. Table B.3.1 summarizes the calculations performed. The first two production runs (Cases 1A and 1B) examined the effect of choosing compartment flame propagation lengths (FPL). FPL are estimates of the path length over which the hydrogen burn can occur in each compartment of the containment. Flame speeds are calculated by HECTR at the beginning of each compartment burn using flame speed correlati in HECTR based on the compartment gas conditions.[3] Dividing each compartment FPL by the flame speed gives the burn time duration. TMI-2 containment FPLs were chosen based on compartment dimensions. Case 1A used maximum compartment dimensions, and Case 1B used minimum compartment dimensions. The long and short dimensions were chosen as bounding lengths over which the burn could occur. Cases 1A and 1B used initial conditions postulated by Henrie and Postma (Case 1 of Table B.2.1) and assumed complete hydrogen burning.

Case 1C examined the effect of varying surface areas in the compartment model. The magnitude of the surface area can have a significant effect on containment gas cooldown after the burn and a moderate effect on gas heat up during hydrogen burning, with more energy being lost by the gas to greater surface areas. Surface areas for the HECTR analyses were calculated by reviewing Final Safety Analysis Report diagrams of the containment. Case 1C used the initial conditions of Case 1A and complete hydrogen burning.

Cases 1D and 1E assumed incomplete hydrogen burning and used completion percentages postulated by Henrie and Postma.[1] Case 1D assumed that hydrogen burned down to 1 percent hydrogen in the dome region; to 2 percent in the steam generator compartments; and to 2.2 percent hydrogen below Elevation 347. Case 1E assumed that hydrogen burned completely in the dome region and burned down to 3.5 percent hydrogen elsewhere in containment. The final hydrogen concentration balances to 1.1 percent for both cases. Initial conditions used were those postulated by Henrie and Postma (Case 1 of Table B.2.1).

The Case 2 calculations did not attempt to establish burn durations through the selection of FPL and use of HECTR flame speed correlations. Total containment burn times of 12 seconds were specified in the HECTR input data deck. Case 2A used the Henrie and Postma initial conditions and assumed complete hydrogen burning. Cases 2B and 2C used the Henrie initial conditions but assumed incomplete burning as in Cases 1D and 1E, respectively. Cases 2D and 2E used the

FMRC initial conditions (Cases 2 and 3 in Table B.2.1 and assumed complete hydrogen burning. Case 2F was essentially a repeat of Case 2B but delayed the hydrogen burn propagation time from the basement to dome region by 50 percent.

Table B.3.1

HECTR TMI-2 Analyses

Case	Burn Time Mode	Burn Completeness	Surface Area	Initial Conditions
1A	Long FPL	100%	Default	A
1B	Short FPL	100%	Default	A
1C	Short FPL	100%	130%	A
1D	Long FPL	X	Default	A
1E	Long FPL	Y	Default	A
2A	Specified	100%	Default	A
2B	Specified	X	Default	A
2C	Specified	Y	Default	A
2D	Specified	100%	Default	B
2E	Specified	100%	Default	C
2F	Specified	X	Default	A

A Case 1 Initial Conditions Table B.2.1
B Case 2 Initial Conditions Table B.2.1
C Case 3 Initial Conditions Table B.2.1

X 1% H_2 left in dome
2% H_2 left in steam generators
2.2% H_2 left below dome

Y 0% H_2 left in dome
3.5% H_2 left elsewhere in containment

B.3.2.4 Results

Table B.3.2 lists the HECTR calculated peak gas pressures and temperatures (P_m and T_m, respectively). The peak safety equipment model temperatures for the lumped mass model, the CAP model, and the three-layer model (Tm_1, Tm_2, and Tm_3, respectively) are also given in Table B.3.2. The peak incident total and radiant heat fluxes (Tm and Rm) to the three-layer model are also listed. The peak temperatures for the three-layer model will be reported on only in this analysis because the three-layer model is most representative of the actual Barton 763.

Table B.3.2

Deflagration Summaries

Case	Compartment	Gas		Barton			Incident Flux	
		Pm (kPa)	Tm (°K)	Tm (°K)[1]	Tm (°K)[2]	Tm (°K)[3]	Tm (kW/m^2)	Rm (kW/m^2)
1A	1	340	920	--	--	--	--	--
	2	340	1020	352	335	333	54	29
	3	340	1030	352	335	333	55	30
	4	340	1040	--	--	--	--	--
	5	340	990	358	338	334	44	30
	6	340	1010	362	340	335	63	35
	7	340	1060	369	343	338	77	43
1B	1	320	870	--	--	--	--	--
	2	320	1000	351	335	333	52	27
	3	320	1010	352	335	333	54	28
	4	320	1020	--	--	--	--	--
	5	320	960	357	338	334	37	24
	6	320	970	357	338	333	50	28
	7	320	1030	369	342	338	70	39
1C	1	330	920	--	--	--	--	--
	2	330	1020	350	335	333	--	--
	3	330	1030	351	335	333	--	--
	4	330	1040	--	--	--	--	--
	5	330	980	355	337	334	--	--
	6	330	1000	358	338	334	--	--
	7	330	1050	365	341	337	--	--
1D	1	310	800	--	--	--		--
	2	310	900	350	335	333		19
	3	310	890	350	335	332	[illegible]	19
	4	310	970	--	--	--	--	--
	5	310	850	354	337	333	30	18
	6	310	890	358	338	333	42	19
	7	310	1000	369	343	338	66	36
1E	1	300	710	--	--	--	--	--
	2	300	780	345	333	333	27	12
	3	300	780	345	333	331	26	12
	4	300	780	--	--	--	--	--
	5	300	760	349	335	331	19	12
	6	300	790	353	336	332	26	14
	7	300	1030	373	344	339	71	41
1F	1	340	800	--	--	--	--	--
	2	340	1010	357	338	335	49	35
	3	340	1020	357	338	335	50	35
	4	340	1060	--	--	--	--	--

Table B.3.2

Deflagration Summaries (Concluded)

Case	Compartment	Gas		Barton			Incident Flux	
		Pm (kPa)	Tm (°K)	Tm (°K)[1]	Tm (°K)[2]	Tm (°K)[3]	Tm (kW/m^2)	Rm (kW/m^2)
	5	340	1020	365	341	336	56	39
	6	340	1030	368	342	337	59	42
	7	340	1070	375	345	340	68	48
2B	1	320	720	--	--	--	--	--
	2	320	890	350	335	332	32	22
	3	320	900	350	335	333	33	21
	4	320	1000	--	--	--	--	--
	5	320	890	355	337	333	35	23
	6	320	900	359	339	334	38	25
	7	320	1010	369	342	338	57	39
2C	1	310	660	--	--	--	--	--
	2	310	790	344	333	331	21	12
	3	310	790	344	333	331	21	12
	4	310	810	--	--	--	--	--
	5	310	800	349	335	331	25	14
	6	310	800	353	336	332	26	15
	7	310	1060	374	344	340	65	46
2D	1	300	730	--	--	--	--	--
	2	300	900	349	335	332	32	21
	3	300	900	349	335	333	32	21
	4	300	930	--	--	--	--	--
	5	300	910	356	338	333	37	24
	6	300	910	359	339	334	39	25
	7	300	940	361	340	336	43	28
2E	1	310	730	--	--	--	--	--
	2	310	930	352	336	333	38	26
	3	310	930	352	336	334	39	26
	4	310	970	--	--	--	--	--
	5	310	940	359	339	334	44	29
	6	310	950	362	340	335	46	31
	7	310	980	366	342	338	53	35
2F	1	320	750	--	--	--	--	--
	2	320	910	350	335	333	33	22
	3	320	910	350	335	333	34	22
	4	320	1010	--	--	--	--	--
	5	320	900	355	337	333	37	24
	6	320	900	359	339	334	40	25
	7	320	1020	369	343	338	64	39

Peak containment gas pressures ranged from 300 kPa to 340 kPa. Peak gas temperatures in the dome region ranged from 940°K to 1070°K. Basement and second floor peak gas temperatures ranged from 760°K and 790°K to 1020°K and 1030°K, respectively.

The lumped mass, CAP, and three-layer models of the Barton 763 pressure transmitter were included to provide continuity with the Surry and hybrid containment analyses presented in Appendices A and C. A more detailed description of these models may be found in Section A.1.1. Peak temperatures of the Barton 763 models never exceeded the LOCA qualification temperature of 444°K. Peak temperatures for the one dimensional three-layer model ranged from 331°K to 340°K. Peak total-incident fluxes in the dome region ranged from 43 kW/m^2 to 79 kW/m^2, while peak total incident fluxes in the lower elevations of containment ranged from 22 kW/m^2 to 64 kW/m^2. The total incident fluxes would be comparable in magnitude to fluxes seen by other equipment or by cable in containment. The possible effect of these fluxes on cable will be addressed later in the report.

Figure B.3.3 shows the Case 1A and 1B HECTR calculated pressure compared to the OTSGA and OTSGB pressure readings. Case 1A used the shorter FPLs which resulted in a burn duration time of approximately 7 seconds while Case 1B, using the longer FPLs, resulted in a burn duration time of approximately 11 seconds. Although Case 1B calculates a reasonable burn time, HECTR does calculate its pressure increase to occur approximately three seconds before the corresponding OTSGA pressure value. Postburn cooling shows good agreement with the TMI-2 OTSG readings.

Figure B.3.4 compares Case 1A and 1C results to the OTSG data. The surface area in containment for Case 1C was increased by 30 percent compared to the containment surface area used in Case 1A. The increased surface area resulted in a 15 kPa decrease in containment pressure at the time when containment spray water entered the containment when compared to the Case 1A pressure response. The initial surface area calculated for the TMI-2 calculations are believed to be adequate due to agreement in postcombustion cooldown slopes between HECTR calculated pressures and the OTSG A pressures.

Figures B.3.5 and B.3.6 show Case 1D and 1E HECTR pressure calculations compared to the Case 1B and OTSG data curves. Recall that Case 1D and 1E assume 1.1 percent total hydrogen left after the burn. Pressure rise during the burn as calculated by HECTR occurs earlier than the OTSG pressure data, but postcombustion gas pressure cooldown results are in excellent agreement with each other.

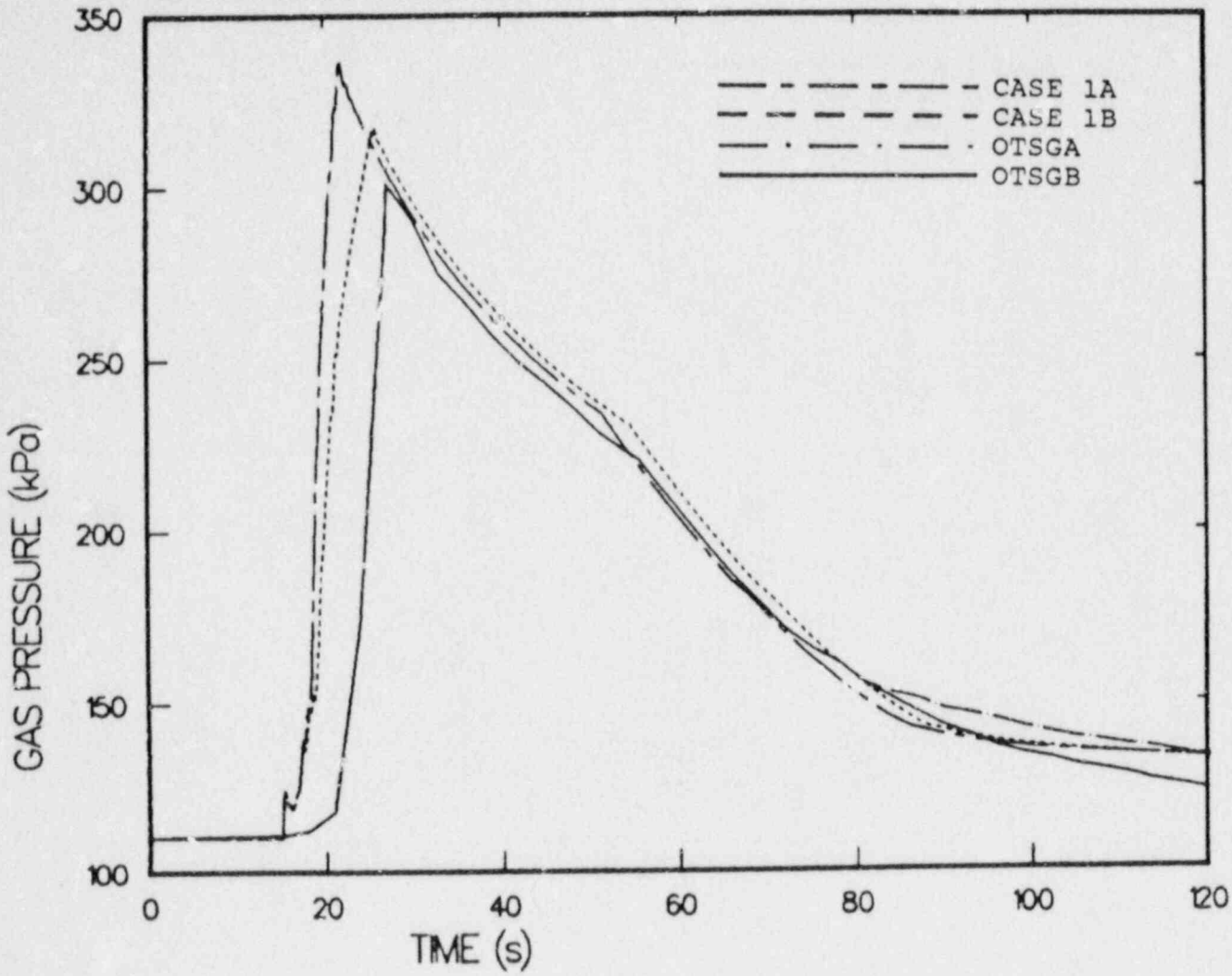

Figure B.3.3. Comparison of Case 1A and Case 1B Pressure Calculations to OTSGA and OTSGB Pressure Measurements

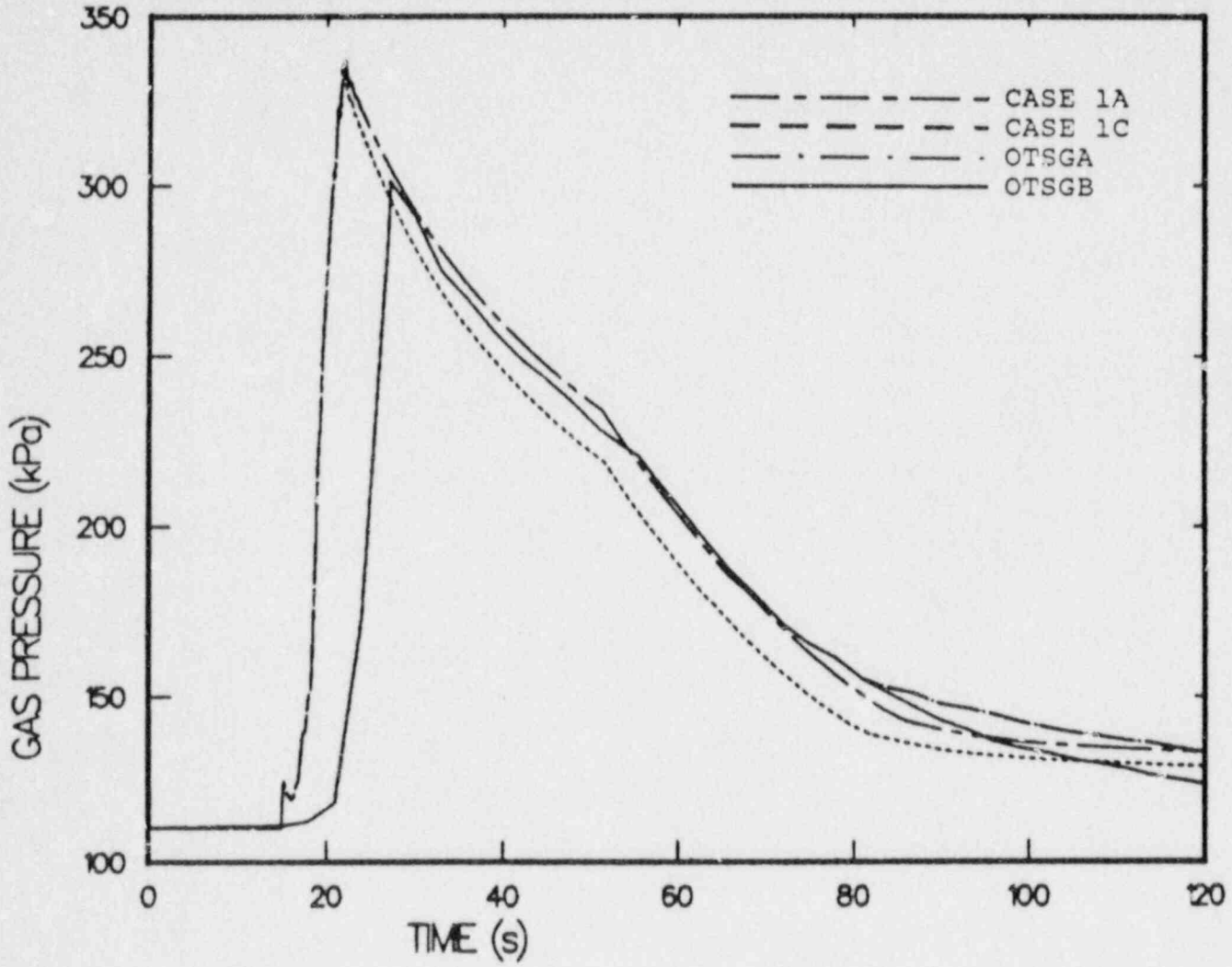

Figure B.3.4. Comparison of Increased Surface Area Pressure Response (Case 1C) to Case 1B, OTSGA, and OTSGB Pressures

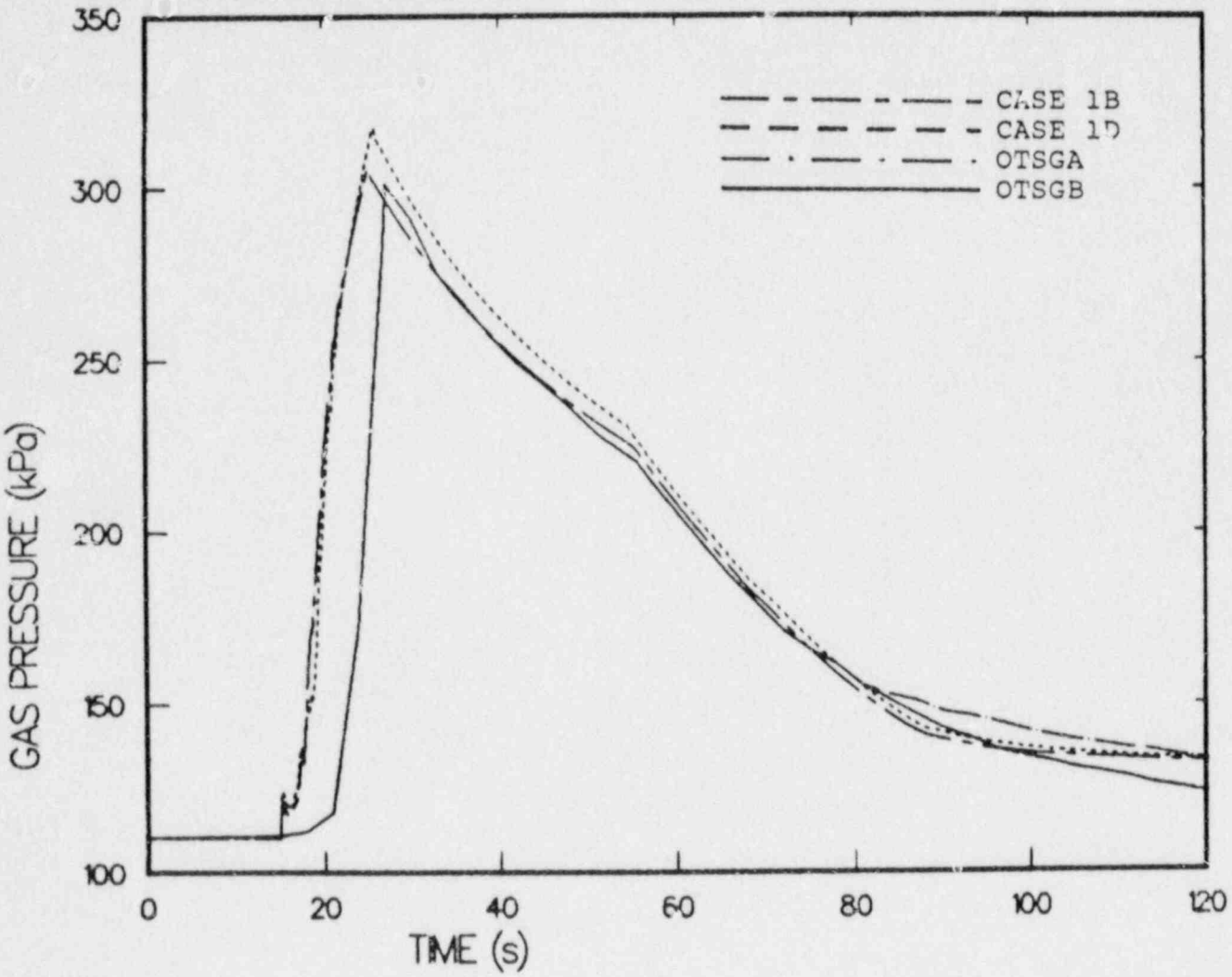

Figure B.3.5. Case 1D Pressure Compared to Case 1B and OTSG Pressures

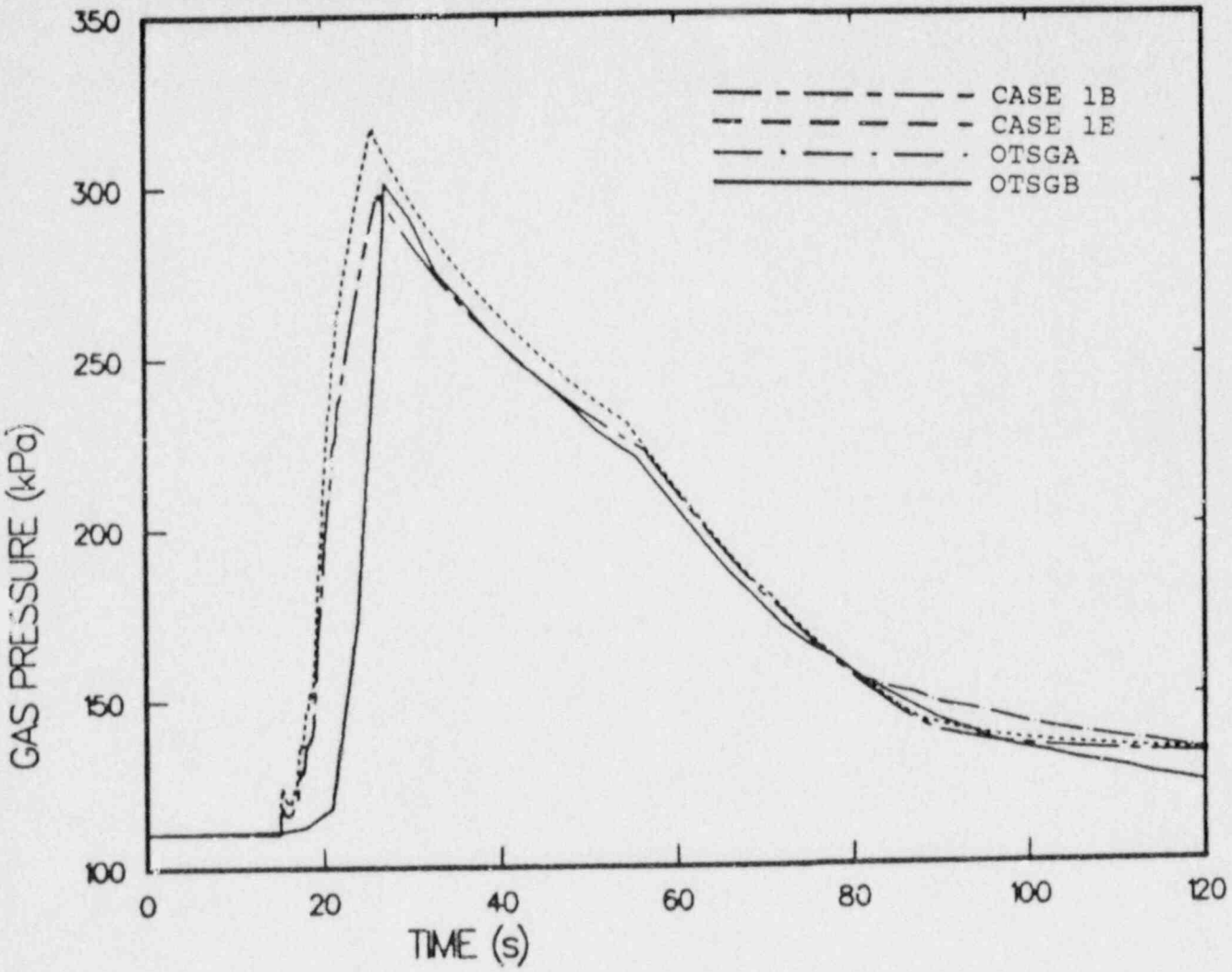

Figure B.3.6. Case 1E Pressure Compared to Case 1B and OTSG Pressures

Figures B.3.7 and B.3.8 show the Case 1D and 1E containment gas temperatures for the basement (C5), second floor (C6), dome region (C7), and steam generator compartments (C2). These temperature patterns are typical for all of the Case 1 calculations. The burn initiated in C5 and propagated to C2 and C6. The burn then propagated to C7 from C6. For all Case 1 calculations, the burns in the compartments below C7 were completed before the burn in C7 was completed. The temperatures in C2, C5, and C6 continued to increase after their hydrogen burns ended due to thermal influence from the hydrogen burning in the dome region. In Case 1E, the thermal influence from the dome region upon C2, C5, and C6 resulted in peak temperatures higher than those due to burning. The phenomenon was true only for C5 in the Case 1D calculation. The duration of the burn times in C1, C4, C5, and C6 may be changed by varying the FPL in each compartment.

It has been postulated that burning occurred simultaneously in all regions of the compartment building.[7] The Case 2 HECTR calculations addressed this issue by forcing the hydrogen burning in each compartment to end concurrently. For the Case 2 calculations, burning was initiated in the basement region and allowed to propagate upward through the second floor and steam generator compartments into the dome region. Burn propagation from the basement into the second floor was delayed for 1.5 seconds, and burn propagation from the second floor to the dome region was delayed for 2 seconds. Therefore, burning occurred for: (1) 12 seconds in the basement and steam generator compartments, (2) 10.5 seconds in the second floor, and (3) 9.5 seconds in the dome region. Hydrogen burning was stopped in the containment building 12 seconds after ignition in the basement. These burn propagation delay times were chosen after a private conversation with O. J. Henrie.

Figures B.3.9 and B.3.10 show HECTR calculated containment pressures for Cases 2B and 2C, respectively. Cases 2B and 2C used the same burning completions as used in Cases 1D and 1E, respectively. The HECTR-calculated pressure agreement with the OTSG pressure data is good. The HECTR pressure increase during burning in Cases 2B and 2C agrees much better with the OTSG pressure data compared to Cases 1D and 1E, but still predicts an earlier pressure rise compared to the OTSG pressure. Figures B.3.11 and B.3.12 show the HECTR containment temperature response for C2, C5, C6, and C7. Since burning below C7 occurs concurrently, the temperature responses of C2, C5, and C6 during burning are very similar with slightly different peak temperatures. The Case 2B C2, C5, and C6 hydrogen burning was more complete than in Case 2C, resulting in higher peak temperatures in those compartments. Case 2B C7 hydrogen burning was less complete than in Case 2C, resulting in a lower dome peak temperature. Before the sprays entered containment, the containment gas cooldown rate was slightly higher in the lower elevations

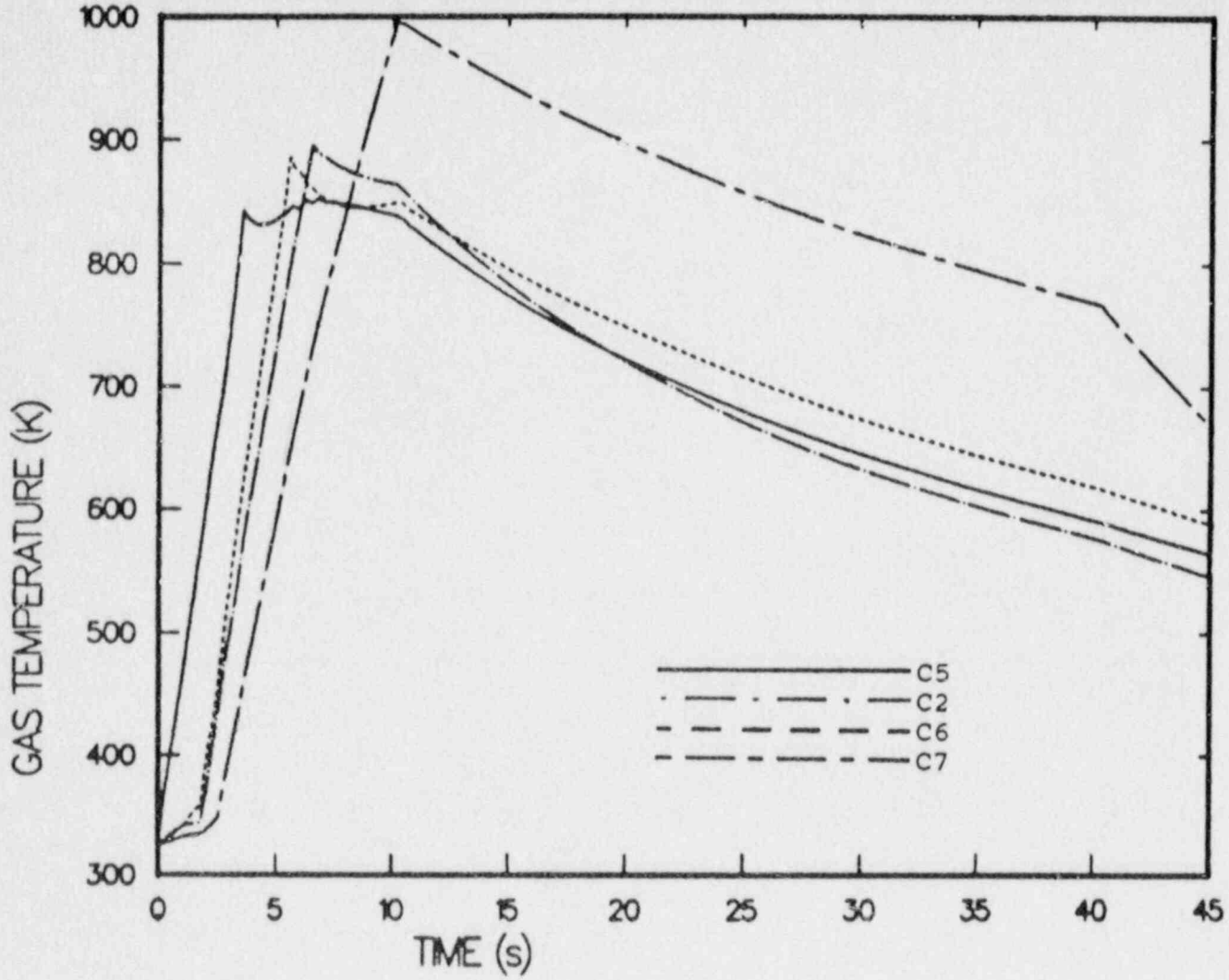

Figure B.3.7. Case 1D Calculated Gas Temperatures from Selected Containment Regions

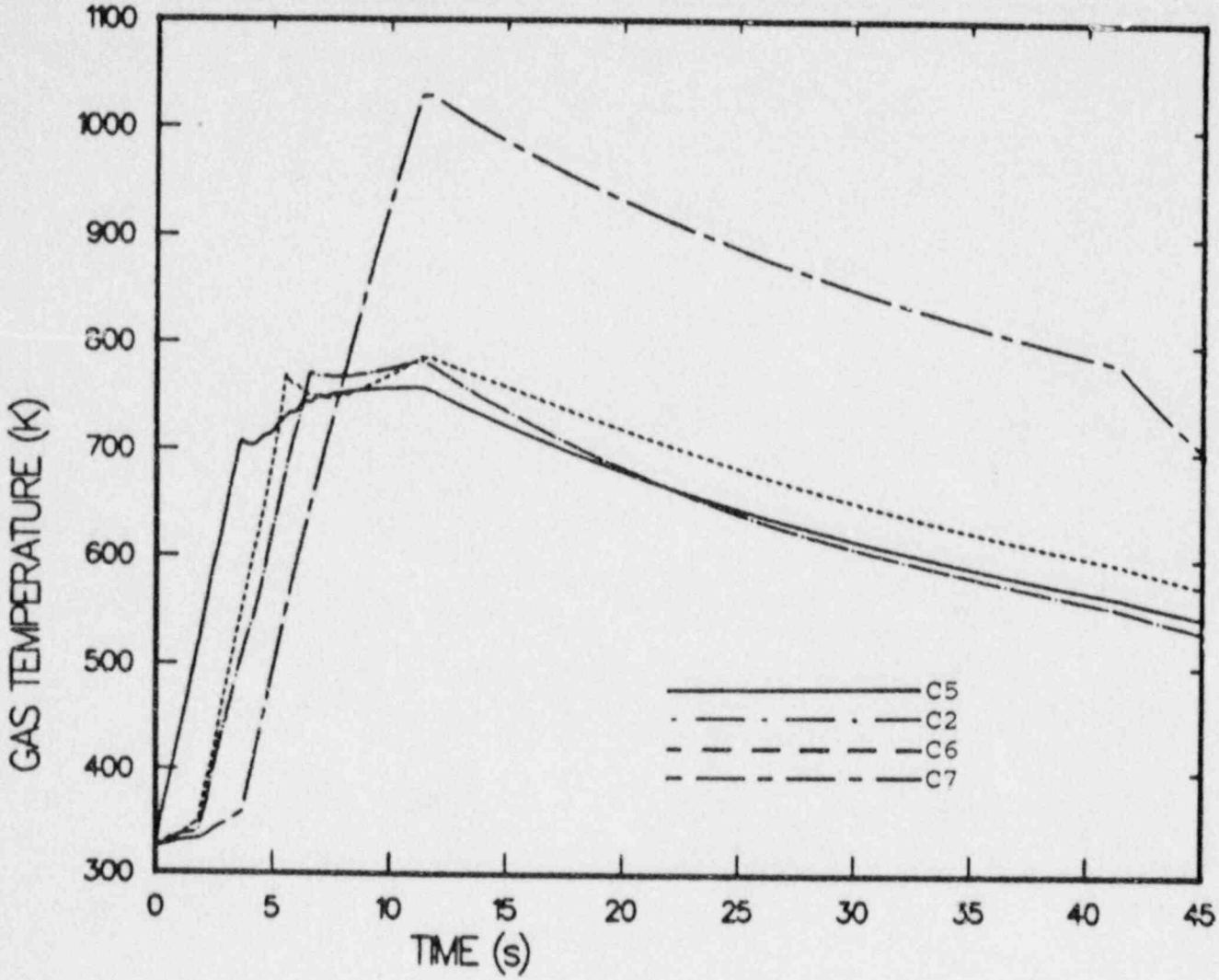

Figure B.3.8. Case 1E Calculated Pressure Compared to OTSGA and OTSGB Measured Pressures

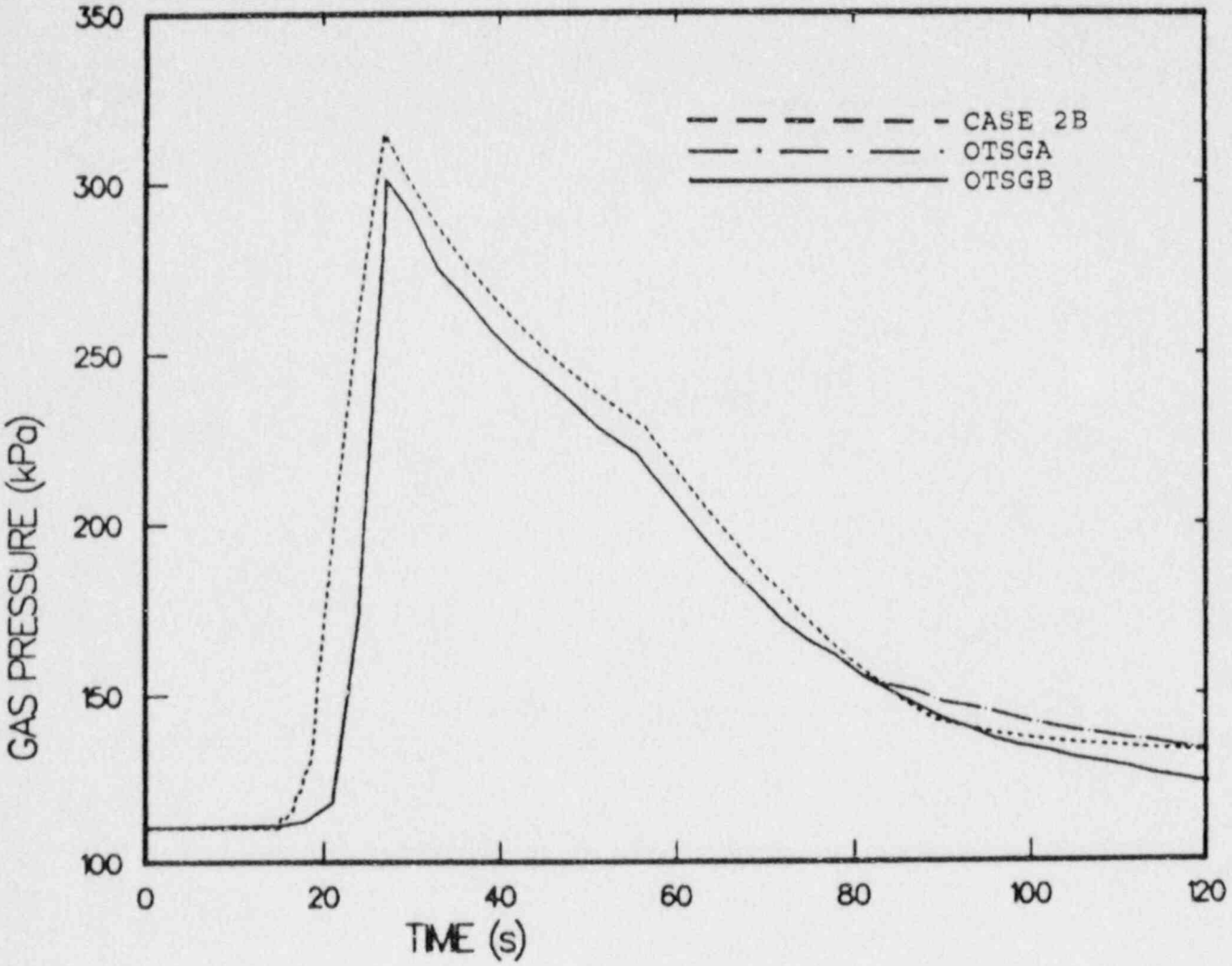

Figure B.3.9. Case 2B Calculated Pressure Compared to OTSGA and OTSGB Measured Pressures

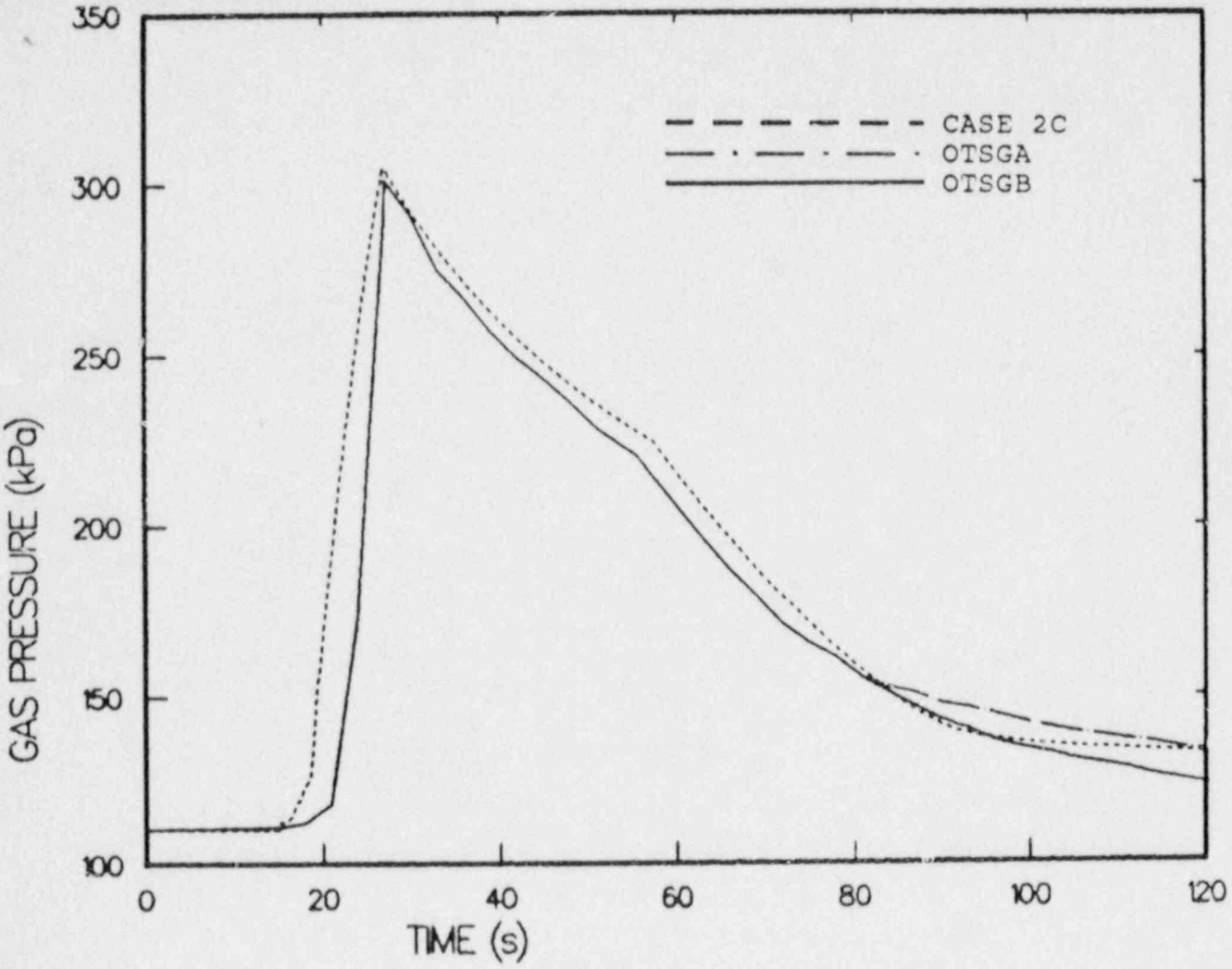

Figure B.3.10. Case 2C Calculated Pressure Compared to OTSGA and OTSGB Measured Pressures

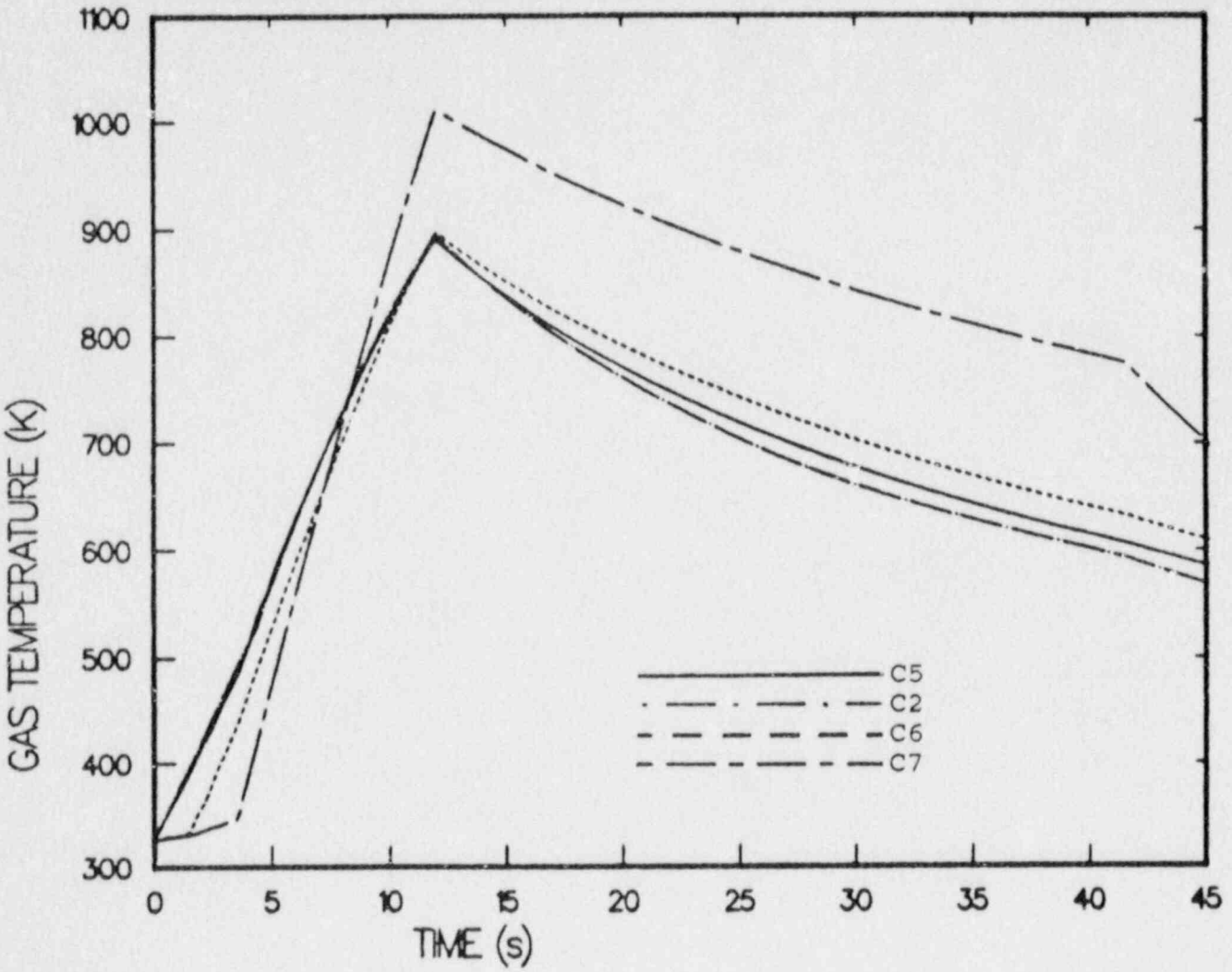

Figure B.3.11. Case 2B Calculated Gas Temperatures

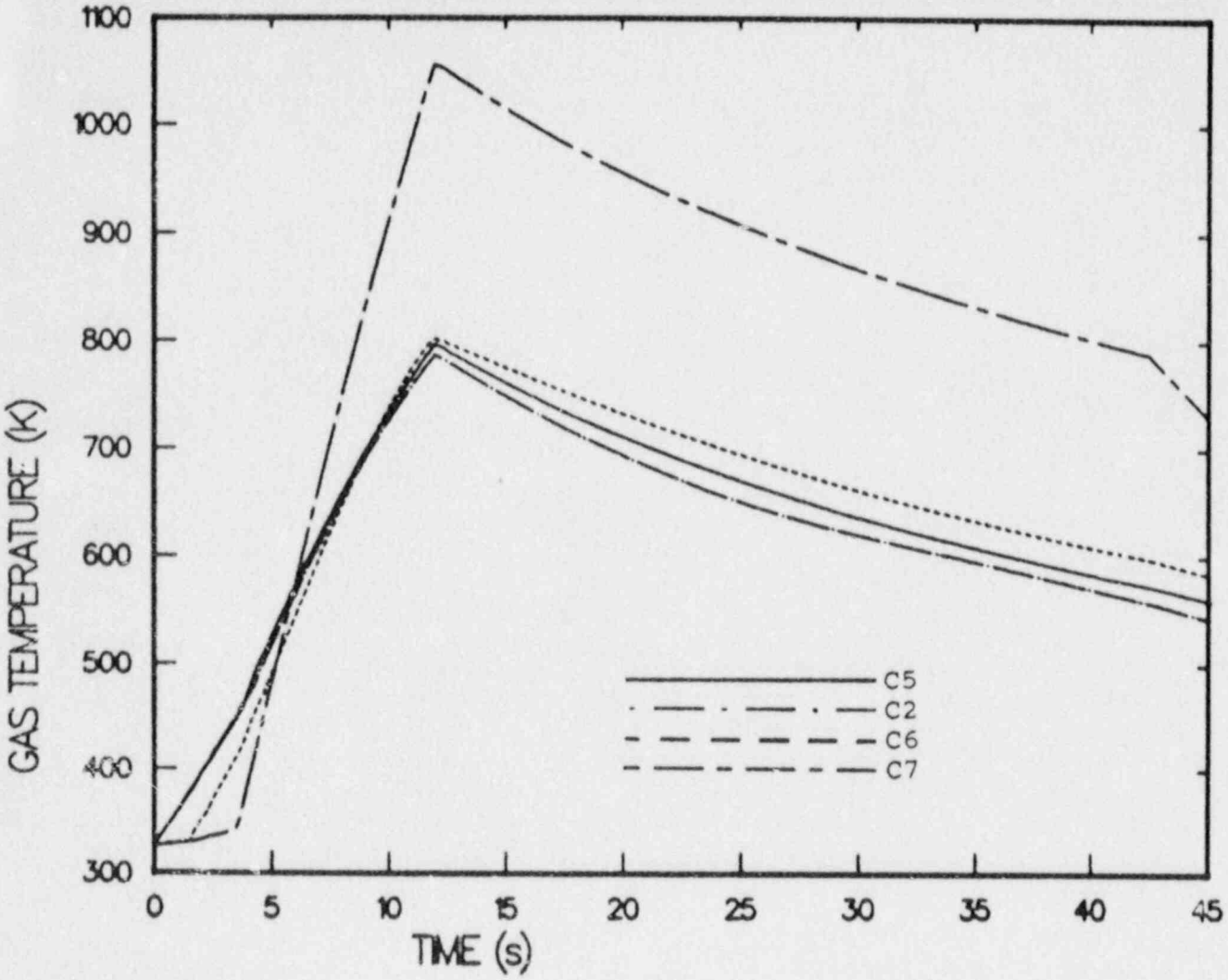

Figure B.3.12. Case 2C Calculated Gas Temperatures

(C5 and C2) of the containment compared to gas cooldown in the dome region.

Spray actuation significantly affected gas cooldown in the dome region. Gas cooldown due to sprays in the C2 spray carryover compartment was much less compared to the dome gas.

Figures B.3.13 through B.3.16 show HECTR gas pressure and temperature calculations for Cases 2D and 2E. Cases 2D and 2E used the FMRC initial conditions: 7.3 percent H_2, 3.6 percent H_2O, and 7.5 percent H_2, 5 percent H_2O, respectively. Both cases assumed complete hydrogen burning. The lower initial hydrogen concentrations resulted in less severe peak pressures and temperatures when compared to the Case 1A, 1B and 2A complete hydrogen burning calculations. The HECTR pressure calculations show good agreement with the OTSG pressure data. The C2, C5, C6, and C7 peak temperatures are close due to complete hydrogen burning in all containment regions occurring concurrently.

The Case 2F calculation attempted to address the earlier pressure increases calculated by HECTR in the prior Case 1 and Case 2 series. The Case 2F calculation delayed the flame propagation from C5 to C6 and then from C6 to C7. The burn propagation from C5 to C6 was delayed by 3 seconds, and the burn propagation from C6 to C7 was delayed by another 3 seconds. Therefore, the burn time in: (1) the basement and steam generator compartments was 12 seconds, (2) the second floor was 9 seconds, and (3) the dome was 6 seconds. The delay in burn propagation from lower to higher elevations would decrease the pressure rise rate early in the burn. Delaying burn initiation in the dome would cause the hydrogen in the dome to be burned at a higher rate to force the burn to end in 12 seconds. The quicker burning in the dome would then cause the pressure increase rate to be larger than the other Case 1 and Case 2 calculations during burning in the dome region. The Case 2F calculation used the Case 2B initial conditions and burning completion.

Figures B.3.17 and B.3.18 show the calculated containment pressure and temperatures. Figure B.3.17 demonstrates that the HECTR-calculated pressure rise rate is much closer to the OTSG pressure data than for the other Case 1 and Case 2 calculations. HECTR pressures lead the OTSG data by approximately 2 seconds. The containment temperature responses are similar to those of Case 2B and demonstrate almost uniform peak temperatures below the dome region.

Figures B.3.19 and B.3.20 show the calculated total incident fluxes to the Barton pressure transmitter for the lower level (C1) and dome region (C7) of containment, respectively. Fluxes are presented for three typical cases:

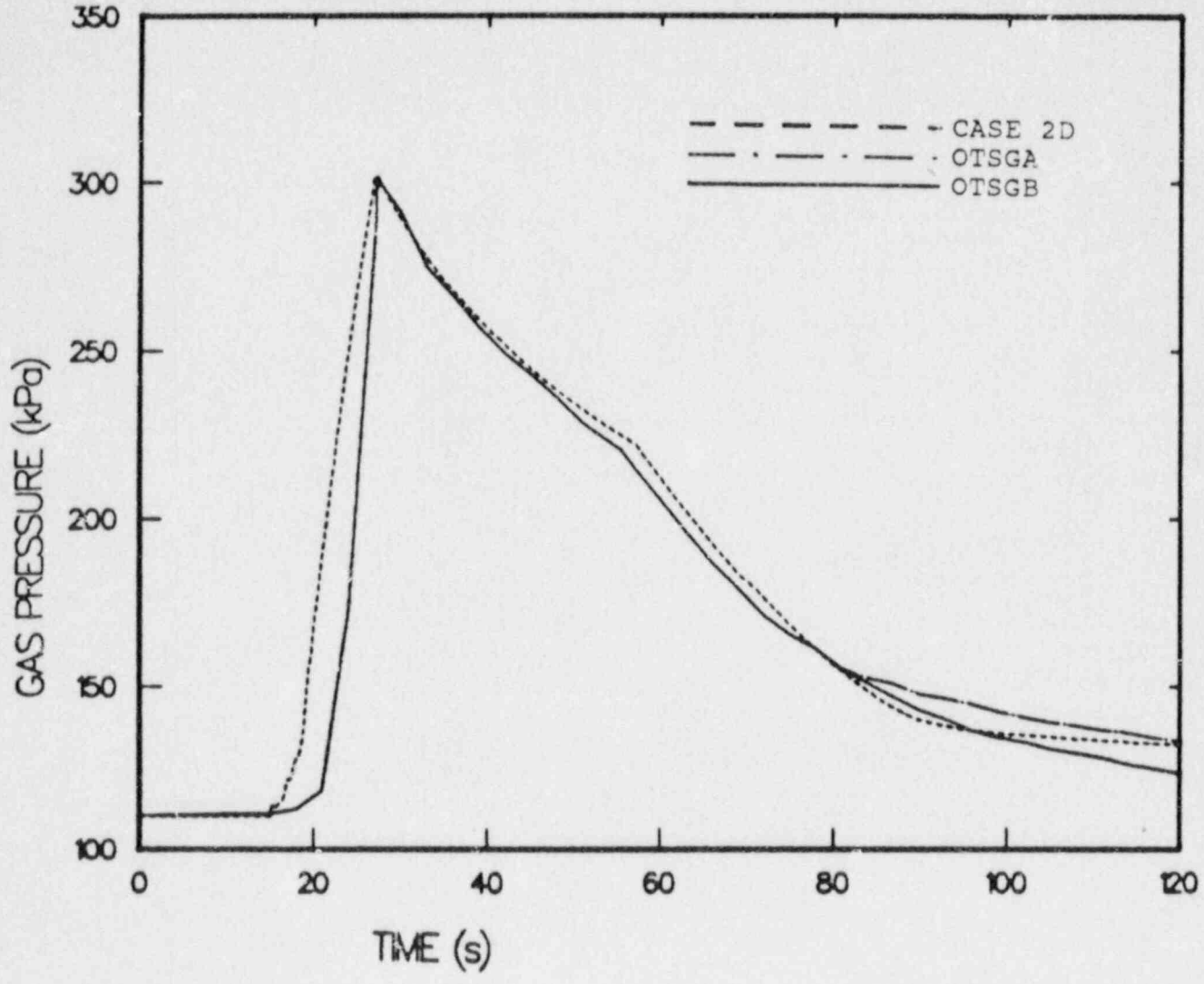

Figure B.3.13. Case 2D Calculated Pressure Compared to OTSGA and OTSGB Measured Pressures

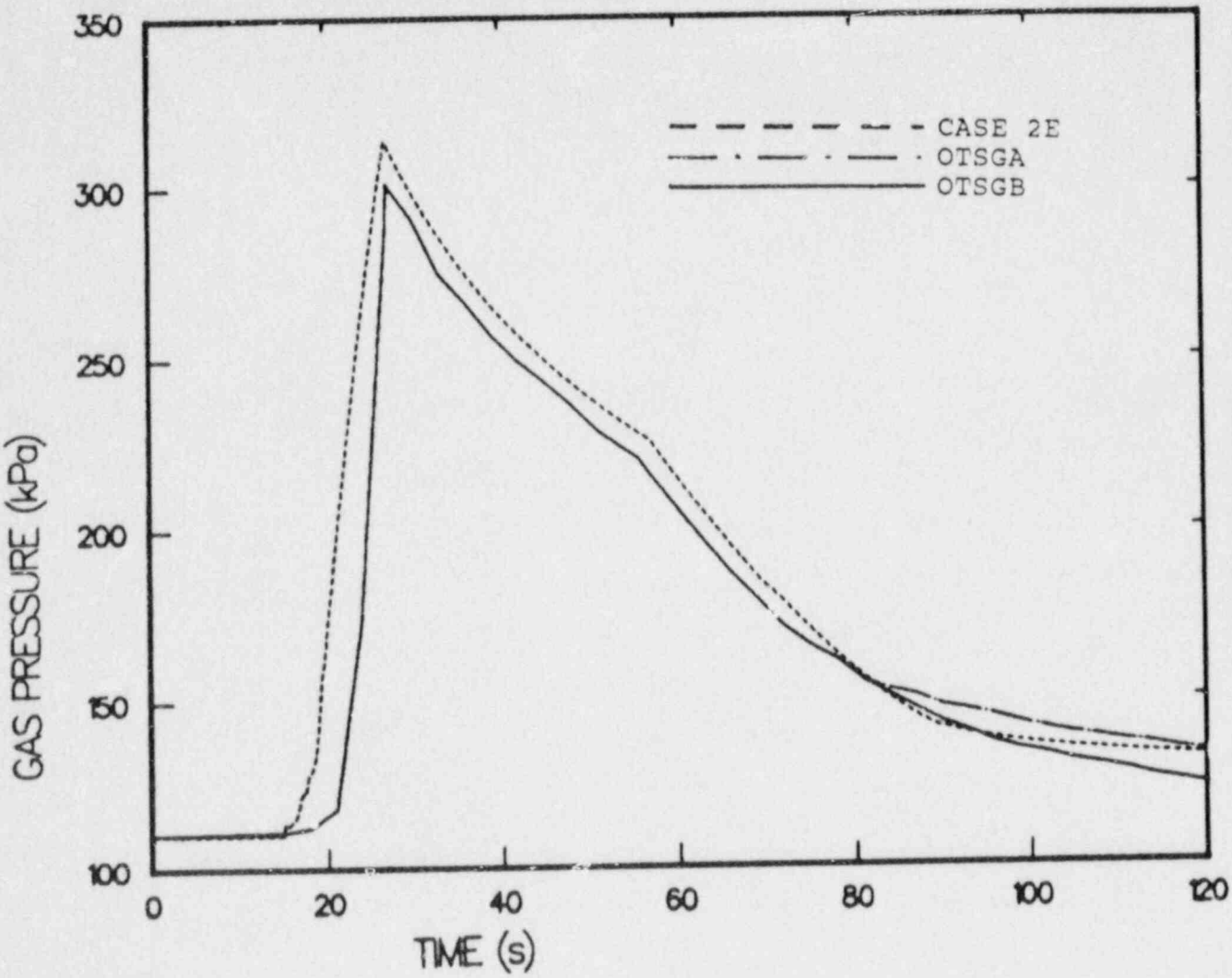

Figure B.3.14. Case 2E Calculated Pressure Compared to OTSGA and OTSGB Measured Pressures

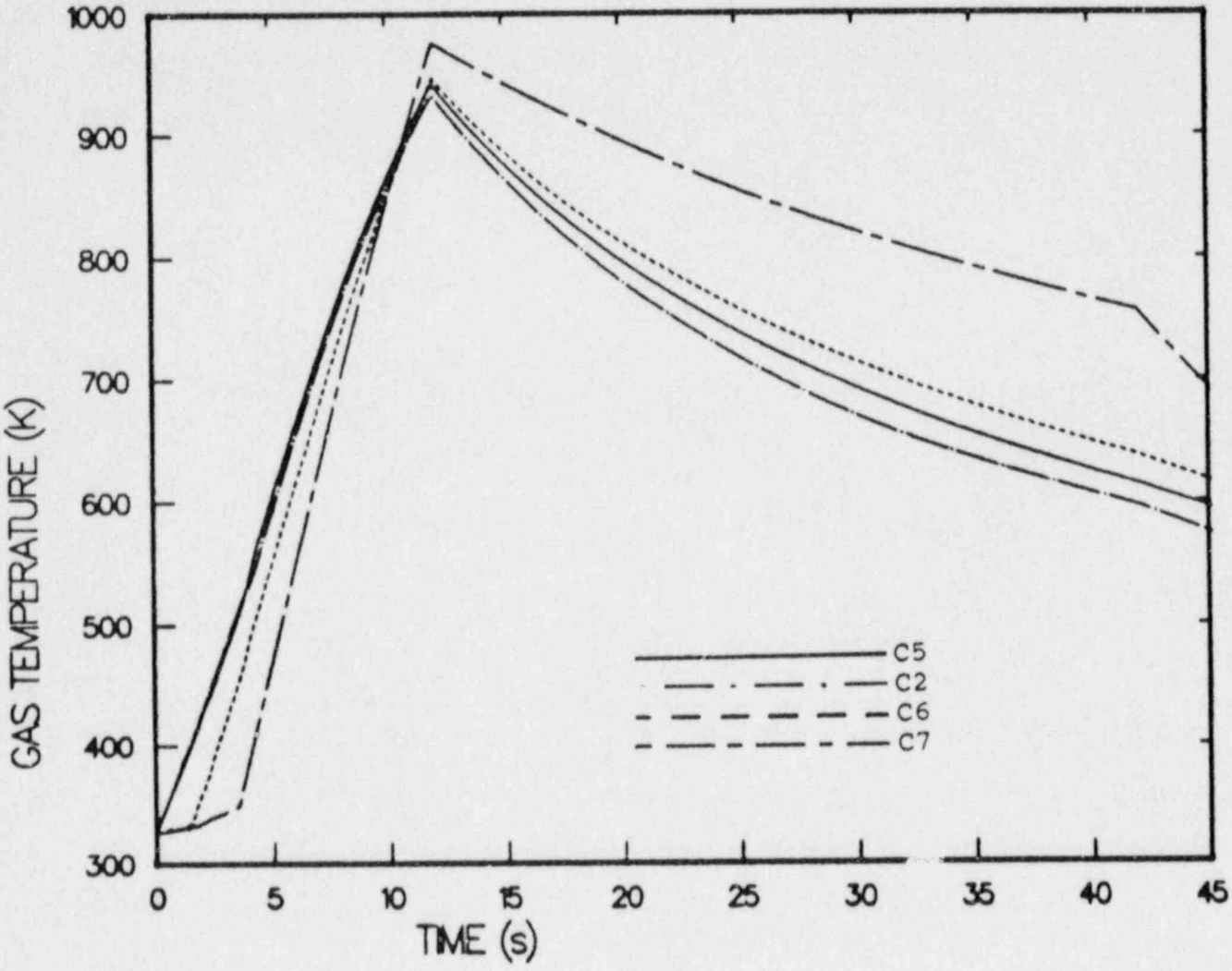

Figure B.3.15. Case 2D Calculated Gas Temperatures

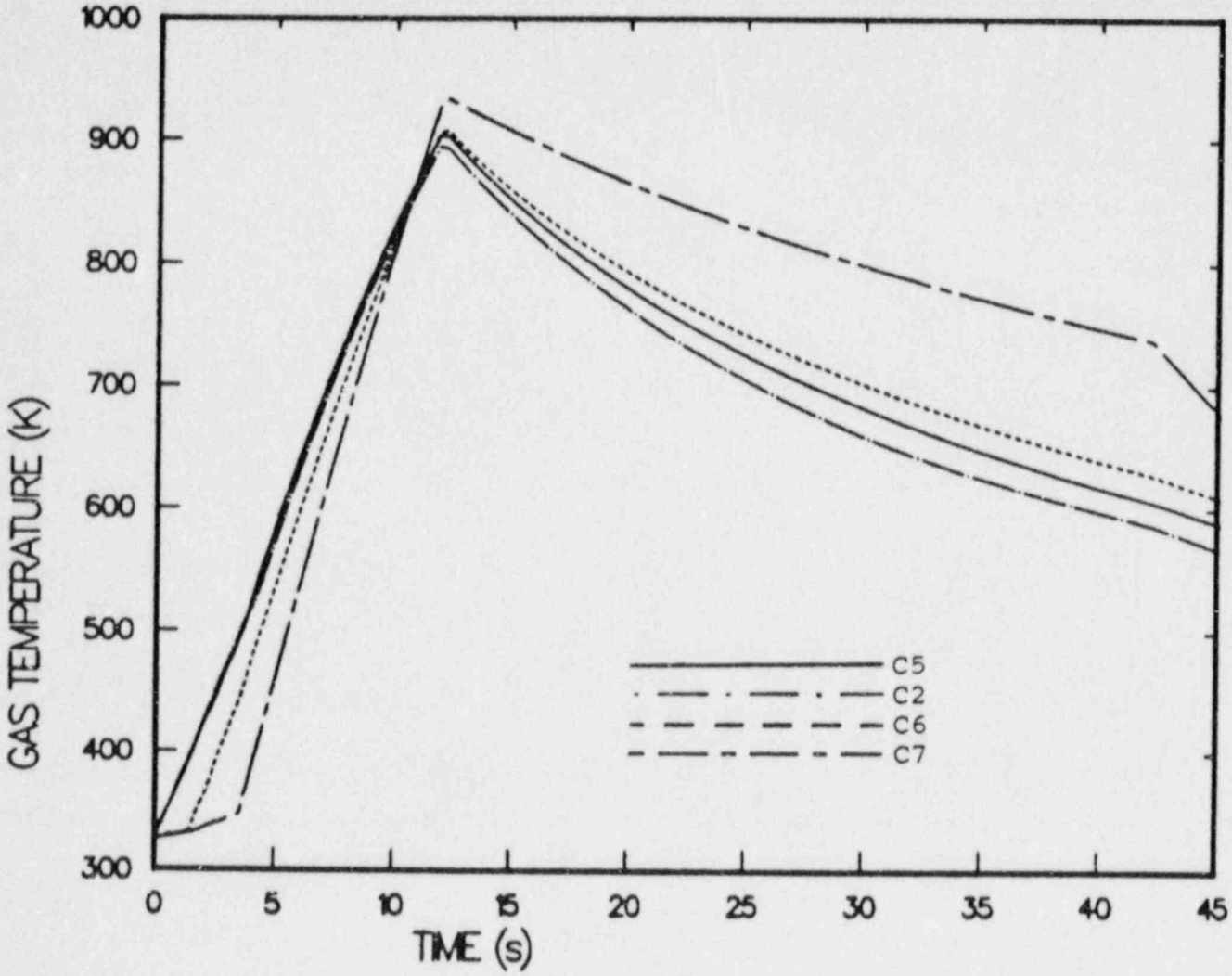

Figure B.3.16. Case 2E Calculated Gas Temperatures

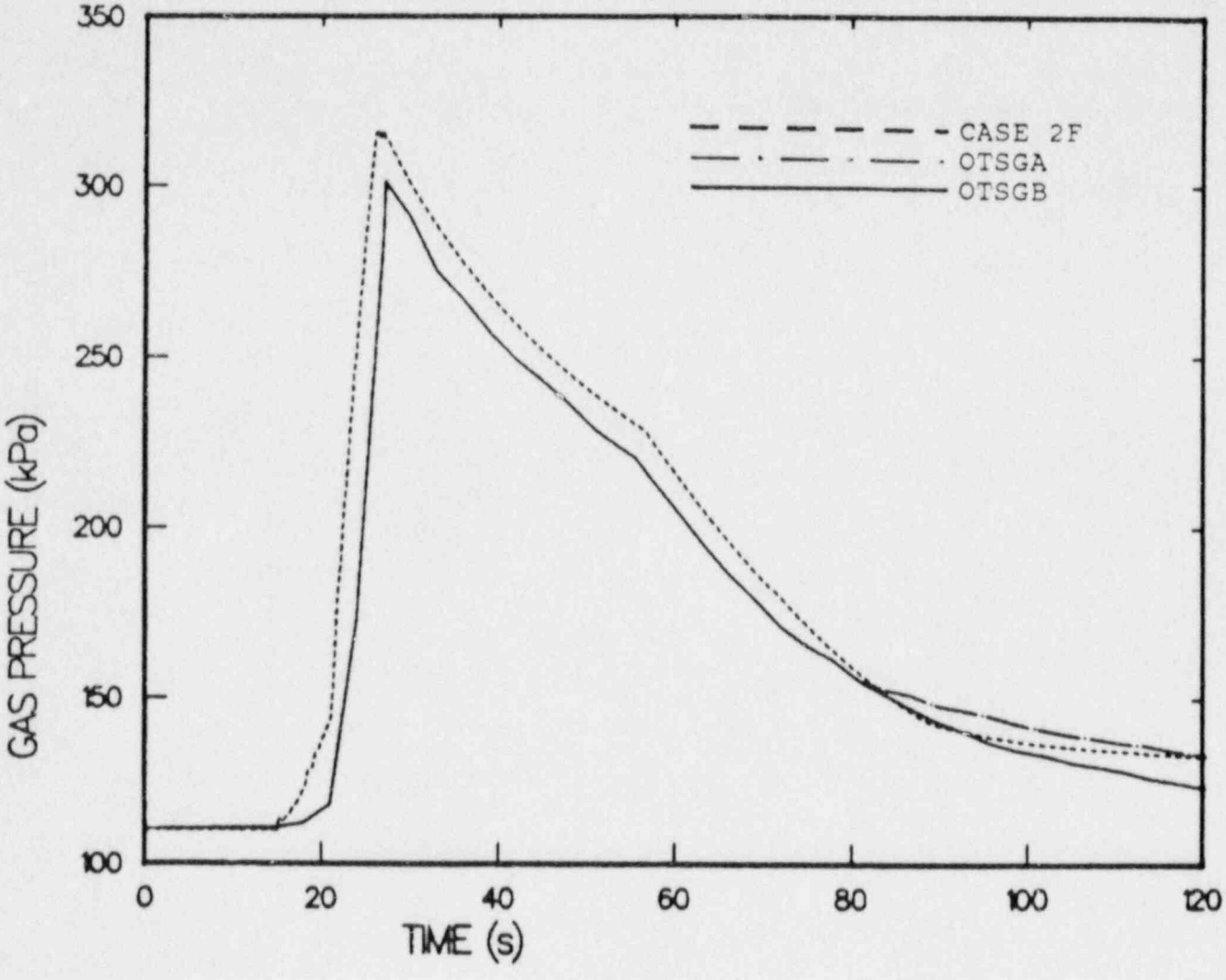

Figure B.3.17. Case 2F Calculated Pressure Compared to OTSGA and OTSGB Measured Pressures

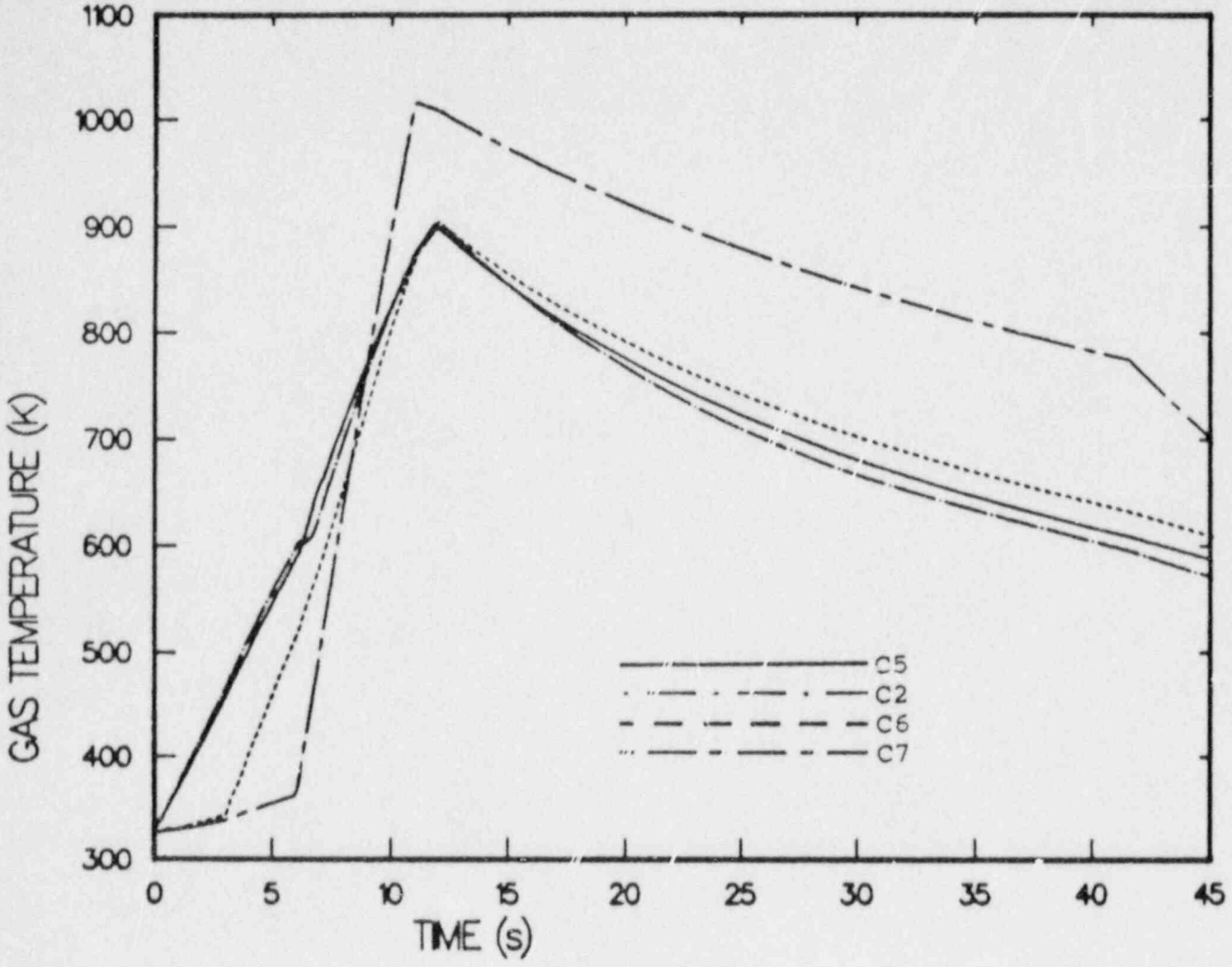

Figure B.3.18. Case 2F Calculated Gas Temperatures

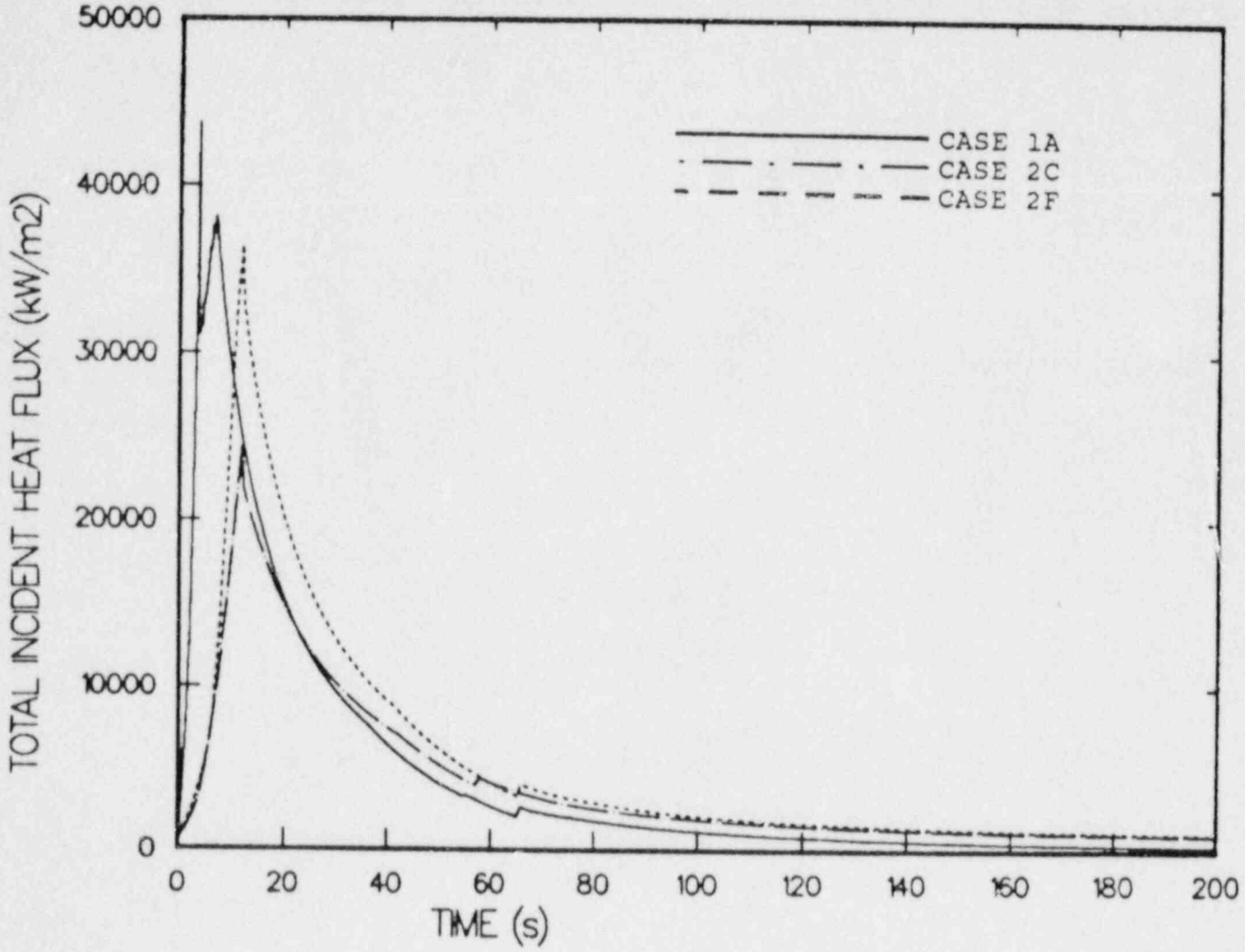

Figure B.3.19. Basement Level Total Incident Fluxes

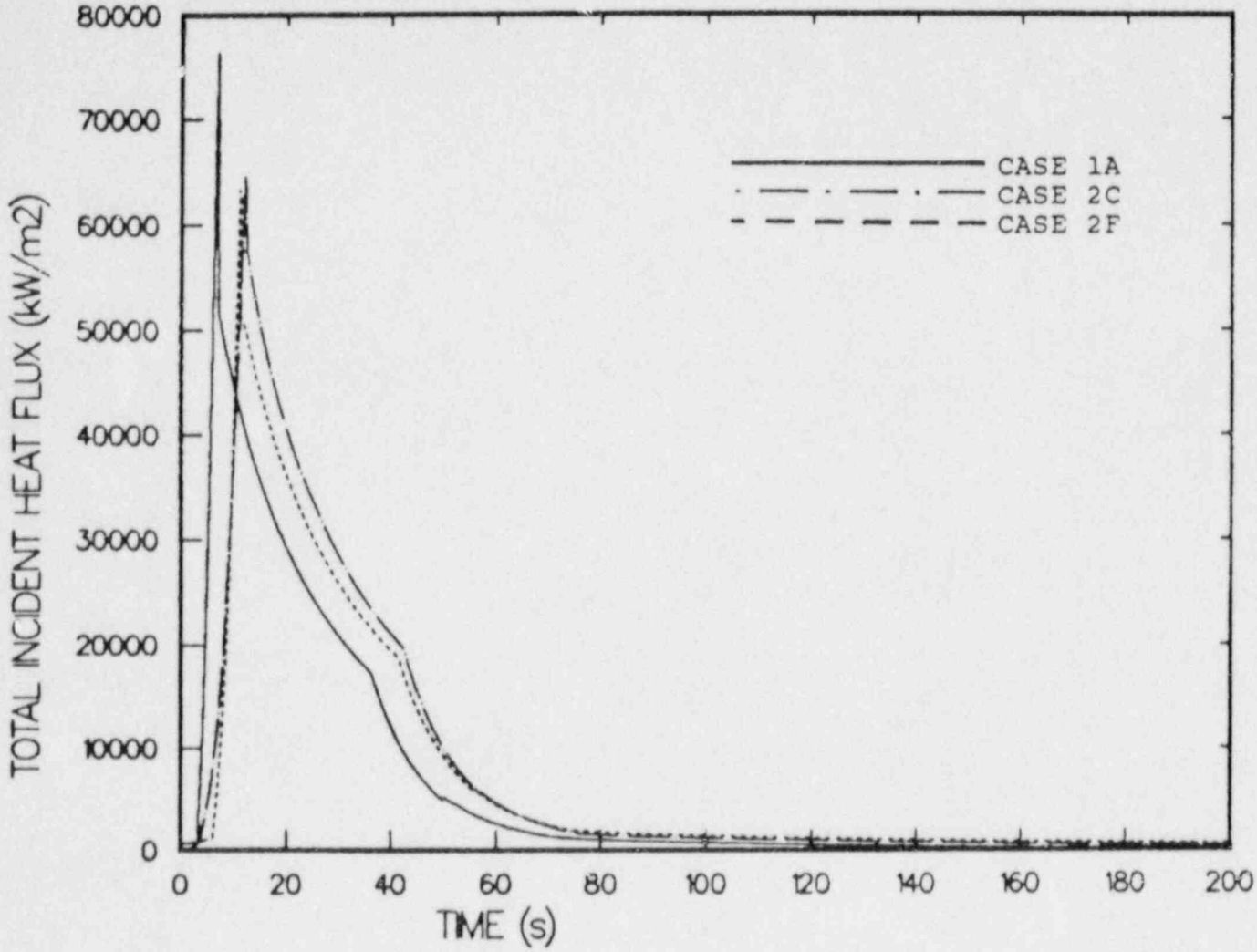

Figure B.3.20. Dome Region Total Incident Fluxes

Case 1A, Case 2C, and Case 2F. The incident total fluxes are calculated with average gas temperatures and therefore represent an average incident flux. Local heat fluxes are influenced by gas turbulence during and after hydrogen burning, by condensation, and by equipment shielding and would vary about the average calculated fluxes. Although the incident fluxes were calculated for the Barton pressure transducer three-layer model, the incident fluxes for the Barton represent upper limits for cable fluxes since the Barton surface temperatures would remain lower than cable surfaces during a burn. Total incident fluxes in the lower containment levels are substantially lower (approximately 30 to 50 percent) than the total incident fluxes in the dome region.

The integrated total incident fluxes are shown in Figures B.3.21 and B.3.22. The integrated energies ranged from 800 to 1010 kJ/m^2 in the basement and from 1250 to 1550 kJ/m^2 in the dome region.

The observed burn damage that occurred in containment during the TMI Unit 2 accident was greater in severity at higher elevations where peak gas temperatures were their highest during the burn. Burn damage also varied with quadrant location for Elevations 305 and 347, with the greatest damage occurring in the south, north, and east quadrants. Major structures and safety-related equipment were not damaged, and burn damage occurred to smaller objects located throughout containment. Items damaged included telephones, wooden scaffolding boards, an instruction manual, and the polar crane pendant cable. The nature of damage to the material was charring or scorching.[1,2]

Cable flammability studies have been performed at FMRC.[8] The results of these studies have been summarized in the FMRC TMI-2 hydrogen burn study.[2] The tests conducted at FMRC base cable flammability on three key parameters: critical heat flux, absorbed damage energy, and absorbed ignition energy. The critical heat flux is defined as a minimum flux above which cable damage or ignition can occur. The absorbed ignition energy is the minimum time integral of external heat flux above which a flammable vapor/air mixture near the surface of the cable can be maintained as long as the external heat flux is above the critical heat flux. A table listing cable ignitablity data has been taken from the FMRC report[2] and is listed in Table B.3.3. The critical heat flux indicates that once Ed (absorbed damage energy) or Ei (absorbed ignition energy) has been obtained, cable damage or ignition will occur as long as the critical heat flux is maintained.

Table B.3.3

FMRC Cable Ignitability Data

Insulation/Jacket Materials	Conductors No.	Conductors Size (AWG)	Outer Diam. (cm)	Critical Heat Flux (kW/m^2)	E_d (kJ/m^2)	E_i (kJ/m^2)	Relevant TMI Cable
EPR/Hypalon	1	2-14	0.5-2.1	14-25	1100	1300-1800	Polar Crane and
EPR/Hypalon	5,7	9-14	1.7-2.5	23-27	--	1900	Power Cables
Hypalon/Hypalon	5	16	1.1	14	900	1300	Central Cable
Silicone/Asbestos	7,9	12-14	2.0	23-25	--	1600-1800	Instrumentation Cable
PTFE/PTFE	1,7	2-1	1.0,1.5	25,26	--	8000-17,000	In-Core Monitoring
Polyolefin/None	1	12	0.4-0.5	25	--	2100-5600	Out of Core Instrumentation

From Reference 2

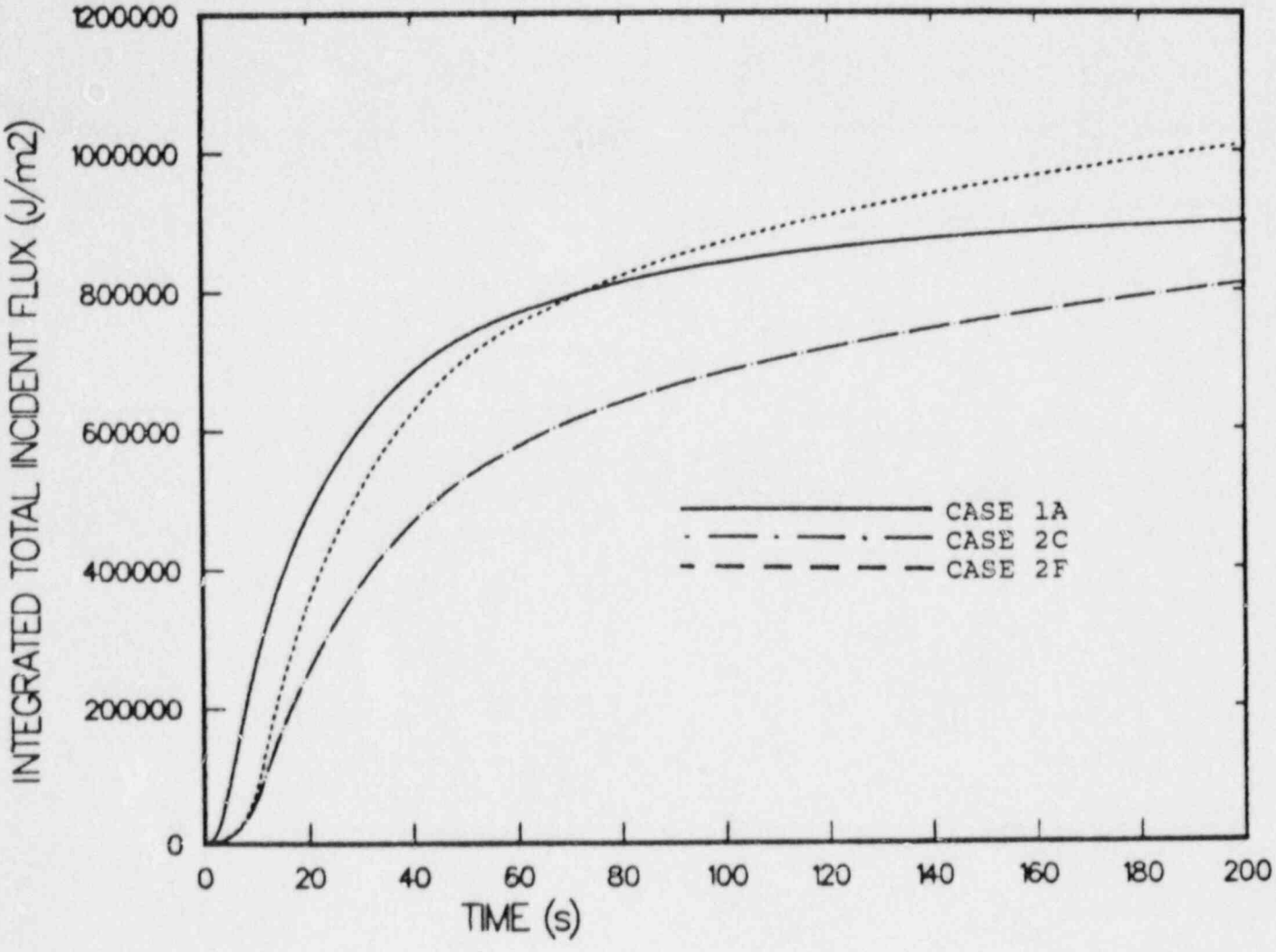

Figure B.3.21. Basement Level, Time Integrated, Total Incident Fluxes

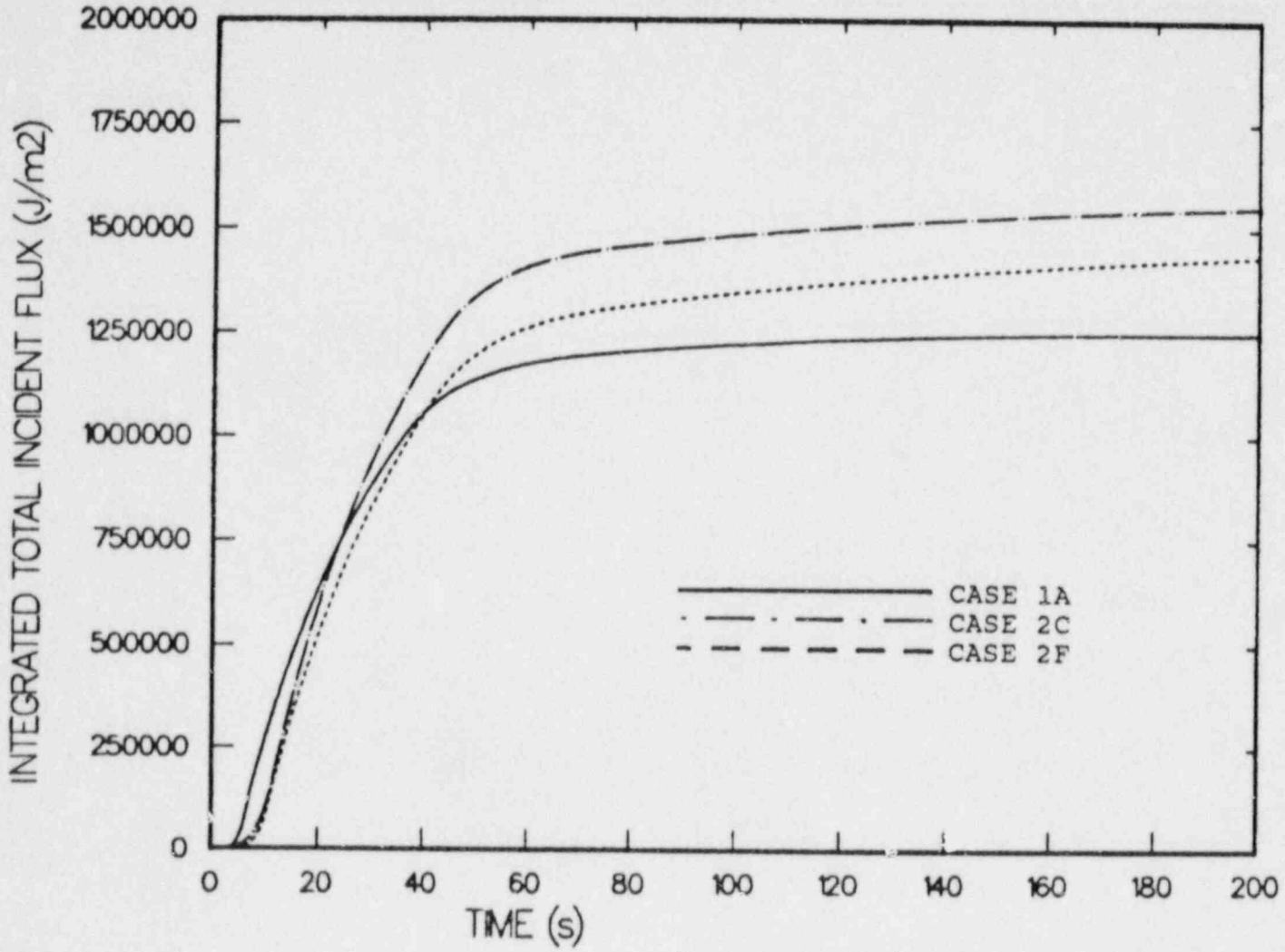

Figure B.3.22. Dome Region Time Integrated, Total Incident Fluxes

Figures B.3.19 and B.3.21 indicate that critical heat fluxes of 14 to 27 kW/m^2 do not exist when integrated flux levels of 900 to 17,000 kJ/m^2 are obtained. Therefore, cable damage or ignition are unlikely below the dome region. Figures B.3.20 and B.3.22 suggest that cable damage may be achieved in the dome but that cable ignition is unlikely. An energy damage level of 1100 kJ/m^2 from Figure B.3.22 corresponds to a flux level of approximately 24 kW/m^2 from Figure B.3.20.

B.4 Summary

HECTR Case 1 and Case 2 deflagration results show good agreement with OTSG pressure data. Case 1 calculations are dependent on FPLs chosen to establish burn times and show the worst agreement with the OTSG data of the Case 1 and Case 2 results. Case 1 calculations show a too rapid pressure rise compared to the OTSG data. Complete burn Case 1 analyses overpredict peak pressures while the noncomplete burn cases predict peak pressures very well. Based upon the Case 1 and Case 2 calculations, better FPL values could be predicted to obtain slower initial pressure rise rates. Case 2 complete burn analyses using Henrie's initial conditions overpredict the peak pressures, but incomplete Case 2 burns agree well with OTSG peak data. Case 2 complete burn analyses using FMRC initial conditions also calculate peak pressures close to the OTSG data.

Peak temperatures are highest in the dome region and decrease with lower containment elevations. Case 1 calculations showed greater variations in peak temperatures with containment elevation than Case 2 calculations did. Less stratification in peak temperatures below the dome region occurs if burning occurs throughout containment simultaneously for greater periods of time.

Incident total flux values and integrated flux values show energy levels below the dome region too low to cause damage to representative cables. Energy levels in the dome region appear too low to ignite cables but may be sufficient enough to damage some cable types. Damage to cables in this context could be described as scorching or charring the cable jacket.

REFERENCES

1. Henrie, J. O. and A. K. Postma, Analysis of the Three Mile Island (TMI-2) Hydrogen Burn, RHO-RE-SA-8, Vol. 3, July 1982.

2. Analysis of the Hydrogen Burn in the TMI-2 Containment, EPRI NP-3975, Electric Power Research Institute, April 1985.

3. Dingman, S. E., et al., HECTR Version 1.5 User's Manual, NUREG/CR-4507, SAND86-0101, Sandia National Laboratories, April 1986.

4. Analysis of the Three Mile Island-Unit 2 Accident, NSAC-1, Electric Power Research Institute, July 1979.

5. Rogovin, M. and F. J. Frampton, Three Mile Island--A Report to the Commissioners and the Public, Vol. I and Vol. II, Part 2, 1980.

6. Dandini, V. J. and W. H., McCulloch, HECTR Analysis of Equipment Temperature Response to Selected Hydrogen Burns in an Ice Condenser Containment, NUREG/CR-3954, SAND84-1704, Sandia National Laboratories, February 1985.

7. Personal Communication with J. O. Henrie, April 1986.

8. Lee, J. L., et al., A Study of Damageability of Electrical Cables in Simulated Fire Environments, EPRI NP-1767, Electric Power Research Institute, March 1981.

APPENDIX C

SURRY EQUIPMENT TEMPERATURE ANALYSIS

APPENDIX C

SURRY EQUIPMENT TEMPERATURE ANALYSIS

C.1 Introduction

The plant chosen for the subatmospheric analyses was the Surry nuclear power plant. Each unit at Surry has a three-loop Westinghouse PWR rated at 775 MW(e). The analyses were performed using the HECTR Version 1.5 hydrogen burn code with a MARCH hydrogen source term.[1,2]

C.2 Containment Model

The volume of the Surry containment building is approximately 1,750,000 cubic ft. The geometry of the structure is considerably different from a large dry containment in that it is highly compartmentalized with the only large open volumes being the dome and operating floor. The containment model used in the Surry analyses was similar to that used in the ANS Source Term Study.[3] For the present study the compartmentalization of the model was refined to conform to characteristics of the HECTR code and to more precisely characterize hydrogen transport in the building. Two longitudinal sections of the building are shown in Figures C.2.1 and C.2.2. The compartments are identified in Table C.2.1.

C.3 Equipment Models

The equipment models used in the analyses were based on the Barton 763 gauge pressure transmitter. This instrument has been extensively tested in the Hydrogen Burn Survival program and its thermal response to simulated hydrogen burn heat flux pulses is well documented.[4]

Four models of the transmitter were used in the analyses. The first model was a one-dimensional slab model of the cover plate of the transmitter only. This model was used in previous analyses whose results are known to be conservative.[5] This model was included in the present work to serve as a check on the results of Reference 5.

The second and third models were the "Case-As-Plate" (CAP) and lumped mass models of the transmitter. The CAP was a one-dimensional slab model, which treated the transmitter as a solid steel plate slab, having the same frontal area as the Barton instrument and a thickness sufficient to account for all the steel in the case. The lumped mass model treated temperature rises as occurring uniformly throughout the transmitter without regard to the transient heat conduction from the front surface included in the slab models.

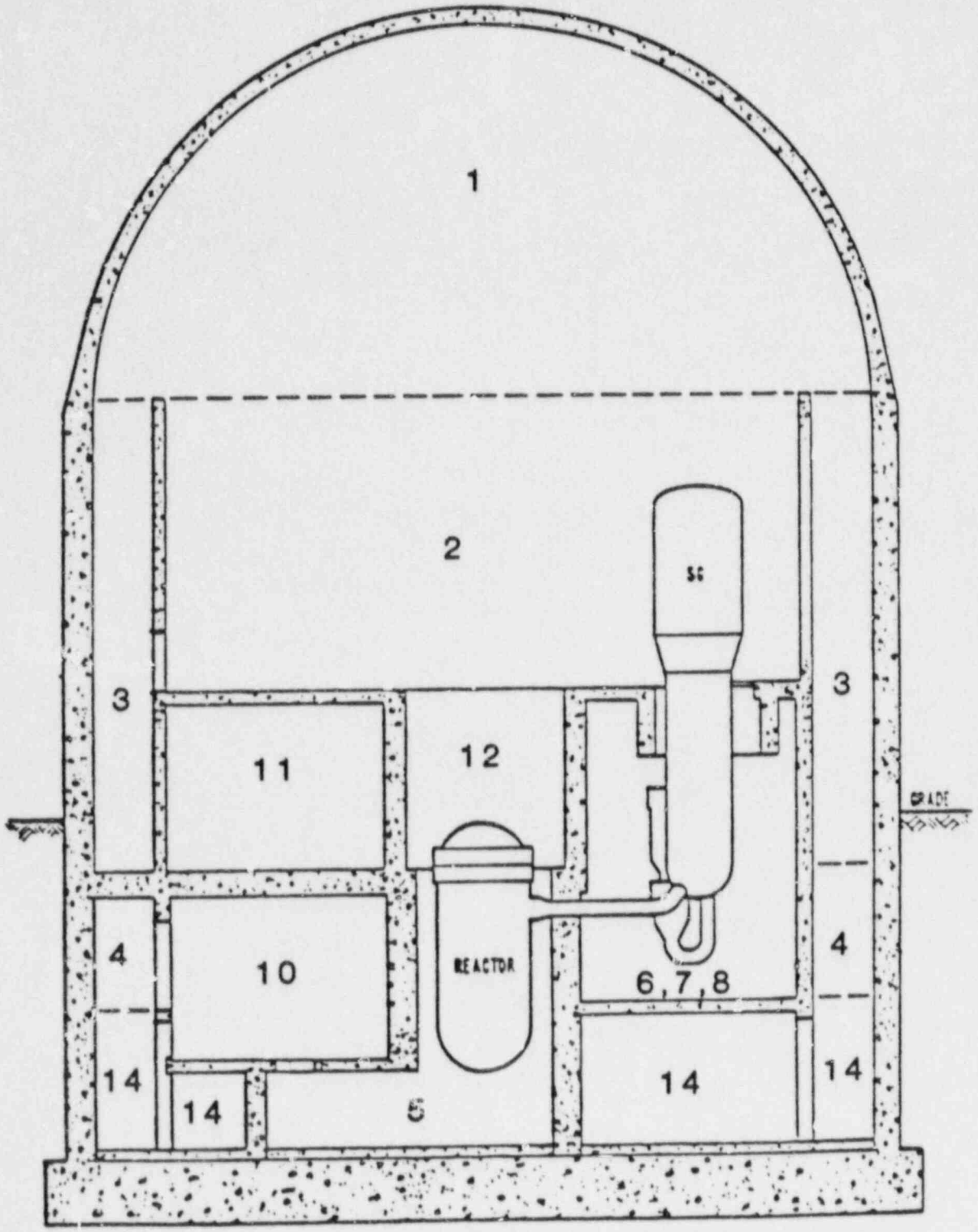

Figure C.2.1. Surry Containment Section A

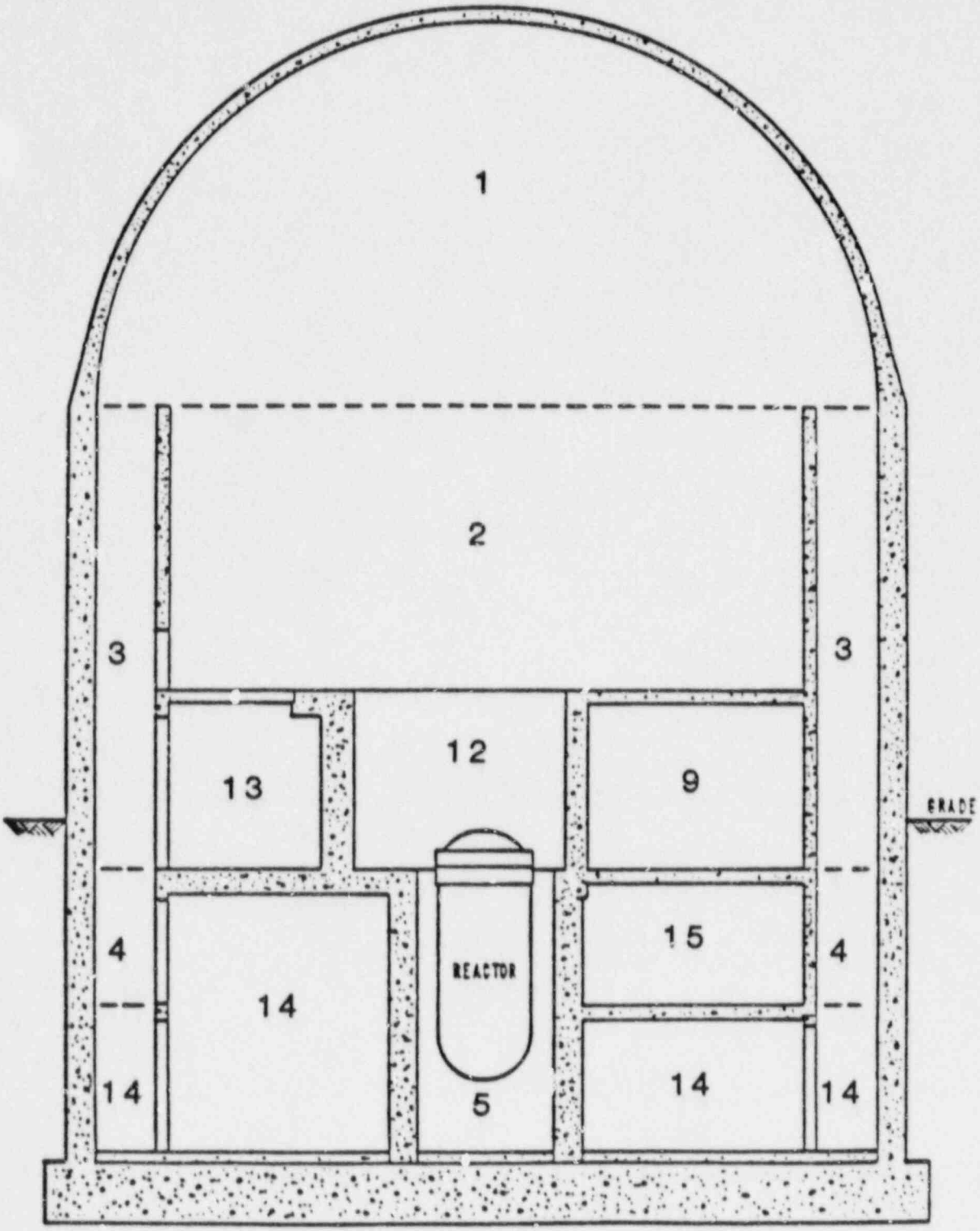

Figure C.2.2. Surry Containment Section B

Table C.2.1

Surry Compartment Identification

Compartment No.	Compartment	Volume (ft^3)
1	Dome	519,633
2	Operating Floor	347,065
3	Upper Annulus	263,512
4	Lower Annulus	75,915
5	Reactor Cavity	11,678
6	Steam Generator A Cubicle	46,834
7	Steam Generator B Cubicle	40,529
8	Steam Generator C Cubicle	42,363
9	Pressurizer Cubicle	24,613
10	RHR Cubicle	30,315
11	Incore Instrumentation Room	31,114
12	Refueling Cavity	33,032
13	Upper Hoist Space	13,847
14	Basement	253,757
15	Pressurizer Relief Tank Cubicle	18,793

The fourth model was a three-layer one-dimensional slab representation of the Barton transmitter. This model accounted for the air volume inside the device by including an air layer sandwiched between two layers of steel (the front and back of the transmitter).

The three-layer representation was the most realistic of the four models. An analysis was performed, which calculated the temperature rise of its front surface when analytically exposed to a heat flux pulse used in hydrogen burn simulation experiments at the Sandia Central Receiver Test Facility (CRTF). The calculated peak temperature was approximately 11°K higher than the peak temperature of an actual Barton transmitter exposed to the same pulse during the CRTF test series. The time responses of the model and test specimen were the same. This comparison is shown in Figure C.3.1. As a result of this analysis it was concluded that this three-layer model provided the most accurate (though mildly conservative) representation of the transmitter temperature response.

Based on discussions with the OIE (NRC Office of Inspection and Enforcement) resident inspector at Surry, it was determined that safety-related equipment should be modeled in several containment compartments. Equipment locations considered in three studies were the upper annulus, the

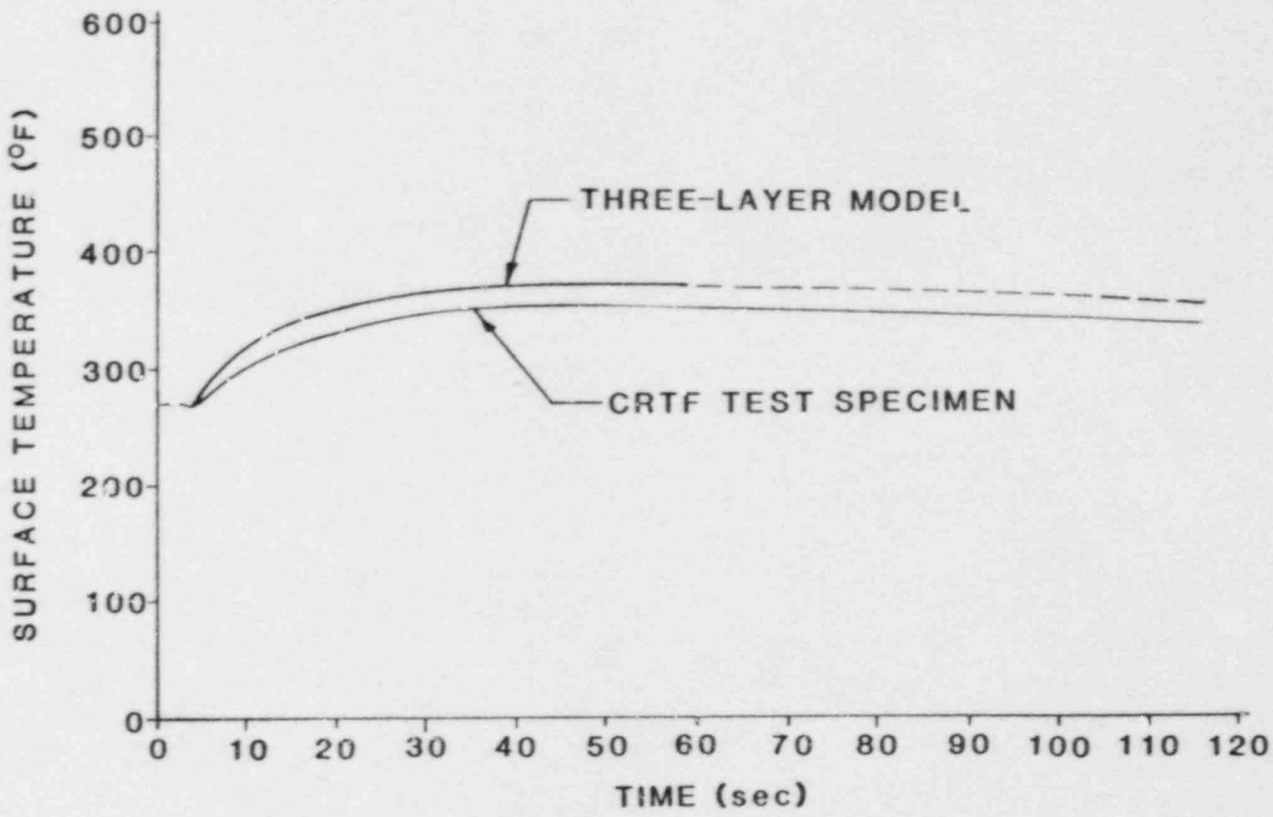

Figure C.3.1. Three-Layer/Experimental Temperature Response Comparison

three steam generator cubicles, the pressurizer and residual heat removal cubicles, the incore instrumentation room, and the basement.

All four equipment models were analyzed in each location. Because the three-layer model was found to be the most realistic representation of a widely used piece of safety equipment (the Barton transmitter), the three-layer results provide the best estimate of the temperature response of safety equipment to hydrogen combustion heat flux pulses. As such, they form the basis of the discussion of equipment temperatures in hydrogen burn environments. However, the results from the other three models may be useful if their thermal characteristics can be related to those of other known pieces of equipment and, for this reason, they are included in the results tables of Section C.5.

C.4 Accident Scenarios

C.4.1 General Description

The accident sequences which formed the basis of these analyses were the S_2D and S_1D events (small and intermediate sized LOCAs with loss of emergency core cooling) with 75 percent of the core Zircaloy assumed to react to release hydrogen prior to the restoration of core cooling.

Different break locations were considered. The break locations (also referred to as source compartments) chosen were steam generator cubicles and the pressurizer relief tank cubicle.

The operation of the safety-related containment spray system was automatically initiated by a containment gas high pressure signal. Operation of the fan coolers was not considered since they are not intended to operate during an accident.[6]

The final accident parameter varied in the study was the ignition criterion, the concentration of hydrogen at which ignition was taken to occur. Two basic ignition criteria were considered. The first assumed that ignition occurred in the basement at the completion of the 75 percent metal-water reaction. The time required for this reaction to go to completion permitted the hydrogen to be transported and evenly distributed throughout the containment prior to the burn. For the S_2D cases, the hydrogen concentration at ignition was roughly 14 to 15 volume-percent with the sprays operating. For S_1D cases the sprays-on concentrations were approximately 15 to 16 volume-percent. This ignition criterion resulted in a single burn in each containment

compartment. While the primary purpose of these analyses was the study of equipment temperature response to hydrogen deflagrations, HECTR also monitored hydrogen concentrations for potentially detonable mixtures throughout the course of the calculations. The HECTR conditions for a detonable mixture are a hydrogen concentration greater than 14 percent, oxygen concentration greater than 9 percent, and a steam concentration less the 30 percent. All three conditions must be satisfied simultaneously. HECTR does not have the capability to analyze detonations. The code is limited to indicating the presence of detonable mixtures. Any ignition of a detonable mixture is treated as a deflagration by the code. The source terms and hydrogen transport are covered in detail in Sections C.4.2 and C.4.3.

The second ignition criterion simulated the use of igniters in the Surry containment. In these cases, ignition occurred at a hydrogen concentration of 7 volume-percent. This is the minimum hydrogen concentration at which HECTR predicts ignition can occur.

These ignition criteria represent extremes in combustion conditions. A single burn generally results in high peak heat fluxes, gas temperatures, and pressures but the heat flux and pressure pulses are of short duration. Deliberate ignition at a lower hydrogen concentration results in lower peak heat fluxes, gas temperatures, and pressures but, because the surfaces are subjected to multiple burns the integrated heat flux can be greater than in the single burn case. Thus, while the individual thermal pulses due to deliberate ignition may be less severe than the single burn pulse, the cumulative effect of these pulses may be higher equipment temperatures than the single burn cases.

C.4.2 Water and Hydrogen Source Terms

The MARCON 2.0 computer code was used to generate the steam and hydrogen source terms. The MARCON 2.0 code includes a replacement of the subroutine that calculates the interaction of the molten debris and the concrete floor in the MARCH 2 (Meltdown Accident Response Characteristics) code with the CORCON Mod 2 code.[2,8] Since this analysis addressed arrested sequences, the CORCON and reactor cavity models were not used in the analyses. The water and hydrogen source terms were calculated only by the models in MARCH 2 version 152D. MARCON 2.0 was used because it is being used for other Sandia programs (SASA and Hydrogen Behavior) and the input models were already developed.

The MARCH models in MARCON 2.0 were used to represent the primary and secondary systems. MARCH models the primary system as a single cylindrical volume with liquid at the bottom and gases or vapor at the top (when present). Figure C.4.1 shows a representation of the MARCON modeling of the primary system. Some characteristics of the Surry primary system are listed in Table C.4.1.

The steam source flow rates are dependent on the primary system pressure and the elevation of the flow junction break relative to the height of liquid in the primary system. Water flow occurs when the break is below the collapsed liquid level and gas flow occurs when the break is above the water level. Two phase (liquid-steam) flow is not modeled. The hydrogen source terms are dependent on the hydrogen generation rate from the zirconium-steam reaction and the leak rate from the primary system into containment. The steam and hydrogen leak rates are proportional to their mass fractions in the vessel. For these degraded core scenarios it was assumed that Emergency Core Coolant (ECC) injection was unavailable for a time period long enough for 75 percent of the clad zirconium to oxidize, but was available to arrest the sequence at 75 percent metal-water reaction. Several runs were required to arrest the sequence at 75 percent clad oxidation, varying the time of initiation of high pressure injection (HPI). Due to the high head and capacity of the HPI pumps, the oxidation was arrested shortly after the initiation of HPI flow. Very large fractions of the core were melted without core slump to obtain the required amount of clad oxidation.

The steam and hydrogen source terms for two LOCAs (S_1D and S_2D) were calculated in this analysis. The S_1D scenario had a break with a 4-inch diameter (S_1D4), and the S_2D scenario had a 2-inch diameter (S_2D2).

C.4.2.1 S_2D2

The S_2D2 water mass flow rate into containment is shown in Figure C.4.2. The initial flow rate was approximately 20,000 lb/min and decreased to 13,500 lb/min as the primary system depressurized. The flow remained constant until the break uncovered at approximately 20 minutes allowing the flow to change from liquid to steam. The steam flow continued to decrease as the primary system depressurized. At 75 minutes, steam flow stopped when the system pressure decreased below the set pressure of the core flood tanks (CFTs) and their liquid was injected into the primary system. The primary system pressure increased due to CFT injection and exceeded the CFT set pressure before the CFTs were completely empty. After CFT injection had stopped, steam continued to flow out of the break from 80 to 145 minutes. During this time period, the primary system

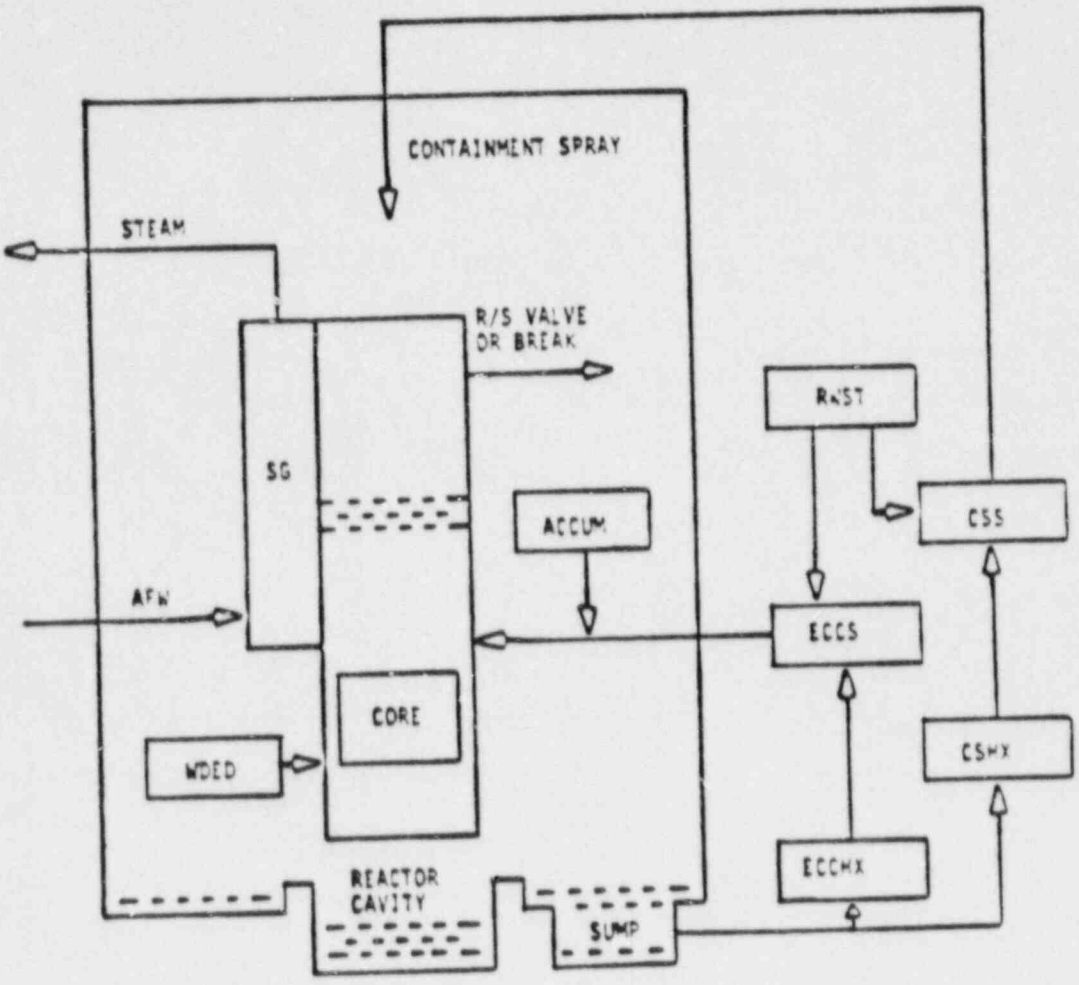

Figure C.4.1. MARCON Model of Primary System

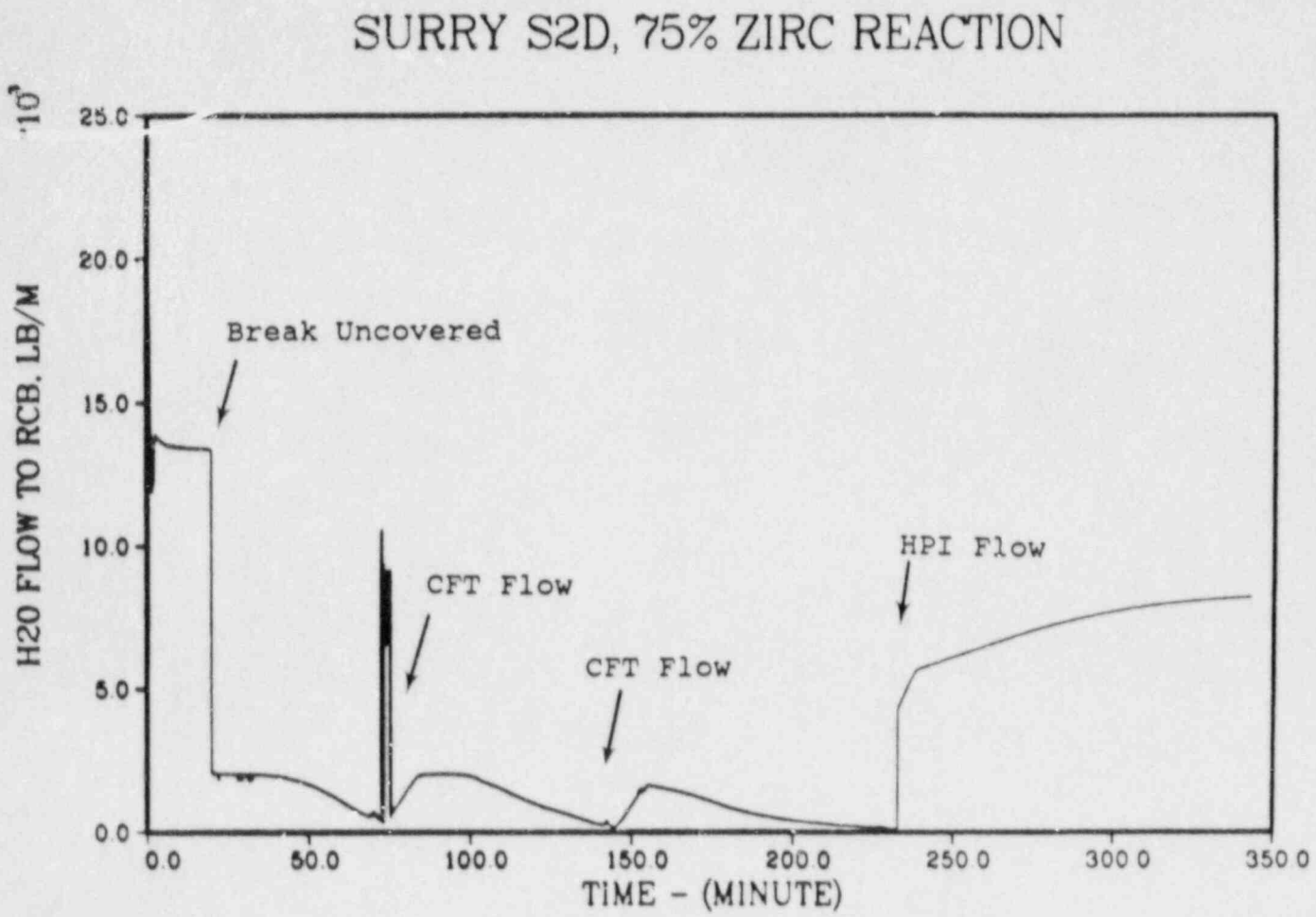

Figure C.4.2. Calculated Water Mass Flow Rate for a Small Break LOCA, S_2D2

pressure depressurized and dropped below the CFT set point at 145 minutes allowing the CFTs to inject their remaining liquid inventory into the vessel. The primary system pressure increased again after the second CFT injection and steam flowed out of the break from 145 to 230 minutes. The high pressure injection (HPI) pumps were started at 230 minutes. The break was covered and water leaked out of the break after 230 minutes.

Table C.4.1

Surry Reactor Characteristics for MARCH Analyses

Reactor Power	2441 MWt
Operating Pressure	2280 psia (15.7 MPa)
Operating Temperature	571.8°F (300°C)
Primary System Volume	11,706 ft^3
Primary System Water	423,200 lb (192,360 kg)
Steam Generator Water	116,808 lb (53,095 kg)
Fuel Rods in Core	32,028
Fuel Rod Diameter	0.422 in (1.072 cm)
Clad Thickness	0.0243 in (0.0617 cm)
Zircaloy in Core	36,300 lb (16,500 kg)
UO_2 in Core	175,600 lb (79,820 kg)

The calculated hydrogen mass flow rate into containment is shown in Figure C.4.3. Hydrogen flow into containment was initiated at 50 minutes and was at a peak flow of 59 lb/min at approximately 64 minutes. CFT injection occurred at 73 minutes and covered the core; the core was quenched and hydrogen production was stopped. The hydrogen flow dropped to zero while the break was covered allowing water only to leave the break. After the break uncovered at approximately 76 minutes, the hydrogen remaining in the primary system continued to leak out until 115 minutes at which time there

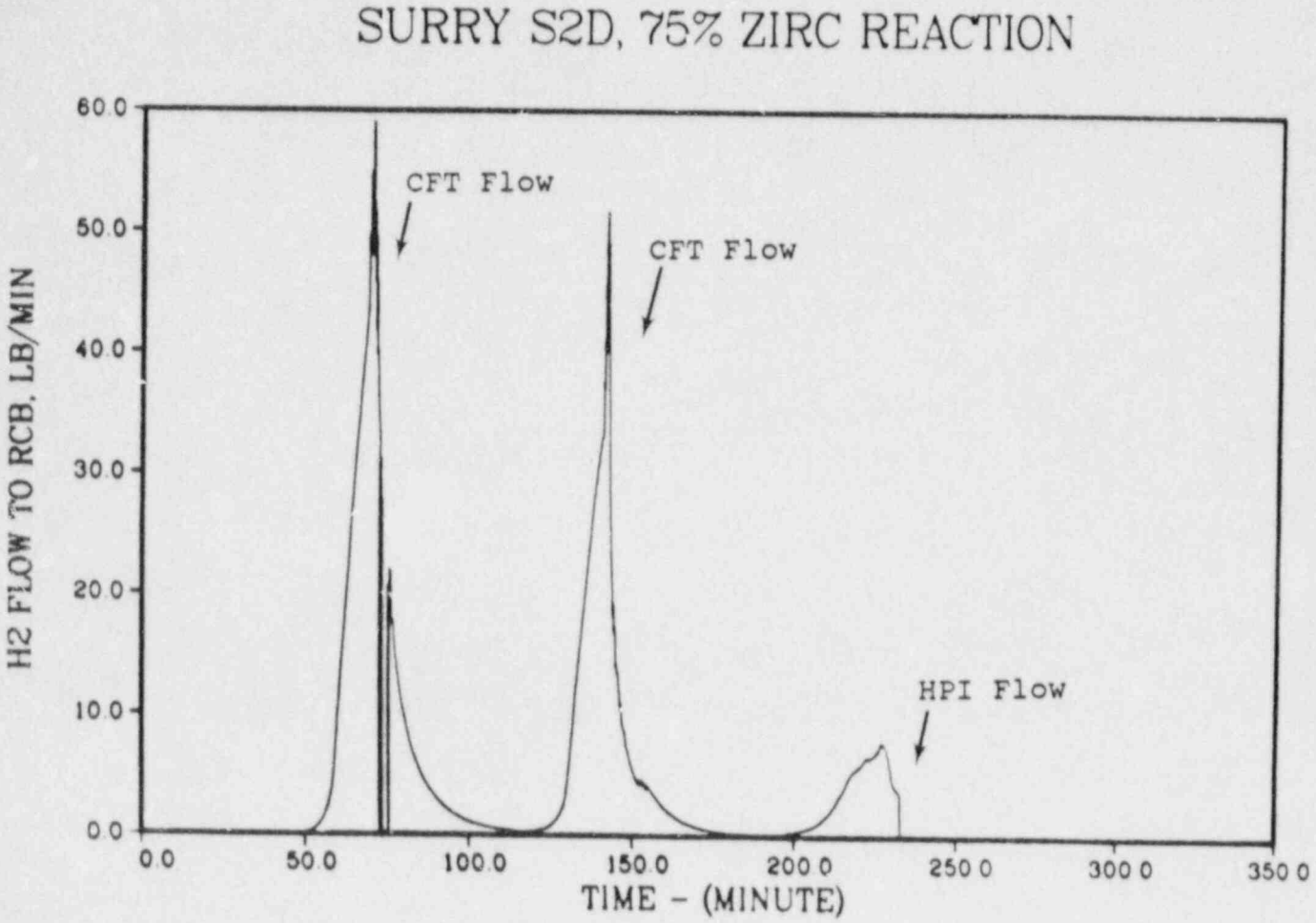

Figure C.4.3. Calculated Hydrogen Mass Flow Rate for a Small Break LOCA, S_2D2

was no hydrogen left in the primary. The core had uncovered sufficiently enough to regenerate hydrogen at approximately 120 minutes. Hydrogen generation and flow to containment increased, reaching a peak value of approximately 33 lb/min at approximately 145 minutes. CFT injection occurred a second time at 145 minutes, and the injected liquid displaced some of the remaining hydrogen in vessel creating a peak hydrogen leak rate of 52 lb/min. The core was quenched again and hydrogen generation was stopped. The hydrogen left in the primary after the second CFT injection continued to leak into containment from 145 minutes to 180 minutes. Hydrogen generation began a third time as the core uncovered and was released into containment until HPI initiation covered the break at 235 minutes.

C.4.2.2 S_1D4

Figure C.4.4 illustrates the calculated water/steam mass flow rate into containment during the S_1D4 scenario. Water initially flowed out of the break at rates between 50,000 lb/min to 65,000 lb/min. The break uncovered at approximately 5 minutes allowing steam to flow out of the break. The primary system depressurized rapidly resulting in CFT injection by 18 minutes. The injected CFT liquid covered the break intermittently until 20 minutes, resulting in liquid water and steam flow into containment. After 20 minutes, steam leaked out of the uncovered break. The break remained uncovered for the rest of the S_1D4 calculation. The steam flowed out of the primary break until the incore steam inventory was depleted; steam flow stopped at 68 minutes. The average core temperature reached its peak value and the primary vessel pressure reached its minimum value during the steam starvation period. HPI flow was initiated at 75 minutes. The HPI flow did not recover the core or the break during its operation. The liquid level in the vessel increased to 10 feet at 100.5 minutes (2 feet below the top of the core) and remained at 10 feet ($\pm$0.5 feet) for the remainder of the accident. Therefore, only steam leaked from the break after 84 minutes as the HPI liquid began to boil. The HPI liquid did not cover the core or the break due to an input error in the MARCH input deck. This error had no adverse effect on the hydrogen transport calculation in containment since the error occurred at 110 minutes, well after the hydrogen injection into containment.

The hydrogen flow rate into containment is shown in Figure C.4.5. Hydrogen flow into containment began at 55 minutes and reached a peak flow rate of approximately 89 lb/min at 67 minutes. As the in-vessel steam inventory decreased, less clad oxidation occurred and the hydrogen

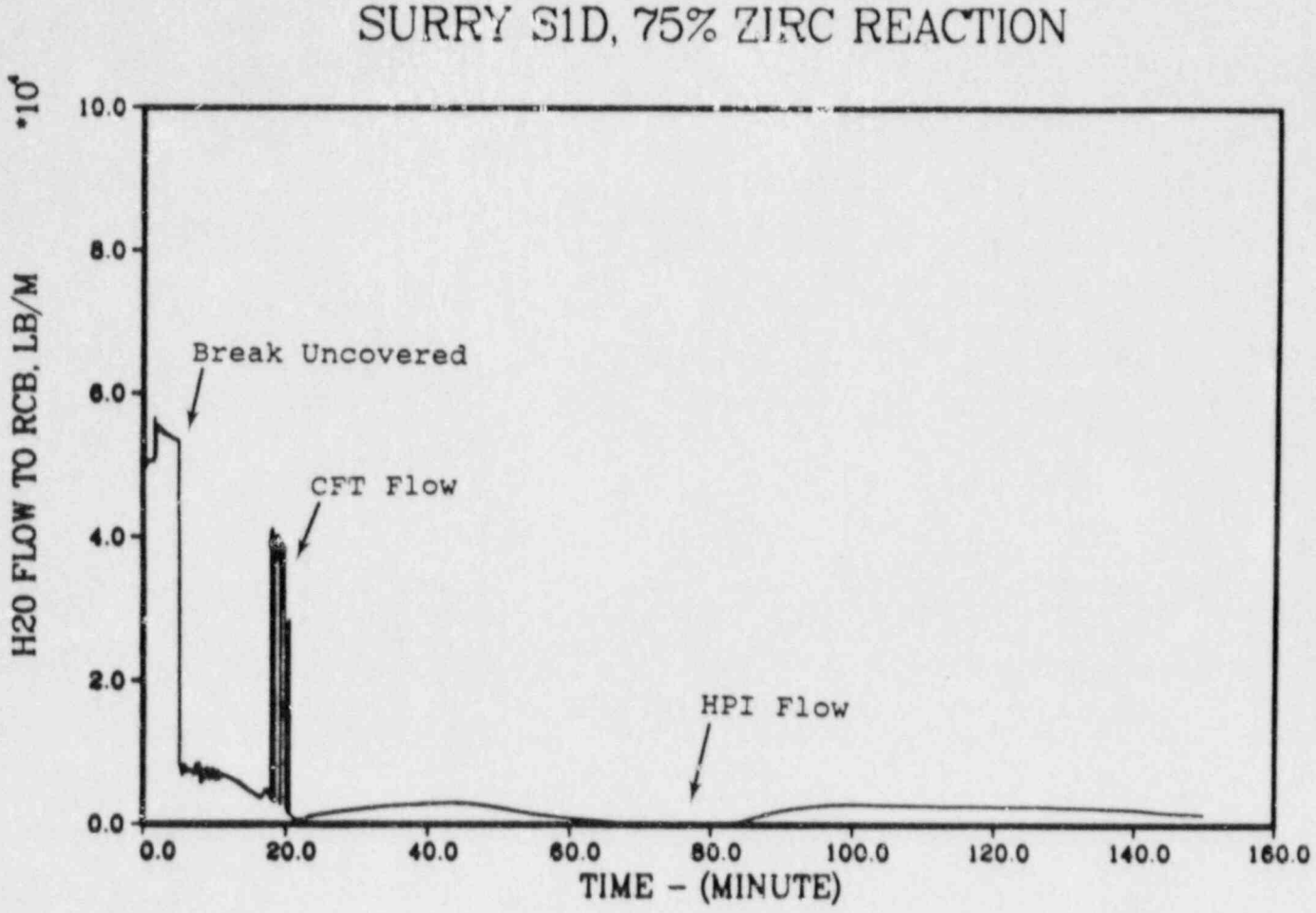

Figure C.4.4. Calculated Water Mass Flow Rate for a Small Break LOCA, S_1D4

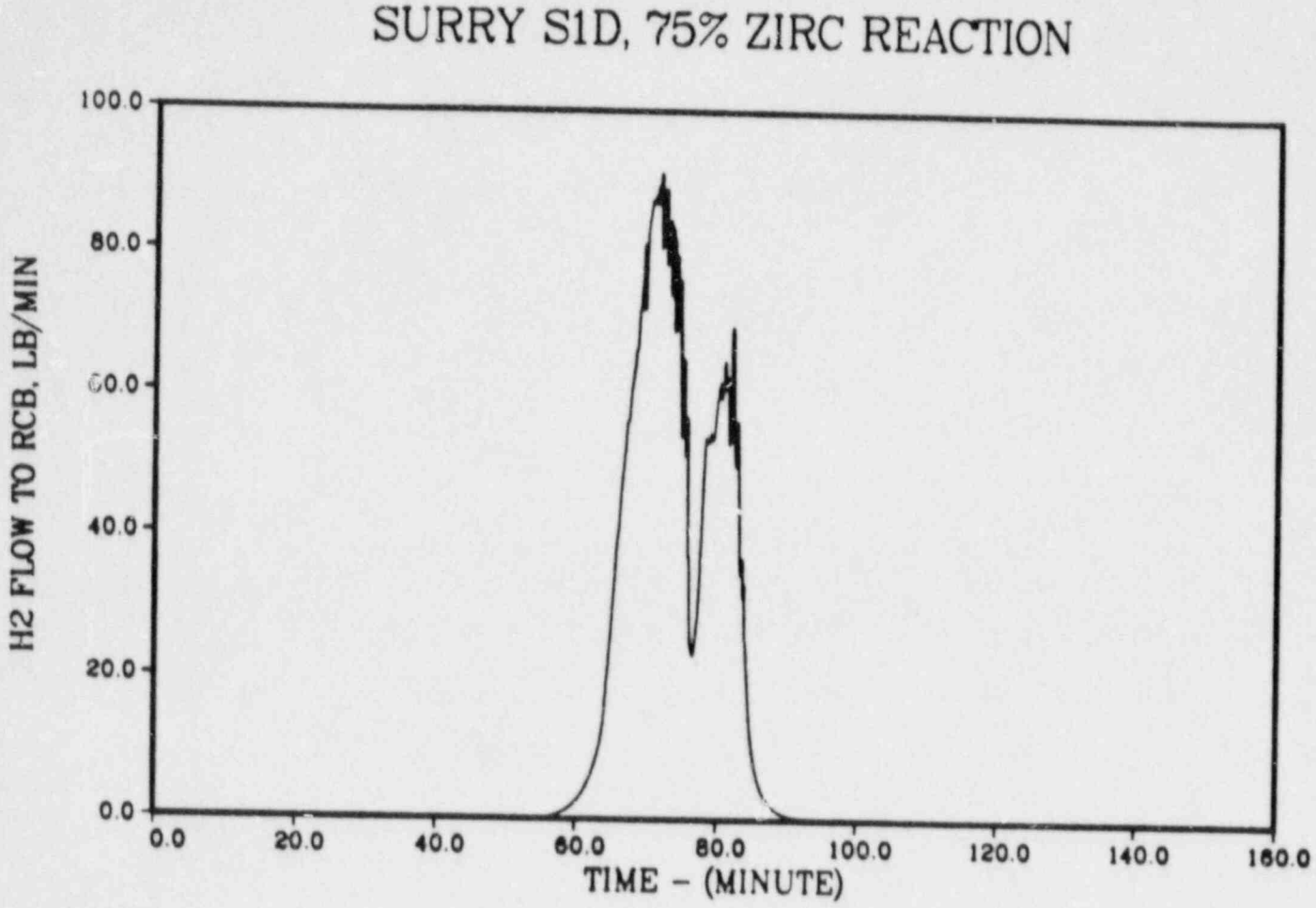

Figure C.4.5. Calculated Hydrogen Mass Flow Rate for a Small Break LOCA, S_1D4

flow rate out of the break decreased (67 to 74 minutes). HPI flow was initiated at 75 minutes but the coolant level remained 2 feet below the top of the core. As the coolant vaporized, its steam allowed hydrogen production to increase a second time (75 to 81 minutes). As the Zircaloy above the 10-foot core level became completely oxidized, hydrogen generation and release decreased (81 to 90 minutes). Hydrogen flow to containment was completed before the error described above occurred in the MARCH calculation at 100.5 minutes. Therefore, the hydrogen and steam release rates up to 100.5 minutes were accurate.

C.4.3 Transport Results

The accident scenarios analyzed in this report are listed in Table C.4.2. Two LOCA scenarios were considered (S_2D and S_1D). The S_2D scenario had a 2-inch diameter break and the S_1D scenario had a 4-inch diameter break. Break locations for the S_1D and S_2D were varied to examine their effect on hydrogen transport in containment. The break locations were located in (1) the reactor cavity; (2) steam generator cubicles A, B, and C; (3) the pressurizer cubicle; and (4) the pressurizer drain tank cubicle. All of the sequences listed in Table C.4.2 began at the initial conditions listed at the bottom of the table.

C.4.3.1 S_2D2

A typical pressure response of the containment gas is shown in Figure C.4.6. This pressure response was similar for all of the S_2D2 scenario break locations with the pressure magnitudes varying by less than 5 kPa for any pressure point. The initial calculated pressure response was dominated by the water/system mass flow rates calculated by MARCON. The containment pressure increased continuously until the break was uncovered at 1500 seconds and flow into containment changed from liquid to steam. The spray system was activated at approximately 6000 seconds. Operation of sprays significantly reduced containment pressure for the remainder of the S_2D2 transport case.

Typical calculated steam, hydrogen and oxygen mole fractions in the containment dome are shown in Figure C.4.7. The reactor building spray system water entered containment at 6100 seconds. The hydrogen mole fraction in the dome was representative of most compartments in containment that were not in direct contact with the source compartment. Hydrogen mole fractions at the end of the sprays on S_2D2 calculation varied by less than 0.01. The average hydrogen mole fraction throughout containment at the end of the S_2D2 calculation was approximately 0.14. The overall containment-wide peak hydrogen mole fractions outside the source compartment occurred between 14,500 and 15,000 seconds and ranged between 0.149 and 0.151. The hydrogen mole fraction

Table C.4.2

Transport Scenarios Analyzed For Surry Containment

Case	Accident Sequence	Source Compartment	Sprays
TA1*	S_2D2	5	automatic
TA2	S_2D2	6	automatic
TA3*	S_2D2	7	automatic
TA4	S_2D2	8	automatic
TA5*	S_2D2	9	automatic
TA6	S_2D2	15	automatic
TB1*	S_1D4	5	automatic
TB2*	S_1D4	6	automatic
TB3	S_1D4	7	automatic
TB4	S_1D4	8	automatic
TB5	S_1D4	9	automatic
TB6	S_1D4	15	automatic

* Parameters went beyond HECTR's range during the run and the run terminated.

Initial containment gas temperature: 314°K
Initial containment gas pressure: 69 kPa

Sprays are automatically initiated at a containment building pressure of 170 kPa.

Each case is identified by an alphanumeric designation as follows: T = transport calculation only (no burns); A = 2_2D; B = S_1D; number = a case within a set of runs with a different source compartment.

mole fraction was above 0.13 throughout the containment after 8500 seconds. HECTR printed detonation messages several times for each compartment from 8600 seconds to 15,860 seconds.

Steam mole fractions were fairly uniform throughout containment after spray activation, varying by less than 0.05 at the end of the transport calculation.

Varying the source compartment locations had little effect on hydrogen and steam mole fractions throughout containment except for in the source compartment. The calculated hydrogen mole fractions and steam mole fractions (after blowdown) in the containment outside the source compartment were similar for all S_2D2 cases.

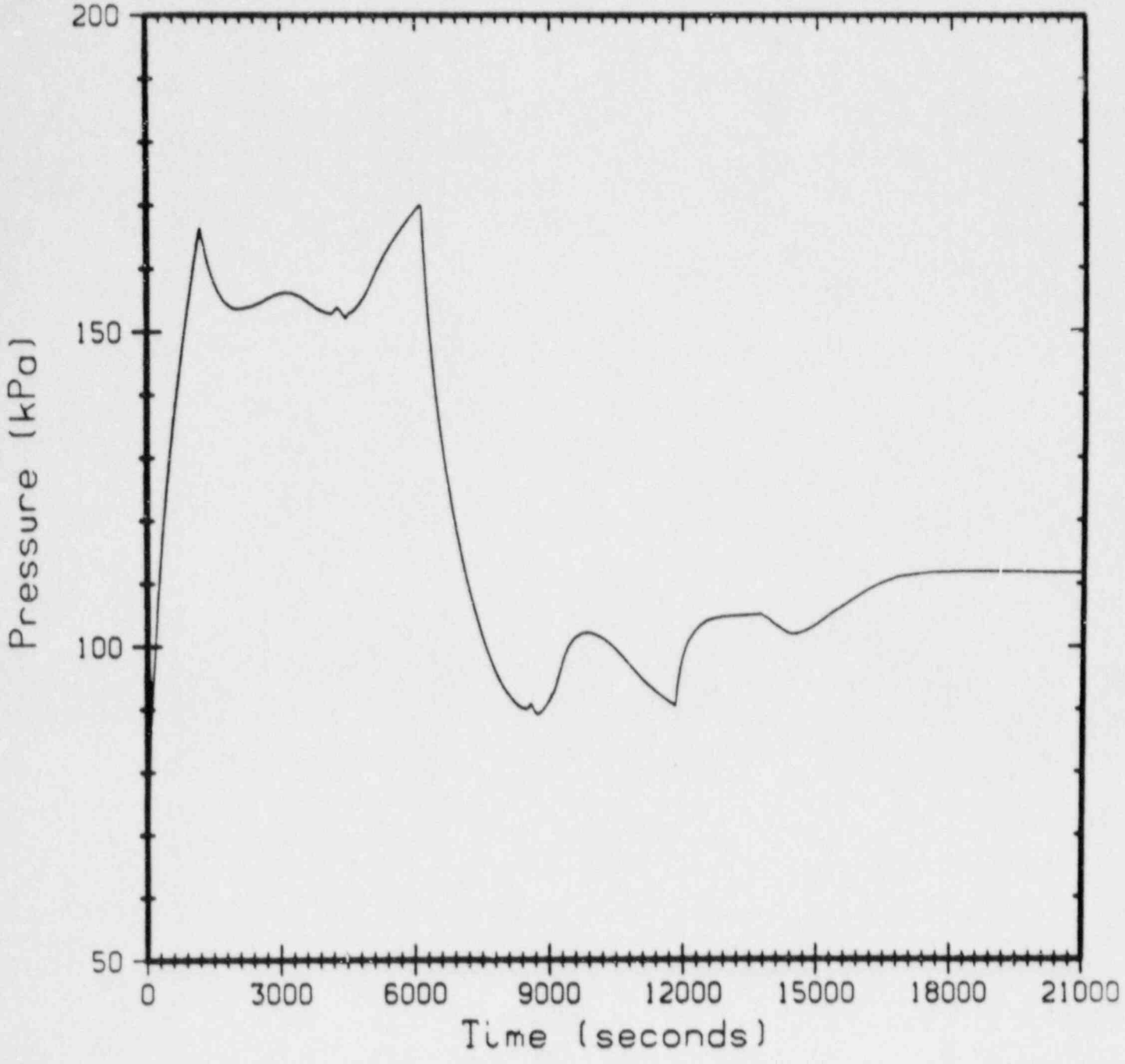

Figure C.4.6. Containment Gas Pressure Response to S_2D2 LOCA with Reactor Building Sprays On

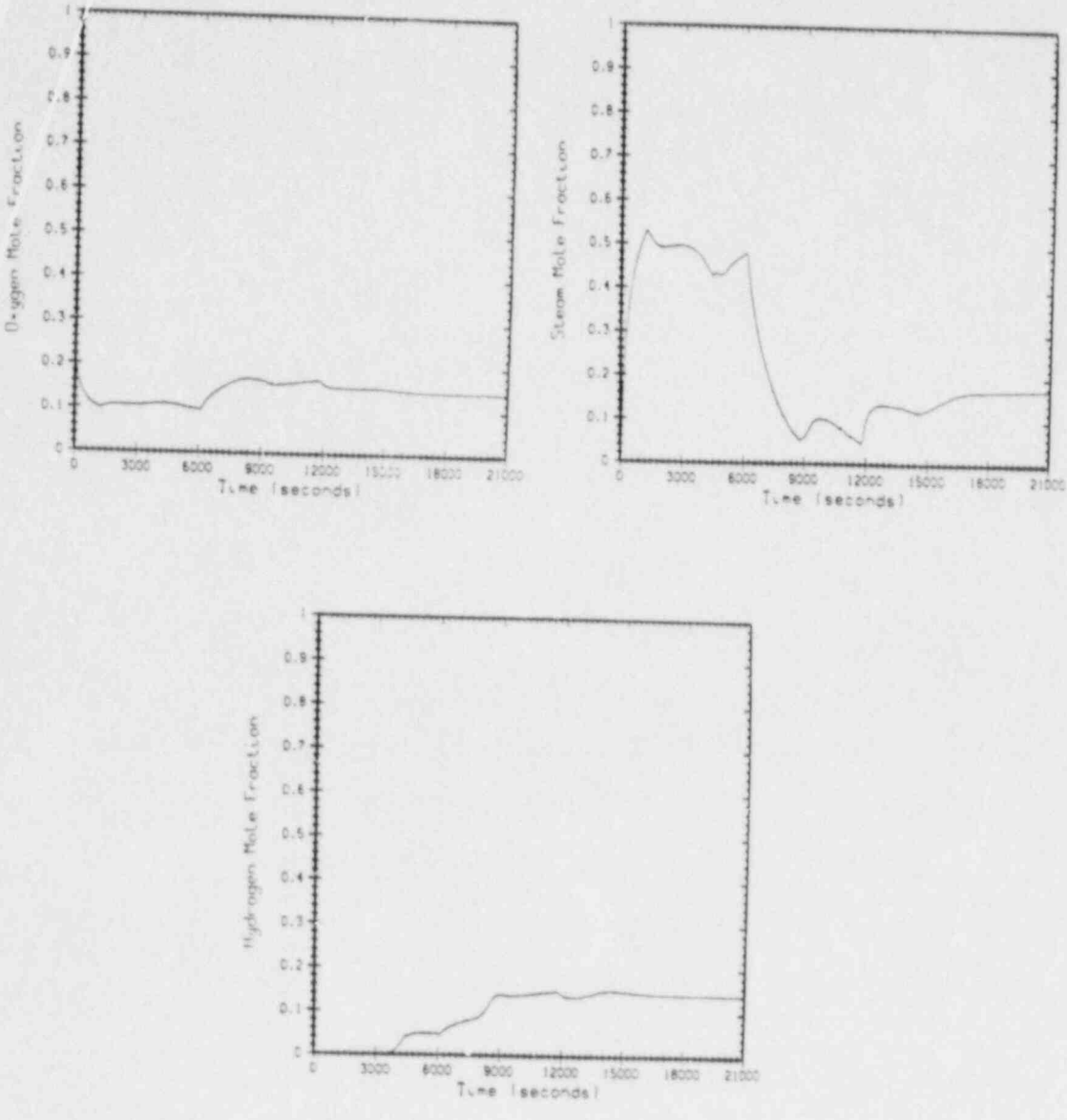

Figure C.4.7. Typical S_2D2 Calculated Gas Mole Fractions in Dome Region

Typical source compartment calculated gas mole fraction trends are shown in Figure C.4.8. The peak hydrogen mole fractions were calculated when the hydrogen leak rate from the primary system was at its maximum value. The source compartment peak hydrogen mole fractions for each S_2D2 case are shown in Table C.4.3. Steam mole fractions at the time of peak hydrogen mole fractions were less than 0.30. The source compartment peak hydrogen mole fractions were higher than the average containment-wide hydrogen mole fractions at the end of the S_2D runs.

The dominant flow directions in containment during the release of water and hydrogen for cases A2S through A6S were similar to one another with respect to flow patterns but different in flow magnitudes. The flow directions were affected primarily by the source terms and also by the hot nuclear steam system surfaces to a lesser extent. Figure C.4.9 shows the average flow patterns. The source term forced flow from the source compartment (compartment 6, for example) up into the operating floor region (compartment 2) and into the dome (compartment 1). Flow into the dome was then directed to the containment basement (compartment 14) through the containment annulus (compartments 3 and 4). Flow then entered the source compartment from the basement, completing the containment air circulation pattern. Flow from the operating floor also entered the refueling canal and reactor cavity (compartments 12 and 5). Flow entering the reactor cavity was then directed into the source compartment.

C.4.3.2 S_1D4

Typical containment gas pressure response to the large break LOCA is shown in Figure C.4.10. The sprays were activated at 300 seconds. Operation of sprays significantly reduced containment pressure for the remainder of the S_1D4 transport case. The pressure response in Figure C.4.10 was roughly equal for all break source locations showing little pressure sensitivity to break location.

Typical calculated steam, hydrogen, and oxygen mole fractions in the containment dome are shown in Figure C.4.11. The hydrogen mole fraction trend in the dome was representative of most compartments in containment except for the source compartment and some of its neighbors. The peak hydrogen mole fractions outside the source compartment occurred between 5000 and 5300 seconds and ranged between 0.155 and 0.168. The hydrogen mole fraction was above 0.13 throughout the containment after 4800 seconds. Detonation messages were printed several times for each compartment in containment from 4100 seconds to 6400 seconds.

Table C.4.3

Source Compartment Peak Hydrogen Mole Fractions

Case	Relative Source Location	Source Compartment Volume (Ft^3)	Peak Hydrogen Mole Fraction
TA1	Reactor Cavity	11689	0.39
TA2	Steam Generator Cubicle A	46834	0.18
TA4	Steam Generator Cubicle B	42363	0.17
TA6	Pressurizer Drain Tank Cubicle	18793	0.24
TB1	Reactor Cavity	11678	Parameters out of range, run terminated
TB2	Steam Generator Cubicle A	46834	Parameters out of range, run terminated
TB3	Steam Generator Cubicle B	40529	0.22
TB4	Steam Generator Cubicle C	42363	0.21
TB5	Pressurizer Cubicle	24613	0.24
TB6	Pressurizer Drain Tank Cubicle	18793	0.28

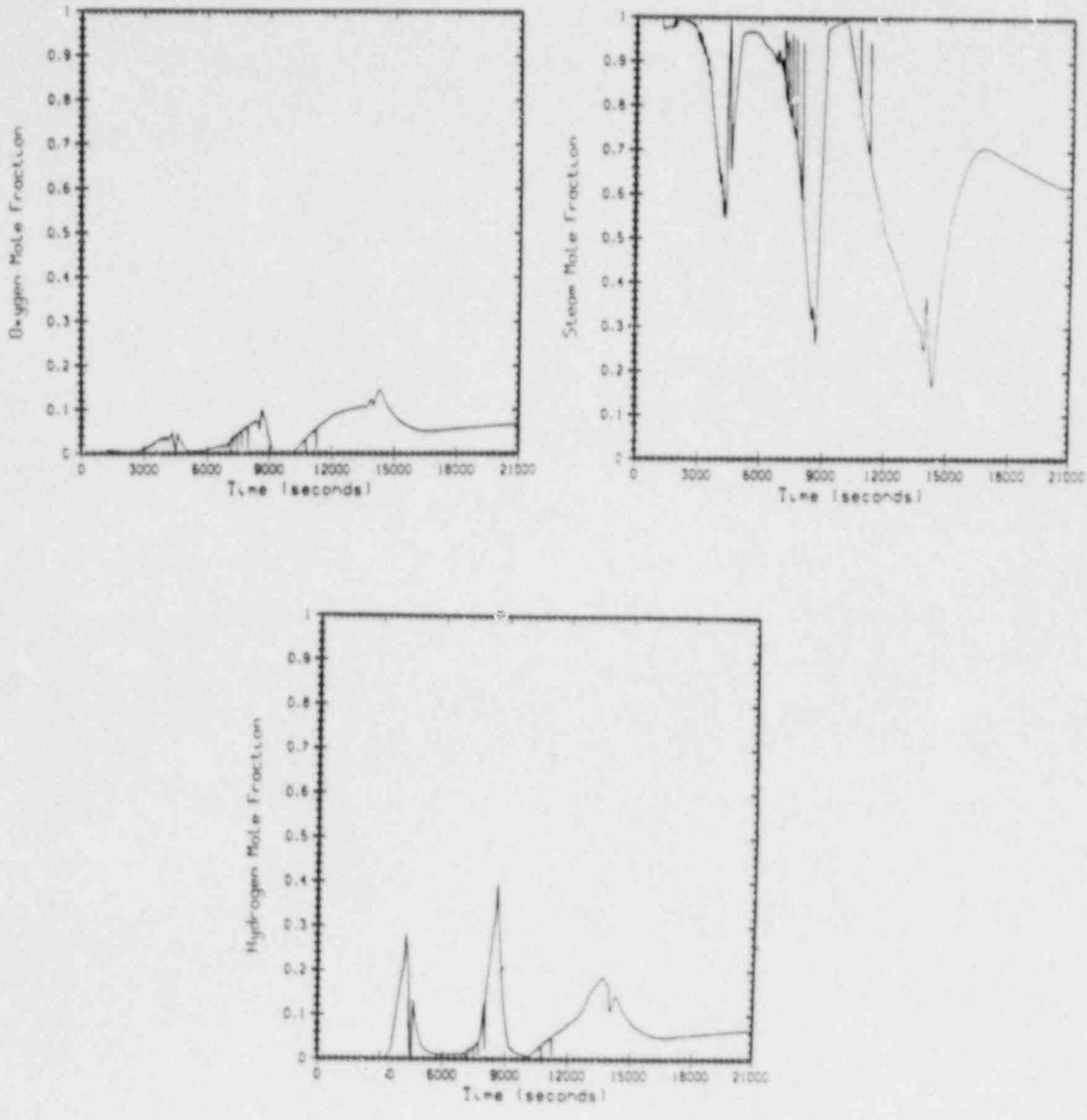

Figure C.4.8. Typical S_2D2 Source Compartment Calculated Gas Mole Fractions

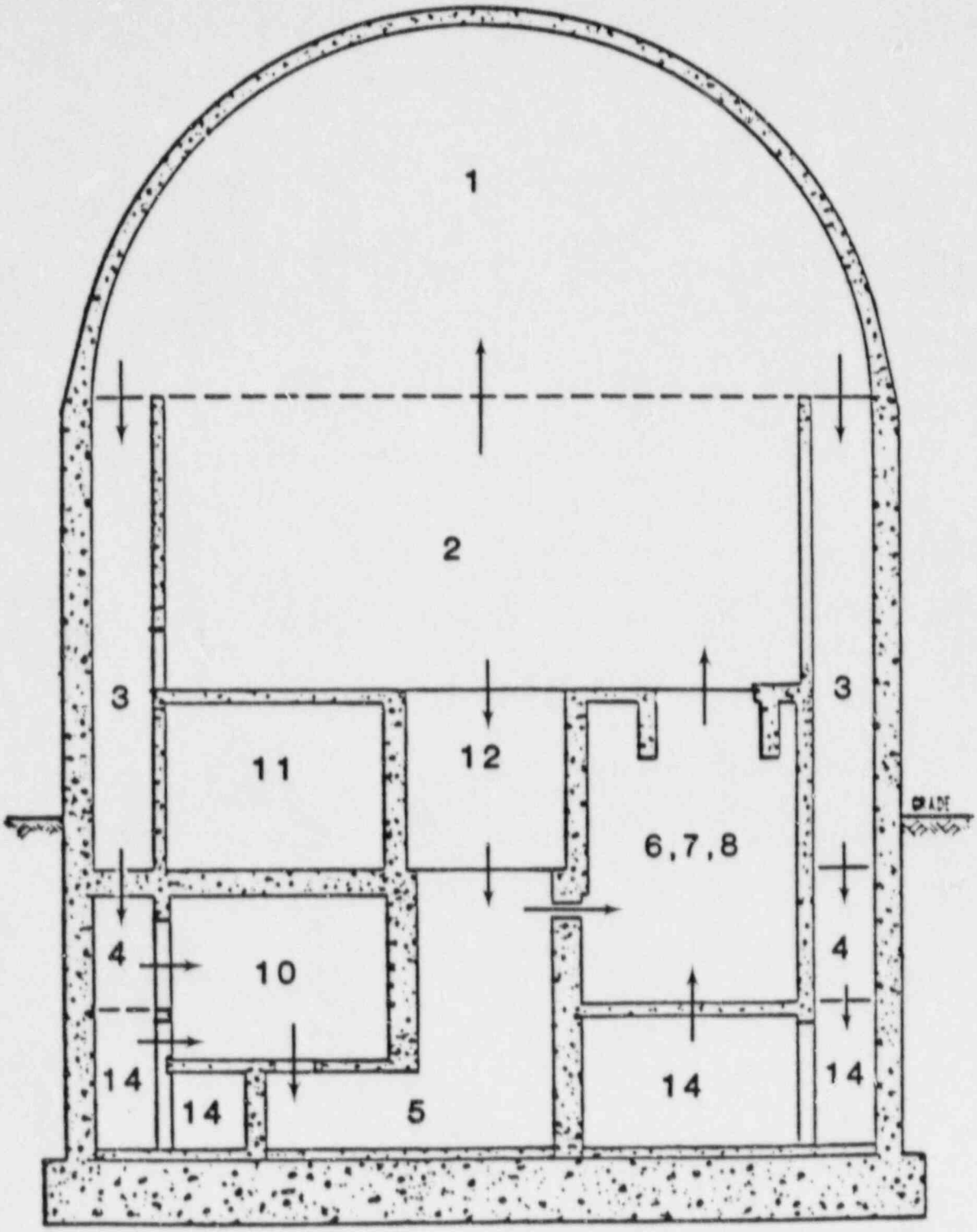

Figure C.4.9. Representative Containment Flow Patterns

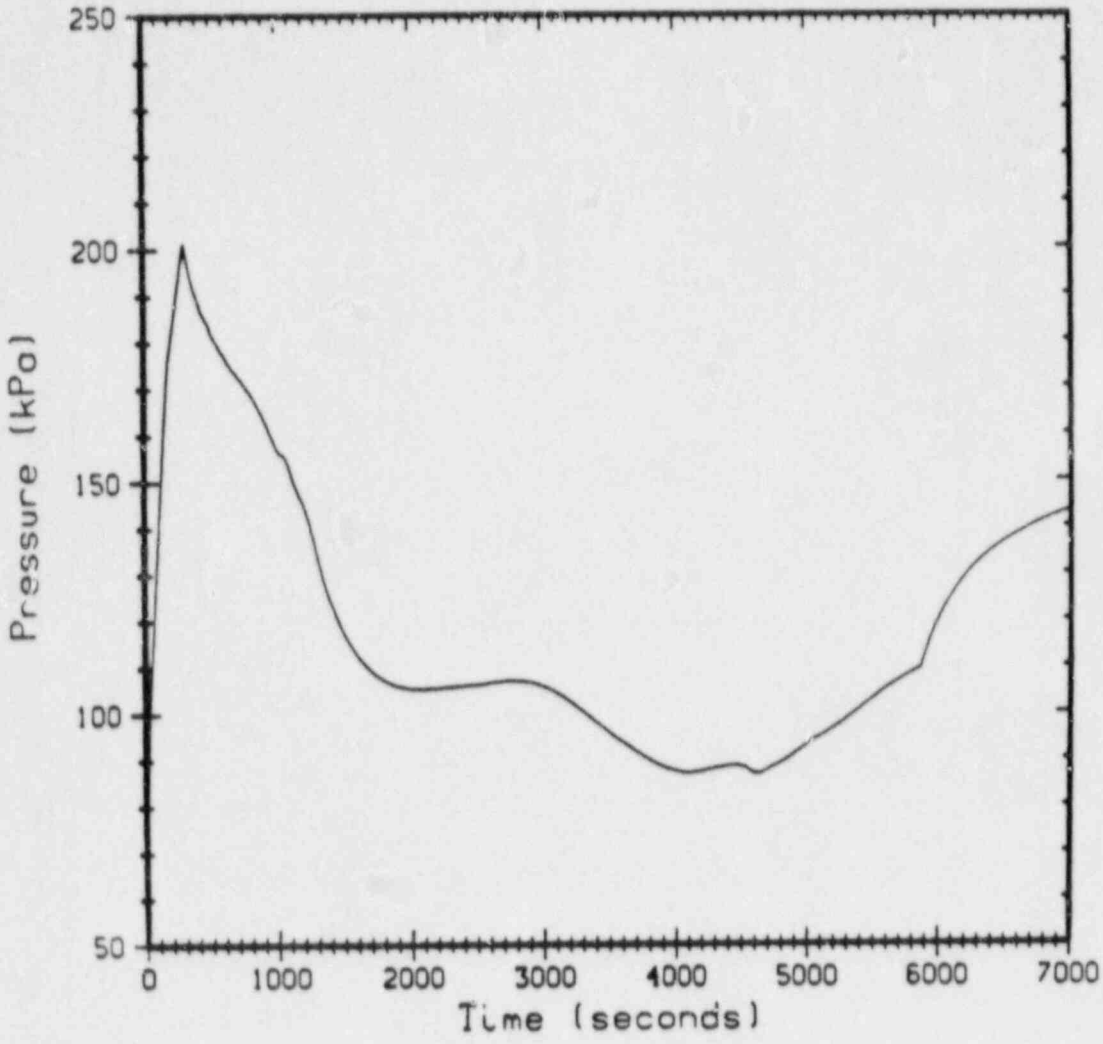

Figure C.4.10. Calculated Containment Gas Pressure Response with Reactor Building Sprays On

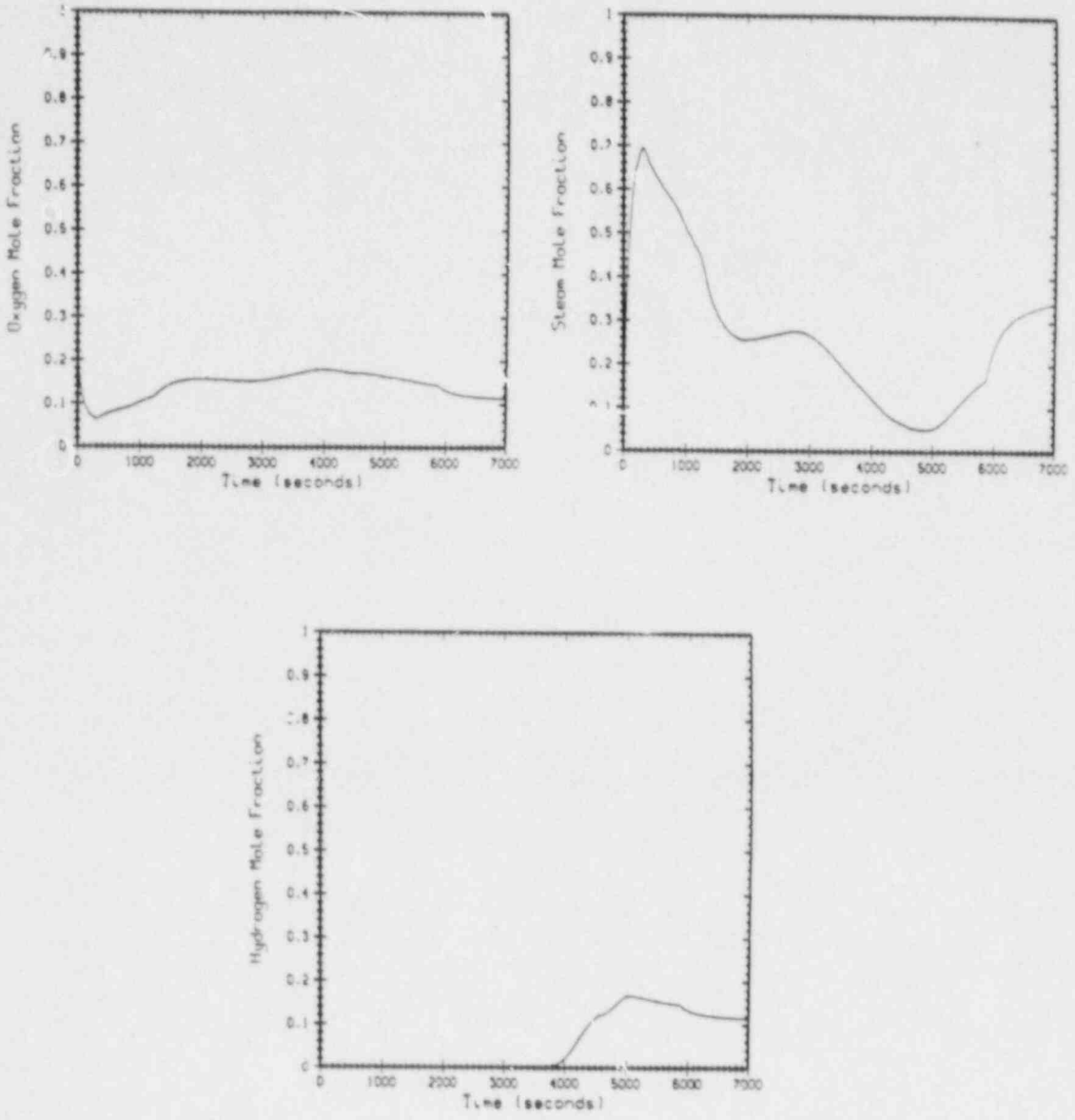

Figure C.4.11. Typical S_1D4 Calculated Gas Mole Fractions in Containment Dome

Varying the source compartment location had little effect on steam and hydrogen mole fractions throughout containment except for in the source compartment.

Table C.4.2 lists the source compartment peak hydrogen mole fractions for the S_1D4 sprays on cases. HECTR indicated that detonable concentrations were present in source compartments for lengthy time periods. The B3S case had a detonable message for 970 seconds.

The dominant flow patterns in containment for the sprays on S_1D4 were similar to those for the sprays on S_2D2 transport calculation.

C.4.4 Transport Summary

Hydrogen generation and release from the primary occurred three times in the S_2D2 and twice in the S_1D4 transport calculations. Hydrogen generation and release stopped when HPI flow was initiated.

The primary leak flow rates were influential in establishing the circulation flow patterns in containment. The calculated circulation flows caused good mixing of hydrogen during and after hydrogen injection into containment. Hydrogen mole fractions were slightly lower in the source compartment for some cases at the end of the scenario because steam was still being injected into the source compartment from the primary, decreasing the hydrogen mole fraction in that compartment. Overall containment-wide average hydrogen concentrations were the highest at approximately 15,000 seconds for the S_2D2 scenario and at 5100 to 5500 seconds for the S_1D4 scenario.

The highest local concentrations of hydrogen were always calculated in the source compartments. These local peak hydrogen mole fractions occurred at the time of maximum hydrogen injection into the source compartment from the primary. Hydrogen mole fractions in other compartments were lower than the peak mole fractions in the source compartment at the time of maximum hydrogen injection. The volume of the source compartment and the venting of the source compartment also affected the calculated peak hydrogen concentrations. In general, smaller volumes or poor venting caused higher peak concentrations.

C.5 Results

The results of the Surry analyses for all four equipment models are given in Tables C.5.1 through C.5.16 at the end of this appendix. There is a separate set of tables for each break size. Thus, the first eight tables (C.5.1 through C.5.8) contain the S_2D results. The second eight (C.5.9 through C.5.16) contain the S_1D results.

Table C.5.1

Compartment 3 Upper Annulus HECTR S_2D Results

Case	Source Compt	No. of Burns	DMs	T_{max} Gas (°K)	P_{max} (kPa)	Cover Plate T_{max} (°K)	Cover Plate t (sec)	Case as Plate T_{max} (°K)	Case as Plate t (sec)	Lumped Case T_{max} (°K)	Lumped Case t (sec)	3-Layer Case T_{max} (°K)	3-Layer Case t (sec)
A1S	5												
A2S	6	1	4	1390	400	390	-	370	-	370	-	390	-
A3S	7												
A4S*	8	1	3	1400	405	390	-	370	-	370	-	390	-
A5S	9												
A6S	15	1	3	1410	403	390	-	370	-	370	-	390	-
A1SD	5												
A2SD	6	1		590	170	370	-	370	-	370	-	370	-
A3SD	7												
A4SD	8												
A5SD	9												
A6SD	15	Exceeded run limit--many burns in Compartment 15											

*Run stopped at 14,616 s. Burns occurred, but peak equipment temps had not occurred. Detonable mixtures are valid results.

Table C.5.2

Compartment 6 Steam Generator A Cubicle HECTR S_2D Results

Case	Source Compt	No. of Burns	DMs	T_{max} Gas (°K)	P_{max} (kPa)	Cover Plate T_{max} (°K)	Cover Plate t (sec)	Case-as-Plate T_{max} (°K)	Case-as-Plate t (sec)	Lumped Case T_{max} (°K)	Lumped Case t (sec)	3-Layer Case T_{max} (°K)	3-Layer Case t (sec)
A1S	5												
A2S	6	1	3	1420	400	450	-	420	-	420	-	450	-
A3S	7												
A4S*	8	1	2	1433	410	390	-	360	-	360	-	380	-
A5S	9												
A6S	15	1	2	1441	410	390	-	360	-	360	-	380	-
A1SD	5								-				
A2SD	6	38		930	170	550	-	460	6069	460	6069	510	5400
A3SD	7												
A4SD	8												
A5SD	9												
A6SD	15	Exceeded run limit--many burns in Compartment 15											

*Run stopped at 14,616 s. Burns occurred, but peak equipment temps had not occurred. Detonable mixtures are valid results.

Table C.5.3

Compartment 7 Steam Generator B HECTR S_2D Results

Case	Source Compt	No. of Burns	DMs	T_{max} Gas (°K)	P_{max} (kPa)	Cover Plate T_{max} (°K)	Cover Plate t (sec)	Case-as-Plate T_{max} (°K)	Case-as-Plate t (sec)	Lumped Case T_{max} (°K)	Lumped Case t (sec)	3-Layer Case T_{max} (°K)	3-Layer Case t (sec)
A1S	5												
A2S	6	1	2	1420	400	380	-	360	-	360	-	380	-
A3S	7												
A4S*	8	1	2	1420	410	390	-	360	-	360	-	390	-
A5S	9												
A6S	15	1	2	1410	410	390	-	360	-	360	-	390	-
A1SD	5												
A2SD	6	0		420	170	370	-	360	-	360	-	370	-
A3SD	7												
A4SD	8												
A5SD	9												
A6SD	15	Exceeded run limit--many burns in Compartment 15											

*Run stopped at 14,616 s. Burns occurred, but peak equipment temps had not occurred. Detonable mixtures are valid results.

Table C.5.4

Compartment 8 Steam Generator C Cubicle HECTR S_2D Results

Case	Source Compt	No. of Burns	DMs	T_{max} Gas (°K)	P_{max} (kPa)	Cover Plate T_{max} (°K)	Cover Plate t (sec)	Case as Plate T_{max} (°K)	Case as Plate t (sec)	Lumped Case T_{max} (°K)	Lumped Case t (sec)	3-Layer Case T_{max} (°K)	3-Layer Case t (sec)
A1S	5												
A2S		1	2	1460	400	390	-	360	-	360	-	390	-
A3S	7												
A4S*	8	1	3	1440	410	430	-	400	-	400	-	430	-
A5S	9												
A6S	15	1	1	1460	410	410	-	380	-	380	-	400	-
A1SD	5												
A2SD	6	0		430	170	370	-	360	-	360	-	370	-
A3SD	7												
A4SD	8												
A5SD	9												
A6SD	15	Exceeded run limit--many burns in Compartment 15											

*Run stopped at 14,616 s. Burns occurred, but peak equipment temps had not occurred. Detonable mixtures are valid results.

Table C.5.5

Compartment 9 Pressurizer Cubicle HECTR S_2D Results

Case	Source Compt	No. of Burns	DMs	T_{max} Gas (°K)	P_{max} (kPa)	Cover Plate T_{max} (°K)	Cover Plate t (sec)	Case as Plate T_{max} (°K)	Case as Plate t (sec)	Lumped Case T_{max} (°K)	Lumped Case t (sec)	3-Layer Case T_{max} (°K)	3-Layer Case t (sec)
A1S	5												
A2S	6	1	2	1440	400	390	-	360	-	360	-	380	-
A3S	7												
A4S*	8	1	2	1420	410	400	-	370	-	368	-	390	-
A5S	9												
A6S	15	1	3	1400	410	440	-	420	-	420	-	440	-
A1SD	5												
A2SD	6	0		430	170	370	-	360	-	360	-	370	-
A3SD	7												
A4SD	8												
A5SD	9												
A6SD	15	Exceeded run limit--many burns in Compartment 15											

*Run stopped at 14,616 s. Burns occurred, but peak equipment temps had not occurred. Detonable mixtures are valid results.

Table C.5.6

Compartment 10 RHR Cubicle HECTR S_2D Results

Case	Source Compt	No. of Burns	DMs	T_{max} Gas (°K)	P_{max} (kPa)	Cover Plate T_{max} (°K)	Cover Plate t (sec)	Case-as-Plate T_{max} (°K)	Case-as-Plate t (sec)	Lumped Case T_{max} (°K)	Lumped Case t (sec)	3-Layer Case T_{max} (°K)	3-Layer Case t (sec)
A1S	5												
A2S	6	1	2	1410	400	370	-	360	-	360	-	370	-
A3S	7												
A4S*	8	1	2	1410	410	380	-	360	-	360	-	370	-
A5S	9												
A6S	15	1	2	1430	410	380	-	360	-	360	-	370	-
A1SD	5												
A2SD	6	0		380	170	350	-	350	-	350	-	350	-
A3SD	7												
A4SD	8												
A5SD	9												
A6SD	15	Exceeded run limit--many burns in Compartment 15											

*Run stopped at 14,616 s. Burns occurred, but peak equipment temps had not occurred. Detonable mixtures are valid results.

Table C.5.7

Compartment 11 Incore Instrumentation Room HECTR S_2D Results

Case	Source Compt	No. of Burns	DMs	T_{max} Gas (°K)	P_{max} (kPa)	Cover Plate T_{max} (°K)	Cover Plate t (sec)	Case-as-Plate T_{max} (°K)	Case-as-Plate t (sec)	Lumped Case T_{max} (°K)	Lumped Case t (sec)	3-Layer Case T_{max} (°K)	3-Layer Case t (sec)
A1S	5												
A2S	6	1	2	1430	400	390	-	360	-	360	-	380	-
A3S	7												
A4S*	8	1	2	1450	410	400	-	370	-	370	-	390	-
A5S	9												
A6S	15	1	2	1440	410	390	-	360	-	360	-	390	-
A1SD	5												
A2SD	6	0		390	170	350	-	350	-	350	-	350	-
A3SD	7												
A4SD	8												
A5SD	9												
A6SD	15	Exceeded run limit--many burns in Compartment 15											

*Run stopped at 14,616 s. Burns occurred, but peak equipment temps had not occurred. Detonable mixtures are valid results.

Table C.5.8

Compartment 14 Basement HECTR S_2D Results

Case	Source Compt	No. of Burns	DMs	T_{max} Gas (°K)	P_{max} (kPa)	Cover Plate T_{max} (°K)	Cover Plate t (sec)	Case-as-Plate T_{max} (°K)	Case-as-Plate t (sec)	Lumped Case T_{max} (°K)	Lumped Case t (sec)	3-Layer Case T_{max} (°K)	3-Layer Case t (sec)
A1S	5												
A2S	6	1	2	1380	400	360	-	350	-	350	-	360	-
A3S	7												
A4S*	8	1	2	1400	410	370	-	360	-	360	-	360	-
A5S	9												
A6S	15	1	2	1380	410	370	-	350	-	350	-	360	-
A1SD	5												
A2SD	6	0		380	170	350	-	350	-	350	-	350	-
A3SD	7												
A4SD	8												
A5SD	9												
A6SD	15	Exceeded run limit--many burns in Compartment 15											

*Run stopped at 14,616 s. Burns occurred, but peak equipment temps had not occurred. Detonable mixtures are valid results.

Table C.5.9

Compartment 3 Upper Annulus HECTR S_1D Results

Case	Source Compt	No. of Burns	DMs	T_{max} Gas (°K)	P_{max} (kPa)	Cover Plate T_{max} (°K)	Cover Plate t (sec)	Case-as-Plate T_{max} (°K)	Case-as-Plate t (sec)	Lumped Case T_{max} (°K)	Lumped Case t (sec)	3-Layer Case T_{max} (°K)	3-Layer Case t (sec)
B1S*	5												
B2S*	6												
B3S	7												
B4S	8	1	1	1560	410	390	–	380	–	380	–	390	–
B5S	9	1	1	1530	410	390	–	380	–	380	–	390	–
B6S	15	1	1	1570	410	390	–	370	–	370	–	390	–
B1SD	5												
B2SD	6												
B3SD	7												
B4SD	8	0		400	220	380	–	380	–	380	–	380	–
B5SD	9												
B6SD	15												
	8	1	1	1600	400	380	–	370	–	370	–	380	–

*Parameters in transport calculation went out of HECTR's range; these cases were not run. Parameters were out of range prior to the start of hydrogen generation. This condition prohibited running the corresponding default cases also.

Table C.5.10

Compartment 6 Steam Generator A Cubicle HECTR S_1D Results

Case	Source Compt	No. of Burns	DMs	T_{max} Gas (°K)	P_{max} (kPa)	Cover Plate T_{max} (°K)	Cover Plate t (sec)	Case-as-Plate T_{max} (°K)	Case-as-Plate t (sec)	Lumped Case T_{max} (°K)	Lumped Case t (sec)	3-Layer Case T_{max} (°K)	3-Layer Case t (sec)
B1S*	5												
B2S*	6												
B3S	7												
B4S	8	1	1	1560	420	390	-	370	-	370	-	380	-
B5S	9	1	1	1520	420	390	-	370	-	370	-	380	-
B6S	15	1	1	1540	420	390	-	370	-	370	-	380	-
B1SD	5												
B2SD	6												
B3SD	7												
B4SD	8	0		390	220	380	-	380	-	380	-	380	-
B5SD	9												
B6SD	15												

*Parameters in transport calculation went out of HECTR's range; these cases were not run. Parameters were out of range prior to the start of hydrogen generation. This condition prohibited running the corresponding default cases also.

Table C.5.11

Compartment 7 Steam Generator B Cubicle HECTR S_1D Results

Case	Source Compt	No. of Burns	DMs	T_{max} Gas (°K)	P_{max} (kPa)	Cover Plate T_{max} (°K)	Cover Plate t (sec)	Case-as-Plate T_{max} (°K)	Case-as-Plate t (sec)	Lumped Case T_{max} (°K)	Lumped Case t (sec)	3-Layer Case T_{max} (°K)	3-Layer Case t (sec)
B1S*	5												
B2S*	6												
B3S	7												
B4S	8	1	1	1520	420	390	-	370	-	370	-	380	-
B5S	9	1	1	1470	420	380	-	370	-	370	-	380	-
B6S	15	1	1	1490	420	380	-	370	-	370	-	380	-
B1SD	5												
B2SD	6												
B3SD	7												
B4SD	8	0		388	220	380	-	380	-	380	-	380	-
B5SD	9												
B6SD	15												

*Parameters in transport calculation went out of HECTR's range; these cases were not run. Parameters were out of range prior to the start of hydrogen generation. This condition prohibited running the corresponding default cases also.

Table C.5.12

Compartment 8 Steam Generator C Cubicle HECTR S_1D Results

Case	Source Compt	No. of Burns	DMs	T_{max} Gas (°K)	P_{max} (kPa)	Cover Plate T_{max} (°K)	Cover Plate t (sec)	Case-as-Plate T_{max} (°K)	Case-as-Plate t (sec)	Lumped Case T_{max} (°K)	Lumped Case t (sec)	3-Layer Case T_{max} (°K)	3-Layer Case t (sec)
B1N	5												
B2N*	6												
B3N	7												
B4N	8	0		640	378	448	507	418	-	418	-	405	-
B5N	9	1		964	382	438	-	404	-	404	-	393	-
B6N	15												
B1ND	5												
B2ND	6												
B3ND	7												
B4ND	8	18		910	226	597	2988	488	3070	488	4391	441	-
B5ND	9	0		494	226	424	-	401	-	401	-	392	-
B6ND	15												
B1S*	5												
B2S*	6												
B3S	7												
B4S	8	1	4	1450	420	440	-	400	-	400	-	430	-
B5S	9	1	1	1550	420	400	-	380	-	380	-	390	-
B6S	15	1	2	1500	420	420	-	390	-	390	-	410	-
B1SD	5												
B2SD	6												
B3SD	7												
B4SD	8	59		1050	220	680	3185	540	5700	540	5200	670	4500
B5SD	9												
B6SD	15												

*Parameters in transport calculation went out of HECTR's range; these cases were not run. Parameters were out of range prior to the start of hydrogen generation. This condition prohibited running the corresponding default cases also.

Table C.5.13

Compartment 9 Pressurizer Cubicle HECTR S_1D Results

Case	Source Compt	Nc. of Burns	DMs	T_{max} Gas (°K)	P_{max} (kPa)	Cover Plate T_{max} (°K)	Cover Plate t (sec)	Case-as-Plate T_{max} (°K)	Case-as-Plate t (sec)	Lumped Case T_{max} (°K)	Lumped Case t (sec)	3-Layer Case T_{max} (°K)	3-Layer Case t (sec)
B1S*	5												
B2S*	6												
B3S	7												
B4S	8	1	1	1450	420	390	-	380	-	380	-	390	-
B5S	9	1	3	1100	420	460	1100	410	-	410	-	440	-
BS6	15	1	1	1510	424	450	600	410	-	410	-	440	-
B1SD	5												
B2SD	6												
B3SD	7												
B4SD	8	0		540	220	390	-	380	-	380	-	390	-
B5SD	9												
B6SD	15												

*Parameters in transport calculation went out of HECTR's range; these cases were not run. Parameters were out of range prior to the start of hydrogen generation. This condition prohibited running the corresponding default cases also.

Table C.5.14

Compartment 10 RHR Cubicle HECTR S_1D Results

Case	Source Compt	No. of Burns	DMs	T_{max} Gas (°K)	P_{max} (kPa)	Cover Plate T_{max} (°K)	Cover Plate t (sec)	Case-at-Plate T_{max} (°K)	Case-at-Plate t (sec)	Lumped Case T_{max} (°K)	Lumped Case t (sec)	3-Layer Case T_{max} (°K)	3-Layer Case t (sec)
B1S*	5												
B2S*	6												
B3S	7												
B4S	8	1	1	1540	420	370	-	360	-	360	-	370	-
B5S	9	1	1	1500	420	370	-	360	-	360	-	370	-
B6S	15	1	1	1510	420	370	-	360	-	360	-	370	-
B1SD	5												
B2SD	6												
B3SD	7												
B4SD	8	0		370	220	370	-	370	-	370	-	370	-
B5SD	9												
B6SD	15												

*Parameters in transport calculation went out of HECTR's range; these cases were not run. Parameters were out of range prior to the start of hydrogen generation. This condition prohibited running the corresponding default cases also.

Table C.5.15

Compartment 11 Incore Instrumentation Room HECTR S_1D Results

Case	Source Compt	No. of Burns	DMs	T_{max} Gas (°K)	P_{max} (kPa)	Cover Plate T_{max} (°K)	Cover Plate t (sec)	Case-as-Plate T_{max} (°K)	Case-as-Plate t (sec)	Lumped Case T_{max} (°K)	Lumped Case t (sec)	3-Layer Case T_{max} (°K)	3-Layer Case t (sec)
B1S*	5												
B2S*	6												
B3S	7												
B4S	8	1	1	1610	420	400	-	370	-	370	-	400	-
B5S	9	1	1	1580	420	400	-	370	-	370	-	400	-
B6S	15	1	1	1610	460	400	-	370	-	370	-	400	-
B1SD	5												
B2SD	6												
B3SD	7												
B4SD	8	0		380	220	380	-	380	-	380	-	380	-
B5SD	9												
B6SD	15												

*Parameters in transport calculation went out of HECTR's range; these cases were not run. Parameters were out of range prior to the start of hydrogen generation. This condition prohibited running the corresponding default cases also.

Table C.5.16

Compartment 14 Basement HECTR S_1D Results

Case	Source Compt	No. of Burns	DMs	T_{max} Gas (°K)	P_{max} (kPa)	Cover Plate T_{max} (°K)	Cover Plate t (sec)	Case-as-Plate T_{max} (°K)	Case-as-Plate t (sec)	Lumped Case T_{max} (°K)	Lumped Case t (sec)	3-Layer Case T_{max} (°K)	3-Layer Case t (sec)
B1S*	5												
B2S*	6												
B3S	7												
B4S	8	1	1	1430	420	360	-	360	-	360	-	360	-
B5S	9	1	1	1410	420	360	-	360	-	360	-	360	-
B6S	15	1	1	1400	430	360	-	360	-	360	-	360	-
B1SD	5												
B2SD	6												
B3SD	7												
B4SD	8	0		370	220	370	-	370	-	370	-	370	-
B5SD	9												
B6SD	15												

*Parameters in transport calculation went out of HECTR's range; these cases were not run. Parameters were out of range prior to the start of hydrogen generation. This condition prohibited running the corresponding default cases also.

There is a separate table for each compartment in which equipment was modeled. Compartment conditions and peak equipment surface temperatures are given for each case. Compartment conditions include the number of burns which occurred in the compartment, the peak gas temperature (T_{max} Gas), and pressure (P_{max}) reached in the compartment and, in cases where HECTR predicted detonable mixtures (DMs), the number of times for that case that a detonable mixture accumulated in the compartment. The peak equipment temperatures and times (t), if any, spent above 444°K are given for each equipment model. The 444 temperature represents a typical maximum equipment qualification temperature.[7] A typical maximum qualification pressure is 483 kPa.[7] During an environmental qualification test of nuclear qualified safety-related equipment, these conditions can last for several hours.

The tables also contain a source compartment number. Using this number, the source compartment can be identified by referring to Table C.2.1 of this appendix.

Each case is identified by an alphanumeric designation as follows: A = S_2D; B = S_1D; number = case within a set; S = sprays set to operate upon high containment building pressure signal; D = default ignition (i.e., ignition by igniter at 7 mole fraction percent hydrogen concentration); no D = ignition in basement at the completion of the 75 percent core metal-water reaction.

Because of the similarity of thermal responses between the three-layer transmitter model and an actual Barton transmitter (Figure C.3.1) the three-layer model was considered as a surrogate for safety-related equipment in these analyses.

The other three models were included for exploratory reasons. However, the results from these models may prove useful provided a relationship between their heat transfer characteristics and those of a known piece of safety-related equipment can be established.

HECTR uses a very simple set of criteria for defining a detonable mixture. The code defines such a mixture as having a hydrogen concentration greater than 14 percent, an oxygen concentration greater than 9 percent, and a steam concentration less than 30 percent. All three criteria must be satisfied simultaneously. In practice, the existence of a detonable mixture depends on several other factors including pressure, temperature, the presence of other gases, and compartment geometry. Thus, any detonable mixture predicted by HECTR should be considered to be potentially detonable pending a detailed analysis which accounts for all pertinent variables.

REFERENCES

1. Dingman, S. E., et al., HECTR Version 1.5 User's Manual, NUREG/CR-4507, SAND86-0101, Sandia National Laboratories, Albuquerque, NM, 1986.

2. Wooten, R. O., et al., MARCH2 (Meltdown Accident Response Characteristics) Code Description and Users Manual, NUREG/CR-3988, BMI-2115, Battelle Columbus Laboratories, August 1984.

3. Report of the Special Committee on Source Terms, American Nuclear Society, September 1984.

4. Dandini, V. J., Testing of Nuclear Qualified Cables and Pressure Transmitters in Simulated Hydrogen Deflagrations to Determine Survival Margins and Sensitivities, NUREG/CR-4324, SAND85-1481, Sandia National Laboratories, Albuquerque, NM, December 1985.

5. Dandini, V. J. and W. H. McCulloch, HECTR Analysis of Equipment Temperature Responses to Selected Hydrogen Burns in an Ice Condenser Containment, NUREG/CR-3945, SAND84-1704, February 1985.

6. Surry Power Station Units 1 and 2 Final Safety Analysis Report, Virginia Electric and Power Company, December 1969.

7. IEEE Standard for Qualifying Class 1E Equipment for Nuclear Power Generating Stations (IEEE Std 323-1974), Institute of Electrical and Electronics Engineers, 1974.

APPENDIX D

TESTING IN THE SEVERE COMBINED ENVIRONMENT TEST CHAMBER

APPENDIX D

TESTING IN THE SEVERE COMBINED ENVIRONMENT TEST CHAMBER

D.1 Introduction

A great deal of research has been conducted to assess the behavior and survivability of nuclear qualified safety-related equipment in hydrogen burns. Testing conducted by the Electric Power Research Institute (EPRI) at the Nevada Test Site (NTS) exposed several samples of different types of equipment to hydrogen burns ignited at different hydrogen concentrations.[1] Testing at Sandia's Central Receiver Test Facility (CRTF) subjected samples of nuclear qualified cables and pressure transmitters to simulated hydrogen burns of varying degrees of severity.[2,3]

The EPRI-NTS tests used new equipment for test samples in most cases. Hydrogen concentrations up to 13 volume-percent were ignited. As the tests progressed, instrumentation in the test vessel which was intended to monitor the environment became degraded due to the test conditions. As a result, the test environments, especially those from the most severe burns, are not well defined. During the course of these tests several samples failed or exhibited erratic behavior which EPRI attributed to faulty installation. After the correction of installation deficiencies the samples performed correctly.

The CRTF tests at Sandia exposed new and thermally aged pressure transmitters and cables to simulated hydrogen burns of varying severity. The most severe had a heat content and peak heat flux equal to 300 percent of those expected from a single hydrogen burn resulting from a 75 percent core Zircaloy-water reaction in a PWR in a large dry containment building. The pressure attendant to a hydrogen burn was not considered. The equipment performed correctly during exposure to the heat flux pulses and in posttest evaluations.

Both the EPRI and CRTF tests considered only the hydrogen burn portion of the accident. No simulation of the pre- or postburn LOCA was conducted. Also, none of the equipment samples had been radiation aged.

Recently, a series of experiments was conducted in Sandia National Laboratories Severe Combined Environment Test Chamber (SCETCh) which evaluated the effects of these other environmental factors. This appendix discusses these experimental efforts.

D.2 SCETCh Description

The SCETCh facility (Figure D.2.1) was designed to simulate severe environments having combined thermal, pressure, and chemical components. The chamber is a cylinder 27 inches long with an inside diameter of 15.25 inches. It is constructed of Inconel 625.

The moisture components of the environment were provided by a supply of water introduced at the beginning of the tests. The water was boiled into the SCETCh atmosphere with quartz lamps located on the outside and at the bottom of the chamber. The excess water was then drained out of the chamber. Heat for the LOCA portion of the tests was provided by 45 quartz lamps around the outside of the chamber. Each lamp was rated at 2.5 kW.

The heat source used for the hydrogen burn simulation was a set of electrically heated austenitic stainless steel foils of thickness equal to one mil (.001 inch). A separate set of foils was used in the cable and transmitter tests to account for the differences in test specimen geometry. These foils are shown in Figures D.2.2 and D.2.3.

An external pressure source (air) was used to establish the necessary preburn oxygen and pressure conditions. Venting of the chamber could be performed as necessary.

The facility is controlled using a Hewlett-Packard 9816 instrument controller and a Hewlett-Packard 3497A data acquisition unit. Instrumentation included a Heise pressure gauge, a digital manometer, and numerous thermocouples.

D.3 Accident Environment

For the single burn tests, the accident simulated was an S_2D event for a PWR in a large dry containment building. The accident was assumed to result in the reaction of 75 percent of the core Zircaloy to produce hydrogen prior to the restoration of core cooling. The hydrogen burn was assumed to occur at the completion of the 75 percent metal-water reaction. Environmental parameters for the LOCA and hydrogen deflagration were obtained from a HECTR analysis of the TMI-hybrid power plant described in Appendix A. The HECTR-determined containment gas temperature, which is an indication of overall environmental conditions, is shown in Figure D.3.1. The actual test environment is discussed in Section D.5.

For the cable multiple burn test, the accident simulated was an S_1D event for the Surry subatmospheric containment building. The accident was assumed to result in a

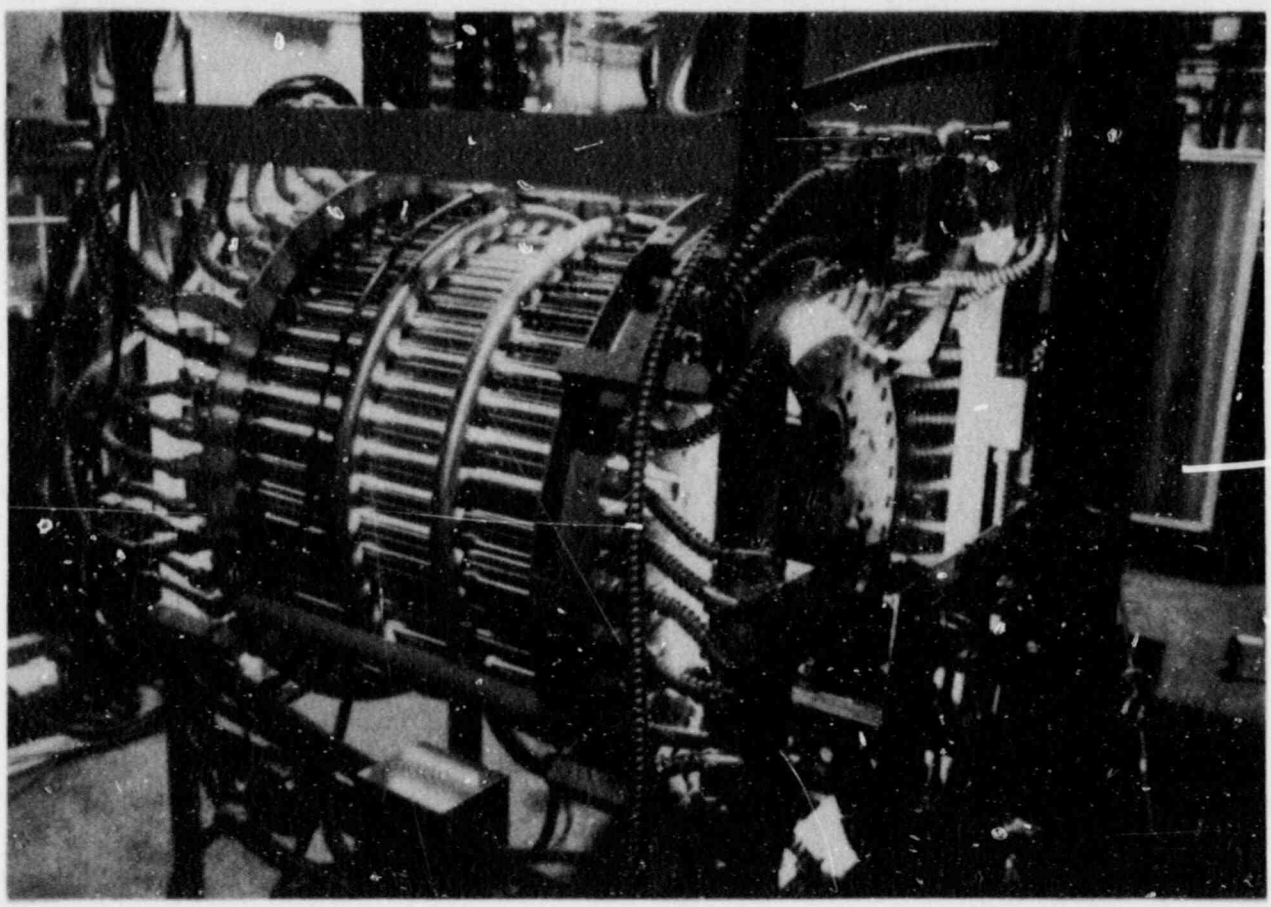

Figure D.2.1. Severe Combined Environment Test Chamber

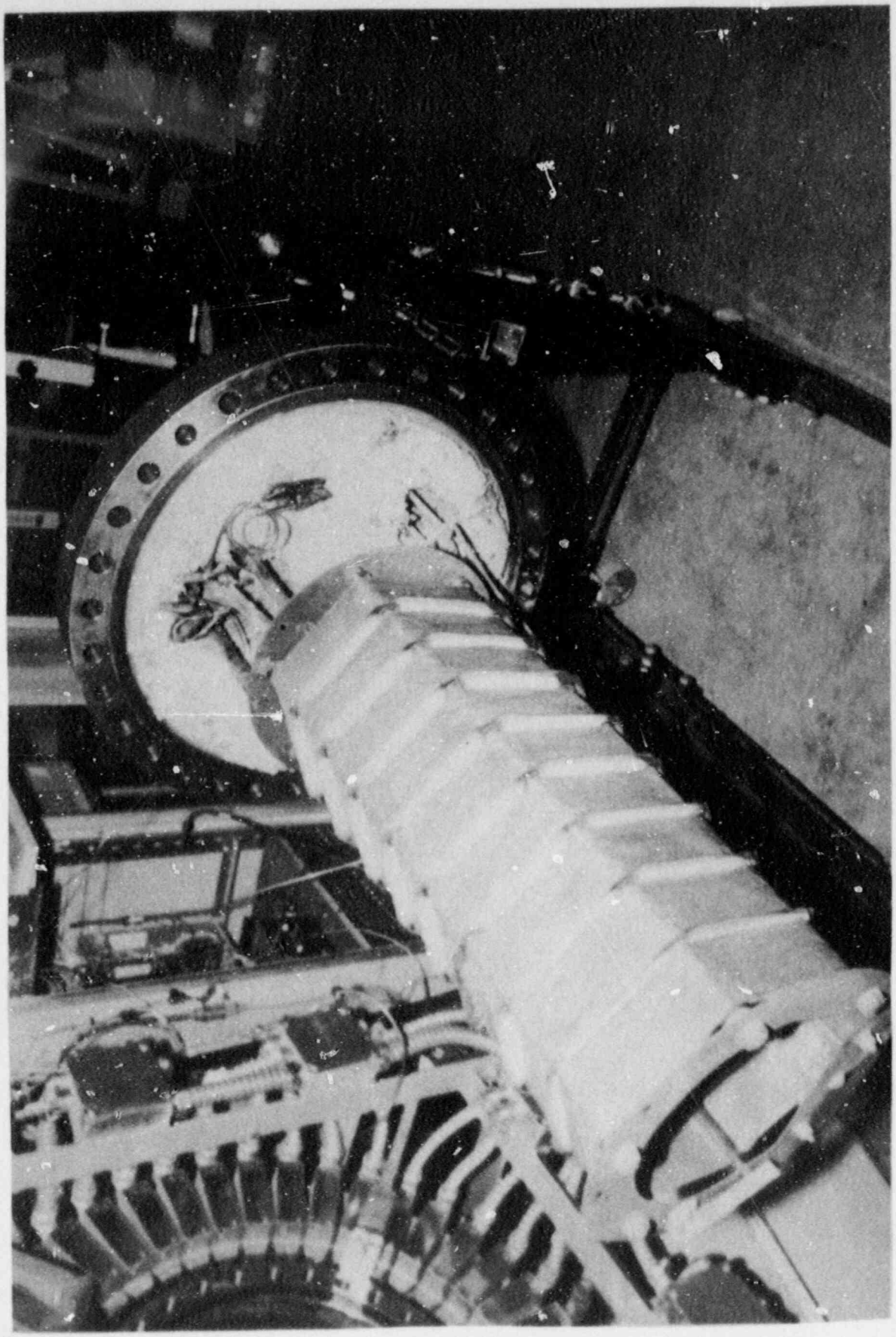

Figure D.2.2. Hydrogen Burn Simulation Cable Foils

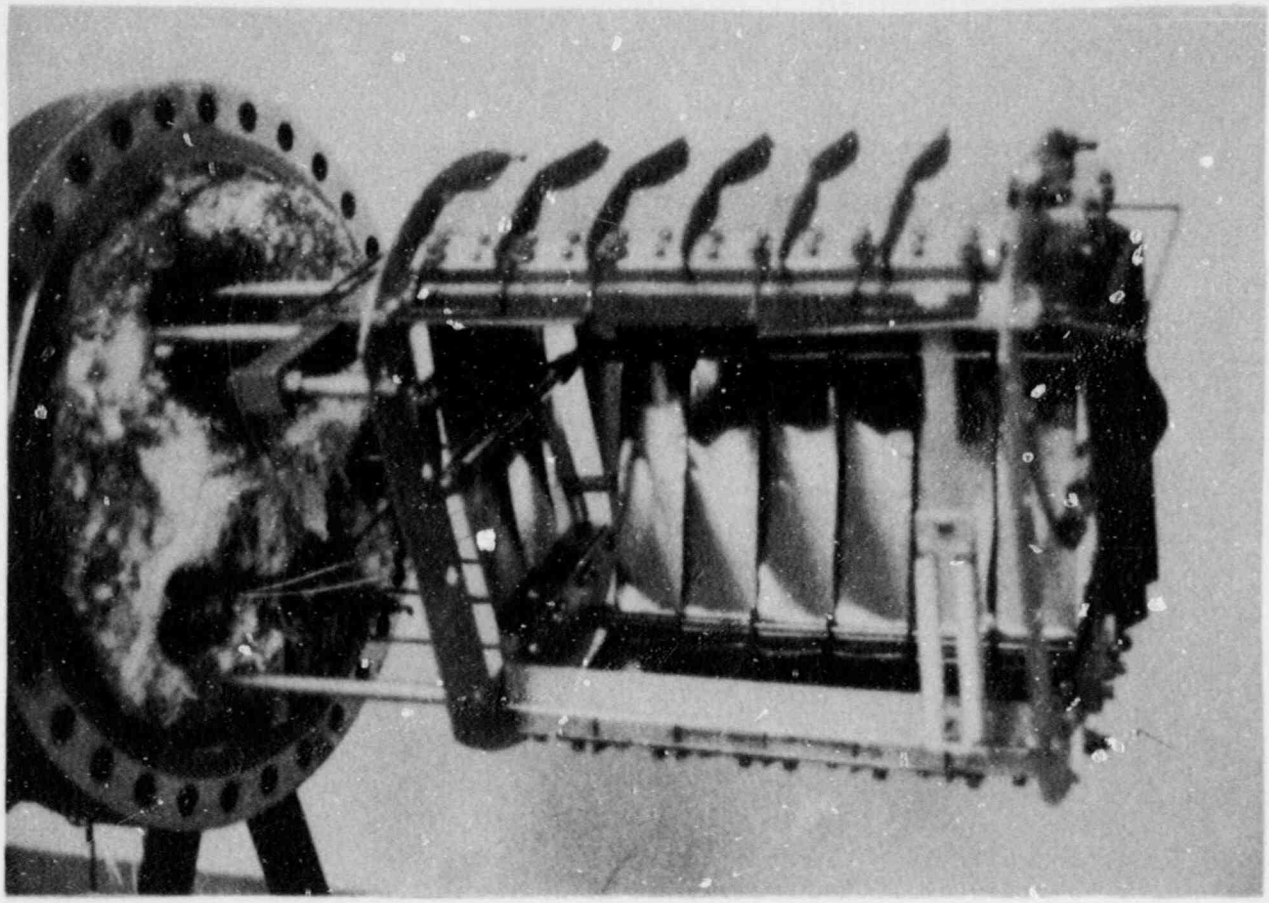

Figure D.2.3. Hydrogen Burn Simulation Transmitter Foils

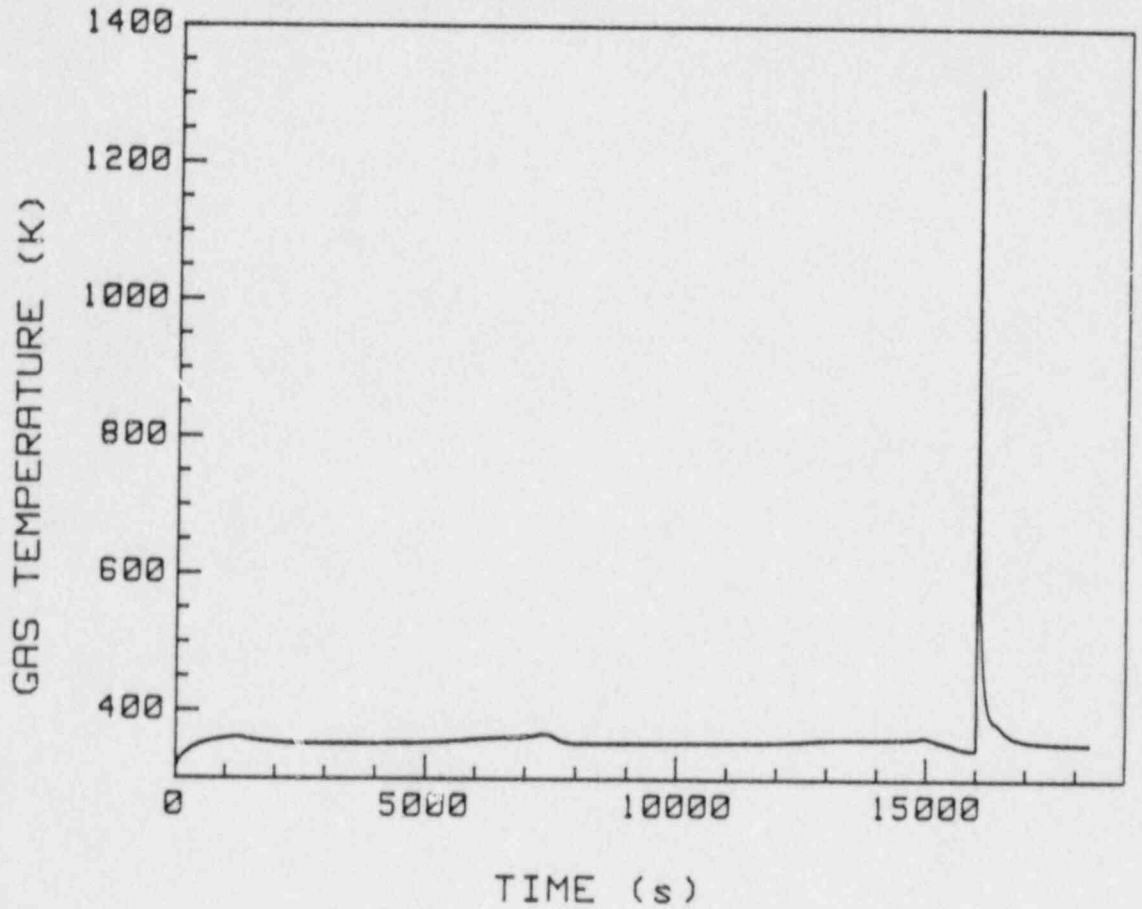

Figure D.3.1. LOCA/Hydrogen Burn Gas Temperature

75 percent core metal-water reaction. Hydrogen ignition was assumed to occur at 7 percent hydrogen concentration as discussed in Appendix C. Environmental parameters were obtained from a HECTR analysis of the Surry power plant.

For the Barton pressure transmitter multiple burn test, an environment was selected based on the results of parametric calculations performed using HECTR. The accident environment selected for the test was representative of HECTR predictions spanning a range of source compartment volumes.

More details on the actual test environments for both cases can be found in Section D.5.

D.4 SCETCh Environment Determination

As stated, predicted thermal and moisture environments during a LOCA and a hydrogen deflagration in a typical large dry containment were generated using the HECTR code. Some of the results are presented in the main body of this report. The predicted hydrogen deflagration environments differ significantly from the LOCA environments in that much higher heat fluxes are present for a much shorter duration. In order to reproduce the high heat flux pulse to the equipment in the hydrogen deflagration scenario, electrically heated foils were used inside the test chamber. The test chamber itself provided the background LOCA environment. This LOCA environment was relatively easy to achieve due to the low heat fluxes, temperatures, and pressures required.

For the hydrogen deflagration scenario, a computer program (FOILTEMP) was written which incorporated all of the important considerations. It was used to predict a priori the feasibility of reproducing the necessary heat fluxes, pressures, and moisture conditions inside the test chamber for the deflagration scenario as well as the required foil temperature and powers. Some of the important considerations and details of the analysis are discussed below.

D.4.1 Translation of Environments

In a typical containment hydrogen deflagration environment the equipment sees a combination of radiative and convective fluxes. In the SCETCh test chamber, only radiative fluxes are possible (neglecting the small contribution from natural convection). Also, in a typical containment the thermal radiation is largely from the surrounding steam, while in the SCETCh chamber it is largely from the foils. In attempting to translate the typical containment deflagration environment to the chamber, these become important considerations.

For a typical containment environment, the energy abscrbed by a piece of equipment is:

$$q_{absorbed} = \int_0^\infty \alpha_{\lambda,eq}\varepsilon_{\lambda,st}F_{st-eq}e_{\lambda b,st}d\lambda + h_x(T_{st} - T_{eq}) \quad (D\text{-}1)$$

where the first term is the absorbed incident radiative flux, and the second is the net convective flux. In (D-1),

$\alpha_{\lambda,eq}$ = spectral absorptivity of equipment,

$\varepsilon_{\lambda,st}$ = spectral emissivity of steam,

F_{st-eq} = viewfactor, steam to equipment,

$e_{\lambda b,st}$ = blackbody emissive power of steam,

λ = wavelength,

h_x = local forced convection heat transfer coefficient (including condensation),

T_{st} = steam temperature, and

T_{eq} = equipment temperature.

For the equipment in the test chamber,

$$q_{absorbed} = \int_0^\infty \alpha_{\lambda,eq}\varepsilon_{\lambda,f}F_{f-eq}\tau_{\lambda,st}e_{\lambda b,f}d\lambda + \int_0^\infty \alpha_{\lambda,eq}\varepsilon_{\lambda,st}F_{st-eq}e_{\lambda b,st}d\lambda + h_x(T_{st} - T_{eq}) \quad (D\text{-}2)$$

where the 'f' subscript indicates a foil property,

$\tau_{\lambda,st}$ = steam spectral transmissivity for foil radiation, and

h_x = local natural convection heat transfer coefficient (including condensation).

The first term in (D-2) represents absorbed foil radiation, the second term represents absorbed steam radiation, and the last, the natural convection contribution.

In comparing (D-1) and (D-2), note that h_x is much larger in (D-1) than in (D-2). Therefore, a larger fraction of absorbed energy must come from thermal radiation exchange in the test chamber. Also, h_x in (D-1) and F_{f-eq} in (D-2) can be highly position-dependent (Figure D.4.1). In attempting to match the typical containment radiation plus convection environment with a test chamber radiation-only environment, exact reproduction of the local heat flux distribution is beyond the present chamber capabilities. Thus, it is the surface-averaged heat flux (obtained from HECTR) which is matched in the chamber.

The spectral dependence of the equipment surface properties plays an important function. If the absorptivity of the surface varies considerably with wavelength, the calculations of absorbed incoming thermal radiation must be appropriately weighted. Since the amount of incoming thermal radiation is itself a function of wavelength (Figure D.4.2), the product of surface spectral absorptivity, $\alpha_{\lambda,eq}$, and incoming radiation at a given wavelength integrated over all wavelengths yields the rate at which thermal radiation is absorbed by the surface (per unit area).

In a typical containment hydrogen deflagration scenario, the majority of incoming radiative flux on a piece of equipment comes from the surrounding hot steam generated in the deflagration process. Since the thermal radiation flux on the equipment in the test chamber originates from electrically heated foils as well as steam with possibly different radiation characteristics (ε_λ, $e_{\lambda b}$), care must be taken to ensure that the fluxes are the same in both the predicted containment environment and the test chamber environment.

Fortunately, both the instrument cable and Barton transmitter tested have relatively flat reflectivity versus wavelength curves. The cable reflectivity is shown for example in Figure D.4.3. They can thus be treated as gray surfaces and $\alpha_{\lambda,eq}$ in (D-1) and (D-2) can be moved outside the integral. If the radiation originates from a gray or black surface (ε_λ constant) and from a "gray" gas with some wavelength averaged emissivity ($\bar{\varepsilon}$) and transmissivity ($\bar{\tau}$), (D-2) reduces to

$$q_{absorbed} = \bar{\alpha}_{eq}\bar{\varepsilon}_f\bar{\tau}_{st}F_{f-eq}\sigma T_f^4 + \bar{\alpha}_{eq}\bar{\varepsilon}_{st}F_{st-eq}\sigma T_{st}^4 + \bar{h}(T_{st} - T_{eq}) \qquad (D-3)$$

where $\bar{h}$ is a surface averaged natural convection heat transfer coefficient. This simplifies the calculations by

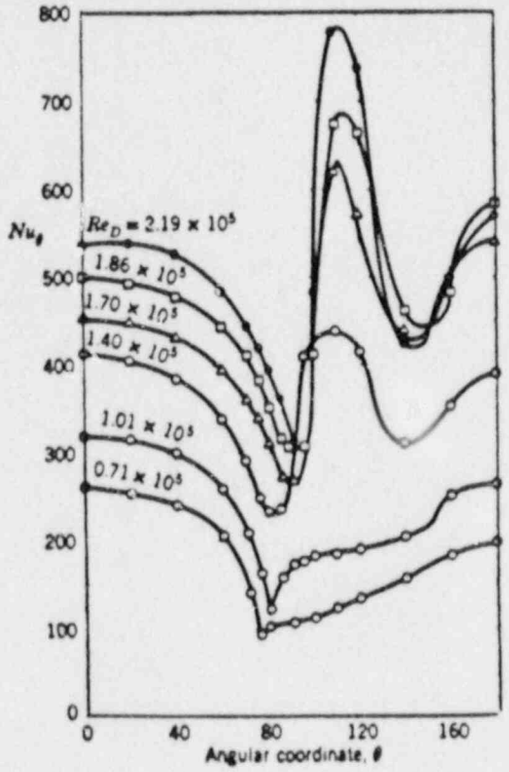

Figure D.4.1. Local Nusselt Number Distribution for Airflow Normal to a Circular Cylinder

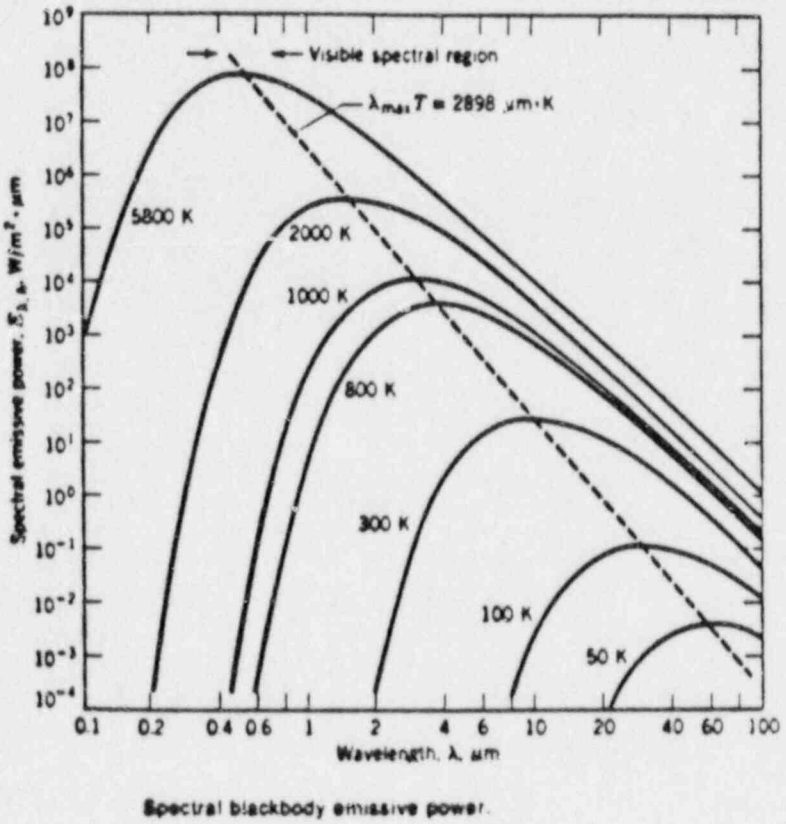

Spectral blackbody emissive power.

Figure D.4.2. Planck Distribution

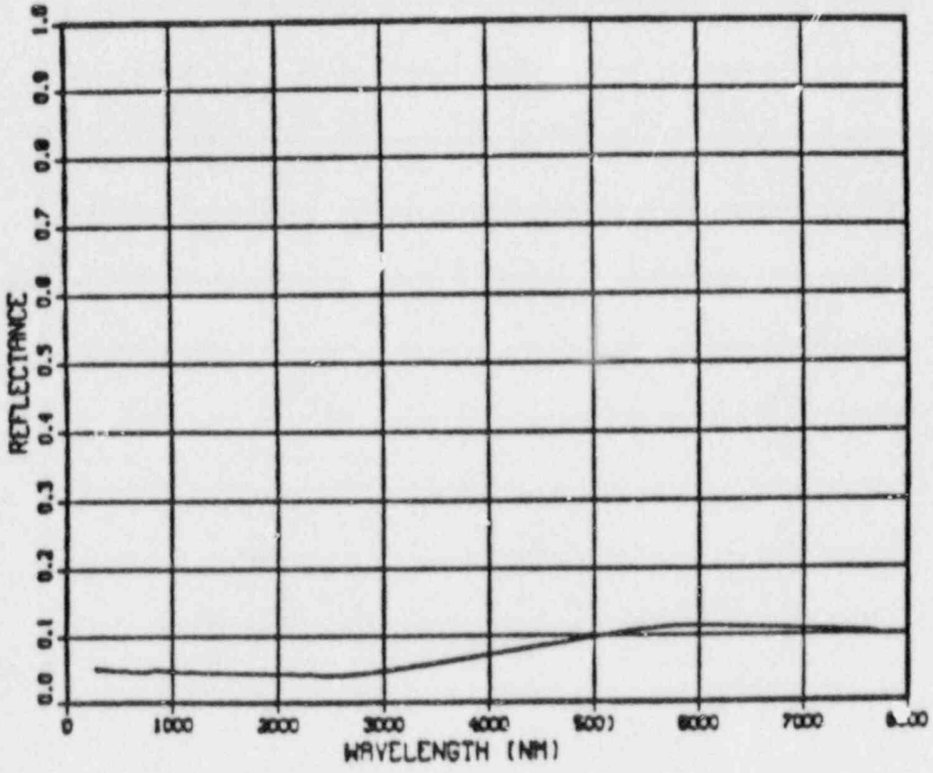

Figure D.4.3. Cable Reflectance Versus Wavelength

avoiding integration over the wavelength. Although the surface properties of the cable are only shown out to 8 μm in Figure D.4.3, the details at longer wavelength are not necessary. It will be shown below that roughly 90 percent of the incident thermal radiation is at wavelengths less than 8 μm.

D.4.2 Steam Spectral Behavior

In order to reproduce the desired moisture environment it is necessary to have steam in the test chamber. Steam behaves as a participating medium and absorbs and emits in discrete wavelength bands (Figure D.4.4). Thus a portion of the thermal radiation incident on the equipment originates from steam emission. Similarly, not all of the foil radiation emitted in the direction of the equipment actually reaches the equipment because of absorption by the steam.

There are two possible methods of accounting for these effects. If there is a strong wavelength dependence of equipment absorptivity or foil emissivity, then the surface properties must be characterized as a function of wavelength. Since the test specimens and foils used in the SCETCh tests behave relatively independent of wavelength, this procedure is not necessary. Instead, the gray behavior of the test specimens and black behavior of the foils enable the steam to be modeled as a gray gas.

Treating the steam as a gray gas involves using a correlation or figure to represent the absorptivity and emissivity integrated over all wavelengths. One such correlation is the well known Cess-Lian correlation:

$$\epsilon_{st} = a_o[1 - \exp(-a_1 x)] \qquad \text{(D-4)}$$

where $x = P_{st}L_e(300/T)(P_{air} + bP_{st})$, and (D-5)

$$b = 5.0(300/T)^{1/2} + 0.5 \quad . \qquad \text{(D-6)}$$

In the above equations, T is the absolute temperature, P is the pressure and L is the mean beam length given by

$$L_e = 0.9(4V/A) \qquad \text{(D-7)}$$

where V is the gas volume and A the surface area to which it radiates. a_o and a_1 are given in Reference 4.

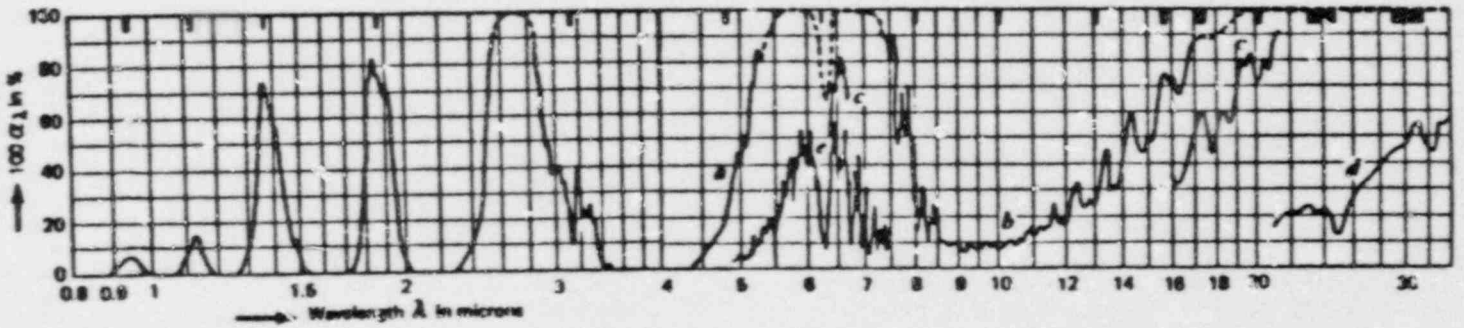

Figure D.4.4. Absorption Coefficient of Steam Versus Wavelength

In calculating the absorptivity of steam for thermal radiation originating from a surface at some temperature not equal to the temperature of the steam, some modification to (D-4) is necessary.[4] For this case,

$$\bar{\alpha}_{st} = \bar{\epsilon}^{*}_{st} \left(\frac{T_{st}}{T_{surf}} \right)^{0.45} \qquad \text{(D-8)}$$

where $\bar{\epsilon}^{*}_{st}$ is obtained from (D-4) using T_{surf} in place of T_{st} and using $P_{st}L_e T_{surf}/T_{st}$ in place of $P_{st}L_e$. The average transmissivity of the steam is then, by Kirchhoff's Law:

$$\bar{\tau}_{st} = 1 - \bar{\alpha}_{st} \qquad \text{(D-9)}$$

D.4.3 Viewfactor Calculations

It can be seen from (D-2) and (D-3) that accurate estimation of the viewfactor from the foil to the equipment (F_{f-eq}) is necessary to determine the amount of radiative foil energy absorbed by the equipment. For the SCETCh tests, a flux gauge was positioned near the equipment being tested. This gauge was used to determine experimentally the flux to the equipment. Thus the viewfactor from the foils to the flux gauge also needed to be determined. Both viewfactors were calculated using a simple computer program to perform the necessary integrations.

The viewfactor from the flux gauge to the foils was calculated treating the sensitive portion of the flux gauge surface as a differential area element (due to its small size). The foil surfaces were divided into a number of small elements. An integration over the entire foil surface was performed according to the equation:

$$F_{dl-2} = \int_{A_2} \frac{\cos\theta_1 \cos\theta_2}{\pi S^2} \, dA_2 \qquad \text{(D-10)}$$

where S is the line joining the flux gauge and the foil surface, and θ_1 and θ_2 are the angles the outward normal make with S.[4] The gaps between foils, the portion of the foils hidden by termination blocks, and the 150° viewing angle of the flux gauge were all accounted for. The resulting viewfactors from the flux gauge to the foils for

the particular foil orientation selected were 0.85 and 0.80 for the cable and transmitter tests, respectively.

It should be noted that the integral in (D-10) is actually a double integral since the integration is over a surface area. The integration was performed numerically using a Gauss quadrature routine accurate to the fourth decimal place.

The foils were oriented to maximize the viewfactor to the equipment (Figure D.4.5). In calculating the average viewfactor from the foils to the cable or transmitter, another integration is needed over the equipment surface. The resulting equation is:

$$F_{f\text{-}eq} = \frac{1}{A_f} \int_{A_f} \int_{A_{eq}} \frac{\cos\theta_1 \cos\theta_2}{\pi S^2} \, dA_{eq} dA_f \quad . \qquad \text{(D-11)}$$

The local viewfactor varies with location along the equipment surface. Thus, there are local areas of higher and lower incident flux. For example, along the cable length the viewfactor varies as shown in Figure D.4.6. The benefit of using a 19-inch length of cable and foil is seen in the relatively flat viewfactor behavior along the middle two thirds of the cable. The viewfactor from the transmitter to the foils is shown in Figure D.4.7.

D.4.4 Chamber Convection

All convection inside the test chamber was assumed to be natural convection since there were no fans or vents present. Correlations from the literature were selected.[5]

It should be noted that the radiative process itself may actually give rise to convective currents. Because the radiant intensity of a beam passing through the steam is a function of position (owing to steam absorption, scattering, and steam emission), the energy deposited in the steam is also a function of position. Thus, thermal radiation can result in virtually instantaneous temperature differences within the steam and thereby produce convective currents. This effect is not believed to be large enough to significantly affect anything.

Because the convective heat fluxes are very small relative to the radiative fluxes in the test chamber, their modeling is not a critical element of this analysis and was selected to be as simple as possible. Although the convective heat fluxes to equipment in a typical containment hydrogen deflagration may be 30 to 40 percent of the total heat flux,

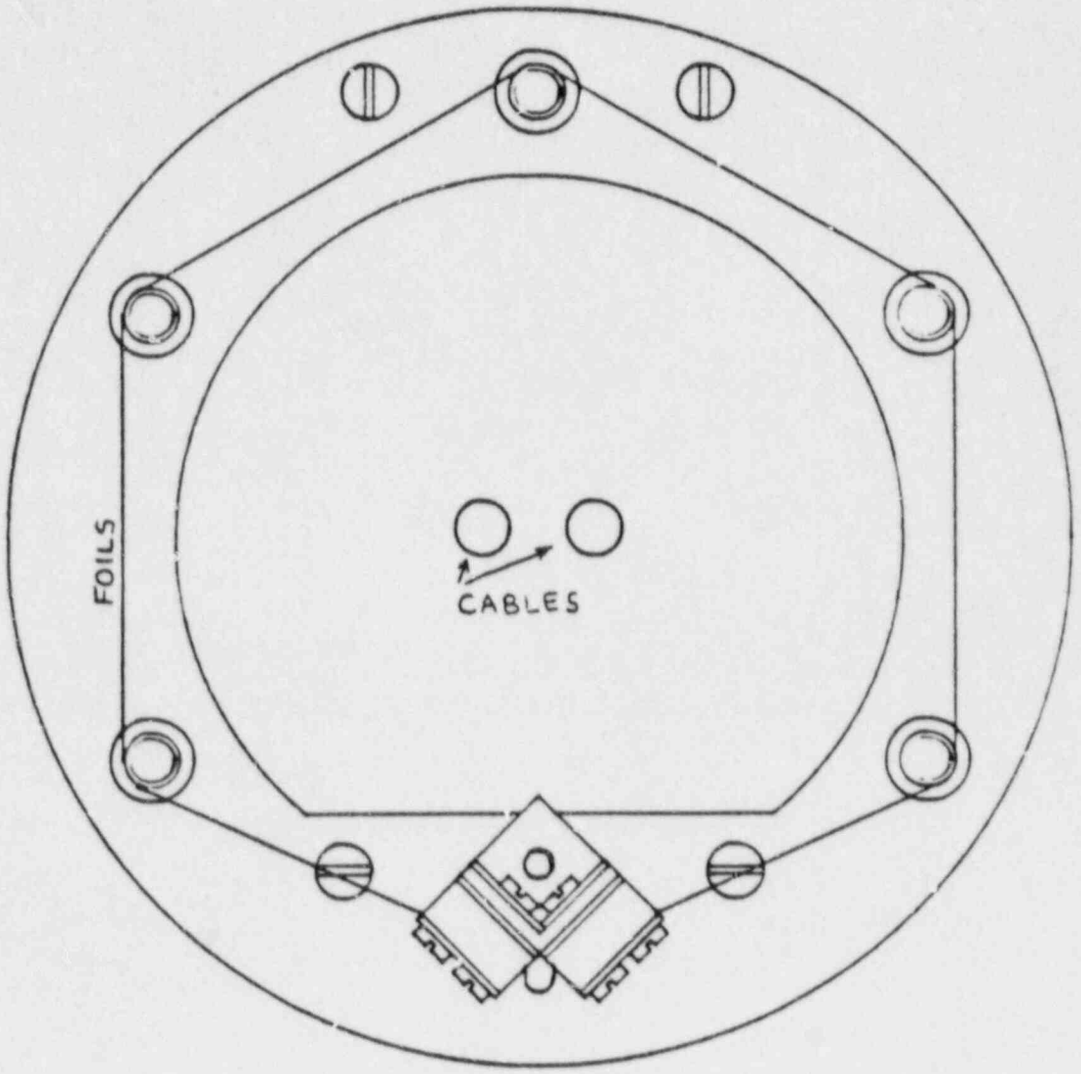

Figure D.4.5. Cable Test Foil Arrangement (End View)

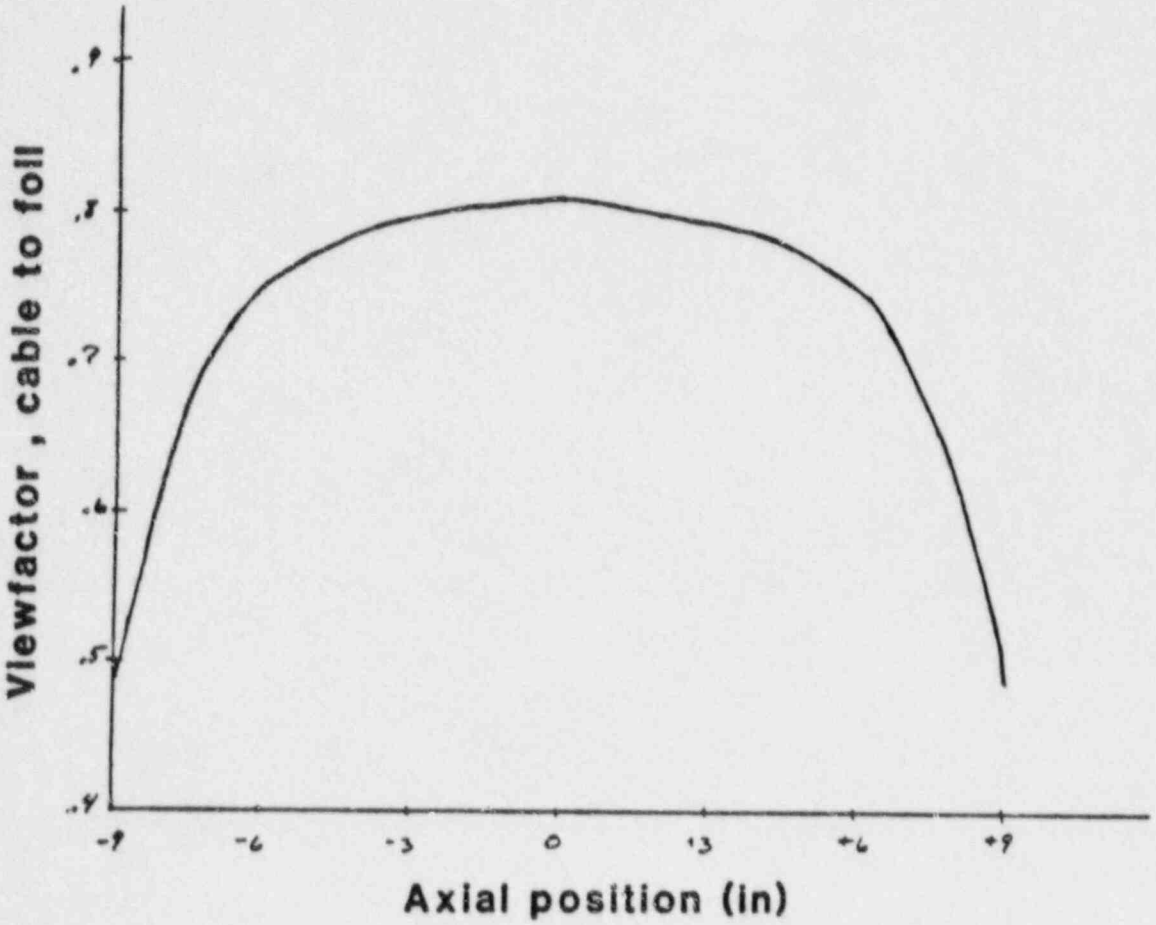

Figure D.4.6. Circumferentially Averaged Cable Viewfactor Versus Length

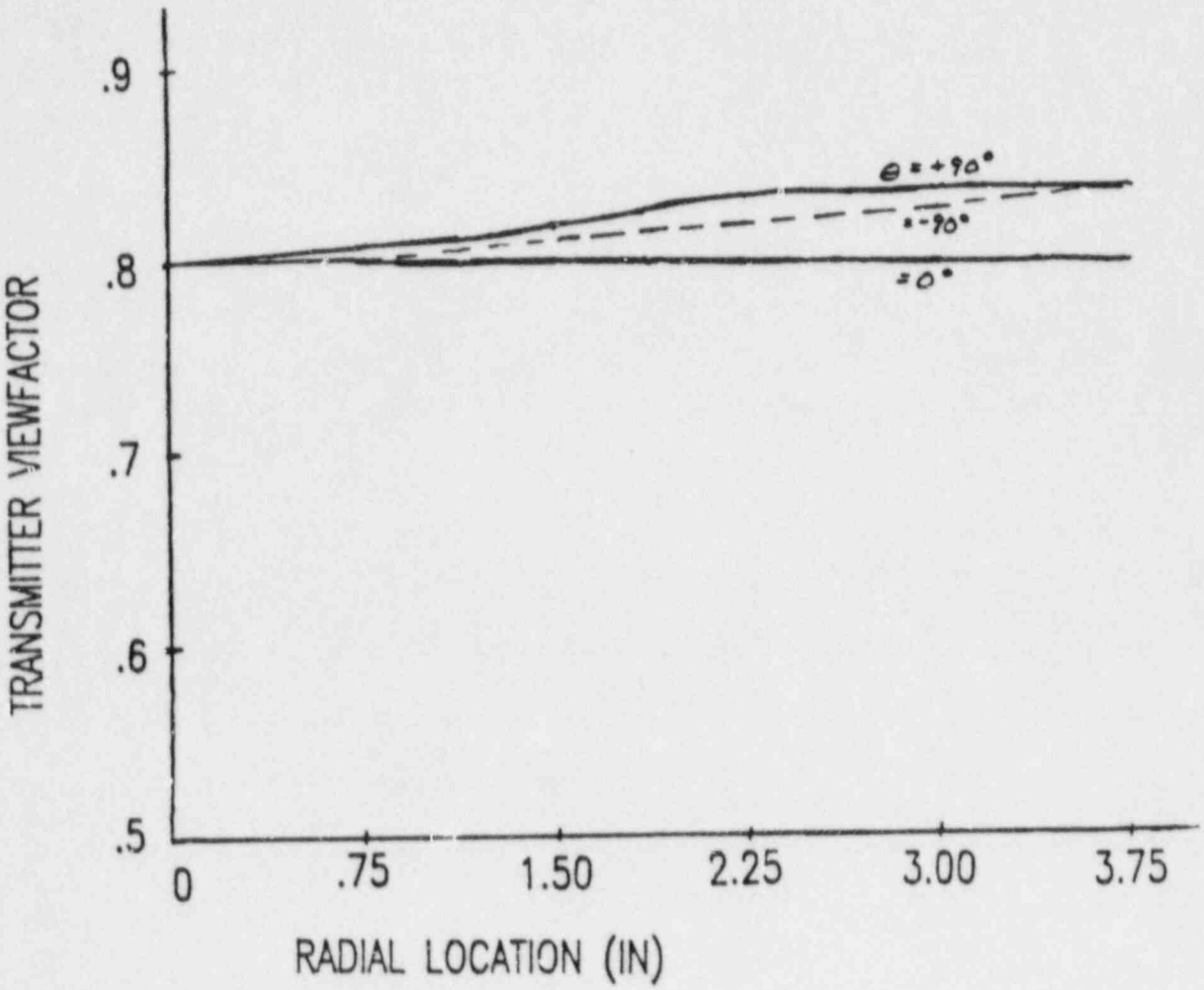

Figure D.4.7. Barton Transmitter Viewfactor Versus θ and Radius

the SCETCh chamber relies only on the radiative power of the foils to deliver the same combined heat flux which the equipment in a typical containment might see.

D.4.5 Condensation

It was also necessary to examine whether or not condensation phenomena would be correctly modeled, since the condensate may eventually be forced through seals or cracks and cause failure. Assuming that the equipment thermal response would be properly modeled (due to correct modeling of the heat flux), correct condensation modeling really entails duplicating the actual containment steam pressure versus time. When the equipment surface temperature falls below the saturation temperature corresponding to P_{st}, condensation occurs on the equipment.

As in the case of convection heat transfer, condensation heat transfer is quite small relative to the radiative flux. It can, however, greatly enhance the absorptivity of a surface since α of water is roughly 0.9. For the equipment tested, $0.80 < \alpha_{eq} < 0.95$. Thus, the condensate does not have a large effect on surface absorptivity in these tests.

It was one of the goals of the analysis to predict whether or not condensation occurred and if so, what effect it had on the foil temperatures and powers. Although HECTR gave condensation predictions for the Barton transmitter, these predictions were not valid for a piece of cable because of the different thermal response of the surface. Finite element models of the transmitter and the cable were constructed (for example, Figure D.4.8). The known HECTR fluxes and thermal environment were input to the two-dimensional finite element code COYOTE.[6] The equipment surface temperature versus time was calculated along with whether or not condensation would occur in the HECTR generated containment environment. This enabled a more accurate prediction of whether or not condensation was actually occurring. The results indicated that condensation would not occur on the cable during the pulse but would occur on the transmitter because of its slower surface thermal response. This necessitated the proper modeling of steam pressure versus time in the test chamber.

D.4.6 Governing Equations

Examples of the analysis involved in deriving the appropriate conservation equations for this problem will now be presented. The goal was to determine what foil temperatures and powers would be necessary to produce the HECTR predicted fluxes inside the SCETCh chamber. Using this information, a foil material and surface area could be selected.

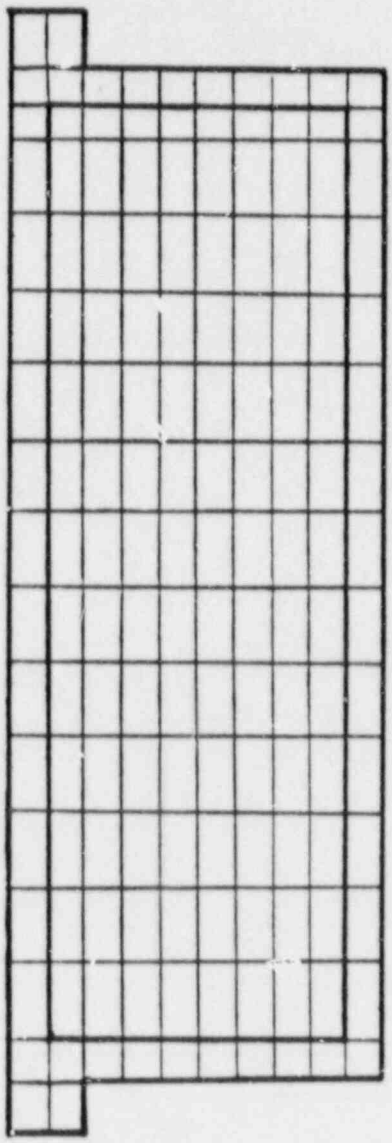

Figure D.4.8. Finite Element Model of Barton Pressure Transmitter

A typical foil and cable arrangement is shown in Figure D.4.5. The three important surfaces are: the foils (subscript 'f'), the equipment (subscript 'eq'), and the chamber wall (subscript 'cw'). The steam and air mixture (subscript 'st') is lumped together and treated as having a uniform temperature, concentration, and pressure which are functions of time.

Energy leaves the foils from both sides. Concentrating first on the energy leaving the outside foil surface in the direction of the chamber walls, some of the energy will be absorbed by the steam and the remainder will reach the chamber wall. Thus the energy leaving the outside of the foils can be written as:

$$Q_f = \epsilon_f \sigma T_f^4 A_f \qquad \text{(D-12)}$$

where A_f is the outside surface area of the foils. This can also be written in terms of the steam absorptivity, α_{st}, as

$$Q_f = F_{f-cw}[\alpha_{st} Q_f + (1 - \alpha_{st}) Q_f] \quad . \qquad \text{(D-13)}$$

where F_{f-cw} equals 1.

The first term in (D-13) is the fraction of foil energy (from the outside surface of the foils) absorbed by the steam, while the second term is the fraction reaching the chamber wall. Of the energy which reaches the chamber wall, only a portion will be absorbed due to the nonblack surface behavior. Thus, the second term in (D-13) could be written:

$$F_{f-cw}(1-\alpha_{st})Q_f = F_{f-cw}\alpha_{cw}(1-\alpha_{st})Q_f + F_{f-cw}(1-\alpha_{cw})(1-\alpha_{st})Q_f \qquad \text{(D-14)}$$

where the first term on the right-hand side (RHS) is the rate of energy absorption by the chamber wall. Some of what is reflected away is absorbed by the steam, some is absorbed by the foils, and some again reaches the chamber walls and continues the cycle. Fortunately the chamber walls absorptivity (~0.8) and the steam absorptivity (0.2 to 0.5) are large enough that consideration of more than one reflection is not worthwhile.

The second term on the RHS of (D-14) represents the reflected energy, which can be further expressed as.

$$F_{f-cw}(1-\alpha_{cw})(1-\alpha_{st})Q_f = \alpha_{st}F_{f-cw}(1-\alpha_{cw})(1-\alpha_{st})Q_f + \alpha_f F_{cw-f}F_{f-cw}(1-\alpha_{cw})(1-\alpha_{st})^2 Q_f + \alpha_{cw}F_{cw-cw}F_{f-cw}(1-\alpha_{cw})(1-\alpha_{st})^2 Q_f \quad \text{(D-15)}$$

where only one reflection has been considered. Therefore, of the energy leaving the outside foil surface, some of it reaches the chamber walls:

$$Q_{f-cw} = \alpha_{cw}F_{f-cw}(1-\alpha_{st})Q_f + \alpha_{cw}F_{cw-cw}F_{f-cw}(1-\alpha_{cw})(1-\alpha_{st})^2 Q_f \quad \text{(D-16)}$$

Some of it returns to the foils:

$$Q_{f-f} = \alpha_f F_{cw-f}F_{f-cw}(1-ast)^2(1-\alpha_{cw})Q_f \quad . \quad \text{(D-17)}$$

The remainder is absorbed by the steam:

$$Q_{f-st} = \alpha_{st}Q_f + \alpha_{st}F_{f-cw}(1-\alpha_{st})(1-\alpha_{cw})Q_f \quad . \quad \text{(D-18)}$$

If the chamber walls and foils were very reflective and steam were not a good attenuator of thermal radiation, many reflections would occur and (D-16) could be written more generally as:

$$Q_{f-cw} = \alpha_{cw}F_{f-cw}Q_f \sum_{n=1}^{\infty} (1-\alpha_{cw})^{n-1}(1-\alpha_{st})^{n}F_{cwcw}^{n-1} \quad . \quad \text{(D-19)}$$

The equations were initially formulated in these generalized forms to examine the effects of covering the chamber interior with a highly reflective coating (such as specular aluminum) to increase the steam absorption and reduce losses to the walls. It was found that the chamber surface emissivity was not a very important parameter because:

1. The foils behave as a blackbody and absorb all incident radiation,

2. The steam has a significant absorptivity (0.2 to 0.4) and reduces the importance of multiple reflections, and

3. The chamber walls respond so slowly that condensation occurs on them. This changes the wall emissivity to that of water (~0.9).

Thus, nothing was done to modify the chamber interior surface.

Note that the equations written in this form are not net energy transfers. They deal only with energy originating at a particular surface or in the steam. When written for every surface and the steam, the set of equations represent a statement of energy conservation. This particular form of the equation was selected because the dependence of the steam absorptivity on the surface temperature from which the radiation originates can be easily taken into account. Additionally, no integration over wavelength is required (assuming wavelength integrated properties are known beforehand).

Equations such as (D-19) were formulated for energy originating at every surface and also in the steam. The net rate of energy transfer to the surface is then the sum of all the energy arriving at the surface minus that which is leaving. For example, for the foils, the total radiant energy leaving, $Q_{f,out}$ is:

$$Q_{f,out} = 2\xi_f \sigma T_f^4 A_f \qquad \text{(D-20)}$$

where the factor of 2 is needed because A_f is the area of only one side of the foils. The total incoming radiant energy, $Q_{f,in}$, can be found by summing the contributions from all the surfaces and the steam. The rather lengthy result is:

$$Q_{f,in} = \alpha_f(1-\alpha_{eq})(1-\alpha_{st})^2 F_{f-eq} Q_f + \alpha_f(1-\alpha_{st}) F_{f-f} Q_f$$

$$+ \alpha_f Q_f F_{f-gap}(1-\alpha_{st}) F_{cw-f} \sum_{n=1}^{\infty} (1-\alpha_{st})^{n+1}(1-\alpha_{cw})^n F_{cw-cw}^{n-1}$$

$$+ \alpha_f Q_f F_{cw-f} F_{f-cw} \sum_{n=1}^{\infty} (1-\alpha_{st})^{n+1}(1-\alpha_{cw})^n F_{cw-cw}^{n-1}$$

$$+ \alpha_f(1-\alpha_{st})Q_{eq}$$

$$+ \alpha_f F_{cw-f} Q_{cw} \sum_{n=1}^{\infty} (1-\alpha_{st})^n (1-\alpha_{cw})^{n-1} F_{cw-cw}^{n-1}$$

$$+ \alpha_f(1-\alpha_{st})(1-\alpha_{st})F_{gap-f}F_{cw-gap}Q_{cw}$$

$$+ \alpha_f q_{st,i} A_f + \alpha_f(1-\alpha_{eq})(1-\alpha_{st})q_{st,i}A_{eq}$$

$$+ \alpha_f q_{st,o} A_f \left[1 + F_{cw-f} \sum_{n=1}^{\infty} (1-\alpha_{cw})^n (1-\alpha_{st})^n F_{cw-cw}^{n-1}\right] . \quad (D-21)$$

$q_{st,i}$ and $q_{st,o}$ are thermal radiation fluxes emitted by the steam as a result of its temperature on the inside and outside, respectively, of the foils.

Equation (D-21) can be understood as follows. The first line models radiation originating on the inner foil surface which returns to the foils via reflection from the equipment (the first term), or via direct communication, foil to foil (the second term). The second line handles radiation from the inner foil surface which passes through gaps in the foils (including any open ends or regions), is reflected from the chamber wall, and returns to the foils. The third line covers radiation emitted from the outer foil surface which returns via reflection from the chamber wall. The fourth line deals with radiation emitted by the equipment to the foils, the fifth and sixth with chamber wall radiation to the foils, and the last two lines with steam emission to the foils.

It should once again be noted that the steam absorptivities (α_{st}) are dependent upon the temperature from which the radiation originates (as well as steam pressure and temperature, total pressure, and pathlength). Hence the α_{st}'s in (D-21) are not identical (see Section D.4.2). Since the steam and foils can have significantly different temperatures in this particular problem, this dependence cannot be overlooked.

The net rate of energy transfer to the foils is then given by:

$$Q_{f,net} = Q_{f,in} - Q_{f,out} . \quad (D-22)$$

Equations similar to (D-20) through (D-22) were formulated for each surface and the air and steam mixture. If the chamber wall and air-steam mixture are treated in lumped fashions, the thermal response is predicted as follows:

$$M_{cw}C_{p,cw}\frac{dT_{cw}}{dt} = Q_{cw,net} + Q_{convection} \qquad \text{(D-23)}$$

$$M_{st}C_{p,st}\frac{dT_{st}}{dt} = Q_{st,net} + Q_{convection} \qquad \text{(D-24)}$$

where M_{st}, $C_{p,st}$, and T_{st} are the mass, specific heat, and temperature of the air-steam mixture. $Q_{convection}$ is added in as it is not accounted for in the radiation balance. These equations can be used to estimate T_{cw} and T_{st} as functions of time. Recall that the equipment temperature versus time was predicted beforehand using a finite element code (Section D.4.5).

The remaining task is to estimate the foil temperature and power versus time. The foil temperature is determined by the required incident flux to the equipment (from HECTR calculations), $q_{incident}$:

$$T_f = \left\{ \frac{q_{incident}A_{eq} - \alpha_{eq}A_{eq}\epsilon_{st}\sigma T_{st}^4 \pm Q_{convection}}{F_{f-eq}A_f(1-\alpha_{st})\sigma} \right\}^{1/4} \qquad \text{(D-25)}$$

Noting from reciprocity that

$$F_{f-eq}A_f = F_{eq-f}A_{eq} \qquad \text{(D-26)}$$

(D-25) can be reduced somewhat if desired.

To estimate the foil power requirements, P_f,

$$P_f = -(Q_{f,net} + Q_{convection}) \quad . \qquad \text{(D-27)}$$

In the actual solution procedure the foil temperature is estimated first using (D-25). The energy balances are then used to calculate the thermal response of the chamber walls and the air-steam mixture. Finally, the foil power requirements are estimated using (D-27).

D.4.7 FOILTEMP Code and Analysis Results

While some preliminary results have been presented (such as transmitter to foil viewfactor), the main goal of the analysis was to examine the feasibility of producing the desired environment inside the SCETCh chamber. Reaching this goal necessitated assimilation of all the preceding considerations into a computer code (FOILTEMP). Some of the important results follow.

The incident thermal radiation on the equipment originates from the foil and steam emission. Figure D.4.9 indicates the relative contribution of each during the pulse. Since the foil temperatures are considerably higher than the chamber steam temperatures (except at very early times), the majority of incident thermal radiation comes from the foils. Because the foils get very hot (~1200°C), most of the radiation is at wavelengths less than 8 μm. In fact, Figure D.4.10 shows that roughly 87 percent of the incident thermal radiation is at wavelengths less than 8 μm.

A typical foil temperature versus time curve is shown in Figure D.4.11. Note that the foil temperatures are in general higher than the HECTR predicted containment steam temperature. This is a result of attempting to reproduce the predicted containment radiative plus convective flux with a purely radiative foil flux.

The FOILTEMP code was also used to examine the feasibility of achieving similar pressure and moisture environments. It was also developed such that it could be used for parametric analyses to determine optimum initial conditions. Figure D.4.12 represents one possible pressure versus time curve for the chamber predicted by FOILTEMP. Several combinations of initial steam and initial total pressure were tried in the code to achieve these results. The desired set of initial conditions (preceding the deflagration environment) had to result in:

1. Following the HECTR predicted steam pressure versus time as closely as possible in order to properly reproduce surface condensation effects.

2. Following the HECTR predicted total pressure versus time to properly reproduce failures associated with moisture penetration.

Additionally, the initial conditions (prior to the pulse) had to be near saturation, as this is where the LOCA environment was.

Several iterations were necessary because increasing the initial steam pressure (holding initial air pressure

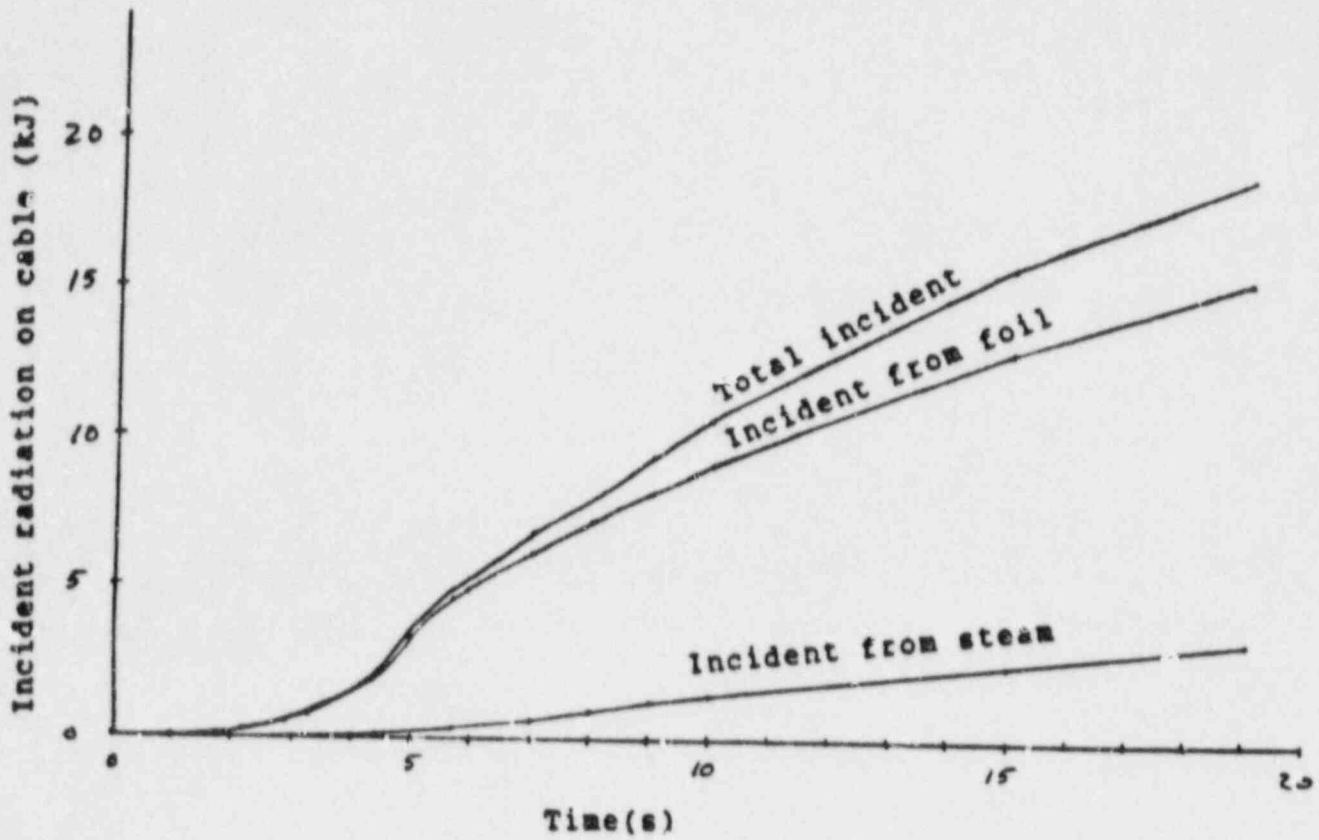

Figure D.4.9. Predicted Incident Radiation From Steam and Foils

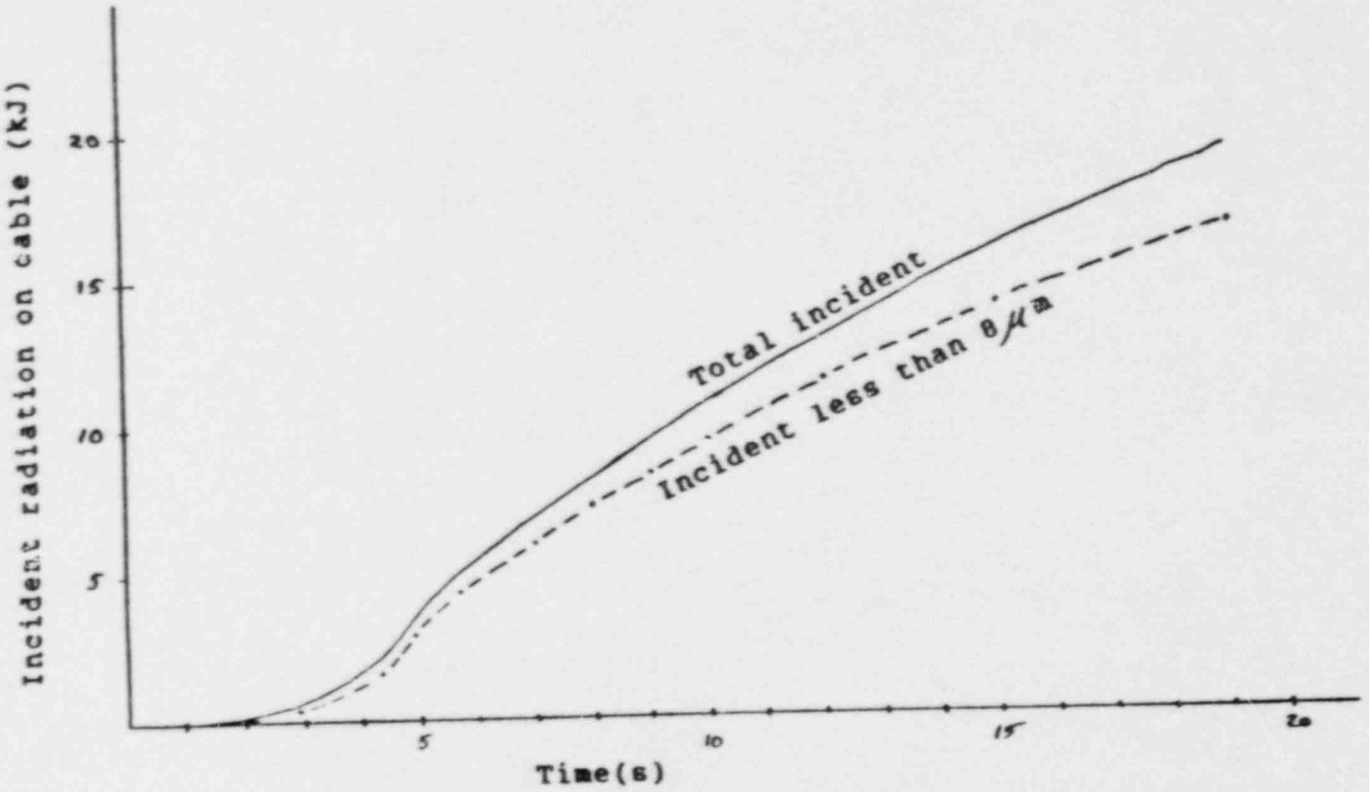

Figure D.4.10. Predicted Incident Radiation Versus Wavelength

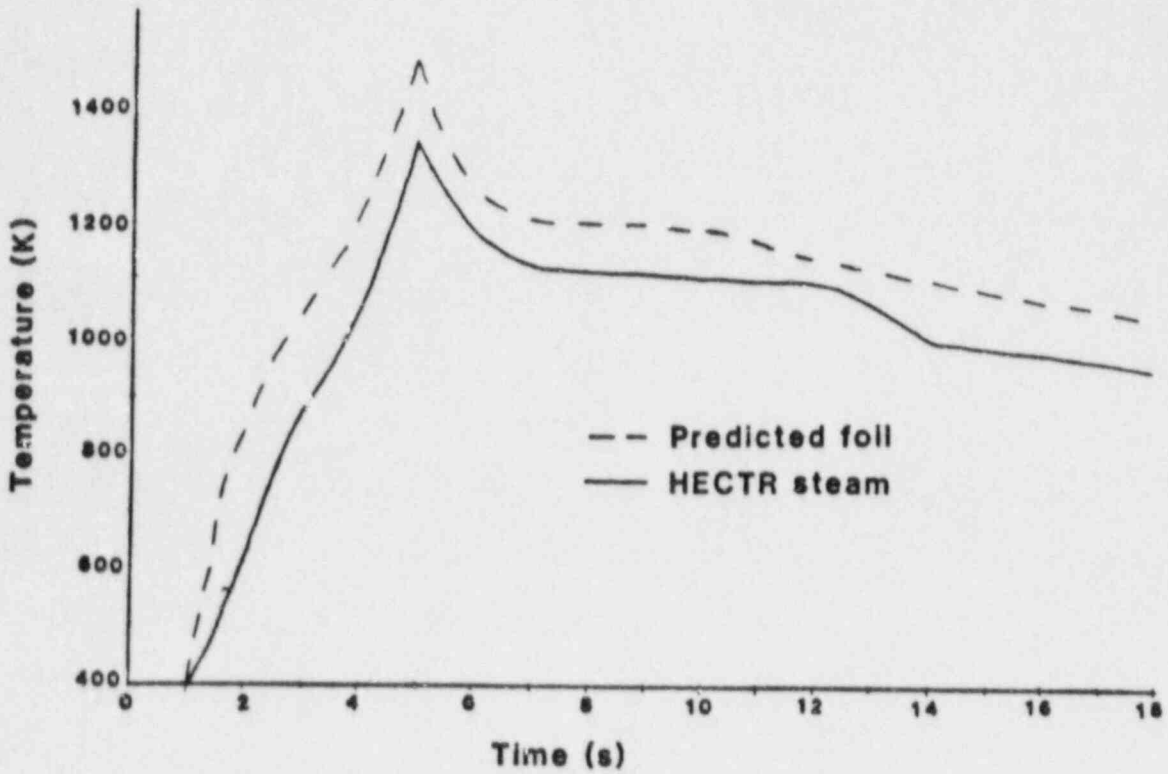

Figure D.4.11. Predicted Foil Temperature Versus Time

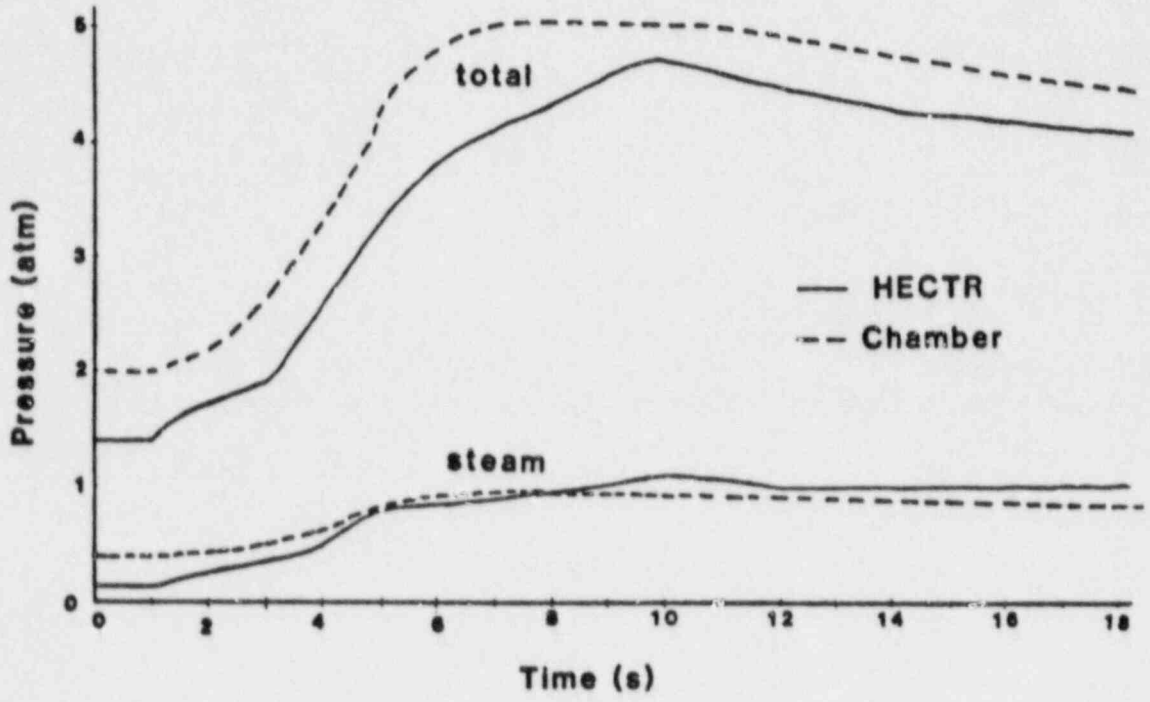

Figure D.4.12. Predicted Steam and Total Pressure Versus Time

constant) had various effects. A higher initial steam pressure meant that there was more steam represent, and thus more mass to heat up. It also resulted in more steam emission and absorption. These two factors affect (oppositely) the steam temperature and thus the pressure. Increasing the initial air pressure had a similar effect, including enhanced emission and absorption by steam due to collision broadening of the spectral bands.

Once the foil temperatures and energy absorption by the surroundings have been calculated, the amount of foil power necessary to keep the foils at the desired temperature is calculated. If the foil temperature and power versus time were not achievable or were not acceptable for control reasons, the foil orientation and/or foil area were changed and the calculations performed again until an acceptable set of curves was obtained.

In summary, the results of the FOILTEMP calculations demonstrated the feasibility of reproducing a typical hydrogen burn deflagration heat flux, pressure, and moisture environment inside the SCETCh chamber. Necessary foil temperatures, powers, areas, and orientations were determined as well as suitable initial conditions. The results were integrated into the foil design, control setup, and test plan.

D.5 SCETCh Results

Using the analytical method discussed above, the HECTR generated accident environments were translated into SCETCh environments. The SCETCh tests included both single and multiple burn simulations. The single burn simulations are discussed in D.5.1 and the multiple burn simulations are discussed in D.5.2.

D.5.1 Single Burn Tests

Cable specimens and two pressure transmitters were exposed in the single burn tests. The results indicate that nuclear qualified safety equipment with similar characteristics and sensitivities can survive a single hydrogen burn inside a large dry containment.

D.5.1.1 Cable Tests

The cable specimens consisted of aged and unaged lengths of Brand Rex three-conductor XLP/CU 12 AWG power and control cable. The specimens were approximately 48 inches long and were looped once such that both ends terminated outside the same end of the test chamber. The aged samples were thermally aged at 136°C for 168 hours.[7] They were radiation aged to a total dose of 200 Mrad at a dose rate of 1 Mrad/hr.

The cable conductors were connected to a three-phase power supply in an arrangement which facilitated the identification of specific conductors which might have shorted to each other or to the cable mount during testing. During the tests, a three-phase 480 V source was placed across the conductors (277 V conductor to tray voltage). Although the cables were subjected to a voltage potential during the tests, they were not electrically loaded (i.e. no current was flowing in the cable).

The test environment simulated the HECTR calculation of an S_2D event in the TMI-hybrid power plant described in Appendix A. A 75 percent metal-water reaction was assumed, with ignition occurring at the highest hydrogen concentration.

The LOCA portion of the experiments was conducted once thermal equilibrium had been reached. The SCETCh LOCA environment maintained a temperature of 358°K, a total pressure of 150 kPa, and a steam partial pressure of about 50 kPa (saturated steam).

The hydrogen burn was assumed to occur 4.4 hours into the LOCA based on the HECTR calculations. At this time the stainless steel foils were energized to provide the heat flux pulse which would simulate the hydrogen deflagration. Following the hydrogen burn simulation, the LOCA was continued for another 2 hours.

A linear ramp up to the peak heat flux was used in the cable tests. This was necessary due to the response time of the foil control algorithm. The actual test heat flux profile is shown in Figure D.5.1 along with the HECTR generated profile. The linear ramp up to the peak results in approximately 30 percent more energy incident on the cable specimens (the difference in areas under the curves in Figure D.5.1). Thus the cable tests are conservative (more severe than the HECTR predicted TMI-hybrid environment).

The test matrix is shown below.

Table D.5-1

SCETCh Cable Test Matrix

Pulse (%)	No. of Tests Aged	Unaged
100	1	1
110	0	3
110+	2	0

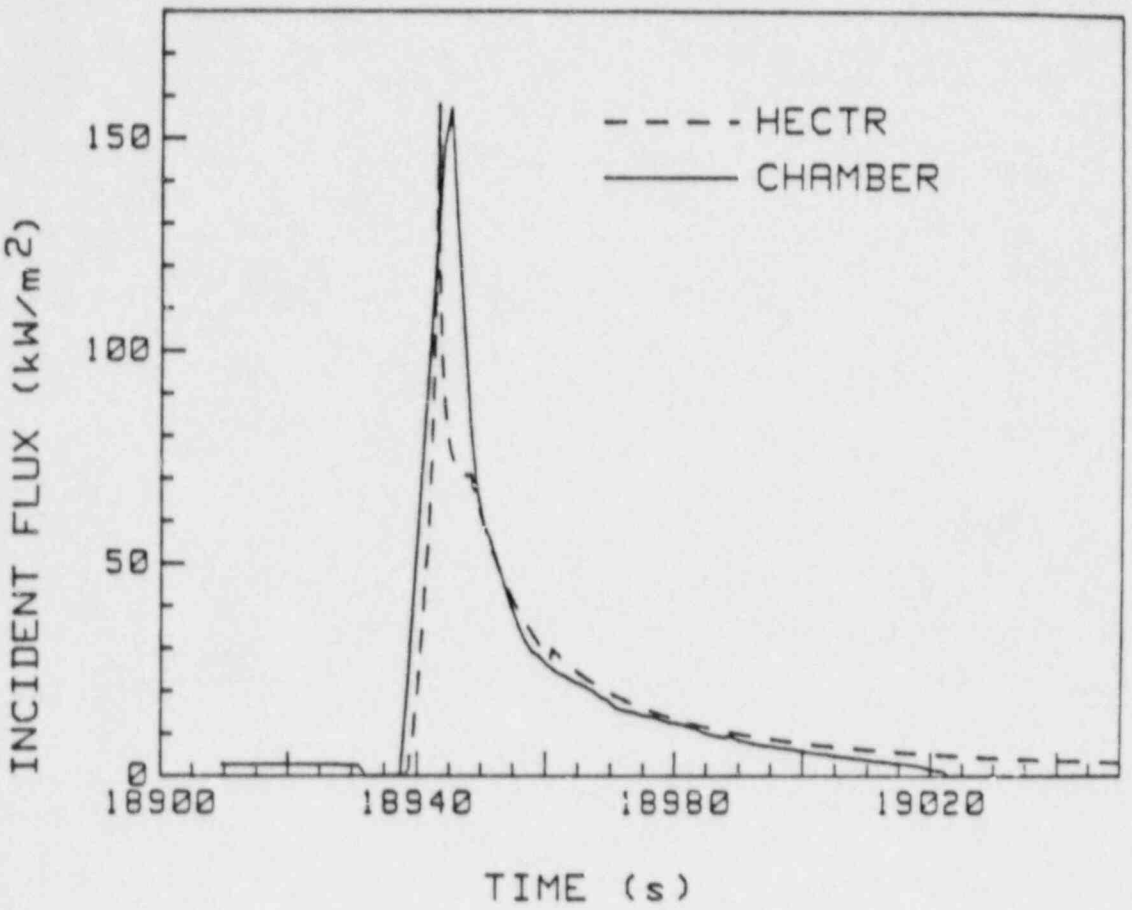

Figure D.5.1. Single Burn Cable 100 Percent Test Heat Flux

The 100 percent tests correspond to the test heat flux profile shown in Figure D.5.1. The 110 percent tests used foil powers which resulted in heat fluxes 10 percent higher than the 100 percent tests. These tests were conducted near the upper limit of foil power. During the two 110 percent tests on aged cables, foils failed after the peak heat flux was attained but prior to the completion of the pulse. The tests were terminated and the foils were replaced. The samples were then subjected to another full LOCA/hydrogen burn test. Thus, the 110+ percent category appears in the test matrix.

Results of the 100 percent tests were given in the main body of this report. The 110 and 110+ percent results are given here. As with the 100 percent tests, all conductors in the 110 and 110+ tests maintained their applied cable to tray voltage.

Flux, pressure, conductor voltage, and posttest photos of one unaged cable subjected to a 110 percent test are given in Figures D.5.2 through D.5.5. Results from other 110 percent unaged cables are similar.

The hydrogen burn simulation resulted in extensive blistering and charring of the unaged cable jacket. There were small surface cracks in the jacket near the wire ties which held the cable to the sample mount. The ties were wrapped tightly around the cable and thus restrained blistering at the tie points. This restraint caused stress concentrations near the ties and resulted in the minor cracking of the jacket. Some melting of the white fibrous filler material occurred in one test but the interior conductors were unaffected. The physical damage was indistinguishable from the 100 percent unaged tests.

Pressure, conductor voltage, and posttest photos for an aged 110+ percent cable test are given in Figures D.5.6 through D.5.8. Results for the other 110+ percent aged cable are similar.

As with the unaged cable, damage to the aged cable was largely confined to the cable jacket. Figure D.5.8 shows that the nature of the damage to the aged cable was different from that of the unaged cable. The jacket charred but no blistering occurred. Deep axial cracks, exposing the cable filler material and interior insulation occurred in all aged samples. The filler material melted but the interior conductors' insulation remained intact.

When the axial cracks in the aged cable reached the tight fitting tie-down wires the cable jacket cracked about its circumference. Damage to the other aged cable was similar but, since it was held on the cable mount with loose fitting

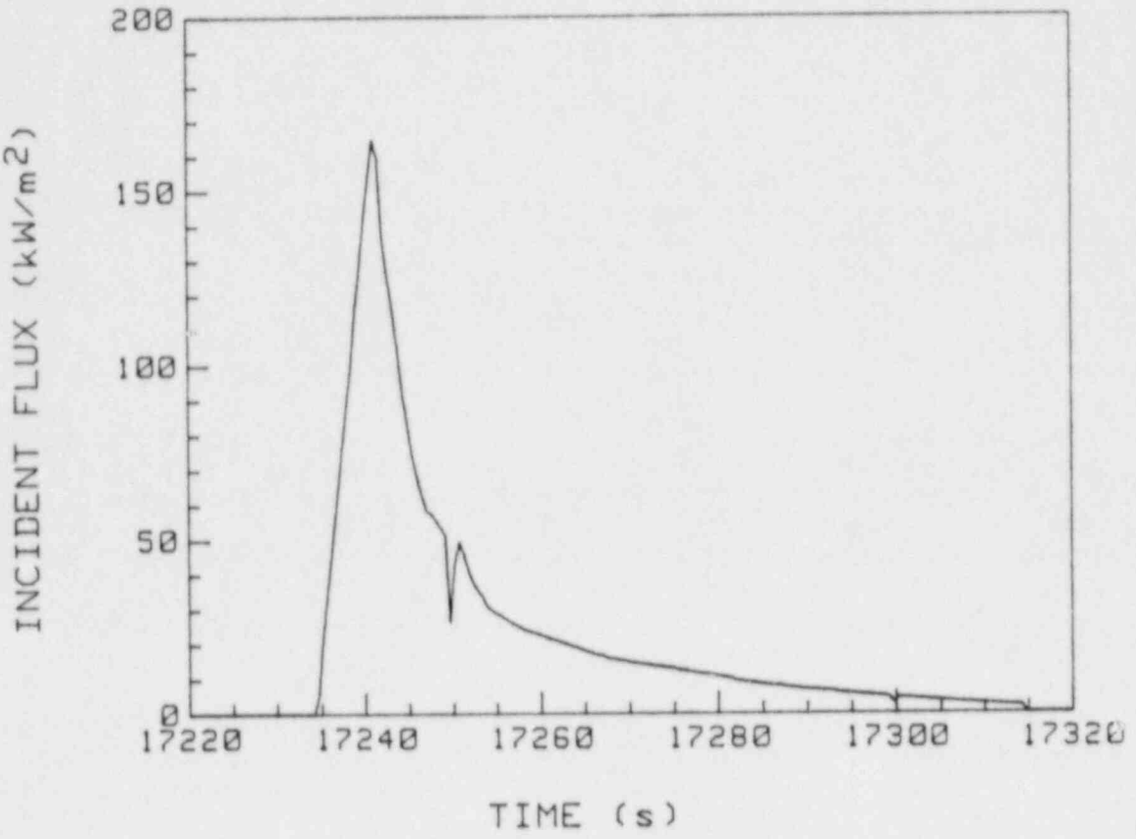

Figure D.5.2. Unaged Cable Heat Flux (110 Percent Test)

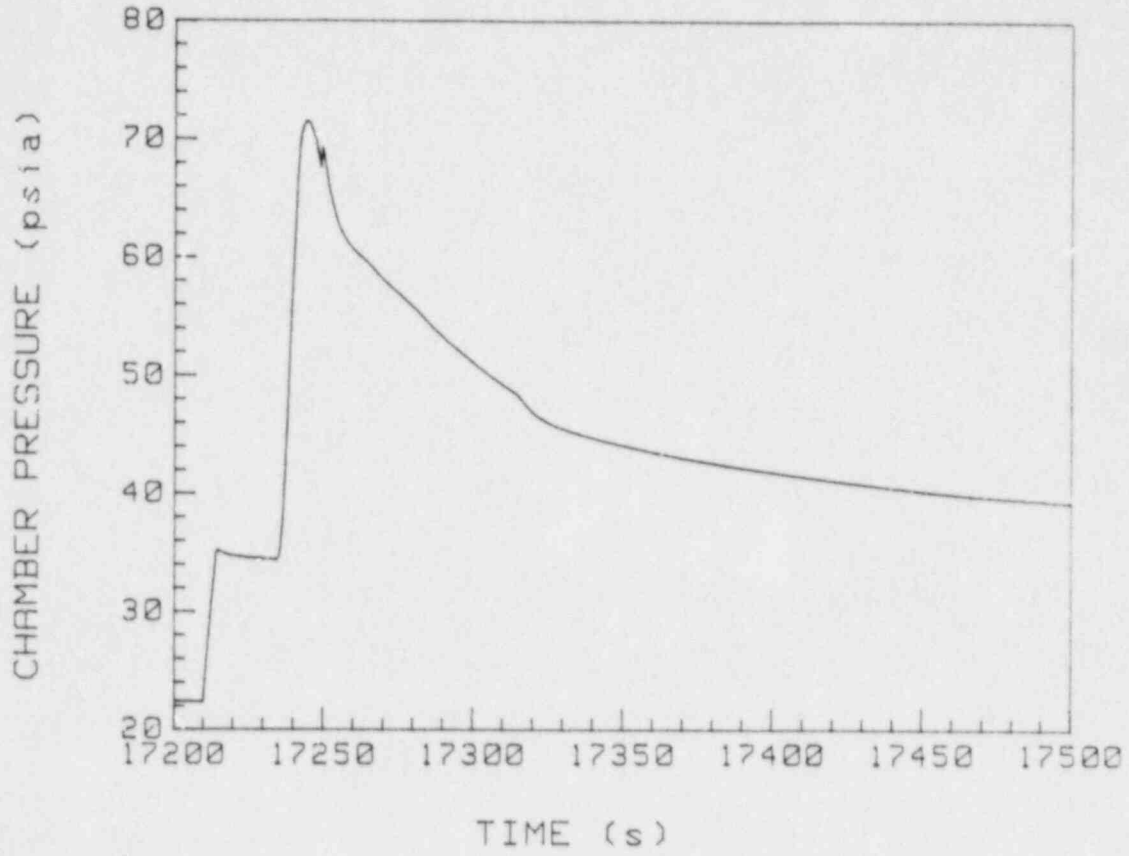

Figure D.5.3. Unaged Cable Chamber Pressure (110 Percent)

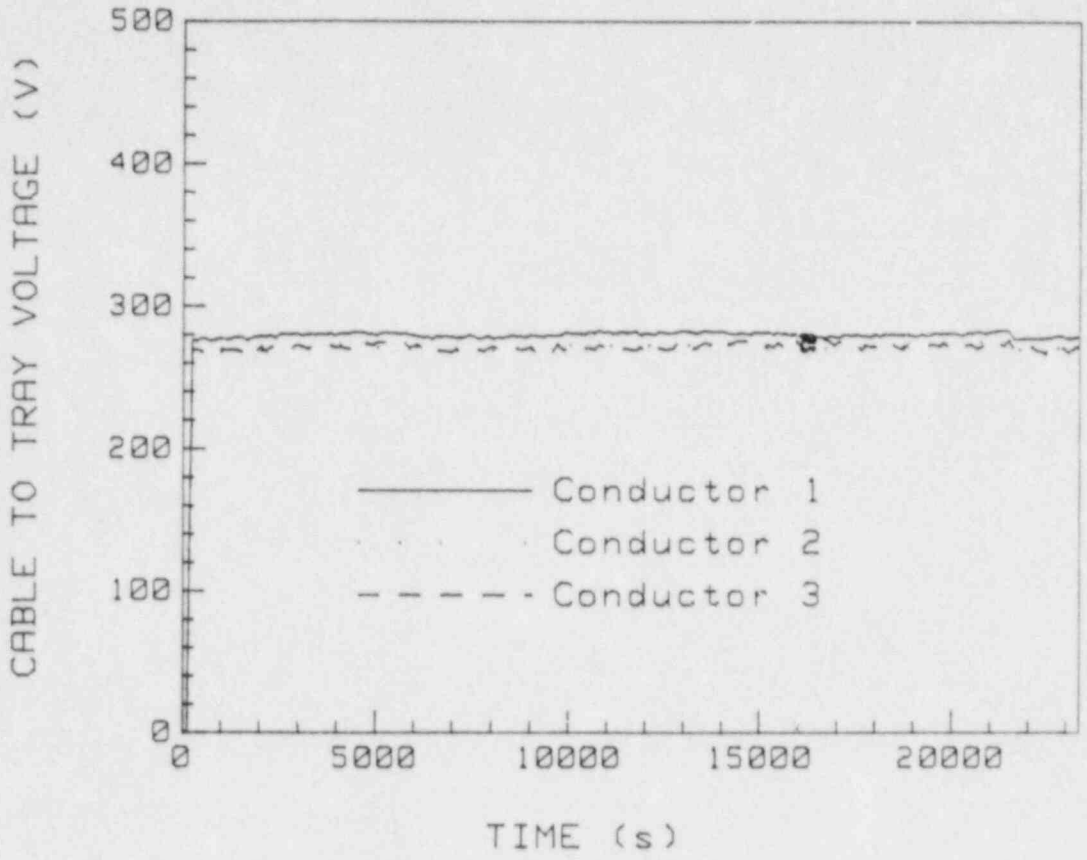

Figure D.5.4. Unaged Cable Conductor Voltages (110 Percent)

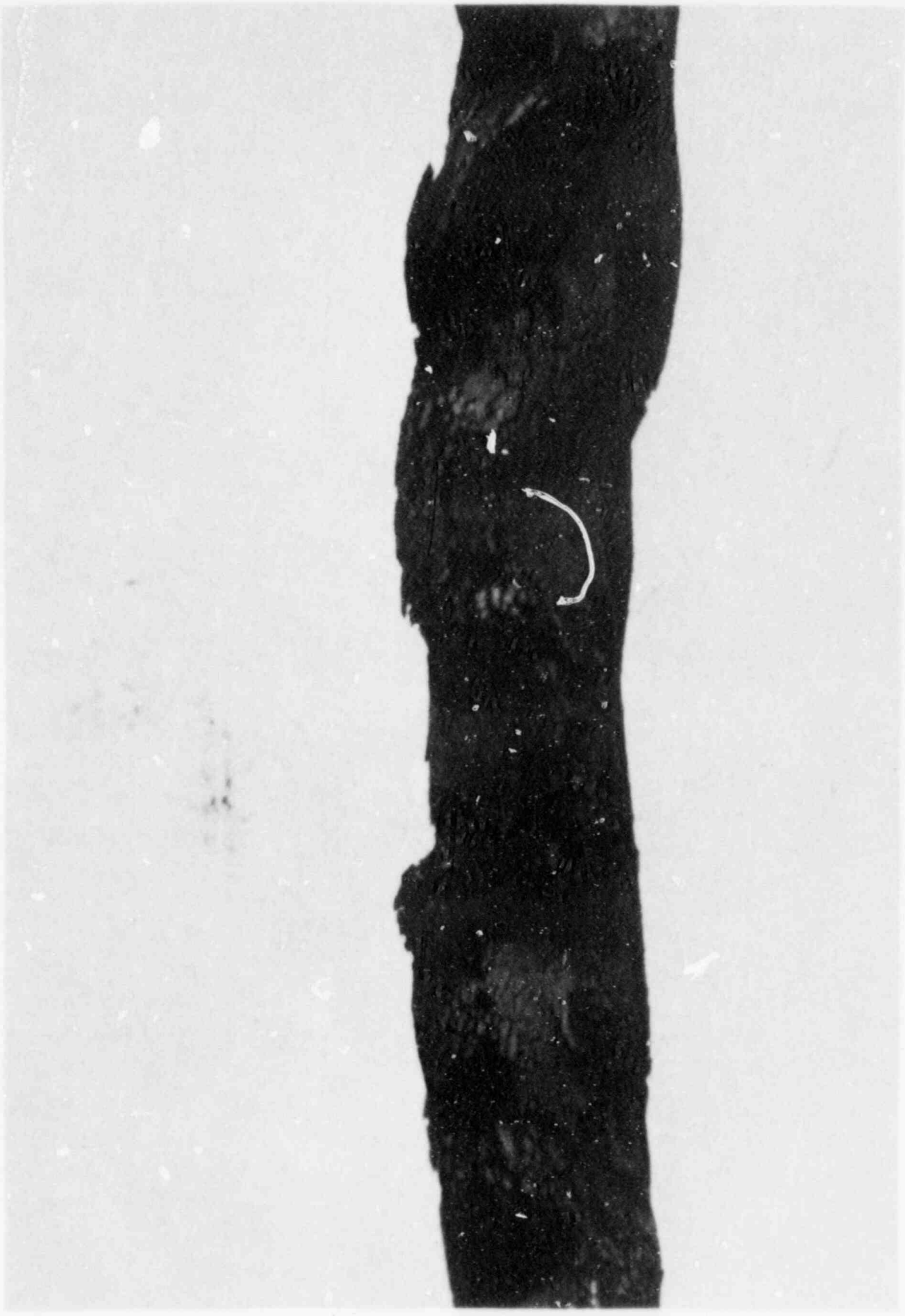

Figure D.5.5. Unaged Cable After Testing (110 Percent)

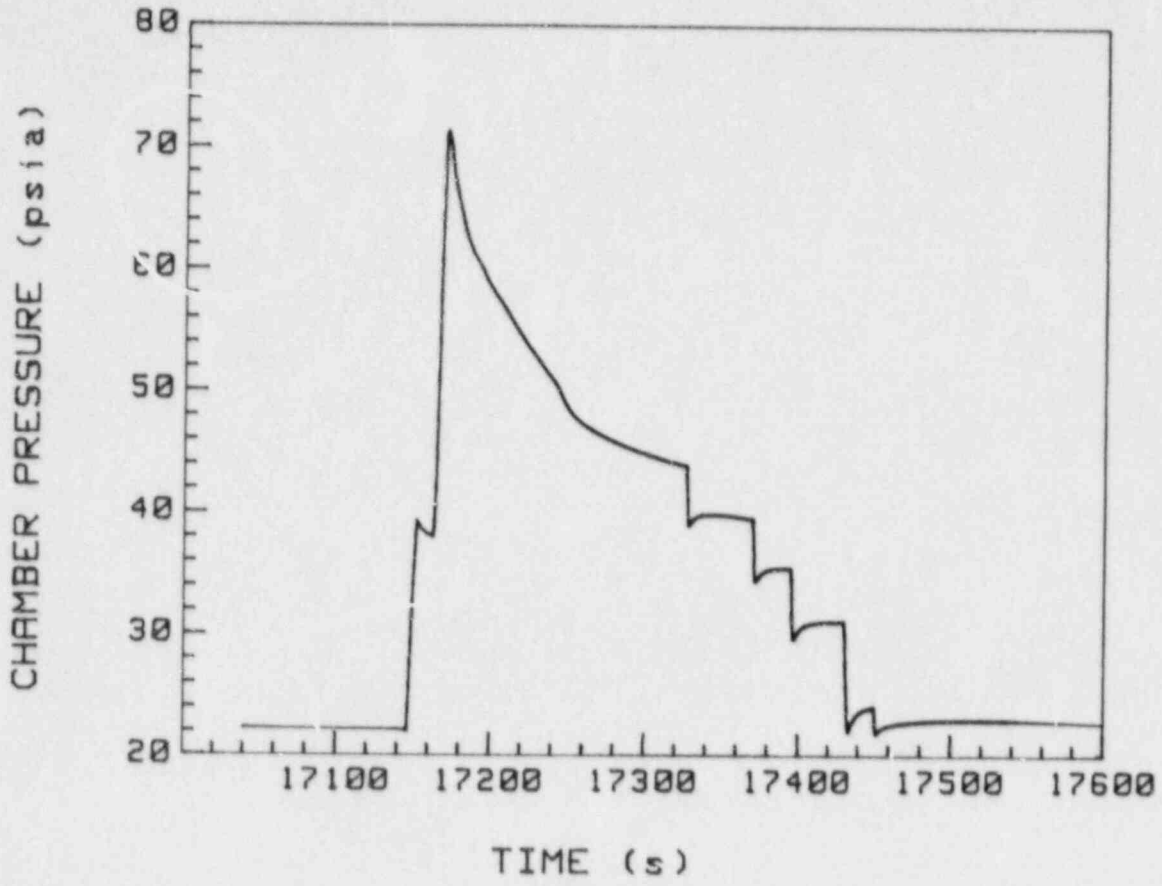

Figure D.5.6. Aged Cable Chamber Pressure (110+ Percent)

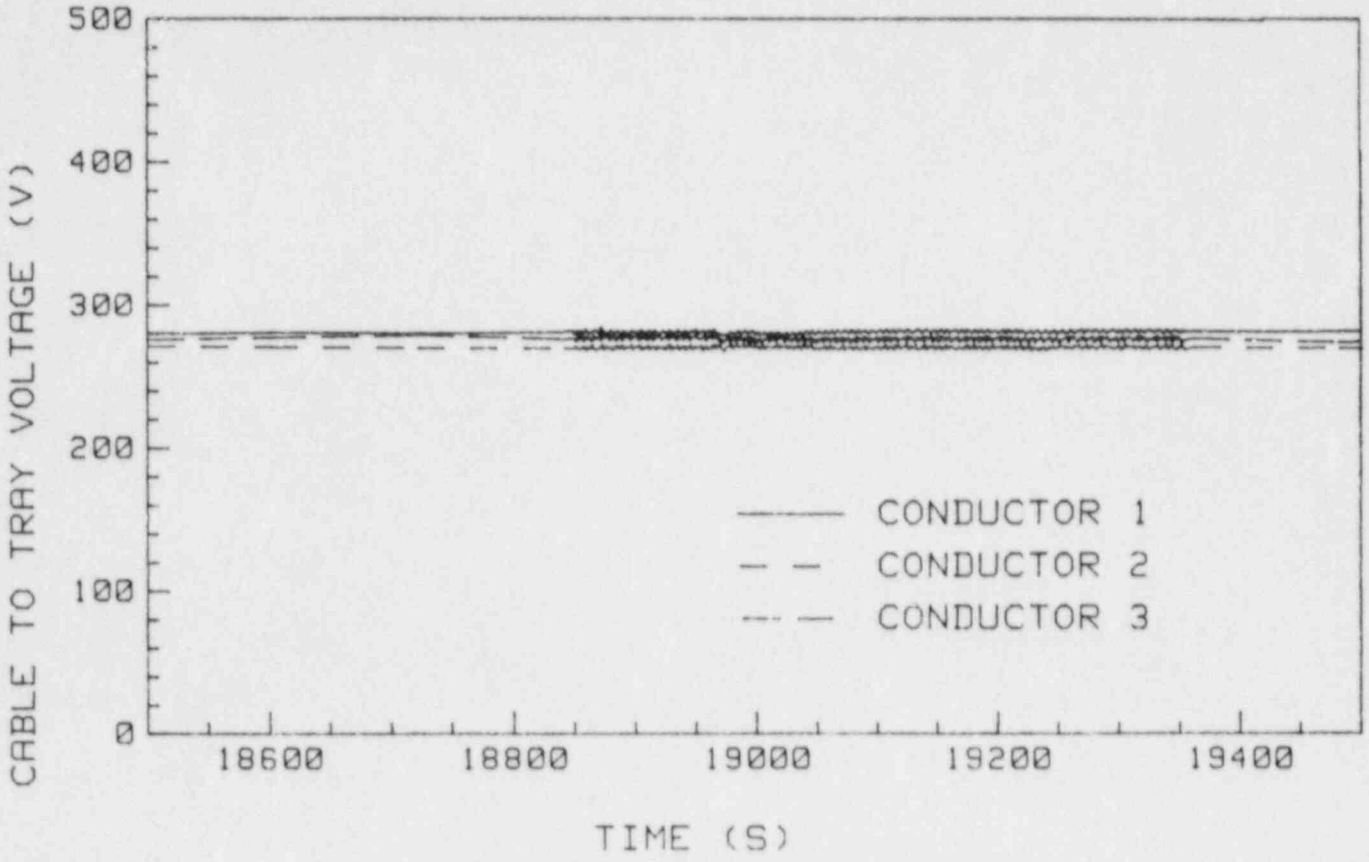

Figure D.5.7. Aged Cable Conductor Voltages (110+ Percent)

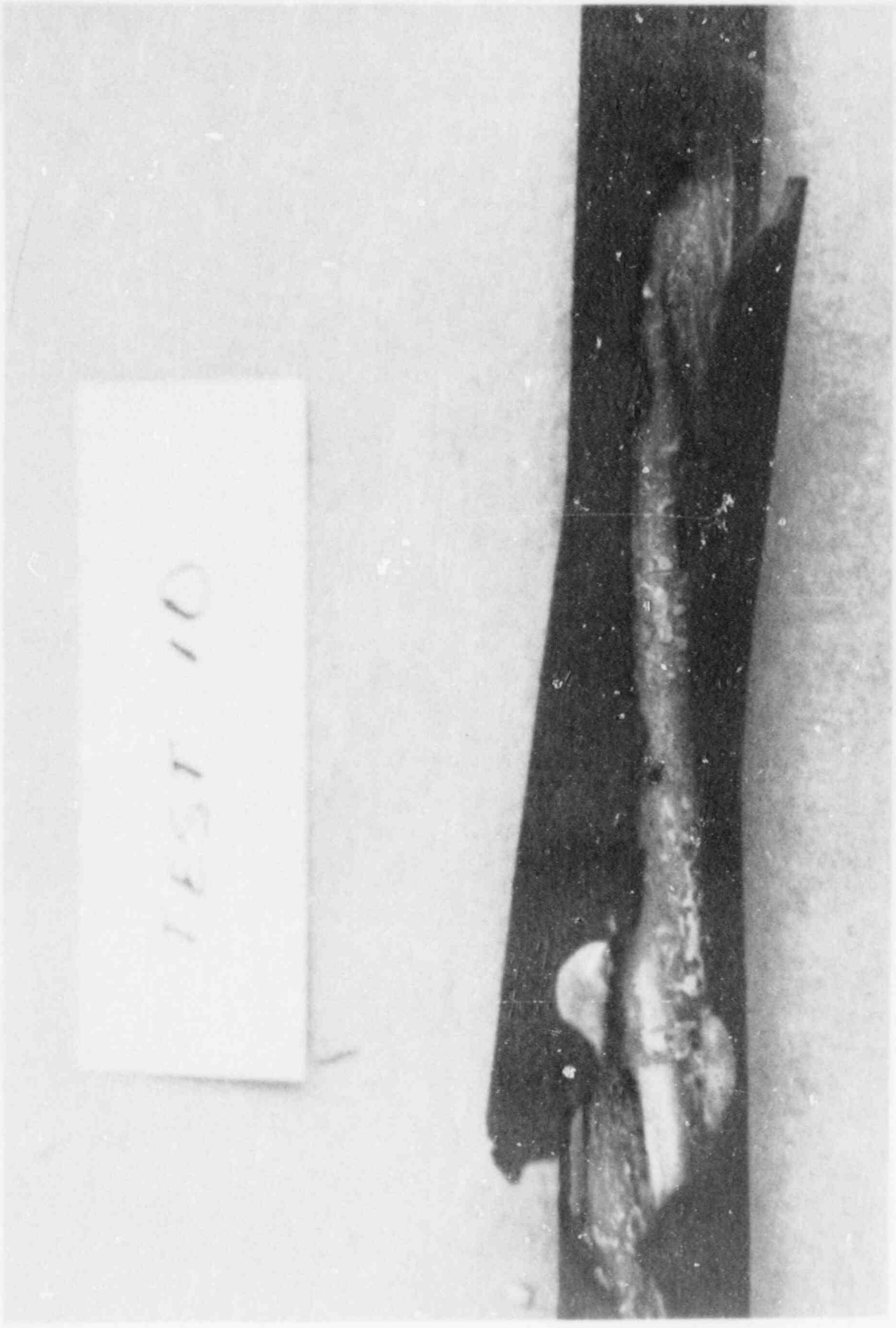

Figure D.5.8. Aged Cable After Testing (110+ Percent)

tie-downs the initiation of the cracking around the periphery of the jacket took a more helical path and the points of origin were more randomly spaced.

There was no discernible difference in the degree of damage between the 100 percent aged cable and the 110+ percent aged cables.

The failure of the foils on the aged 110+ percent tests provided the opportunity to determine when in the testing the cracking occurred. The specimens which had experienced the foil failure were removed from the test chamber with their jackets intact. The foils failed within a few seconds after they reached their peak temperature. Since the 100 percent aged sample experienced the entire pulse and emerged from the chamber with a cracked jacket and melted filler the cracking occurred during the tail of the pulse.

One exploratory test of an unaged cable was conducted on a new cable outside the chamber to assess the effect of a higher oxygen concentration. Only the hydrogen burn portion of the test profile was used; the LOCA portion was not. Prior to the initiation of the heat flux pulse the cable was at ambient temperature. Shortly before the peak flux was reached the cable ignited and burned vigorously for approximately 40 seconds. The cable is shown in Figure D.5.9. Damage to the unaged cables tested in the chamber and chamber pressure measurements are not consistent with the level of combustion which occurred outside the chamber. As discussed in the previous paragraphs, unaged cable subjected to pulses inside the SCETCh blistered but did not burn. Apparently the 15 to 16 percent oxygen atmosphere in the SCETCh (corresponding to HECTR calculations of containment environments) suppresses cable burning. Thus, matching initial oxygen concentrations is important in this type of testing.

As mentioned previously, the linear ramp up to the peak heat flux used in the cable tests results in approximately 30 percent more energy incident on the cable specimens compared to the HECTR calculations for the particular S_2D event studied in the TMI-hybrid analysis. Thus all of the single burn cable test environments were more severe than any of the HECTR calculated TMI-hybrid environments.

After the cable tests had been performed, Surry calculations (which were not available prior to the testing) were completed which indicated possibly more severe environments in Surry. Figure D.5.10 shows the most severe heat flux from the Surry calculations and the TMI-hybrid calculations along with the heat flux profile used in the 100 percent cable tests. Although the Surry peak heat flux is greater than the test peak heat flux, the energy incident on the

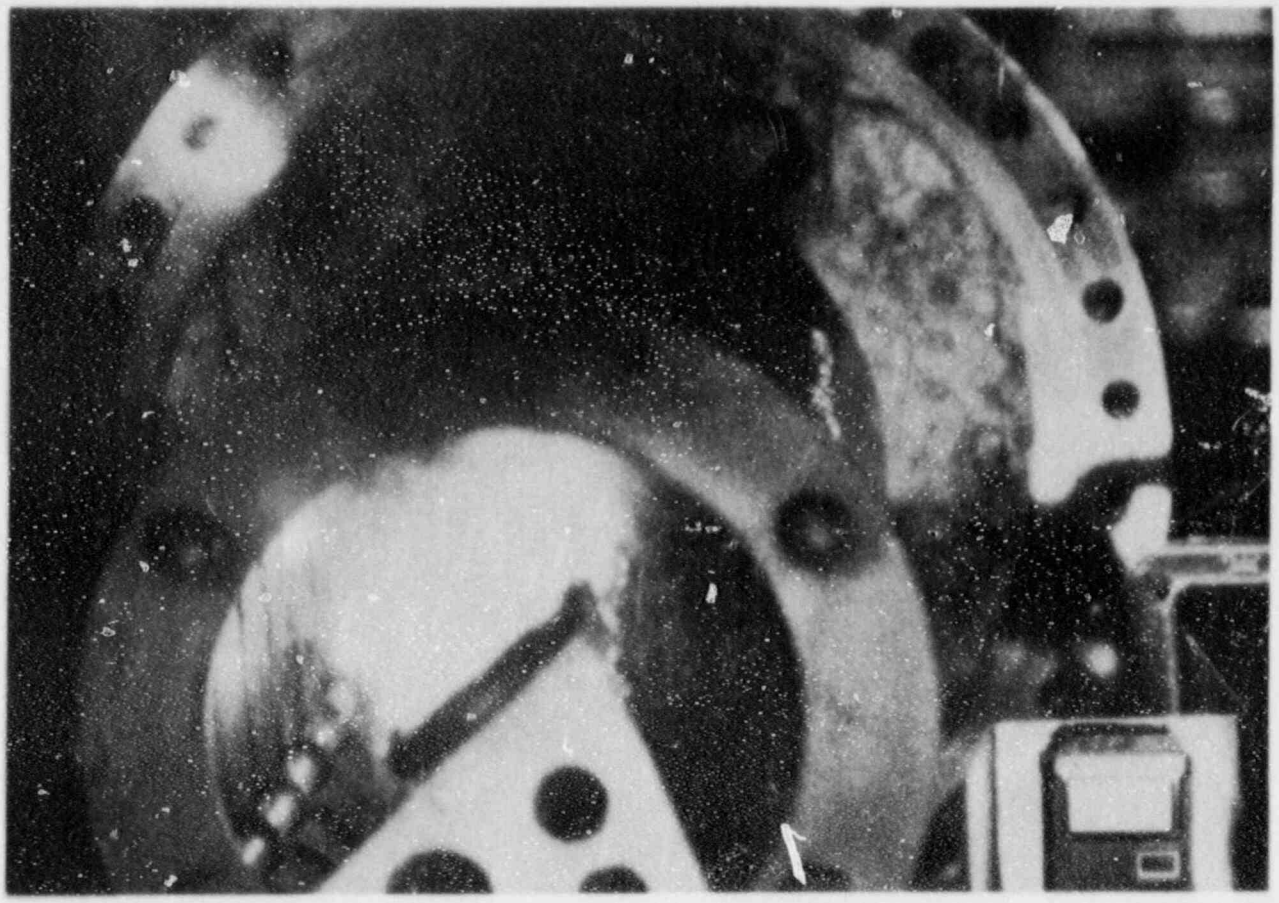

Figure D.5.9. New Cable Tested Outside of the SCETCh

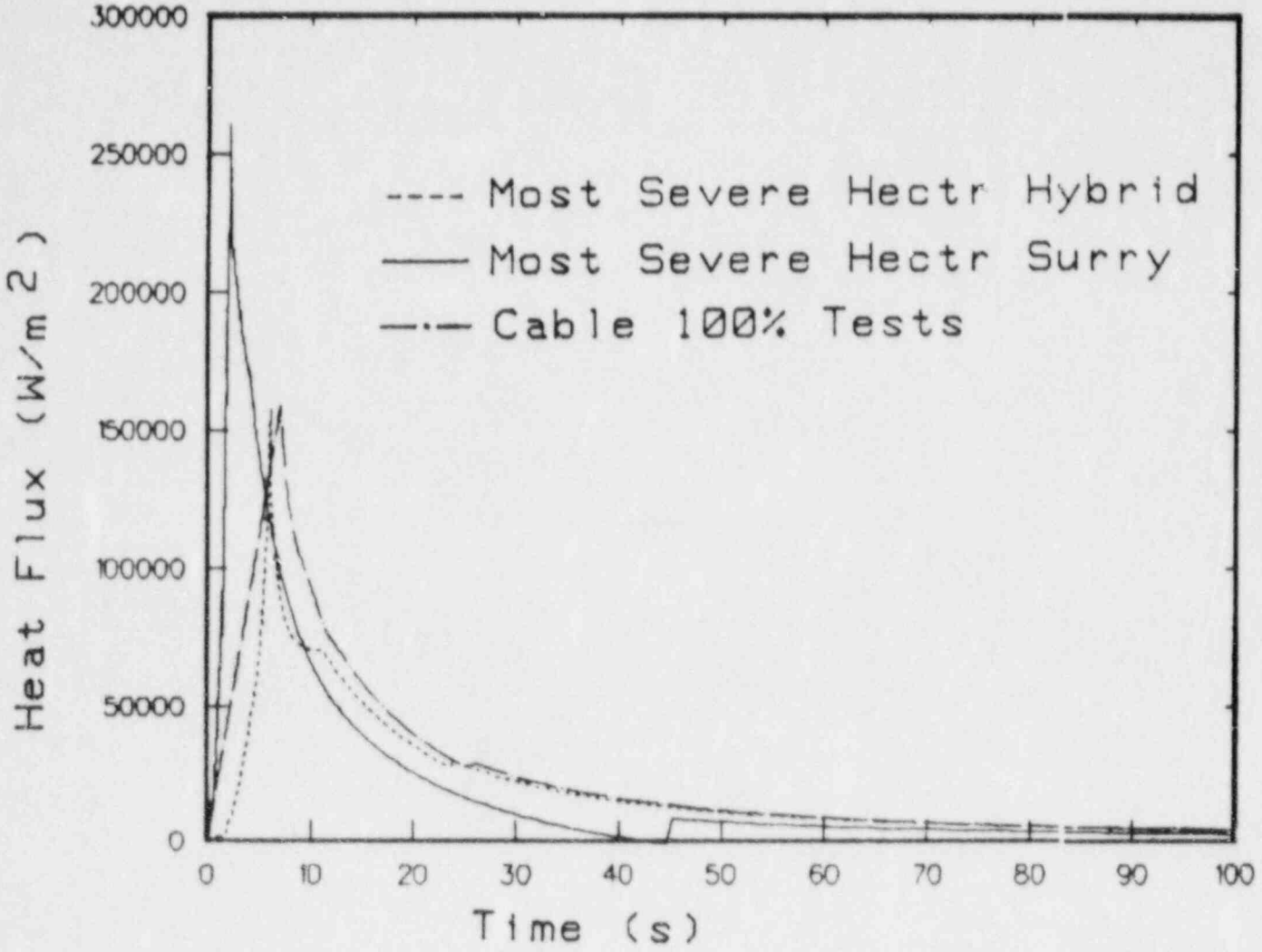

Figure D.5.10. Experimental Versus Most Severe Calculated Peak Heat Fluxes

cable specimens is actually greater (by about 20 percent) in the experimental heat flux profile as shown in Figure D.5.11. Thus in terms of energy deposition, the cable tests were more severe than either the worst-case Surry or worst-case TMI-hybrid environments calculated.

A calculation was performed including the effects of initial temperature, peak heat flux, and integrated energy deposition, to determine if these environments would result in significantly different cable temperatures. Using a one-dimensional finite difference model of the cable jacket and ignoring the effects of pyrolysis and combustion, a calculation of the cable thermal response indicated only slight differences between the test and the most severe Surry environments. The results of the calculation are shown in Figure D.5.12 for the cable surface temperature versus time. There is a slightly slower increase in surface temperature in the test case due to the linear ramp up to the peak, but this represents only a 2 or 3 second delay. Based on these results, it can be concluded that the test environment was representative of the most severe single burn environments observed in any of the calculations.

In light of the discussion concerning Table 3.5 of the main body, it can therefore be concluded that the cable tests were representative of the most severe environments expected in a LOCA and subsequent single deflagration of the hydrogen resulting from a 75 percent metal-water reaction in a large dry or subatmospheric power plant. Thus, the single burn cable test results indicate that nuclear qualified class 1E cable can survive a LOCA and severe single hydrogen burn environment inside a large dry or subatmospheric containment.

D.5.1.2 Transmitter Tests

The single burn transmitter tests were performed in two phases, a calorimetry phase and a performance phase. Both phases used the same LOCA/hydrogen environment as the cable tests with changes in foil temperatures and geometries to account for differences in the transmitter absorptivity and geometry. The calorimetry tests were conducted to determine the temperature response of the Barton 763 pressure transmitter electronics and case to the simulated accident environment. The test specimen used in these tests was a Barton 763 pressure transmitter which had been used in previous testing at the Central Receiver Test Facility.[3] The transmitter was equipped with thermocouples on the inside surface of the casing cover plate and on the electronics. Since the transmitter was previously exposed to a harsh environment it was not a valid specimen for testing transmitter performance (though it was operated during the tests). Also, routing the thermocouple wires from the interior of the transmitter to the data acquisition system

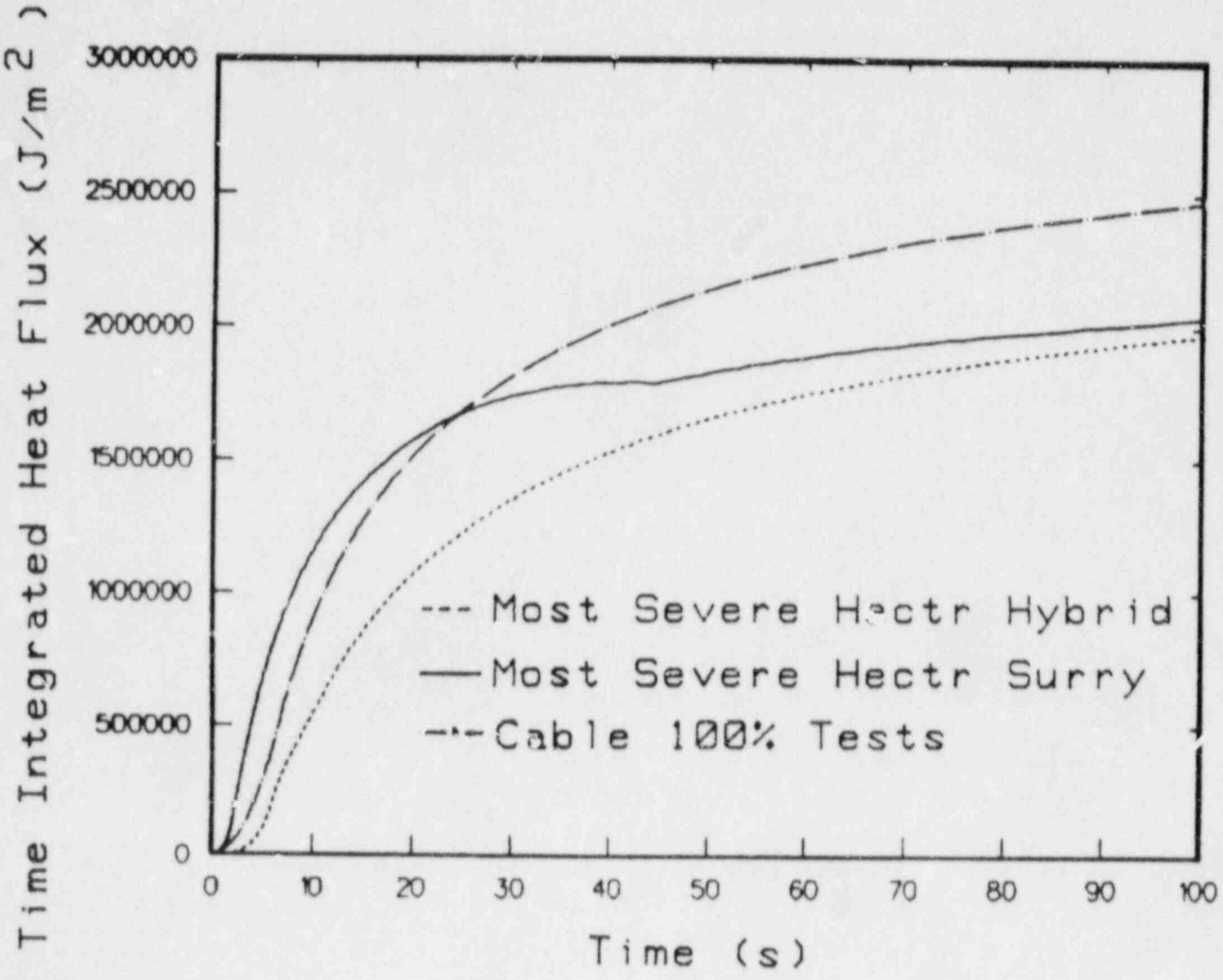

Figure D.5.11. Experimental Versus Most Severe Calculated Integrated Incident Energies

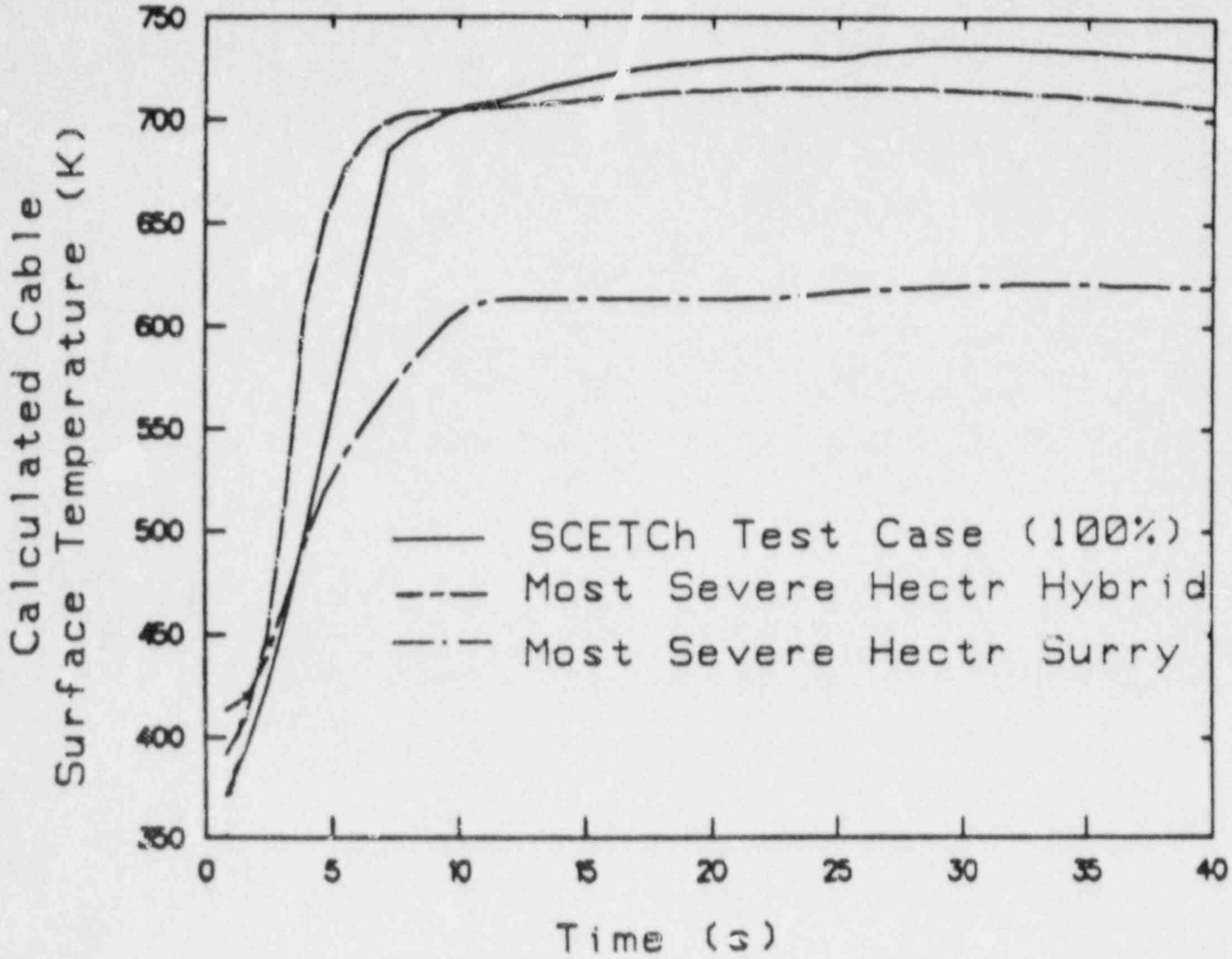

Figure D.5.12. Calculated Cable Responses

required removal of a seal gland intended to protect the interior of the instrument from moisture intrusion. However, the transmitter was suitable for measuring equipment temperature response.

The performance test investigated the operational characteristics of the Barton 763 pressure transmitter under LOCA/hydrogen burn conditions. The test specimen was a Barton 763 transmitter, identical to the calorimetry specimen but without thermocouples, which had been thermally aged to the equivalent of 40 years (125°C for 1830 hours[8]) and radiation aged to the equivalent of 40 years of in-plant radiation exposure plus the radiation dose due to the accident (200 Mrad at 1 Mrad/hr). The performance (aged) specimen included the gland to prevent moisture intrusion.

Both specimens had an operating range of 0 to 1000 psig and a signal output of 4 to 20 mA. The signal was monitored by passing the signal current through a 500 ohm resistance and measuring the voltage drop across the resistance. Both specimens were pressurized to 750 psig during their respective exposures to the accident environment.

By the time the Barton tests were conducted, an improved foil control algorithm had been developed. Thus the linear ramp in heat flux used in the cable tests was not necessary and a more accurate heat flux profile was used in the pressure transmitter tests. This profile closely follows the HECTR predicted heat flux curve shown in Figure D.5.1. In addition the SCETCh control algorithm was modified to follow more closely the HECTR predicted post-burn pressure profile. The experimentally measured and HECTR predicted pressures for one of the Barton tests is shown in Figure 5.13.

The problems encountered during the 110 percent single burn cable test (i.e. foil failures) resulted in a decision to conduct the pressure transmitter tests only at the 100 percent HECTR predicted heat fluxes. Thus, no 110 percent tests were conducted on the pressure transmitters.

The results of the calorimetry tests are shown in Figures D.5.14 and D.5.15. Figure D.5.14 shows that the casing front face temperature approached 133°C (406°K) and the capacitor temperature reached a maximum of 113°C (386°K). The thermal lag between the case and electronics is consistent with the temperature response of the instrument from previous tests.[3]

The HECTR three-layer model predictions of the front surface peak temperature are higher by 3°C than the measured temperature. The excellent agreement is an indication of the accuracy and mild conservatism of the Barton three-layer

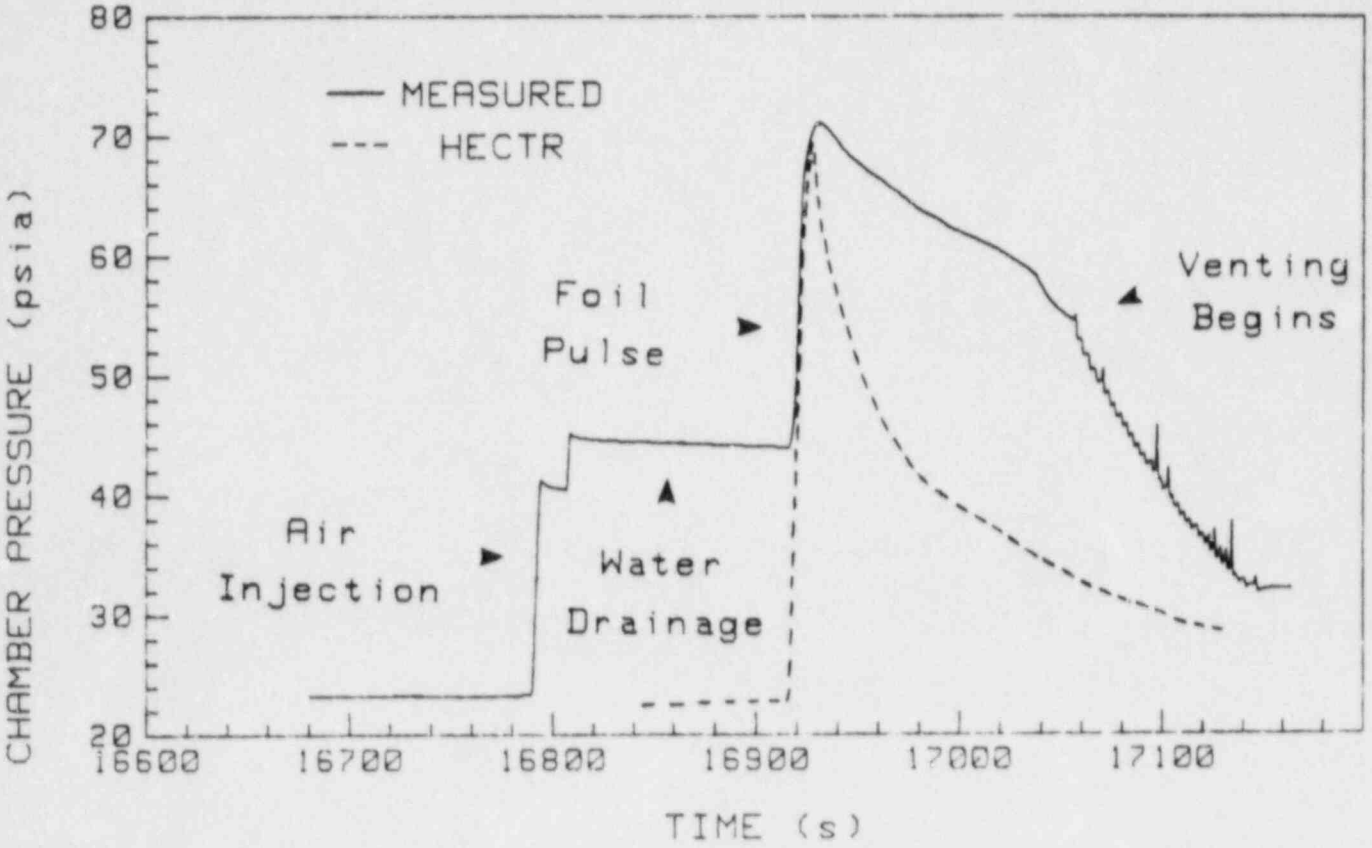

Figure D.5.13. Measured SCETCh Pressure for Transmitter Calorimetry Test

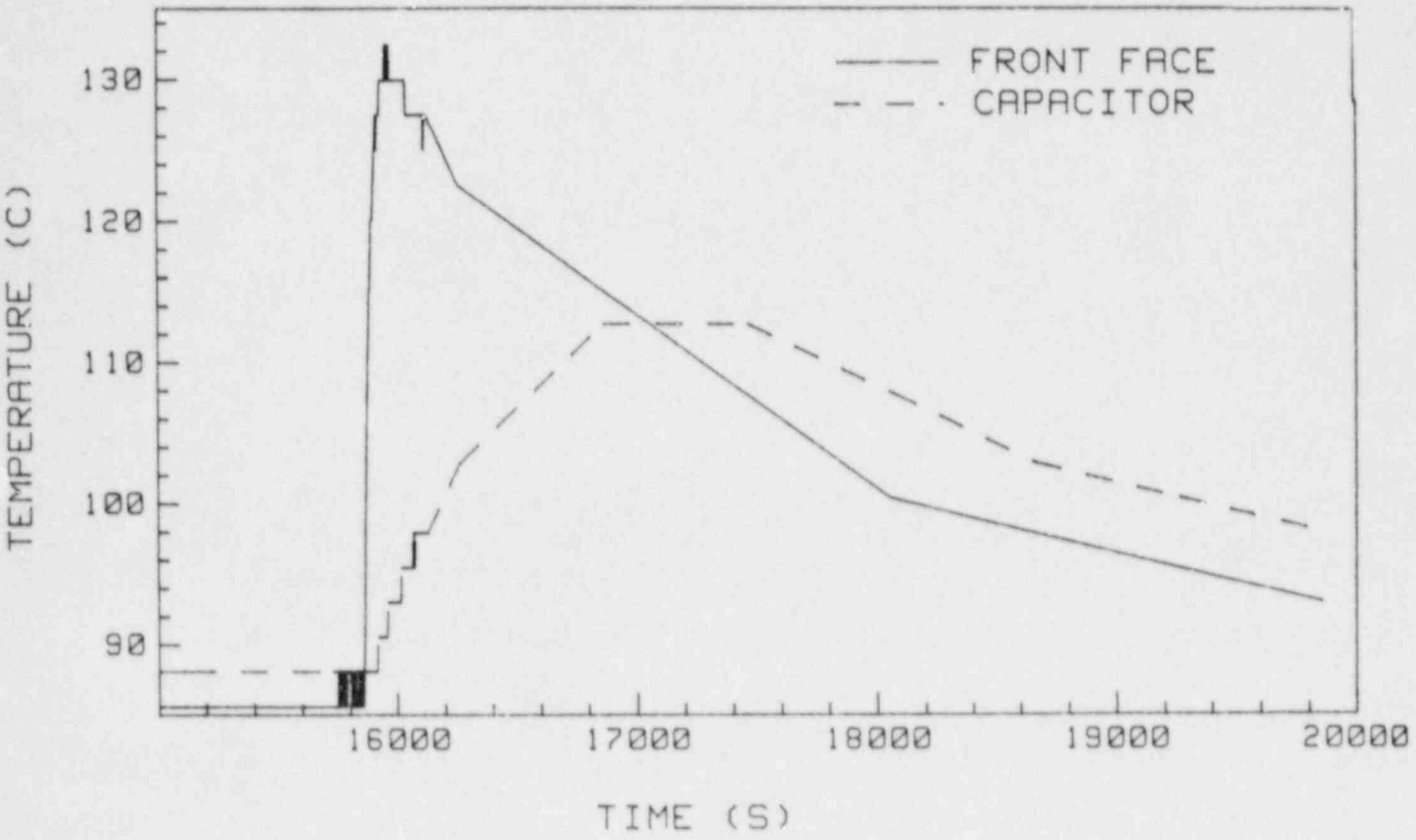

Figure D.5.14. Calorimetry Specimen Temperatures

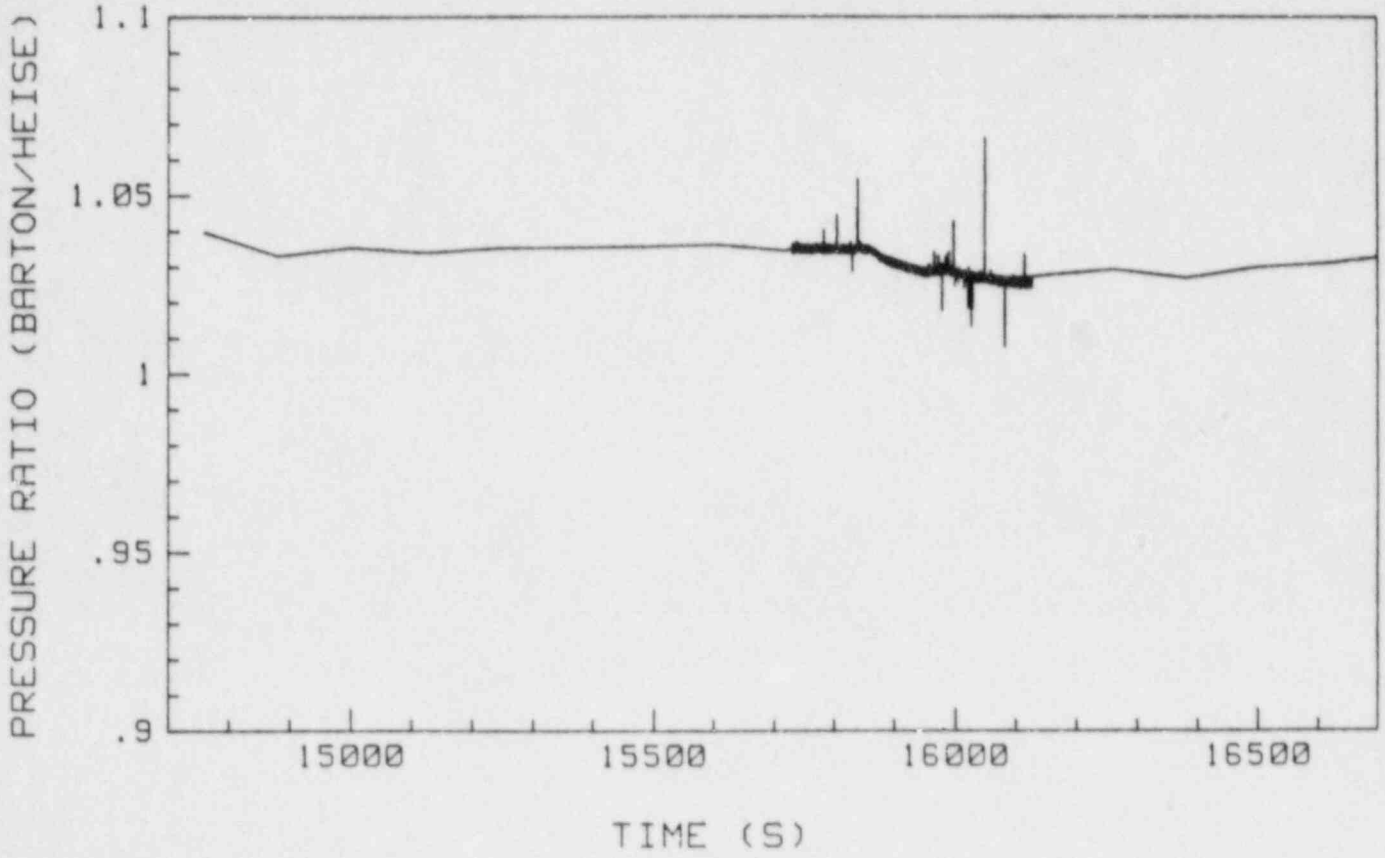

Figure D.5.15. Calorimetry Specimen Signal

model employed in the HECTR calculations, as well as an additional check on the test environment.

The ratio of the Barton pressure output to that of a Heise gauge is shown in Figure D.5.15. The fluctuations from the pre-burn readings were less than four percent during the burn simulation indicating acceptable accuracy during the test.

Another test was run using the aged Barton pressure transmitter (the performance test). Throughout the performance testing the aged transmitter also performed properly. The ratio of Barton to Heise pressure is shown in Figure D.5.16. The fluctuations from the pre-burn readings were less than two percent.

Both Barton pressure transmitters performed well during the tests. The slight fluctuations during the burn simulations could be due to small adjustments made by the pressure regulation on the system supplying nitrogen to the transmitter. Another possible cause of the fluctuations is electromagnetic interference from the foils. In either case the fluctuations were not large enough to be interpreted as an impairment to the operation of the pressure transmitter.

The heat flux profile used in the single burn pressure transmitter tests was the most severe environment seen in the TMI-hybrid calculations. Subsequent to these tests, Surry calculations were completed which indicated more severe environments in terms of maximum equipment temperature. However, the most severe of these environments resulted in a HECTR predicted peak front face temperature exceeding the qualification limit of 444°K by about 6°K for about 10 minutes. In view of the mild conservatism in the HECTR three-layer model and the considerably longer LOCA qualification test which the Barton has been tested to, HECTR-predicted front face temperatures of 450°K for 10 minutes should not be reason for concern. And in light of Table 3.5 of the main body of this report, this Surry calculation represents the bounding case.

For the single burn scenarios, the most likely threat to the survival of thermally massive equipment such as a Barton pressure transmitter is from moisture penetration through seals. For the single burn tests, the total pressure and steam concentration used were as severe as any seen in the HECTR single burn calculations. Thus from a pressure and moisture standpoint, the Barton tests were as severe as warranted by the calculations.

The results of these tests indicate that the Barton 763 pressure transmitter can withstand a large dry containment

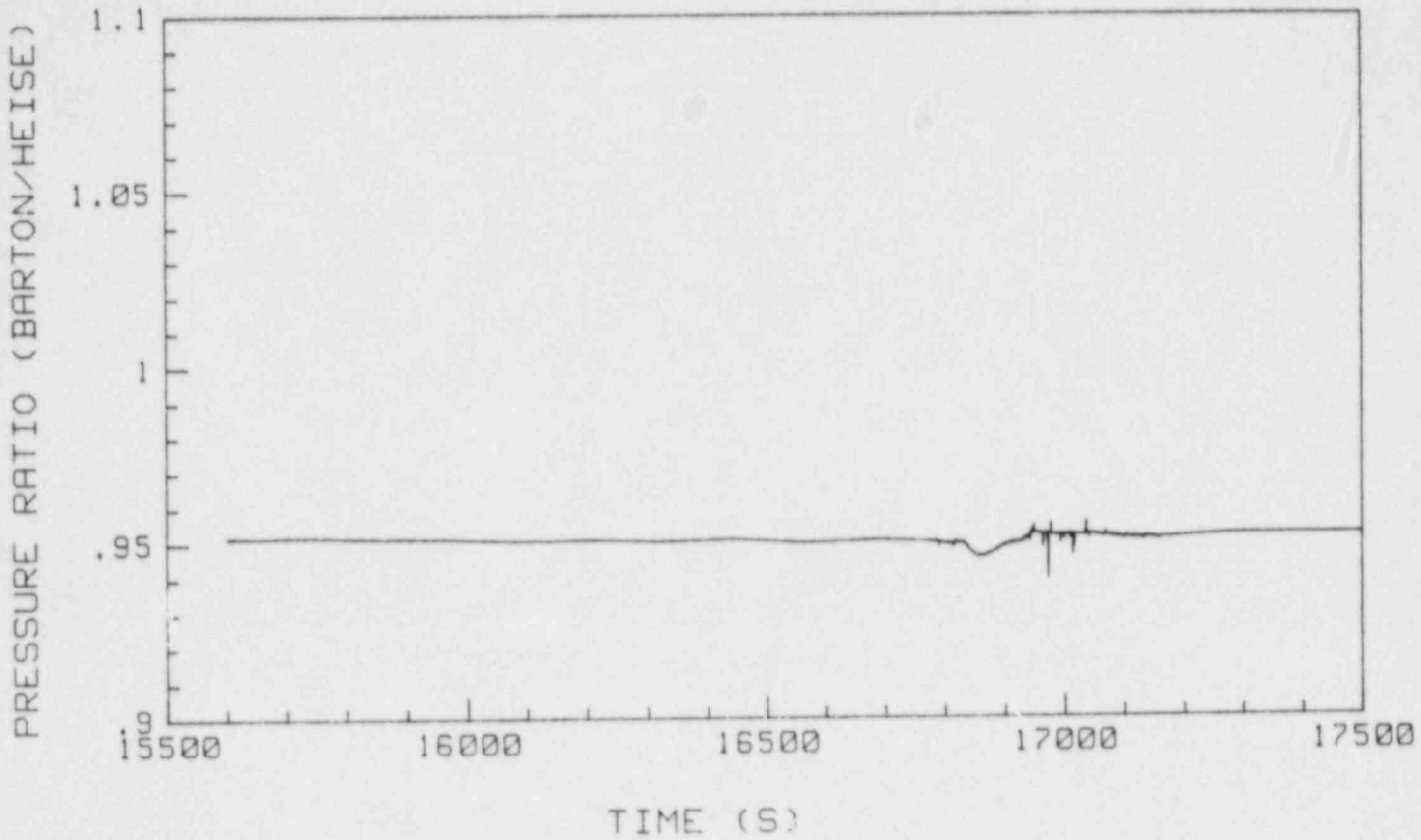

Figure D.5.16. Aged Barton Transmitter Signal

LOCA and hydrogen burn environment with a single deflagration of hydrogen released in a reaction involving 75 percent of the core Zircaloy.

D.5.2 Multiple Burn Tests

During the single burn cable tests, most of the visually observed damage occurred after the peak flux during the tail portion of the heat flux pulse. The damage to the cable jacket appeared to be a strong function of the energy deposited therein. This raised concern that an environment which results in a considerably larger energy deposition (such as occurs in a multiple burn scenario) may pose a serious threat to the survival of safety-related equipment. Although multiple burn experiments were beyond the program scope, two quick look multiple burn tests were conducted in an attempt to address this concern.

Two cable specimens and one Barton pressure transmitter were exposed in the multiple burn tests. The results (presented below) indicate that multiple burns pose a serious threat to the survival of safety equipment located in the source compartment of a large dry containment.

D.5.2.1 Cable Test

Two specimens of Brand Rex cable approximately .3 m long were exposed in the cable multiple burn test. The two specimens were taken from the ends of an aged cable specimen previously exposed in a 110 percent single burn test in which the foils failed. These specimens were used because one half of each specimen had been thermally and radiation aged (the other half had not). Although these specimens had been previously exposed in a 110 percent aged cable single burn test, the portions selected for the multiple burn test had been located outside of the foils during the 110 percent test and thus showed no evidence of cracking or charring. One specimen was placed in thin-walled 1/2 inch galvanized steel conduit with swage lock plugs to simulate any shielding that conduit may provide.

The two specimens are shown as mounted before the test in Figure D.5.17. The foreground cable is shown inside of the conduit (as tested). The background cable is shown fully exposed (as tested). The left half of both cables has not been aged, while the right half has. The specimens were not powered or monitored during the test.

HECTR predicts that multiple burns may occur with anywhere from two to more than 100 burns in a source compartment. The frequency of the burns, the peak heat fluxes, and the total incident energy are also highly variable.

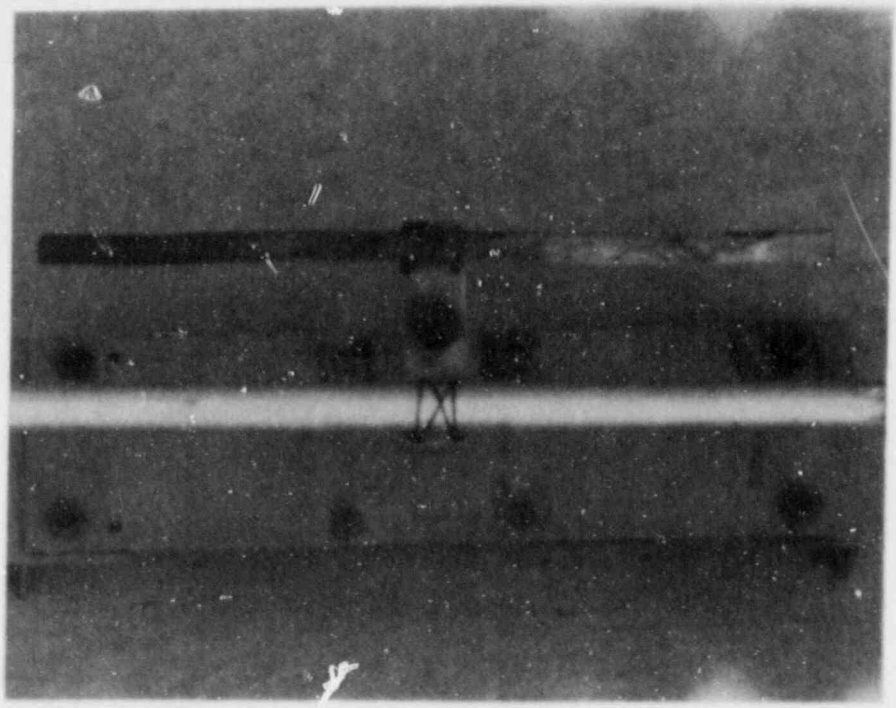

Figure D.5.17. Cable Multiple Burn Specimens (Pre-Burn)

For the cable multiple burn test, a heat flux profile from a HECTR simulation of an S_1D event in Surry was selected. This heat flux profile consisted of 58 burns in the source compartment (steam generator cubicle) and is shown in Figure D.5.18. This particular profile is believed to be representative of multiple burn scenarios and does not constitute the worst case possible. The integrated energy incident on the bare cable is shown in Figure D.5.19.

The results of the test are best described by referring to Figure D.5.20. With the exception of a very thin layer of ash over a portion of the copper conductors, only the bare copper strands remain. The jacket, filler material, and conductor insulation have been burned off exposing the bare copper wire. The results were similar for the cable specimen in conduit, with slightly more ash present. Thus, both the exposed cable specimen and the cable specimen in conduit did not survive the multiple burn environment simulation.

The results of this test indicate that multiple burn environments pose a serious threat to cables located in the source compartment of a large dry containment.

D.5.2.2 Transmitter Test

The instrumented Barton pressure transmitter which had been previously exposed in one of the single burn tests was selected as the test specimen for the multiple burn test. The thermocouples and pressure output were monitored during the test. The Barton was maintained at 750 psig during the burn simulations.

There are many combinations of burn frequency, number of burns, incident energy, and peak heat fluxes possible for defining a multiple burn environment. The source compartment volume has a strong influence on which combination of the above occurs in a given scenario. In order to examine this influence, parametric calculations using HECTR were performed over a range of source compartment volumes to determine possible effects on the multiple burn scenario. The multiple burn scenario selected for the Barton multiple burn test was a representative scenario and does not constitute the worst case possible. The 39 burn scenario selected produced the heat flux profile shown in Figure D.5.21. The integrated energy incident on the Barton from this flux profile (Figure D.5.22) is 20 percent greater than for the multiple burn cable test profile, even though there are fewer burns in this scenario. The source compartment volume used to obtain this heat flux profile is representative of a steam generator cubicle in the TMI containment.

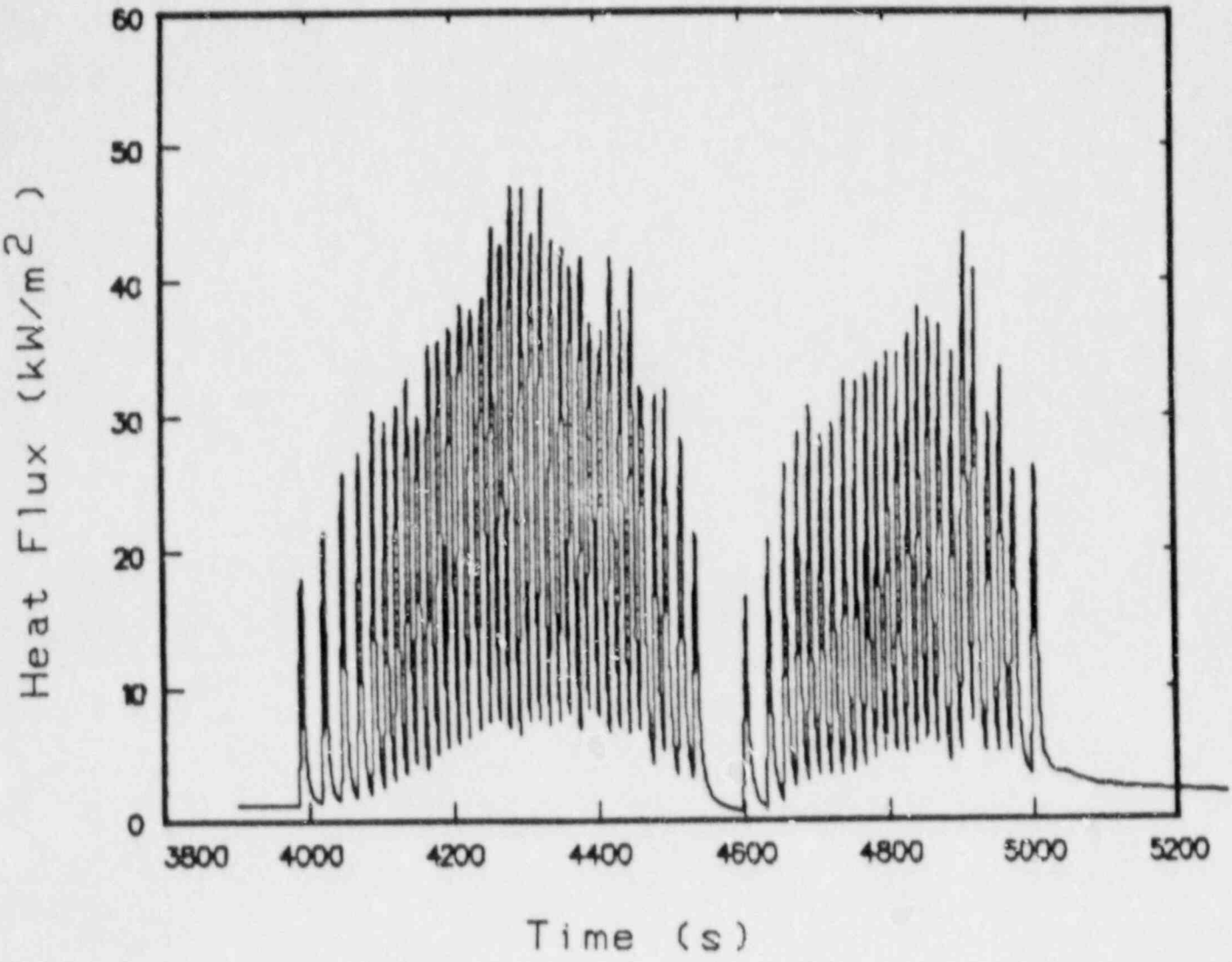

Figure D.5.18. Cable Multiple Burn Heat Fluxes

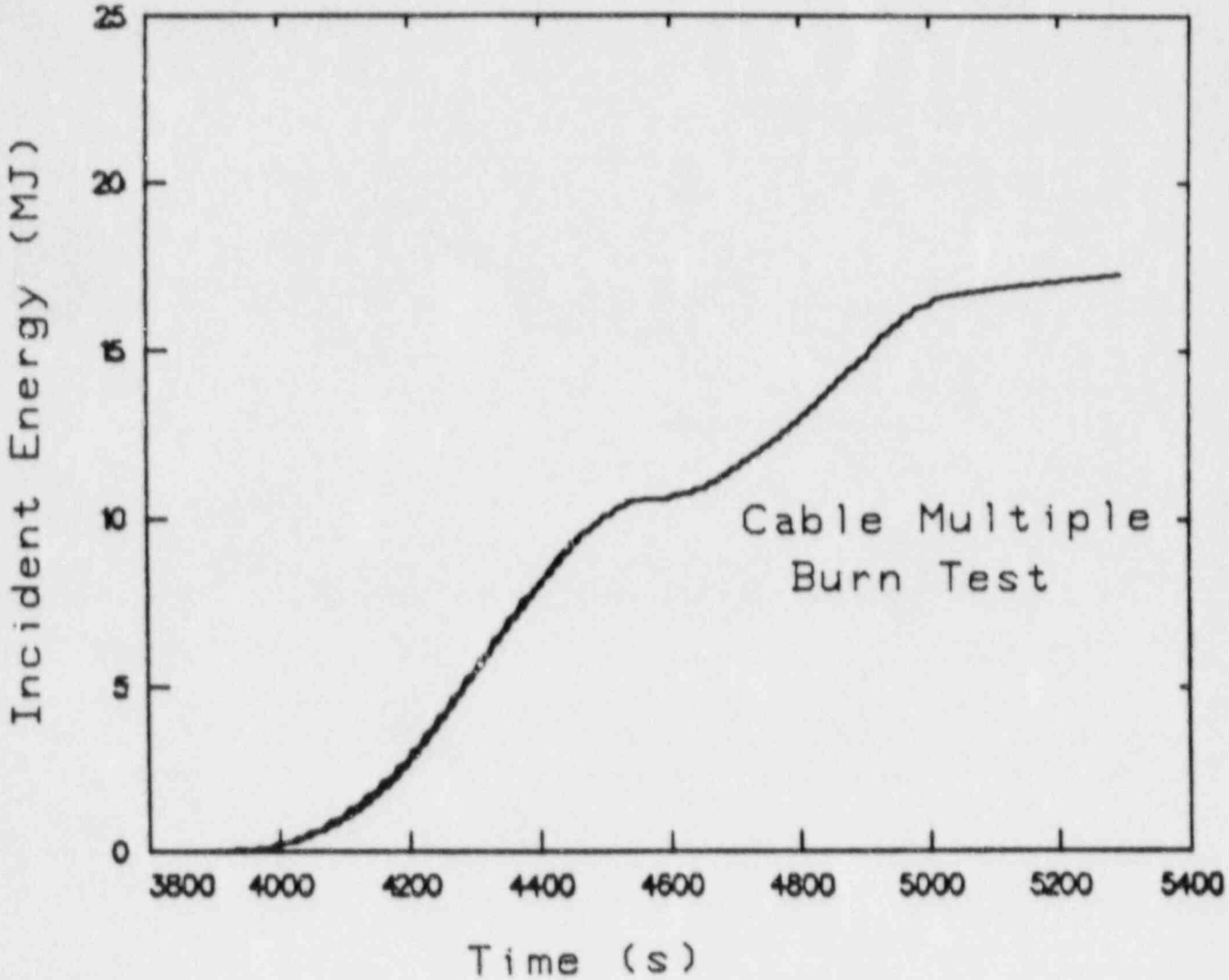

Figure D.5.19. Cable Multiple Burn Incident Energy

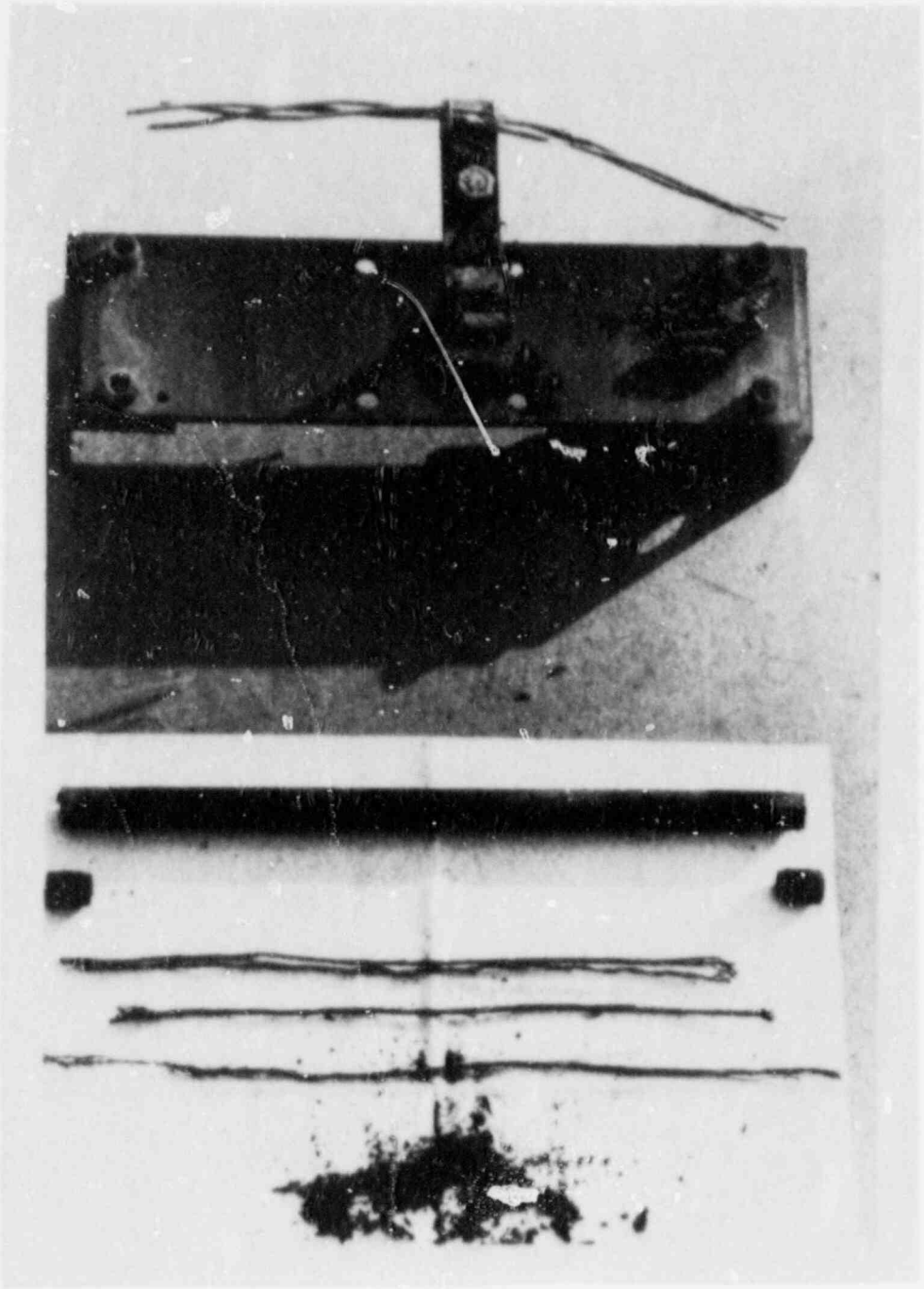

Figure D.5.20. Cable Multiple Burn Specimens (Post-Test)

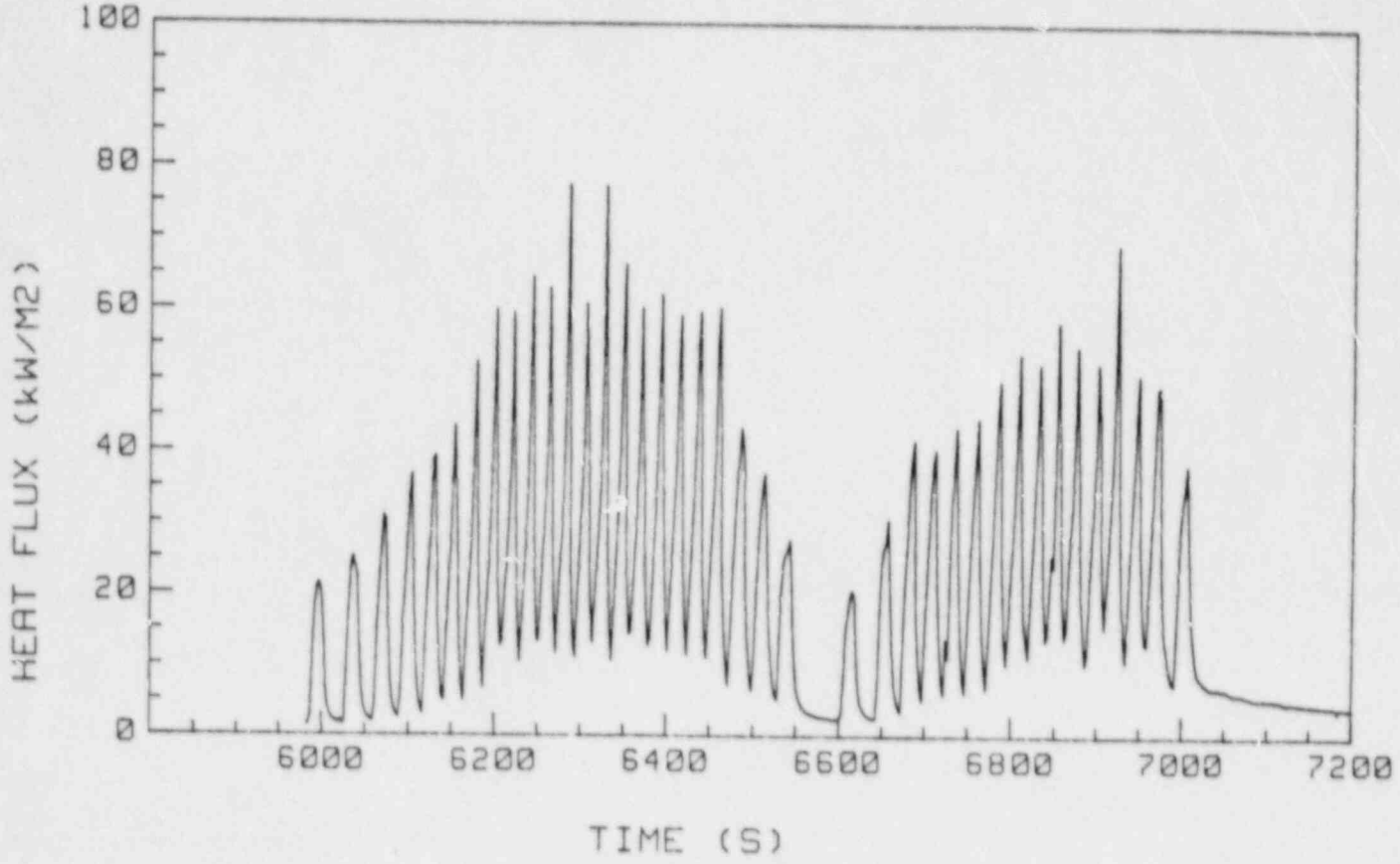

Figure D.5.21. Barton Multiple Burn Heat Fluxes

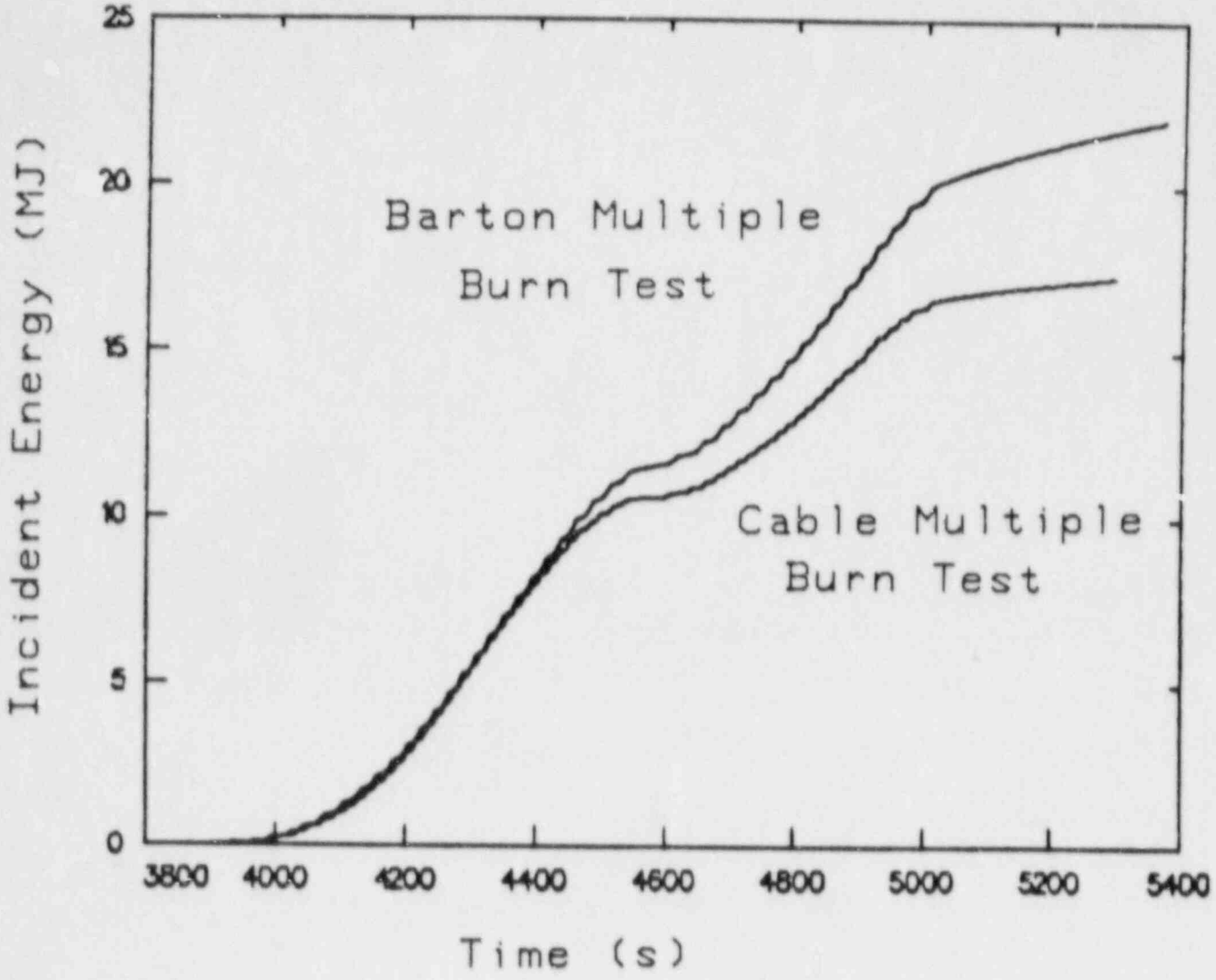

Figure D.5.22. Barton Multiple Burn Incident Energy

About one third of the way through the multiple burn scenario, the Barton pressure transmitter became erratic and failed. The ratio of Barton pressure output to that of a Heise gauge is shown in Figure D.5.23. The performance began to degrade at about 6350 seconds into the test and completely failed at about 6480 seconds. The integrated incident energy at this point in time was less than 50 percent of the total energy which the heat flux profile shown in Figure D.5.21 generated. The temperature of the capacitor at the point of failure was approximately 195°C (468°K), as shown in Figure D.5.24. The front face temperature at this time was in excess of 357°C (630°K). The momentary decline in front face temperature at 6450 seconds was a result of the thermocouple pulling away from the front plate due to the melting of the epoxy which held it in place. Thereafter the front face thermocouple gave an indication of air temperature inside the Barton.

Blistering of the paint on the surface of the transmitter was observed (Figure D.5.25) upon post-test inspection. The electronics were charred (Figure D.5.26) indicating possible combustion or smoldering inside the transmitter.

The results of this test indicate that multiple burns pose a serious threat to pressure transmitters and other similar safety-related equipment located in a source compartment.

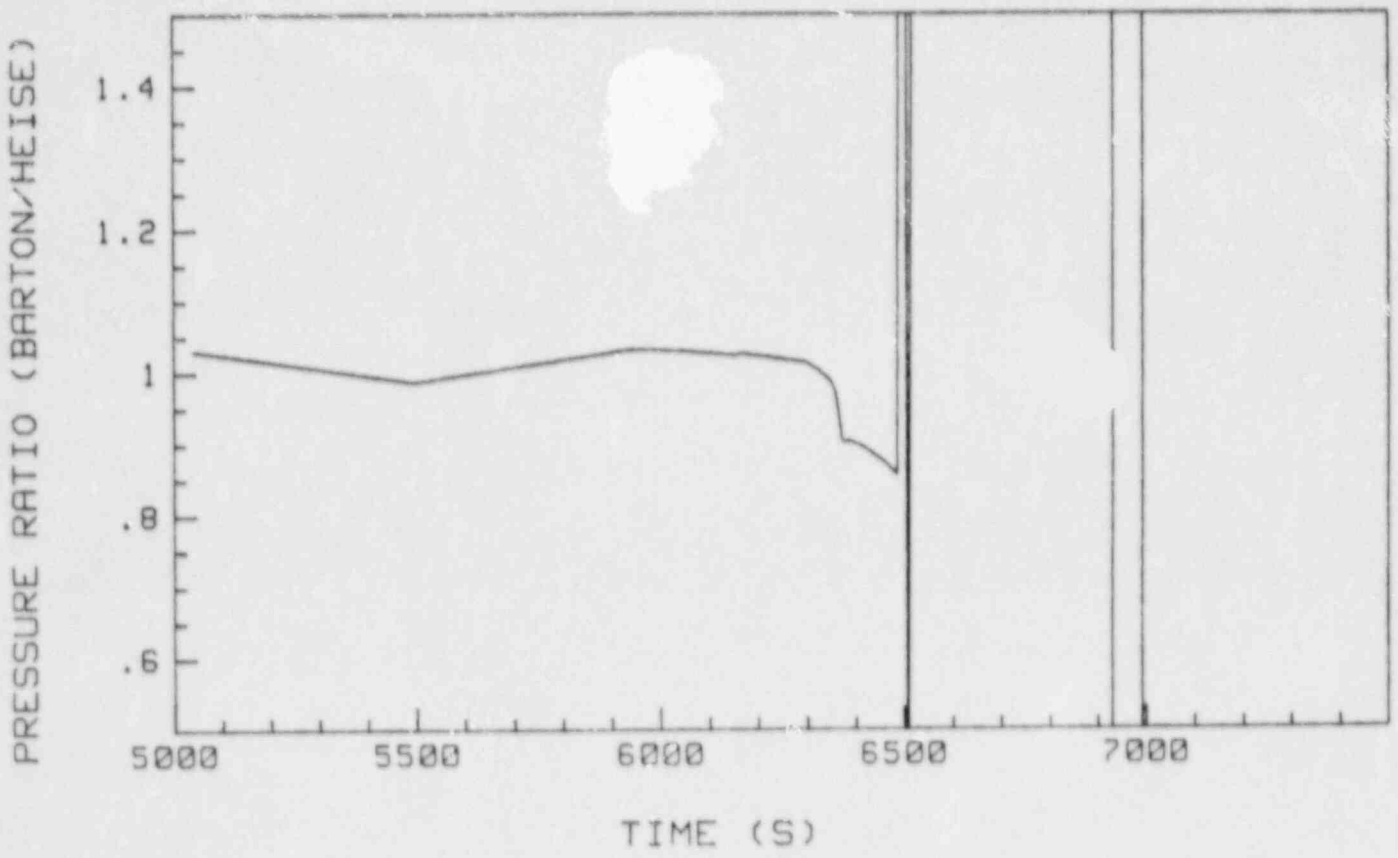

Figure D.5.23. Barton Multiple Burn Signal

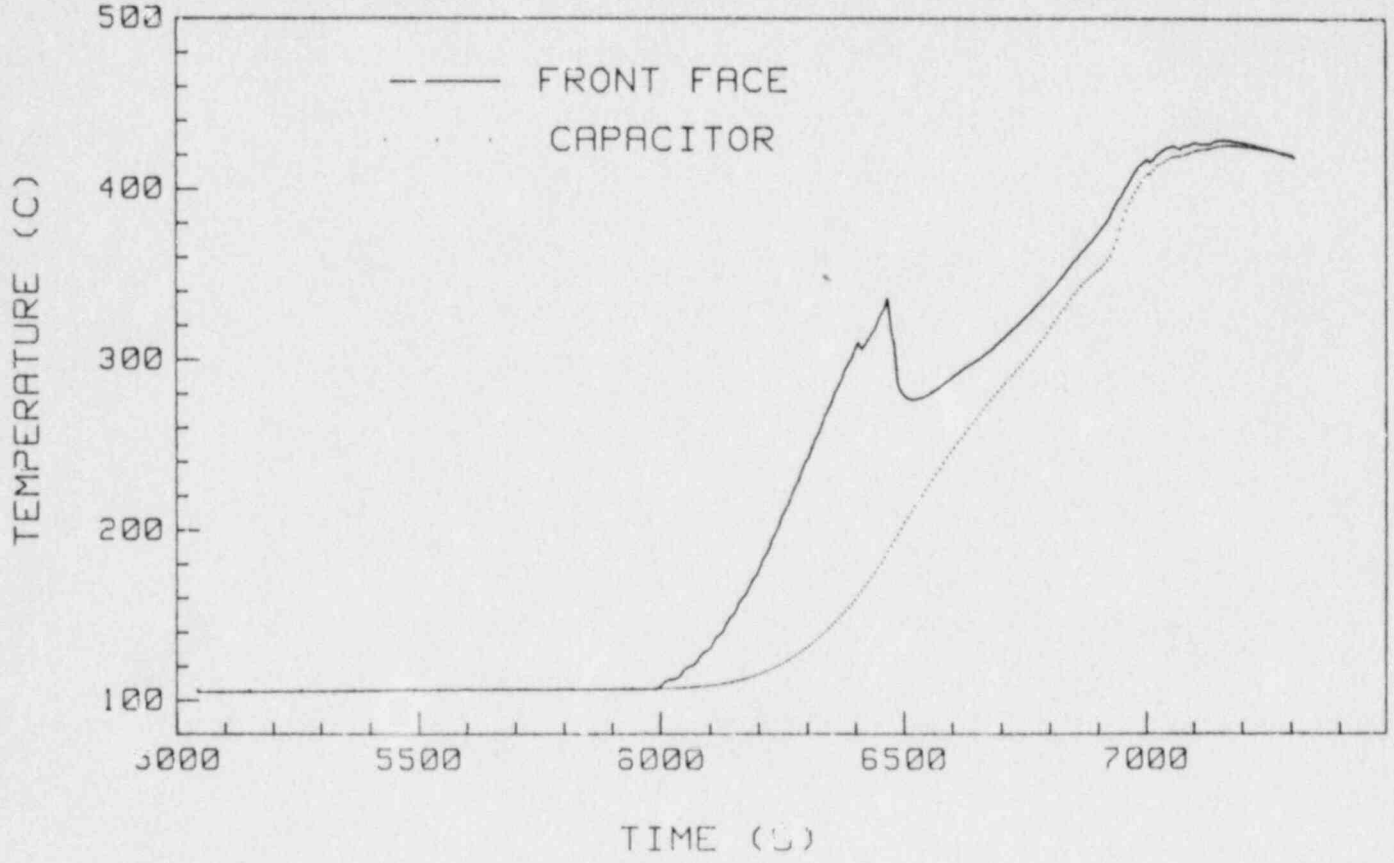

Figure D.5.24. Barton Multiple Burn Temperatures

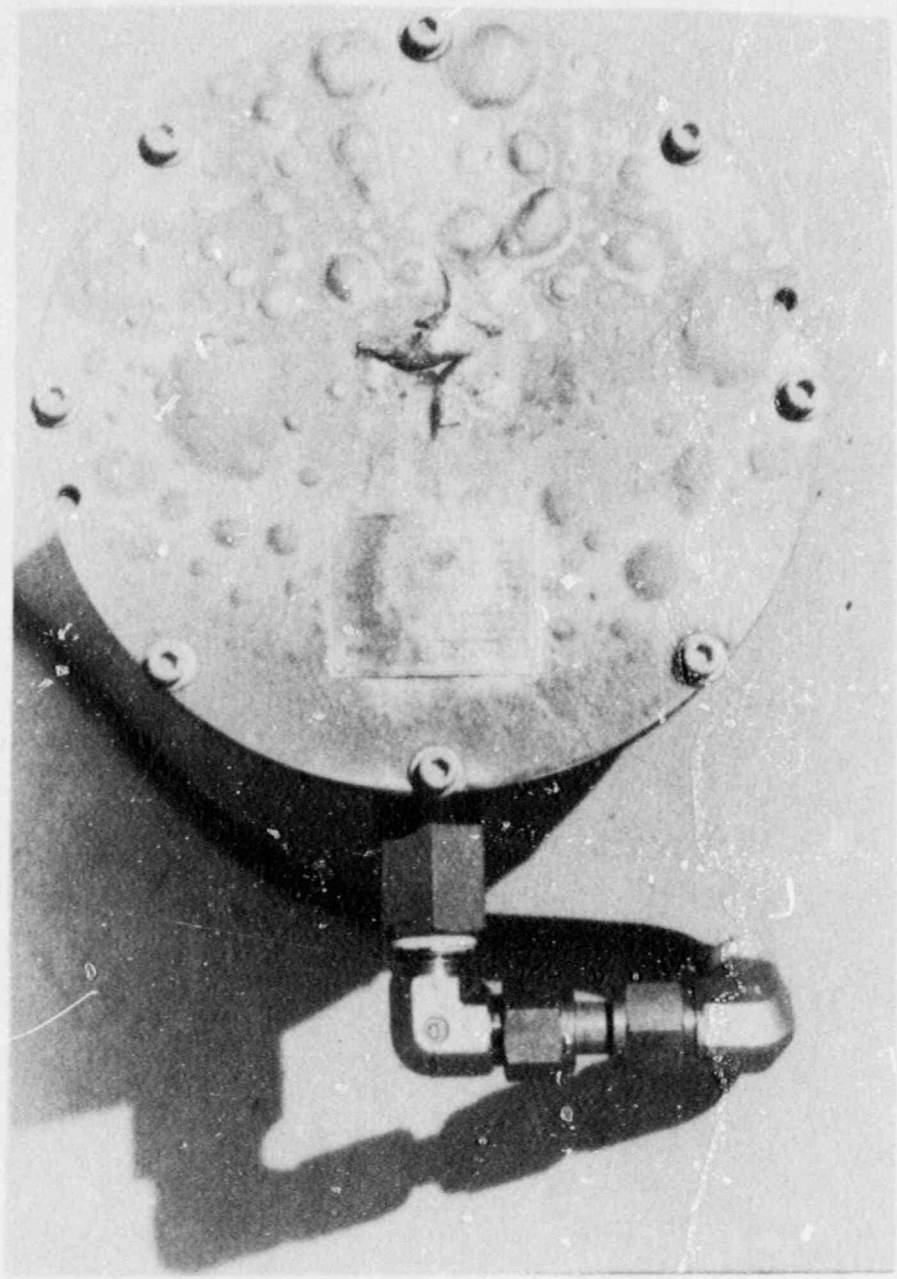

Figure D.5.25. Barton Casing (Post-Test)

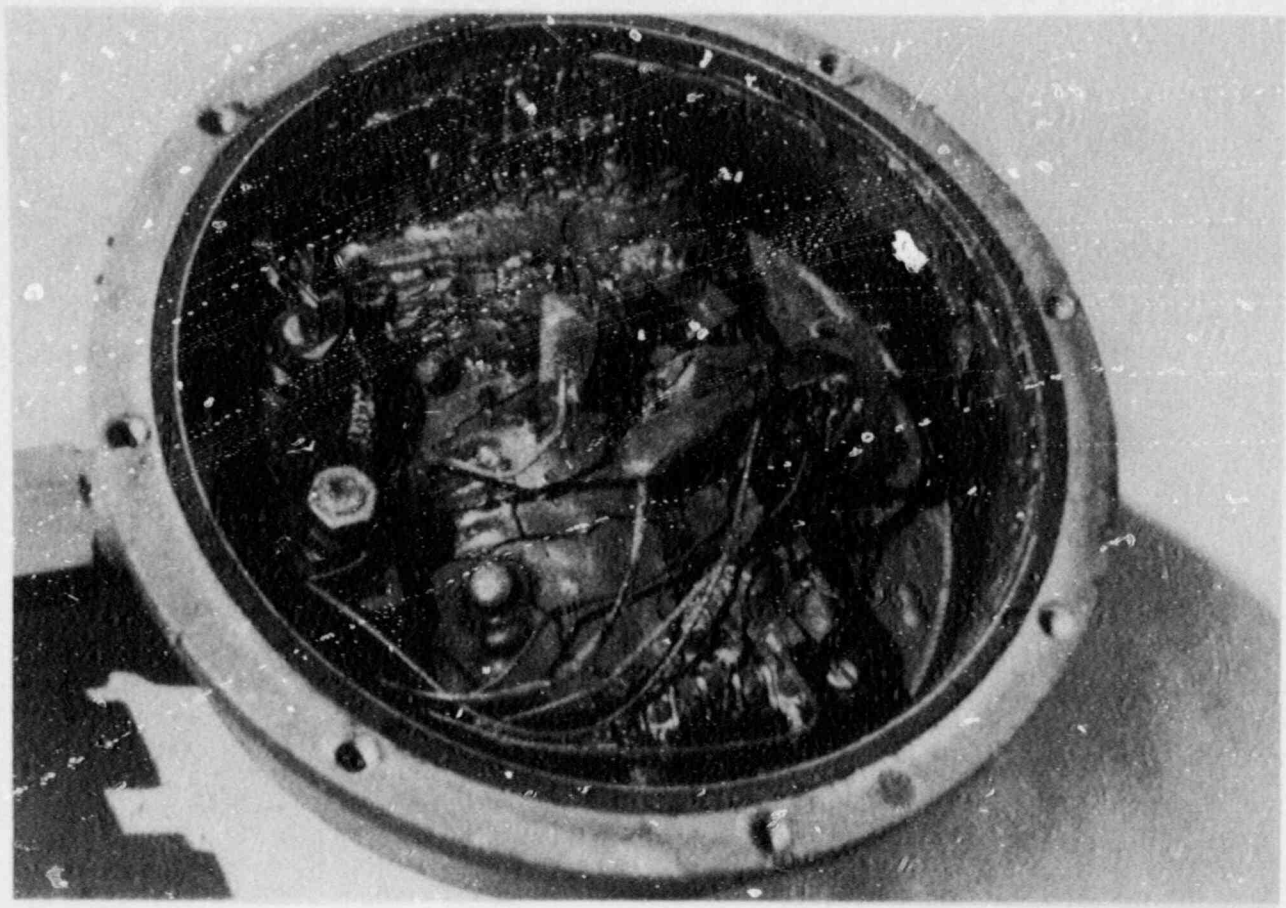

Figure D.5.26. Barton Electronics (Post-Test)

REFERENCES

1. Achenbach, J. A., et al., Westinghouse Electric Corporation, Large Scale Hydrogen Burn Equipment Experiments (EPRI NP-4354).

2. Dandini, V. J. and J. J. Aragon, Simulation of an EPRI-Nevada Test Site (NTS) Hydrogen Burn Test at the Central Receiver Test Facility (NUREG/CR-4146, SAND85-0205), Sandia National Laboratories, June 1985.

3. Dandini, V. J., Testing of Nuclear Qualified Cables and Pressure Transmitters in Simulated Hydrogen Deflagrations to Determine Survival Margins and Sensitivities (NUREG/CR-4324, SAND85-1481), December 1985.

4. Siegel, R. and J. R. Howell, Thermal Radiation Heat Transfer, 2nd ed., 1981.

5. Incropera, F. P. and D. P. DeWitt, Fundamentals of Heat Transfer, 1981.

6. Gartling, D. K., COYOTE--A Finite Element Computer Program for Nonlinear Heat Conduction Problems, SAND77-1332, October 1982.

7. IEEE Standard for Qualifying Class 1E Equipment for Nuclear Power Generating Stations (IEEE Std 323-1974), Institute for Electrical and Electronics Engineers, 1974.

8. Barton Model 763 Gauge Pressure Electric Transmitter Qualification Test Report, Report No. R3-763-6, ITT Barton, September 1982.

DISTRIBUTION

U. S. Government Printing Office
Receiving Branch (Attn: NRC Stock)
8610 Cherry Lane
Laurel, MD 20707
250 copies for R3

W. S. Farmer (5)
U.S. Nuclear Regulatory Commission
Office of Nuclear Regulatory Research
Division of Engineering
Washington, DC 20555

L. C. Shao
U.S. Nuclear Regulatory Commission
Office of Nuclear Reactor Regulation
Division of Engineering and Systems Technology
Washington, DC 20555

J. L. Telford
U.S. Nuclear Regulatory Commission
Office of Nuclear Regulatory Research
Division of Regulatory Applications
Washington, DC 20555

M. R. Fleishman
U.S. Nuclear Regulatory Commission
Office of Nuclear Regulatory Research
Division of Regulatory Applications
Washington, DC 20555

Z. Rosztoczy
U.S. Nuclear Regulatory Commission
Office of Nuclear Regulatory Research
Division of Regulatory Applications
Washington, DC 20555

L. Hulman
U. S. Nuclear Regulatory Commission
Office of Nuclear Regulatory Research
Division of Reactor Accident Analysis
Washington, Dc 20555

C. M. Ferrell
U. S. Nuclear Regulatory Commission
Office of Nuclear Regulatory Research
Division of Reactor Accident Analysis
Washington, DC 20555

P. Worthington
U.S. Nuclear Regulatory Commission
Office of Nuclear Regulatory Research
Division of Reactor Accident Analysis
Washington, DC 20555

G. Arlotto
U.S. Nuclear Regulatory Commission
Office of Nuclear Regulatory Research
Division of Engineering
Washington, DC 20555

M. Vagins
U.S. Nuclear Regulatory Commission
Office of Nuclear Regulatory Research
Division of Engineering
Washington, Dc 20555

S. Carfagno
Franklin Research Center
Valley Forge Corporate Center
2600 Monroe Blvd.
Norristown, PA 19403

B. Saffel
Battelle Columbus Laboratory
505 King Avenue
Columbus, OH 43201

E. Rumble
Science Applications, Inc.
Suite C-31
5150 El Camino Real
Los Altos, CA 94022

H. J. Kouts
Dept. of Nuclear Energy
Brookhaven National Laboratory
Upton, Long Island, NY 11973

G. Sliter
EPRI
3412 Hillview Ave.
Palo Alto, CA 94304

Sandia Distribution:

6400 D. J. McCloskey
6500 A. W. Snyder
6411 S. E. Dingman
6427 C. C. Wong
6440 D. A. Dahlgren
6442 W. A. von Riesemann
6447 M. P. Bohn
6447 D. B. King (15)
6447 V. F. Nicolette
6447 L. D. Bustard
6448 D. L. Berry
6448 B. L. Spletzer
6512 V. L. Dandini
6513 D. D. Carlson
3141 S. A. Landenberger (5)
3151 W. L. Garner
8524 P. W. Dean

NRC FORM 335 (2.84) NRCM 1102, 3201, 3202

U.S. NUCLEAR REGULATORY COMMISSION

BIBLIOGRAPHIC DATA SHEET

SEE INSTRUCTIONS ON THE REVERSE

1 REPORT NUMBER (Assigned by TIDC add Vol. No., if any)

NUREG/CR-4763
SAND86-2280

2 TITLE AND SUBTITLE

Safety-Related Equipment Survival in Hydrogen Burns in Large Dry PWR Containment Buildings

3 LEAVE BLANK

4 DATE REPORT COMPLETED

MONTH | YEAR

5 AUTHOR(S)

D. B. King, W. F. Nicolette, V. J. Dandini, B. L. Spletzer

6 DATE REPORT ISSUED

MONTH | YEAR

March 1988

7 PERFORMING ORGANIZATION NAME AND MAILING ADDRESS (Include Zip Code)

Sandia National Laboratories
Albuquerque, NM 87185

8 PROJECT/TASK/WORK UNIT NUMBER

9 FIN OR GRANT NUMBER

A1270

10 SPONSORING ORGANIZATION NAME AND MAILING ADDRESS (Include Zip Code)

Division of Engineering
Office of Nuclear Regulatory Research
U.S. Nuclear Regulatory Commission
Washington, DC 20555

11a TYPE OF REPORT

11b PERIOD COVERED (Inclusive dates)

12 SUPPLEMENTARY NOTES

13 ABSTRACT (200 words or less)

Analytical and experimental investigations of equipment survival in hydrogen burns in large dry PWR containment buildings have been conducted. Both atmospheric and subatmospheric containments were considered. Two sets of analytical studies were carried out for atmospheric large dry containments. One set analyzed the hydrogen burn that occurred as a result of the March 1979, accident at Three Mile Island. The other set considered a hybrid power plant consisting of the Zion reactor housed in the TMI-2 containment building. An analytical study of subatmospheric containments was also carried out using a model of the Surry nuclear power plant. To complement the analyses, a series of experiments simulating hydrogen burns in large dry containments was also conducted using the Sandia severe combined environment test chamber (SCETCh). The experiments investigated the survivability of thermally and radiation aged nuclear qualified Brand Rex power and control cable and a Barton 763 pressure transmitter in a simulated LOCA/hydrogen burn environment.

14 DOCUMENT ANALYSIS - a KEYWORDS/DESCRIPTORS

b IDENTIFIERS/OPEN ENDED TERMS

15 AVAILABILITY STATEMENT

NTIS
GPO Sales

16 SECURITY CLASSIFICATION

(This page)
Unclassified
(This report)
Unclassified

17 NUMBER OF PAGES

18 PRICE

☆ U.S. GOVERNMENT PRINTING OFFICE: 1988—573-049/61041